ERROR ANALYSIS OF ANALYTICAL AND NEURAL REAL-TIME RECONSTRUCTION OF ANALOG SIGNALS

Jerzy JAKUBIEC
Jerzy ROJ

WYDAWNICTWO POLITECHNIKI ŚLĄSKIEJ
GLIWICE 2024

MONOGRAFIA

Jerzy JAKUBIEC Jerzy ROJ

ERROR ANALYSIS OF ANALYTICAL AND NEURAL REAL-TIME RECONSTRUCTION OF ANALOG SIGNALS

WYDAWNICTWO POLITECHNIKI ŚLĄSKIEJ
GLIWICE 2024
UIW 48600

ISBN 978-83-7880-959-3

CONTENTS

SPIS TREŚCI

INTRODUCTION

Many modern digital instruments are designated for delivering suitably accurate samples of varying in time measuring signals – they are called sampling instruments [J14]. Such signals are deformed by the analog parts of the instruments [J14, M2] because of both nonlinearities of converters and the dynamic properties of them. For this reason, the samples of the signal obtained in the output of the analog part of a sampling instrument can differ substantially from the suitable instantaneous values of the input signal. The aim of the signal reconstruction is to process the output samples of the analog part in such a way as to obtain enough accurate values of the samples of in the instrument input [J14, M3, M4].

In a sampling instrument, an analog input signal is usually converted to a voltage, which is sampled, and then the values of the samples are measured by an analog-to--digital (AD) converter [J14]. The obtained digital results are processed by a microprocessor or a microcontroller accordingly with static and dynamic reconstruction algorithms oriented to achieving minimum calculation times. This enables real-time work of the instrument, which means that all calculations are performed in the time between successive sampling instants. This causes a sampling instrument to deliver in its output samples of the input signal with a frequency that depends on the instrument sampling period.

We can point to two basic ways of building the reconstruction algorithms dependently on mathematical tools used to model metrological properties of analog converters of the instruments. The first way, called analytical, consists in determining expressions that are directly coded as programs performed by a processor [J9, S3]. The parameters of the expressions are determined on the basis of measured data obtained during an identification process of the analog conversion model. The second way basis on properties of artificial neural networks, parameters of which are determined in a learning process of them by using these data [C1, C2, R5, R7]. The basic difference between these ways consists in obtaining the models: a neural network builds them themselves, while parameters of expressions that create the model are coded by a programmer.

It should be noticed that both mentioned ways considered here are performed, in the final stage, by a processor because activity of the neural networks is treated in this book as execution of a suitable program. In the real-time mode, the execution time of the reconstruction program should be as short as possible, which can be achieved in practice by applying linear segmental approximations of nonlinear functions and using look-up tables to store their parameters [R10, S4, W1]. This method is usable for both considered types of reconstruction algorithms because it enables the neural reconstruction by using microcontrollers.

The presented algorithms are limited to the simplest numerical forms, not only to enable their realization in real-time. The second reason, even more important, is connected with analysis of inaccuracy of the algorithms – simple forms of the algorithms make error analyzing easier and more transparent from these error propagation points of view [J9]. The method of the error description is independent of the forms of the algorithms; therefore, conclusions from the error analysis carried out for a simple reconstruction algorithm can be applied for every kind of it.

Reconstruction is carried out on signals in the digital form obtained as an effect of sampling and quantization of analog signals [J14, M2]. It means that the properties of the AD converter, being the measuring component of the sampling instrument, impose a definition of a measurement error. The definition used for the error analysis is based on the description of a measurement as a quantization process considered in probabilistic categories [J7, J9]; thus, all errors of the reconstruction are treated as random. The influence of errors on the inaccuracy of the sampling instrument is described by an uncertainty considered here as the parameter of a set of error values [J1, J10]. Based on the reconstructed value (estimate) of the input sample and the uncertainty, representation of the sample (being a measurand [Y2], [M5]) in a form of a numerical interval, called here an interval of a measurand, is proposed in Chapter 1.

The inaccuracy is interpreted as a property of a measuring instrument, which points out that a measurement result differs from a true value of a measured quantity (a measurand). Therefore, the inaccuracy characterizes the instrument qualitatively – it measures better if its inaccuracy is lower. To describe the inaccuracy quantitatively, one uses uncertainty [Y1] being a probabilistic measure of the error defined as adifference between a true value of a measured quantity and its estimate obtainedas a result of a suitable measurement process.

Due to the specificity of the errors that arise in the reconstruction process, the general model of the analog conversion in the sampling instrument is decomposed into two parts: static and dynamic, discussed in Chapter 2. In the same chapter, based on the decomposed models, fundamentals of static and the dynamic reconstruction are considered.

The static and dynamic reconstruction algorithms are presented in Chapters 3 and 4 for both analytical and neural forms of the algorithms. To discuss the metrological properties of the algorithms, an exemplary sampling instrument is used, which is dedicated to measuring instantaneous values of temperature that varies under time in industrial conditions. Theoretical considerations are illustrated by examples that show practical aspects of applications of sampling instruments. The results of probabilistic experiments carried out using Monte Carlo method [K4] to determine error distributions are the basis for analysis of factors that influence inaccuracy of the exemplary sampling instrument.

The propagation of errors from the input to the output of the instrument is described in Chapter 5 on the basis of the error propagation model, which enables tracking changes in distributions of different kinds of errors during the processing of measurement data by the reconstruction algorithms. The final effect of the application of the error propagation model is its use in calculating the uncertainty of the reconstructed signal samples obtained in the instrument output.

The last Chapter 6 is devoted to analysisof the execution time of the reconstruction algorithms by microcontrollers that realize them both in the programmed and neural forms. The analysis results make it possible to evaluate their usefulness for the real--time reconstruction for varying in time analog signals.

1. MEASUREMENT PROCESS IN SAMPLING INSTRUMENT

Generally, a signal reconstruction is that kind of the measurement process which consists in determination of the signal at the input of an instrument on the basis of the measurement results of the signal at the output of its analog part [J9, M4]. The reconstruction performed by a sampling instrument is carried out in a digital way, i.e. instantaneous values (samples) of the instrument input signal are calculated on the basis of measurement results being indications of an AD converter, which measures samples of the signal after its conversion by the analog part of the instrument. The general structure of the sampling instrument is shown in Fig. 1.1.

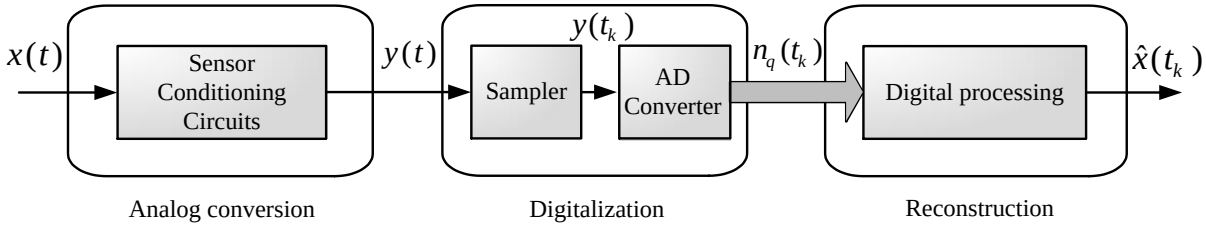

Fig. 1.1. General structure of the sampling instrument

As presented in Fig. 1.1, the sampling instrument consists of three parts. The first part performs the analog conversion of the input analog signal $x(t)$, varying in time t, into the electrical signal $y(t)$ (usually a voltage or a current). For this purpose, the appropriate sensor and signal conditioning circuits are used. In the second part, digitalization of the signal $y(t)$ is carried out, which consists in sampling the signal $y(t)$ and next, in quantization of the samples by an AD converter. The sampling is performed at instants $t_k = kT$, where k is the sample number, T the sampling period. The quantization result of the sample $y(t_k)$ is obtained in the form of an indication $n_q(t_k)$, which determines the number of quanta assigned to the sample $y(t_k)$ [J5, J9]. In the last part of the sampling instrument, the estimate $\hat{x}(t_k)$ of the instantaneous value (sample) of the input signal at the instant t_k is calculated by using areconstruction algorithm, which uses one indication or a sequence of them to obtain one estimate.

Asampling instrument can be used as an element of a measuring system and as an individual device. In both applications, it can work in batch mode or in real-time mode. In batch mode, a sequence of indications is collected at first and, at any time, they are used to reconstruct a sequence of the input signal samples. In the real-time mode, the instrument aims at current delivering accurate enough estimates of the input signal samples on the basis of the measurement results of the samples [R7]. If asampling instrument works in real-time, it repeats its activity between succeeding instants t_k and t_{k+1}, i.e. in the sampling period T. Independently of the mode, the obtained estimates have to be treated as measurement results of the input samples. This means that values of the estimates have to be close enough to the suitable true values of the input signal samples, and this property should be described quantitatively in categories of inaccuracy. In [Y1] a measurand is defined as "specific quantity subject to measurement". Accordingly with this definition, one input sample is treated in this book as the measurand. The measured (input) quantity of the sampling instrument is represented by a series of samples, the estimates of which are results of the reconstruction. The inaccuracy of every reconstructed sample is described by its uncertainty interval calculated on the basis of errors that burden the estimate [J10]. A value of the estimate and the uncertainty interval determine an interval of the measurand, which is a probabilistic representation of the input sample after its measurement on principle of the reconstruction.

1.1. Error of measurement result

A single realization of a reconstruction procedure results in obtaining one estimate of the input signal sample. This estimate is defined as a number that is the closest to true value of the input signal sample under the measurement conditions, in which the sampling instrument works. Such a definition means that the errors that burden the estimate take the lowest values possible to obtain under the assumption that all errors described deterministically are corrected (eliminated). This correction causes that the remaining errors of the estimate are of random nature. To make their values as low as possible, it is necessary to remove the constant component from the set that contains the error values. The set without this component is the basis of determination of the uncertainty interval, which expresses quantitatively the inaccuracy of every estimate obtained as a result of the signal reconstruction.

As in Fig. 1.1, all measurement results used for the signal reconstruction are obtained from an AD converter; thus, considerations dealing with a description of the errors that arise during the reconstruction should be based on analysis of the metrological properties of the AD conversion. The AD converter, considered as a measuring instrument, compares the measured quantity with a standard, which is built from quanta which are elementary standards with the same values considerably less than the range of the converter [J9]. A simple way of the quantization analysis, representative of all AD converters, can be presented on an example of the flash AD converter shown in Fig. 1.2, which is often applied to measure high-frequency signals.

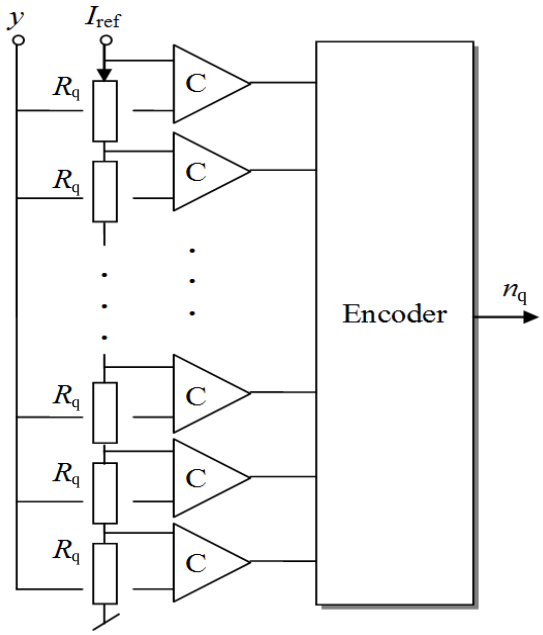

Fig. 1.2. General scheme of flash AD converter

The flash AD converter compares instantaneous valuesof the input voltage signal y with the set of quanta obtained as drops of the voltages on the resistors connected in the chain. The resistors with the same nominal values R_q are supplied by the accurate current source I_{ref}. The state of set of the electronic comparators denoted as **C** is determined at the output of the AD converter as the number n_q of quanta assigned to the instantaneous current value (sample) of y.

Generally, based on the presented example, one defines the quantization as comparing the measured quantity with the standard composed of quanta that are a set of elementary standards, the values of which are the same and significantly less than the quantizer measuring range. The quantized signal is denoted here as y (see Fig. 1.2). For varying in time signals, their physical carriers are, as a rule, voltages (as in the exemplary AD converter) or currents [J9].

The mathematical model of quantization, which describes the relationship between the number n_q obtained as the result at the output of the AD converter and the sample value of the signal y (sampling instant is not taken into account), can be written as:

$$n_q = \mathrm{ent}\left(\frac{y}{q}\right) \tag{1.1}$$

where the symbol "ent" denotes the function "entier", the value of which is equal to the integer part of its argument, q is the quantum value. Multiplying number n_q by the value of q, one obtains the row result of the quantization (measurement):

$$\breve{y} = q \cdot n_q \tag{1.2}$$

Example 1.1. Let us take that the standard of the exemplary AD converter consists of $N_q = 2^8 = 256$ resistors having the same value $R_q = 100\ \Omega$ and supplied by the reference current $I_{\mathrm{ref}} = 100\ \mu\mathrm{A}$. This means that the quantum value is: $q = I_{\mathrm{ref}} R_q = 100 \cdot 100 \cdot 10^{-6} = 0.01$ V and the voltage range of the converter is from 0 to $N_q \cdot q = 256 \cdot 0.01 = 2.56$ V. If the true value of the sample is equal, for example, $y = 1.577$ V, the number obtained as the quantization result is:

$$n_q = \mathrm{ent}\left(\frac{y}{q}\right) = \mathrm{ent}\left(\frac{1.577}{0.01}\right) = 157$$

In this case, the row measurement result takes the value:

$$\breve{y} = q \cdot n_q = 0.01 \cdot 157 = 1.57\ \mathrm{V}$$

Analyzing the scheme from Fig. 1.2, one can state that the quantization result points out the maximum number of quanta, the sum of which is less than the value of the measured quantity (sample). This means that the true value of the measured quantity y meets the inequality:

$$n_q q < y \le (n_q + 1) q \tag{1.3}$$

The effect of the quantization process described by the expression (1.3) can be graphically illustrated as shown in Fig. 1.3.

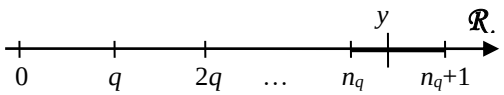

Fig. 1.3. Graphical interpretation of a quantization result

Accordingly with inequality (1.3), the real (true) value y of the quantized quantity is in the interval:

$$\breve{y} = \left[n_q q,\ \left(n_q + 1\right)q\right] \tag{1.4}$$

containing the real numbers $\mathbb{R}$. It means that the quantization process assigns the interval of real numbers (1.4) to the true value y of the measured quantity. The number n_q describes the row measurement result obtained by using an AD converter; however, one should emphasize that the mathematical model of this result takes the form of the interval (1.4). Based on Eq. (1.2), this interval may be written as:

$$\breve{y} = \left[\breve{y},\ \breve{y} + q\right] = \breve{y} + \left[0,\ q\right] \tag{1.5}$$

Inequality (1.3) can be converted to the form:

$$0 < y - n_q q \le q \tag{1.6}$$

and, after introducing Eq. (1.2) to it, written as:

$$0 < y - \breve{y} \le q \tag{1.7}$$

Inequality (1.7) is very important from error analysis point of view because, based on it, the definition of the measurement error e can be obtained. Although this definition is derived from the mathematical description of the quantization, it is of universal character and can be used for every measurement result. From (1.7), we have:

$$e = y - \breve{y} \tag{1.8}$$

which means that the measurement error in the considered case is defined as the difference between a true value y of the measured quantity and the value $\breve{y}$ obtained as a row measurement result of y.

The conception of error is commonly used in measurement practice to describe inaccuracy of measurements both in the phase of planning measurement experiments and in the analysis of metrological properties of the obtained results. One should emphasize that the definition (1.8) can be used not only in the second case, i.e. after a measurement realization but also for the error analysis as illustrated by Experiments 1 and 2.

Accordingly with Eqs. (1.7) and (1.8), the values of the quantization error are somewhere between 0 and q; therefore, these values determine the limits of the interval in the form of Eq. (1.5). It means that definition (1.8) suggests description of a measurement result in the interval form, as it is presented in Section 1.2.

Realizations of measurement error can be described in different ways depending on their applications. A deterministic description is very useful in the case where a relationship between the error and the measured quantity or another quantity being a source of this error is considered. For example, properties of the quantization error, which, accordingly with Eqs. (1.1), (1.2) and (1.8), are described by the deterministic equation:

$$e_{\mathrm{q}} = y - \breve{y} = y - n_q q = y - q\,\mathrm{ent}\left(\frac{y}{q}\right) \tag{1.9}$$

and, in the graphical form, can be presented as in Fig. 1.4.

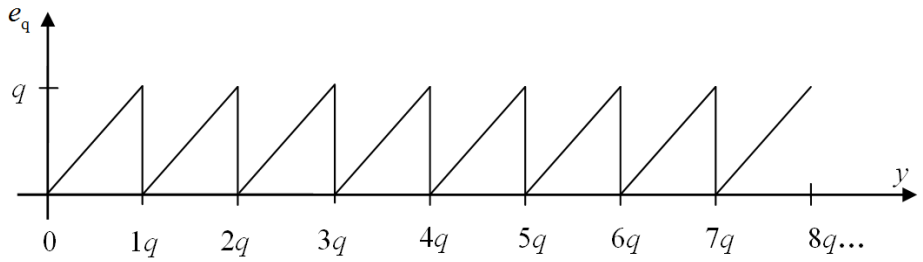

Fig. 1.4. Dependence of quantization error e_{q} on the measured quantity y expressed in values of quantum q determined for 8 beginning values of the standard with the quantum structure

The relationship between y and e_{q} presented in Fig. 1.4 shows that the values of the quantization error are strictly connected to the quantum structure of the standard. Such a deterministic description of the error as in Fig. 1.4 is useful for carrying out analysis of the measurement process before its realization. To describe an error after performing a measurement, the best way is to determine the dependence of the frequency of the error occurrence in relation to the error values. One obtains a set of possible values of the error in selected measurement conditions, which is here called as the set of error values. It contains information about frequency of occurrence of an error values that can burden a measurement result.

There are two ways of obtaining the set of error values: deterministic and probabilistic (statistical). The basis of the first way is such a deterministic function as presented in Fig. 1.4, which is a dependence of the error on the measured quantity. The second way consists in carrying out a physical (measurement) or a simulation experiment to obtain a representative set of error values. This way is usable if deterministic characteristics of an error are difficult to obtain in real physical conditions, which causes that the most effective tool to determine the set of error values consists in carrying out a probabilistic simulation using Monte Carlo method.

Both ways are presented on examples described in the following experiments performed for the exemplary AD converter.

Experiment 1.1. Let us use the characteristic of Fig. 1.4 to determine the set of quantization error valuesof the AD converter described in Example 1.1. Taking into account that the error values change periodically (the period is equal to the quantum value q = 0.01 V) one can use only one period to achieve this aim. Determining, in the interval from 0 to q, 100,000 points uniformly distributed and then, calculating the error values for these points, one obtains the set of values which, in histogram form, is shown in Fig. 1.5a with the assumption that the number of histogram classes is equal to 100.

Experiment 1.2. Let us take the Monte Carlo method to determine the set of the quantization error values. The experiment was carried out in 100 000 steps with the assumption that the input voltage of the exemplary AD converter is sampled randomly in the AD converter range from 0 to $q \cdot 2^8 = 0.01 \cdot 256 = 2.56$ V. In every step, first, a value of the input quantity y is taken from the ADC range with the assumption that all values have the same probability, i.e., the population of these values is described by the rectangular distribution. Every value of y is quantized accordingly with Eq. (1.1); next, the error value is calculated with using Eq. (1.9) and is located in the set of the quantization error values. After the experiment, the obtained set of error values is shown in Fig. 1.6b in the form of a histogram.

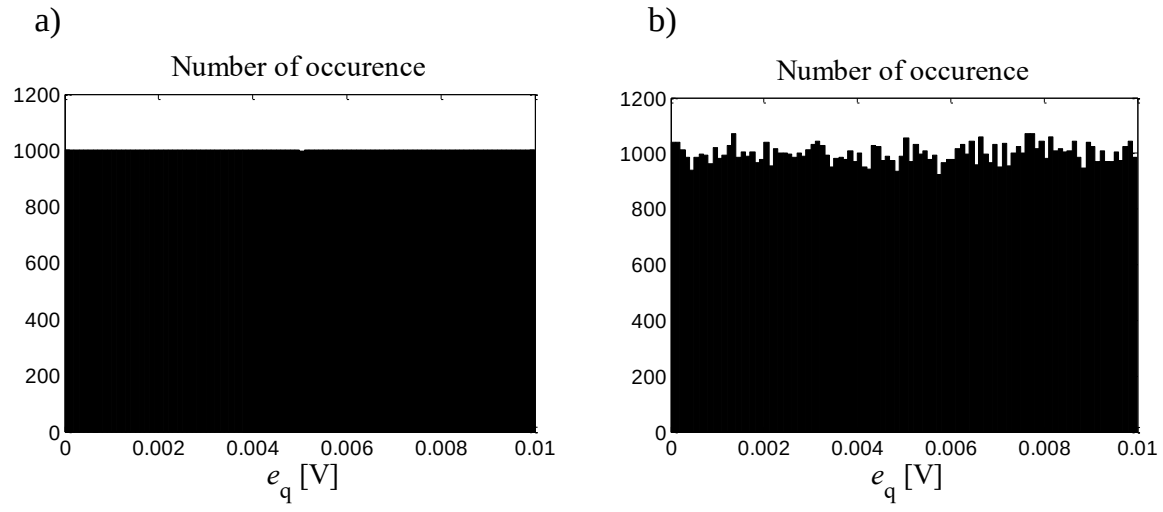

Fig. 1.5. Histograms of the quantization error of the exemplary AD converter obtained: a) in the deterministic way, b) by using the Monte Carlo method

The histograms, both this one from Fig. 1.5a and Fig. 1.5b, describe the same set of error values, although these histograms have been obtained in different ways: the first one in the deterministic way and the second in the probabilistic. From the measurement practice point of view, these histograms differ in non-essential

degree. Moreover, both histograms determine the frequency of the error occurrence; therefore, they can be interpreted as discrete representations of probability density functions. This means that a distribution of a set of error values can be described in a discrete form by a histogram or in an analytical form by a probability density function, which can be treated as an estimate of the suitable histogram.

The determination of a probability density function of an error can be performed on the basis of the histogram, as this from Fig. 1.6, or in an analytical way. Every probability density function $g(e)$, i.e. of any error e, has to fulfill the normalizing expression [P1], accordingly with which we have:

$$\int_{-\infty}^{\infty} g(e)\,\mathrm{d}e = 1 \tag{1.10}$$

For the rectangular distribution, as results from Fig. 1.5, the probability density function of the error e_q is constant in the interval from 0 to q and equal to zero outside these limits. Denoting this constant value as a, one obtains on the basis of (1.10) that:

$$\int_{0}^{q} a\,\mathrm{d}e_\mathrm{q} = 1 \tag{1.11}$$

from which it is:

$$aq = 1 \tag{1.12}$$

Therefore, we have:

$$a = \frac{1}{q} \tag{1.13}$$

The probability density function determined for the quantization error in the presented analytical way is shown in Fig. 1.6.

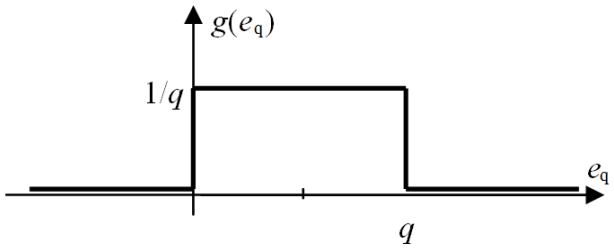

Fig. 1.6. Probability density function of the quantization error presented in Fig. 1.4

As result from Fig. 1.5a, the error can be treated as random, even if the basis of such a perception comes from its primary description, which is deterministic. In measurement practice, a quantization result is burdened by errors connected with

several physical phenomena of random character, mainly by noise. It causes one to assume that for further considerations all measurement errors are described in probabilistic categories, which means that every error is expressed by its realizations taken randomly from the set containing possible values of the error.

The row measurement result is not the best representation of the true value of the measurand because the error burdening this result may contain systematic components, which increases absolute values of the error [J12]. This component can be eliminated from the row result by subtracting a correction from every value of the error.

From Eq. (1.8), which definesthe error of the row measurement result $\hat{y}$, it results that the measurand may be described in the form of the equation:

$$y = \breve{y} + e_{\text{row}} \tag{1.14}$$

where, in place of the general error symbol e, the error e_{row} of the row result is used. After introducing the correction c to Eq. (1.14), we have:

$$y = \breve{y} + c + e_{\text{row}} - c \tag{1.15}$$

The expression:

$$e = e_{\text{row}} - c \tag{1.16}$$

that describes the error without the systematic component takes the least absolute values. It means that the corrected measurement result $\hat{y}$ burdened by this error is closest to the true value from all that are possible to obtain in selected measurement conditions. Accordingly with Eq. (1.15), the corrected result $\hat{y}$ is such an estimate of the measurement result, which is described as:

$$\hat{y} = \breve{y} + c \tag{1.17}$$

The systematic component c of the random error e_{row} is defined as the expected value:

$$c = E\left(e_{\text{row}}\right) \tag{1.18}$$

where the population of this error is represented by the set of the error values. If the probability density function $g(e_{\text{row}})$ is known, the expected value is defined as:

$$E\left(e_{\text{row}}\right) = \int_{-\infty}^{\infty} g\left(e_{\text{row}}\right) e_{\text{row}} \, \mathrm{d}e_{\text{row}} \tag{1.19}$$

For the set with limited error values, the expected value is estimated by the average value:

$$\hat{E}(e_{\text{row}}) = \frac{1}{N}\sum_{i=1}^{N} e_{\text{row}}(i) \tag{1.20}$$

where $e_{\text{row}}(i)$ is a realization of the error, i is the number of the error values in the set, N is the total number of the error values and $N < \infty$.

Example 1.3. Calculating the expected value of the quantization error described by the probability density function of Fig. 1.6, we have:

$$E(e_{\text{q}}) = \int_{-\infty}^{\infty} g(e_{\text{q}})\, e_{\text{q}}\, \mathrm{d}e_{\text{q}} = \int_{0}^{q} \frac{e_{\text{q}}}{q}\, \mathrm{d}e_{\text{q}} = \frac{q}{2} \tag{1.21}$$

For the AD converter described in Example 1.1, the expected value (1.21) of the quantization error is equal: $q/2 = 0.01/2 = 5 \cdot 10^{-3}$ V. The same value one obtains on the basis of Eq. (1.20) after using it for calculation of the average value of the error in the form of the histogram presented in Figs. 1.6a or 1.6b.

Accordingly with Eq. (1.16), elimination of the systematic component from a set of error values consist in subtraction the expected value from all realizations of the error. Subtracting the value (1.21) from each value of the error with the distribution described by Fig. 1.6, we obtain the symmetrical probability density function shown in Fig. 1.7. The absolute values of this error are in the interval from $-q/2$ to $q/2$ and they have minimal values among those that are possible to obtain if measurements using an AD converter are performed for the quantum value equal to q.

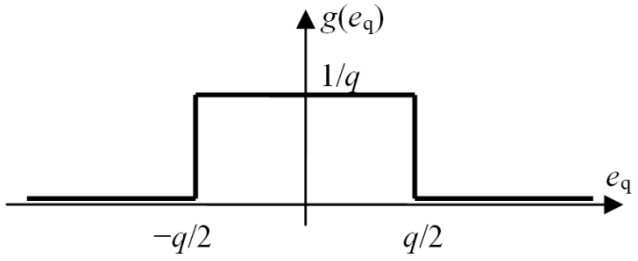

Fig. 1.7. Distribution of the quantization error after correction of the systematic component

Accordingly with Eq. (1.21), the correction appropriate for the row quantization error is $c = E(e_{\text{q}}) = q/2$, which means that the estimate (1.17) of a single quantization result is expressed as:

$$\hat{y} = \breve{y} + c = q \cdot \mathrm{ent}\left(\frac{y}{q}\right) + \frac{q}{2} = q\left[\mathrm{ent}\left(\frac{y}{q}\right) + \frac{1}{2}\right] \tag{1.22}$$

Analysis of this expression leads to the conclusion that the correction of the quantization results can be done both by adding 0.5 to an AD converter indication and by introducing the correction c to the row quantization result.

From Eqs. (1.15), (1.16) and (1.17), it results that the error of the corrected result is defined as:

$$e = y - \hat{y} \tag{1.23}$$

i.e. as the difference between a true value of a measurand and its estimate devoid systematic components. First of all, this definition is the basis for determining the uncertainty of a single measurement result, which is presented in the next section.

The sampling instrument delivers in its output a sequence of the estimates dedicated for sampling instants t_k, k is the number of the sample, k = 0, 1, ... Based on Eq. (1.23), the error burdening the estimate at instant t_k is described as:

$$e(t_k) = y(t_k) - \hat{y}(t_k) \tag{1.24}$$

The probabilistic description of this error maybe the same for subsequent samples or change if measurement conditions under which the sampling instrument works vary over time.

The error definition (1.24) is widely used in the analysis of errors that burden the estimate. But for the analysis of dynamic errors, it is necessary to describe quantities as functions of time. In these cases, the error is defined in deterministic categories in the analog form as:

$$e(t) = x(t) - y(t) \tag{1.25}$$

where $x(t)$ is the input signal of a converter and $y(t)$ is its output signal. In this definition, the input signal represents true values of the converted signal, while the output signal represents the values that can be potentially measured. Every signal is described as functions of time t.

The deterministic form (1.25) of the error can be the basis of its probabilistic description. To obtain such a description, one uses the Monte Carlo method. The error is randomly sampled in its period, and the obtained samples are located in the set of error values, on the basis of which probabilistic parameters of the uncertainty interval are calculated.

1.2. Determination of measurand interval

Distribution of the total error contains complete probabilistic information about inaccuracy of the measurand estimate; thus, it should be the basis of determination such a kind of parameter which describes this inaccuracy quantitatively in probabilistic categories. The commonly used parameter is defined in [Y1] as uncertainty of measurement understood as "a parameter, associated with the result of a measurement, that characterizes the dispersion of the values that could reasonably be attributed to the measurand". In a sampling instrument, the measurand is a single sample of the reconstructed signal, which is expressed by its estimate obtained as a result of a single performance of a reconstruction process. The probabilistic properties of the estimate are described by an uncertainty interval which is determined on the basis of set of the total error values. This means that uncertainty of a reconstruction result is treated in this book more widely than in the mentioned definition. Such an approach is connected with the fact that characteristics of some elements of the sampling instrument can be nonlinear which causes non-symmetrical distributions of some errors. If nonlinearity is significant, the inaccuracy cannot be expressed by one parameter of the error set.

In general, independently of the symmetricity of the error distribution, the error influence on the inaccuracy of the estimate is described as the uncertainty interval [J7, J10] that is defined as such a set of real numbers, which contains the true value of the measured quantity y with a given probability determined by the confidence level p. The uncertainty interval is built in relation to the known estimate, which means that the definition of this interval may be formally written as follows:

$$\mathbf{P}\left[\underline{u} \le \left(y - \hat{y}\right) \le \bar{u}\right] = p \tag{1.26}$$

where **P** denotes probability, $\underline{u}$ and $\bar{u}$ are the limits of the uncertainty interval, low and high, respectively. Accordingly with this definition, the probability of occurence in the interval the difference between the mesurand value and its estimate is equal to p.

The difference in round brackets of the expression (1.26) defines the measurement error (1.8), which means that the limits of the uncertainty interval can be determined as parameters of the error distribution. Assuming that the error values outside the uncertainty interval on the left and on the right are probable at the same level $p/2$, one can calculate the lower limit of the interval as:

$$\int_{-\infty}^{\underline{u}} g(e)\mathrm{d}e = \frac{1-p}{2} \tag{1.27}$$

and the upper one as:

$$\int_{\bar{u}}^{\infty} g(e)\mathrm{d}e = \frac{1-p}{2} \tag{1.28}$$

where $g(e)$ is the probability density function of the error.

From expression (1.26), it results that inequality:

$$\underline{u} \le (y - \hat{y}) \le \bar{u} \tag{1.29}$$

is fulfilled with probability p. After conversion of inequality (1.29), one obtains the expression:

$$\underline{u} + \hat{y} \le y \le \bar{u} + \hat{y} \tag{1.30}$$

on the basis of which the measurand interval is defined as:

$$\vec{y} = \left[\underline{y},\ \ \bar{y}\right] = \left[\hat{y} + \underline{u},\ \ \hat{y} + \bar{u}\right] \tag{1.31}$$

This interval contains the true value of y with probability p; thus, it can be treated as the interval representation of the measurand$y$ after performing its measurement and calculating the estimate of the measurement result.

The interval (1.31) can be expressed as:

$$\vec{y} = \hat{y} + \left[\underline{u},\ \bar{u}\right] \tag{1.32}$$

which means that it is the sum of the estimate and the interval:

$$\vec{u} = \left[\underline{u},\ \bar{u}\right] \tag{1.33}$$

called an uncertainty interval. Taking the above into account, expression (1.32) can be interpreted as an interval model of a measurand after its measurement. In this model, the uncertainty interval (1.33) describes inaccuracy of the estimate $\hat{y}$.

Example 1.4. Let us determine the measurand interval of the voltage sample quantized by the AD converter in the way described in Example 1.1. The exemplary row measurement result is: $\breve{y} = 1.57$ V and the quantum value $q = 0.01$ V. To obtain the estimate of the measurand that is the true value of the voltage sample, one should correct this result by adding to it the expected value of the quantization error which, accordingly with Eq. (1.21), is equal: $c = q/2 = 0.01/2$ V = 0.005 V. After the correction, the estimate takes the value:

$$\hat{y} = \breve{y} + c = 1.57 + 0.005 = 1.575 \text{ V} \tag{1.34}$$

The probability density function of the quantization error, shown in Fig. 1.7, is described as:

$$g(e)=\begin{cases}\dfrac{1}{q} & \text{for} \quad -\dfrac{q}{2}\le q\le\dfrac{q}{2}\\ 0 & \text{in the other cases}\end{cases} \tag{1.35}$$

The lower limit of the uncertainty interval, determined for the function (1.35) accordingly with Eq. (1.27), is calculated from the equation:

$$\int_{-\frac{q}{2}}^{\underline{u}}\frac{1}{q}\,\mathrm{d}e=\frac{1-p}{2} \tag{1.36}$$

For the commonly used value of the confidence level p = 0,95 and the quantum value equal to q = 0.01 V, one obtains from expression (1.35) that the value of the lower limit is: $\underline{u}=-4.75\cdot10^{-3}$ V. The higher limit calculated in the same way on the basis of expression (1.28) has the value: $\overline{u}=4.75\cdot10^{-3}$ V. Therefore, the uncertainty interval is described as:

$$\vec{u}=\left[\underline{u},\ \overline{u}\right]=\left[-4.75,\ 4.75\right]\cdot10^{-3}\ \text{V}$$

thus, the measurement result expressed as the measurand interval has the form:

$$\vec{y}=\hat{y}+\vec{u}=1.575+\left[-4.75,\ 4.75\right]\cdot10^{-3}\ \text{V}=\left[1.57025,\ 1.57975\right]\text{V}$$

In addition to the described limits, two other parameters can be used to characterize an interval [N1]. The first one, called the middle of the interval, is defined as:

$$\operatorname{mid}(\vec{y})=\frac{\overline{y}+\underline{y}}{2} \tag{1.37}$$

and the second, the radius, as:

$$\operatorname{rad}(\vec{y})=\frac{\overline{y}-\underline{y}}{2} \tag{1.38}$$

Based on Eq. (1.31) and the definitions (1.35) and (1.36), one can write that:

$$\operatorname{mid}(\vec{y})=\frac{\hat{y}+\overline{u}+\hat{y}+\underline{u}}{2}=\hat{y}+\frac{\overline{u}+\underline{u}}{2}=\hat{y}+\operatorname{mid}(\vec{u}) \tag{1.39}$$

and:

$$\operatorname{rad}(\vec{y})=\frac{\hat{y}+\overline{u}-\hat{y}-\underline{u}}{2}=\frac{\overline{u}-\underline{u}}{2}=\operatorname{rad}(\vec{u}) \tag{1.40}$$

From Eq. (1.40), it results that the measurand interval and the uncertainty interval have the same radiuses.

For the symmetrical distribution of the error as in Fig. (1.7), the absolute values of the limits of the uncertainty interval are the same (see Example 1.4). Denoting these values as:

$$|\underline{u}| = |\overline{u}| = u \tag{1.41}$$

and taking into account that it is:

$$\overline{u} = -\underline{u} = u \tag{1.42}$$

we have, from Eq. (1.39), that the middle of such a symmetrical measurand interval is:

$$\mathrm{mid}(\vec{y}) = \frac{\hat{y} + u + \hat{y} - u}{2} = \hat{y} \tag{1.43}$$

and, from Eq.(1.40), its radius is:

$$\mathrm{rad}(\vec{y}) = \frac{\hat{y} + u - (\hat{y} - u)}{2} = u \tag{1.44}$$

This means that, for the symmetrical error, the middle of the measurand interval is equal to the estimate $\hat{y}$ of the true value and the radius of this intervalis equal to u. Thus, the measurand interval can be written as:

$$\vec{y} = [\hat{y} - u,\ \hat{y} + u] = \hat{y} + [-u,\ u] \tag{1.45}$$

The measurand interval (1.45) is described by two parameters: the estimate $\hat{y}$ and the uncertainty u which, accordingly with [Y1] can be called an uncertainty of a measurand. From Eq. (1.45), we see that the radius of the uncertainty interval is:

$$\mathrm{rad}(\vec{u}) = \frac{\overline{u} - \underline{u}}{2} = \frac{u - (-u)}{2} = u \tag{1.46}$$

in the case considered. The middle of the interval takes the value:

$$\mathrm{mid}(\vec{u}) = \frac{\underline{u} + \overline{u}}{2} = \frac{-u + u}{2} = 0 \tag{1.47}$$

For the symmetric error, the expression (1.26), which defines the uncertainty interval, can be written as the following expression:

$$\mathbf{P}[-u \le (y - \hat{y}) \le u] = p \tag{1.48}$$

which means that the uncertainty can be calculated on the basis of the probability density function $g(e)$ by solving the functional:

$$\int_{-u}^{u} g(e)\mathrm{d}e = p \tag{1.49}$$

Example 1.5. Using the functional (1.49) to determine the uncertainty for the quantization error distribution presented in Fig. 1.7, one obtains the expression:

$$\int_{-u}^{u} \frac{1}{q} \mathrm{d}e = p$$

on the basis of which it is:

$$u = \frac{q}{2} p$$

The confidence level most commonly used is $p = 0.95$ [Y1, K3], for which the uncertainty is called expanded and denoted as U. If we take $q =$ 0.01 V, this uncertainty takes the value:

$$U = \frac{0.01}{2} 0.95 = 4.75 \cdot 10^{-3} \text{V}$$

The estimate of the exemplary mesurand is $\hat{y} = 1.575$ V. Having given the uncertainty value, one can write this measurand as the interval which can be presented in the form shorter than in Example 1.2 as:

$$\tilde{y} = \hat{y} + [-U,\ U] = \hat{y} \pm U = 1.575 \pm 4.75 \cdot 10^{-3} \text{ V}$$

This means that for the symmetrical distribution of the error that burdens the estimate, its inaccuracy can be described quantitatively by using only one parameter, i.e. the measurement uncertainty.

1.3. Determination of total error distribution

In measurement practice, every obtained result is burdened by many errors, which means that the total error should be treated as a composition of partial errors. Analyses of the physical properties of errors arising in measurement chains that applied quantization [J5, J9] let us treat these errors as additive; therefore, the total (combined) error e can be described as the sum of partial errors e_1, e_2, …, e_J :

$$e = e_1 + e_2 + \ldots + e_J \tag{1.50}$$

where J is the number of all errors. In accordance to this equation, every realization of the total error is the sum of suitable realizations of partial errors. For further consideration, we assume that all partial errors are random and are devoid of systematic components.

Equation (1.50) is treated as the general error model. It is widely used in this book in simulative experiments realized by using the Monte Carlo method because it enables the composition of partial errors by adding its realizations at every step of the experiment. The realization of the total error calculated on the basis of Eq. (1.50) is located in the set of error values. The size of this set was assumed to be 100,000, which is sufficient from the point of view of metrological experiments.This means that after 100,000 steps, the obtained set is presented as a histogram that is treated as a specific estimate of the probability density function of the total error. Based on this histogram and using functionals (1.27) and (1.28), the parameters of the uncertainty interval of the total error are calculated.

The Monte Carlo experiment is the most effective and simplest way for the composition of errors in the measurement conditions which are analyzed in this book. This is connected with the nonlinear properties of analog elements of the exemplary sampling instrument considered in this book and the need for a composition of different kind of errors such as static and dynamic errors. Analytical description of nonlinear static errors is practically impossible, which causes a simulative experiment to be the only way to obtain a distribution of the total error.

With the assumption that the partial errors are not correlated and they are described by suitable probability density functions $g_1(e_1)$, $g_2(e_2)$, …, $g_J(e_J)$, the distribution of the total error can be determined by using the expression:

$$g(e) = g_1(e_1) \otimes g_2(e_2) \otimes \ldots \otimes g_J(e_J) \tag{1.51}$$

where $\otimes$ denotes operation of the convolution [P1, J15]. Except for some simple cases, the mathematical operations necessary to execute operations accordingly with the expression (1.51) are sophisticated. Moreover, analytical descriptions of distributions of errors arising in real measurement instruments are often very difficult to obtain or even this is impossible. This property causes that the expression (1.51) is used mainly in theoretical considerations because of its little usefulness in practice to evaluate the inaccuracy of the measurement results.

Error analysis is often sufficient if one uses only standard deviations (or variances) to describe relationships between error distributions. Accordingly with Eq. (1.50), the variance of the total error is the following sum of variances of the partial errors:

$$\sigma^2 = \sigma_1^2 + \sigma_2^2 + \ldots + \sigma_J^2 \tag{1.52}$$

in the case if the partial errors are uncorrelated. For correlated errors, the relationship between variances can be generally described in the matrix form as follows [Y1, J6]:

$$\sigma^2 = \boldsymbol{\sigma}_{\mathrm{p}}^{\mathrm{T}} \mathbf{C} \boldsymbol{\sigma}_{\mathrm{p}} \tag{1.53}$$

where:

$$\boldsymbol{\sigma}_{\mathrm{p}} = \begin{bmatrix} \sigma_1 & \sigma_2 & \dots & \sigma_J \end{bmatrix}^{\mathrm{T}} \tag{1.54}$$

is the vector containing standard deviations of the partial errors. Matrix **C** is of the form:

$$\mathbf{C} = \begin{bmatrix} 1 & c_{1,2} & \cdots & c_{1,J} \\ c_{2,1} & 1 & \cdots & \\ \vdots & \vdots & \ddots & \vdots \\ c_{J,1} & c_{J,2} & \cdots & 1 \end{bmatrix} \tag{1.55}$$

where it is: $c_{i,j} = c_{j,i}$, $i, j = 1,\ldots, J$ are correlation coefficients.

1.4. Random model of single measurement result in application to algorithmic processing

The error definition (1.23) can be the basis for the determination of a random model of a single measurement result. After transformation Eq. (1.23), we obtain the expression:

$$y = \hat{y} + e \tag{1.56}$$

accordingly with which a true value y of a measured quantity is the sum of its estimate $\hat{y}$ and a realization of a random error e which has no systematic component in the sense of Eq. (1.16). Moreover, Eq. (1.56) means that the estimate contains the same error value as error e but with the opposite sign; thus, a description of probabilistic properties of the estimate can be obtained on the basis of a probability density function of the error.

The model (1.56) is the basis for all algorithmic processing applied in the reconstruction process that is performed in a sampling instrument. Let us denote as **R** the arithmetical operations connected with a reconstruction algorithm, which transform generally a series of n measurements results to one value of the reconstructed sample. Based on the model (1.56), one can write for the linear algorithms that it is:

$$\mathbf{R}(y_n) = \mathbf{R}(\hat{y}_n + e_n) = \mathbf{R}(\hat{y}_n) + \mathbf{R}(e_n) \tag{1.57}$$

The expression $\mathbf{R}(y_n)$ is a formula that describes the mathematical operations performed by the algorithm on a series of *n* true values of the measured quantity. Thus, if a sampling instrument is considered, this formulae describes one output result of the reconstruction algorithm, i.e. the true value $x(t_k)$ of the reconstructed sample at instant t_k. Realization of the formulae results in obtaining this value which, accordingly with Eq. (1.56), is the sum:

$$\mathbf{R}(y_n) = x(t_k) = \hat{x}(t_k) + e \tag{1.58}$$

where $\hat{x}(t_k)$ is the estimate of the reconstructed sample, *e* denotes the error of this estimate.

Based on Eqs. (1.57) and (1.58), one obtains the equation:

$$\hat{x}(t_k) + e = \mathbf{R}(\hat{y}_n) + \mathbf{R}(e_n) \tag{1.59}$$

which can be split into two expressions:

$$\hat{x}(t_k) = \mathbf{R}(\hat{y}_n) \tag{1.60}$$

and

$$e = \mathbf{R}(e_n) \tag{1.61}$$

The first expression generally describes mathematical operations carried out on the series of estimates of measurement results to obtain one estimate of the reconstructed sample. The second one (1.61) means that the same operations as in (1.60) are performed on realizations e_n of the error that burden the estimates. These realizations are taken from the same random population, which causes that the population of resultant error depends both on the primary population and coefficients of the algorithm.

In the case if the algorithm is a linear combination of constant coefficients and none of the coefficients has an extremely high value, the Central Limit Theorem [P1, Y1] is fulfilled, which means that the resultant population tends to a normal distribution. Taking into account that the realizations of partial errors are from the same distribution, the standard deviation of which is denoted as σ_p, one can write that it is:

$$\sigma = \sqrt{(a_1\sigma_\mathrm{p})^2 + (a_2\sigma_\mathrm{p})^2 + \ldots + (a_n\sigma_\mathrm{p})^2} = \sigma_\mathrm{p}\sqrt{a_1^2 + a_2^2 + \ldots + a_n^2} \tag{1.62}$$

where σ is the standard deviation of the resultant error that burdens the estimate of the reconstructed sample, a_1, a_2,..., a_n are coefficients of the algorithm.

The resultant error described by a normal distribution is symmetrical; thus, the uncertainty interval can be characterized only by one parameter that is the uncertainty u. In this case, the expanded uncertainty can be calculated on the basis of the standard deviation by multiplying its value by the coverage factor k [Y1], the value of which is equal to $k = 2$ for the normal distribution. Taking this into account and based on Eq. (1.62), the expanded uncertainty of the estimate at the output of the reconstruction algorithm in the form of linear combination of coefficients is described as follows:

$$U = 2\sigma = 2\sigma_{\mathrm{p}}\sqrt{a_1^2 + a_2^2 + \ldots + a_n^2} \tag{1.63}$$

1.5. Final remarks

The concept of creating means of mathematical description of the inaccuracy of the measurement result presented in this chapter is based on the definition of measurement error determined in a deductive way, which is derived from the analysis of the measurement process by quantization. This definition makes it possible to express the inaccuracy of the result in the form of a measurand interval, which is the sum of the measurand estimate and the uncertainty interval determined on the basis of a probabilistic description of the total measurement error. The error definition is also the starting point for obtaining a probabilistic model of the measurement result, which enables determining the interval expression of the final inaccuracy of algorithmic processing. The error model is a component of the model of the measurement result and it determines the composition of random measurement errors, thanks to which it is possible to analyze the propagation of various types of errors during algorithmic processing.

The most effective way to obtain the distribution of the total error is the Monte Carlo method, which can also be used when a non-linear processing of measurement signals is performed. In the case of algorithmic processing of a series of measurement data, the distribution of the total error is generally close to normal. Then the uncertainty interval is determined by one parameter, i.e. uncertainty that can be estimated from the standard deviation of the error distribution. If the total error distribution is not normal, the uncertainty of the total error can be calculated from the uncertainties of the partial errors using reductive interval arithmetic [J4, J6, J15], which also allows correlations between partial errors to be taken into account.

2. MATHEMATICAL FUNDAMENTALS OF SIGNAL RECONSTRUCTION

Generally, reconstruction, from the physical point of view, is treated as an inference about a cause of a knowledge about its result [M2, S6]. Therefore, such an indirect getting information about a physical reality is performed in two stages presented in Fig. 2.1.

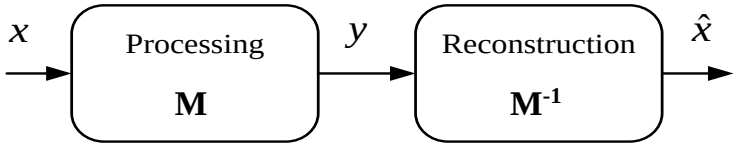

Fig. 2.1. The general structure ofreconstruction

Taking only physical quantities into account, the first stage from Fig. 2.1 is indirect observation of the quantity x by using the measurable quantity y with the assumption that the relation between y and x is known and generally described by a mathematical model $\mathbf{M}$. Thus, the first stage can be written as:

$$y = \mathbf{M}(x) \tag{2.1}$$

The second stage, that is the reconstruction, consists in solving the model $\mathbf{M}^{-1}$ inverse to $\mathbf{M}$ on the basis of measurement results of the quantity y. Operations performed in this stage result in obtaining the output quantity $\hat{x}$ which is an estimate of the observed quantity x. This stage can be described as:

$$\hat{x} = \mathbf{M}^{-1}(y) \tag{2.2}$$

The composition of Eqs. (2.1) and (2.2) leads to the expression:

$$\hat{x} = \mathbf{M}^{-1}\left[\mathbf{M}(x)\right] = x \tag{2.3}$$

according to which the output quantity $\hat{x}$ of the reconstruction chain from Fig. 2.1 is equal to the input (being reconstructed) quantity x. If one takes the metrological point of view into account, Eq. (2.3) means that the chain with reconstruction, as a whole, realizes functionality of the ideal measuring converter, the output signal of which $\hat{x}$ is equal to the input signal x in given measurement conditions.

2.1. General description of reconstruction algorithm

A measurement conversion is always connected with arising of errors; therefore, the reconstruction can be seen as elimination from the quantity y such errors which can be deterministically described and contained by model **M**. Random errors that burden the quantity y influence inaccuracy of the reconstruction. In the considerations presented in this book, it is assumed that the influence of random errors is minimized; thus, the output quantity $\hat{x}$ is treated as the estimate of the input quantity x in this sense.

Quantities x, y and $\hat{x}$ can be considered as signals, i.e., as varying over time t quantities that are carriers of information about another quantity called a measurand. Accordingly with the scheme of the sampling instrument presented in Fig.1.1, every sample of the signal $x(t)$ at the instant t_k is the measurand. Its estimate $\hat{x}(t_k)$ is calculated using a reconstruction algorithm on the basis of one or more quantized samples of the analog output signal $y(t)$. The sequence of these samples necessary to obtain one estimate $\hat{x}(t_k)$ creates the measurement window shown in Fig. 2.2.

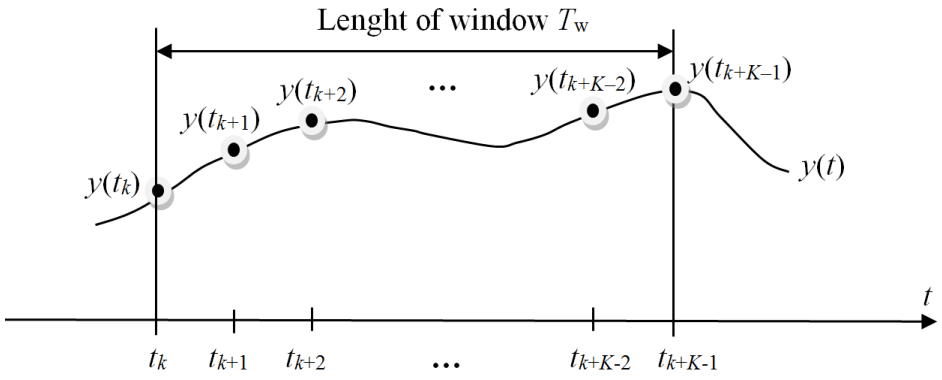

Fig. 2.2. Digital representation of a signal in the measurement window

Usually, the output signal $y(t)$ is represented by a sequence of equally spaced samples, which means that the distant between them is given by the sampling period T_s that is constant and for K samples in the window its length is $T_w = KT_s$. The window begins at the instant k interpreted as the number of the first sample in the window as well as the current number of the measurement window and it is: $k = 0,1,\ldots$. After a realization of a single reconstruction, the index k is increased by 1 and the windowis shifted one period T_s to the right. One should notice that in the case if the reconstruction is performed in real-time, all the calculations have to be ended before the window is shifted, i.e. in the time which is shorter than the sampling period T_s.

Generally, a reconstruction algorithm denoted **R** is a series of calculations performed on samples contained in the measurement window, which gives as the result the single estimate $\hat{x}(t_k)$ of the input signal sample, which is described as:

$$\hat{x}(t_k) = \mathbf{R}\{y(t_{k+i}), i = 0,1,\ldots,K-1\} \tag{2.4}$$

where k is the current number of the window, i = 0, 1,..., K-1 is the current number of the signal sample in the window.

The basic form of a reconstruction algorithm, resulting from expression (2.4), consists in writing it as a linear combination of the output samples and coefficients. The samples are measured on the principle of quatization, which results to obtaining estimates of the output samples. This means that the reconstruction algorithm can be written in the form of the equation:

$$\hat{x}(k) = a_0\hat{y}(k) + a_1\hat{y}(k+1) + \ldots + a_{K-1}\hat{y}(k+K-1) \tag{2.5}$$

in which the symbol t of time is omitted. In Eq. (2.5), $\hat{x}(k)$ denotes the estimate of the reconstructed value of the input signal sample at the instant t_k, $a_0, a_1, \ldots a_{K-1}$ are coefficients of the algorithm and $\hat{y}(k), \hat{y}(k+1), \ldots \hat{y}(k+K-1)$ are estimates of the quantized signal samples contained by the measurement window.

Describing the samples of the analog output signal as the vector:

$$\hat{\mathbf{Y}}_k = [\hat{y}(k) \quad \hat{y}(k+1) \quad \ldots \quad \hat{y}(k+K-1)]^{\mathrm{T}} \tag{2.6}$$

and the vector of coefficient as:

$$\mathbf{A} = [a_0 \quad a_1 \quad \ldots \quad a_{K-1}]^{\mathrm{T}} \tag{2.7}$$

where T denotes the transformation of the vector, one can write Eq. (2.5) in the following matrix form:

$$\hat{x}(k) = \hat{\mathbf{Y}}_k^{\mathrm{T}}\mathbf{A} \tag{2.8}$$

The vector of coefficients (2.7) of the reconstruction algorithm can be the same in the succeeding reconstruction instants k, which means that the coefficients in this vector are constant and the same for all succeeding windows. In this case, the number k of the window can be omitted and algorithm (2.5) is written in the simpler form:

$$\hat{x} = a_0\hat{y}(0) + a_1\hat{y}(1) + \ldots + a_{K-1}\hat{y}(K-1) \tag{2.9}$$

The number K of samples in the window depends on the kind of reconstruction algorithm. For a static reconstruction algorithm, the vector **A** reduces to one coefficient a_0 (the window contains only one sample), which for a linear static algorithm is constant. For a nonlinear static algorithm, values of a_0 depend on a working point on astatic characteristics of an analog part in a sampling instrument. If the characteristic is dependent on influence quantities, a_0 is a linear or nonlinear function of them [L1, P2].

For a dynamic reconstruction algorithm, the window contains more than one sample (for the simplest dynamic algorithms it is equal to 2) depending on that how many samples is needed to calculate one input estimate with required accuracy. The dynamic algorithm is linear if vector **A** is constant. If the coefficients change its values depend on time or influence quantities, the reconstruction algorithm can be considered as adaptive to actual measurement conditions [M7]. One can point to further ways of the algorithm adaptation to the reconstruction requirements connected with the fact that the number of samples in the window and the sampling period T_s can change and in some cases the input signal can be sampled irregularly [G2]. Moreover, a group of nonlinear algorithms one can be pointed that perform operations on multiplicative forms of samples (for example, the algorithm used for calculation of the effective value of a voltage processes squared samples) [J9].

Reconstruction algorithms can be realized by a processor or by an artificial neural network [J16]. The algorithm in the form of a program needs a mathematical description of the inverse model $\mathbf{M}^{-1}$ (see Eq. 1.2) as one or more equations, while a neural network creates the algorithm itself on the basis of learning data. Independently of the algorithm form, execution of a reconstruction process results in the same estimate $\hat{x}(k)$ for the same input data, although its value and inaccuracy depend on properties of the used algorithm.

The signal reconstruction can be carried out in batch mode if it is performed after recording of a series of measurementresults or in real-time [R7, S1]. The algorithms presented in the book are dedicated to realize them in real-time but the described methods of analysis of reconstruction errors can be used in both modes of the reconstruction realization.

2.2. Decomposition of reconstruction process

Propagation of a signal from the input to the output of the sampling instrument is connected to the arising errors in all elements of the reconstruction chain. Every error, which can be described deterministically (often called the systematic error [J12, R8, R10, Y2]) and contained by the analog conversion model **M**, can be eliminated from the signal $y(t)$ using the reconstruction. This means that signal reconstruction can be seen as a correction process of systematic errors that burden the signal $y(t)$ [J9]. The realization of a reconstruction algorithm consists in solving equations inverse to the equations that describe the model **M**.

The general model **M** should contain mathematical descriptions of static and dynamic properties of the analog conversion in the sampling instrument. Because of nonlinearities, representation of this model by one equation is usually a very difficult problem, so there is a need to present the model in a decomposed form to solve the partial equations by a processor. But in some cases if one uses the neural reconstruction, such a decomposition is not necessary [M10]. However, independently of the reconstruction method, the decomposition is indispensable for analysis of the errors that burden the output estimate. The decomposition enables the extraction of partial errors and analysis of their propagation through the succeeding elements of the sampling instrument. It means that the decomposition is the basis for the inaccuracy evaluation of the reconstructed signal samples [J9].

The decomposition of the general model **M** consists in presenting this model as a system of equations in a general case nonlinear. From the point of view of the propagation of errors, every partial equation should describe only the static or dynamic properties of the analog converter and represents one partial model. For varying over time signals, the static properties are described by equations not dependent on the signal variations, while the equations describing the dynamic properties contain expressions which depend on the signal variations [J9].

After decomposition, the general model **M** of the analog conversion can be written as a chain of I equations:

$$\begin{aligned} u_1 &= f_1(x) \\ u_2 &= f_2(u_1) \\ &\vdots \\ y &= f_i(u_{i-1}) \end{aligned} \tag{2.10}$$

where: x and y are the input and output signals of partial conversions, u_1, u_2,…, $u_{i\text{-}1}$ are the go-between signals introduced for the objectives of the decomposition.

Carrying out the reconstruction needs to solve the inverse model $\mathbf{M}^{-1}$. In the case where it is given as the chain of equations (2.10), the reconstruction consists of the successful solution of the appropriate equations inverse to these in the chain (2.10) [J9] and performed in the inverse order. These operations can be written as:

$$\begin{aligned} \hat{u}_{i-1} &= f_i^{-1}(y) \\ &\vdots \\ \hat{u}_1 &= f_2^{-1}(\hat{u}_2) \\ \hat{x} &= f_1^{-1}(\hat{u}_1) \end{aligned} \tag{2.11}$$

where $\hat{x}$ is the estimate of the input signal, $\hat{u}_{i-1}$, ..., $\hat{u}_1$ are estimates of go-between signals in the system of equations (2.10).

After decomposition, the total analog conversion is presented as a chain of partial analog converters, while the reconstruction as the chain of algorithms performing partial reconstructions. The interdependence of the analog conversions and the suitable algorithms of reconstruction is shown in Fig. 2.3 which is the graphical presentation of Eqs. (2.10) and (2.11). In this figure, the suitable analog converters and partial reconstruction algorithms create couples in the mathematical sense resulting from these equations. However, another interpretation of these couples is important. Namely, from the error point of view, an analog conversion is a source of systematic errors that are eliminated from the reconstructed signals by the suitable algorithms. After the whole reconstruction process, all systematic errors that burden the signal *y* are corrected.

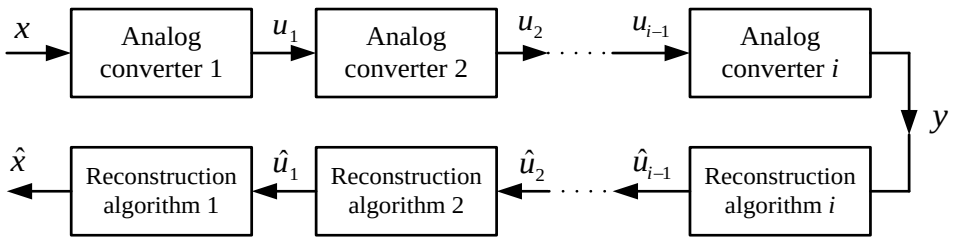

Fig. 2.3. General structure of the decomposed reconstruction chain

The decomposed model from Fig. 2.3 consists of two kinds of partial model that describe static or dynamic properties of the analog conversion, responsibly. Dynamic partial models contain elements that depend on derivatives of the signal, which means that their mathematical models have the forms of ordinary or partial differential equations [L1]. The static partial models are devoid derivatives and describe relations between the output and the input with taking into account all quantities that influence conversion of the input signal.

With assumption that the general model is given in the form of a non-linear differential equation, the decomposition consists in separation of the analog conversion model on two or more partial models that describe exclusively static or dynamic properties. In the literature, the most common point of view on the decomposition consists in using two kinds of elements: nonlinear static NS and linear dynamic LD. The structure LD-NS is called the Wiener model [H2] and NS-LD is known as the Hammerstein model [W2]. In some cases, to describe complex dynamic systems, Wiener-Hammerstein models (LD-NS-LD) and Hammerstein--Wiener models (NS-LD-NS) are also used [G3, S7] and, in addition, multi-element models built as the Volterra series [M11]. The general rules of error analysis are independent of the kind of the decomposed model. Taking this into account, the analysis method of the reconstruction errors described in this book is considered for the Wiener model that is suitable for the sampling instrument taken as exemplary.

To begin detailed considerations on the decomposition procedure, let us assume that the general properties of the analog conversion are described by the ordinary differential equation:

$$a_n y^{(n)} + a_{n-1} y^{(n-1)} + \ldots + a_1 \dot{y} + y = S(x) \tag{2.12}$$

where$x$ is the input signal, y – is the output signal of the analog conversion (both are varying over time), a_1, ..., a_n are constant coefficients, $S(x)$ is the function that contains expressions without derivatives denoted as $y^{(n)},\ldots,\dot{y}$. The function $S(x)$ describes static properties of the analog conversion and in a general case is nonlinear, while expressions with derivatives describe dynamic properties of the conversion.

The decomposition procedure used for the separation of static and dynamic properties of the general model is performed in several steps. In the first step, one should extract the static properties by zeroing all the derivatives in the general model. After that, for Eq. (2.12), one obtains the following static equation:

$$y = S(x) \tag{2.13}$$

The basic assumption of the decomposition procedure is that the equations representing dynamic or static properties have to be ideal in the sense of Eq. (1.3). It means that, after zeroing derivatives, the dynamic equation has the form of the equation, the static transfer function of which equals 1. To achieve this effect, one should define the new auxiliary variable:

$$u = S(x) \tag{2.14}$$

After introduction Eq. (2.14) to Eq. (2.12), we obtain the system of two equations:

$$u = S(x) \tag{2.15}$$

$$a_n y^{(n)} + a_{n-1} y^{(n-1)} + \ldots + a_1 \dot{y} + y = u \tag{2.16}$$

where the first equation (2.15) is dynamically ideal (there are no derivatives in it) and represents static properties, while the second is statically ideal (after zeroing derivatives $y = u$) and describes dynamic properties of the analog conversion. For the decomposed conversion model, the reconstruction of the input quantity consists in solving equations inverse to partial equations (2.15) and (2.16) and in the inverse order if the static equation (2.15) is nonlinear. Thus, the reconstruction process is described in this case by the system of two equations:

$$\hat{u} = a_n y^{(n)} + a_{n-1} y^{(n-1)} + \ldots + a_1 \dot{y} + y \tag{2.17}$$

$$\hat{x} = S^{-1}(\hat{u}) \tag{2.18}$$

The whole processing, consisting of two partial analog conversions and suitable reconstructions, is graphically presented in Fig. 2.4.

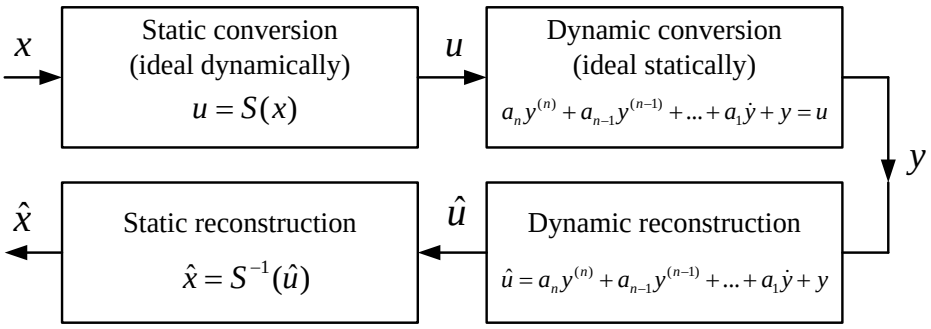

Fig. 2.4. Illustration of partial conversions and reconstructions for the analog conversion modeled by the equations from (2.15) to (2.18)

It should be noticed that the presented decomposition of the general model of the analog conversion corresponds to the Hammerstein model that is used not only for measuring chains but also for description of others systems such as control systems, in which actuators characterizing nonlinear properties (servomechanisms, solenoid valves etc.) are used.

In some cases, physical conditions of the analog conversion cause it should be described by the system of equations:

$$a_n u^{(n)} + a_{n-1} u^{(n-1)} + \ldots + a_1 \dot{u} + u = x \tag{2.19}$$

$$y = S(u) \tag{2.20}$$

which are the same as expressions (2.15) and (2.16) but their order is inverse. In this situation, the reconstruction consists in solving, at first, the static inverse equation:

$$\hat{u} = S^{-1}(y) \tag{2.21}$$

Next, the dynamic reconstruction is carried out, which consist in solving the differential equation:

$$\hat{x} = a_n \hat{u}^{(n)} + a_{n-1}\hat{u}^{(n-1)} + \ldots + a_1 \hat{u} + \hat{u} \tag{2.22}$$

The chain of operations (2.19) and (2.20) performed by the analog chain and reconstruction algorithms described by equations (2.21) and (2.22) are presented in Fig. 2.5.

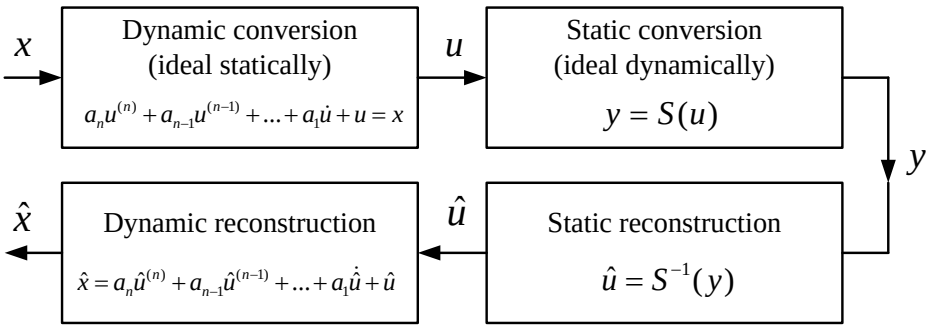

Fig. 2.5. Scheme of the chain composed of partial analog conversions described by equations (2.19), (2.20) and suitable reconstructions by (2.21), (2.22)

The structure of the analog conversion that is described first by a linear dynamic equation and then by a nonlinear static one, corresponds to the Wiener model [G3]. Such a model can be used for a sensor working in dynamic conditions (the sensitive element of the sensor is characterized by an inertia) described by a linear differential equation, while the static characteristic of the sensor is nonlinear. It should be noticed that in the most often cases the remaining elements of the analog converter, such as measuring amplifiers, sample and hold circuits and AD converters are so fast that their dynamic properties do not significantly affect on the dynamics of the whole conversion [J14]. This applies to the exemplary instrument, in which the temperature sensor Pt100, described by the Wiener model, is used.

In a general case, the static transfer function $S(x)$ can be written in the form:

$$y = S(x, w_1, w_2, \ldots, w_s) \tag{2.23}$$

which means that the output signal is dependent not only on the input signal x but also on the influence quantities w_1, w_2, …, w_s, where s is the number of all these quantities. In many practical situations, Eq. (2.23) is nonlinear, which means that is a difficult

problem to describe it in analytical form as one equation or even as a system of equations [M10, P2]. One of the solutions that can be used of this case consists in writing the inverse static transfer function:

$$x = S^{-1}(y, w_1, w_2, \ldots, w_s) \tag{2.24}$$

as a system of linear equations obtained as an effect of the linear segmental approximation. Coefficients of these equations can be stored in microprocessor memory, which enablesa fast execution of the static reconstruction algorithm [R10]. The other solution consists in the application of artificial neural networks to realize reconstruction [R5]. The network builds the reconstruction algorithm itself on the basis of measuring data that must be delivered to its input during a teaching process.

All influence quantities must be measured, which means that their values used for solving the inverse model (2.24) should be obtained as estimates by using suitable measuring chains. The scheme of the static reconstruction in the case where only one influence quantity is contained by the static transfer function is presented in Fig. 2.6.

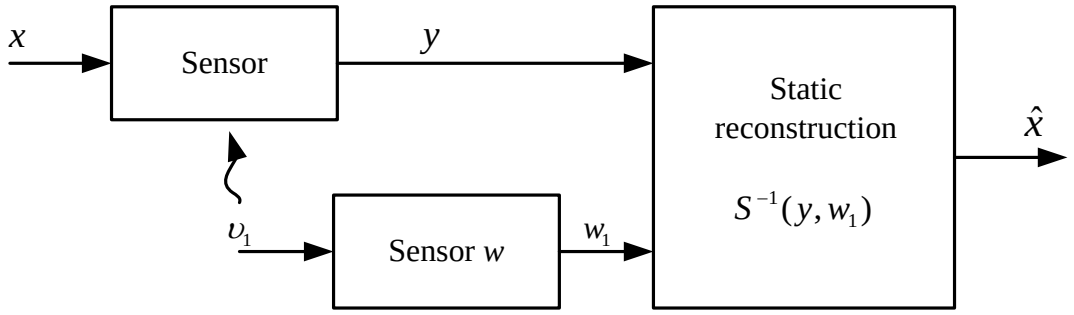

Fig. 2.6. Scheme of static reconstruction performed accordingly with Eq. (2.24) for the single influence quantity w_1

Usually, the influence quantities are static, which means that their measuring chains are described by static equations. But some of these quantities can be dynamic so they need more than one sample to perform reconstruction. In such cases, the reconstruction process should be considered as a parallel multi-reconstruction, in which many dynamic reconstructions are performed at the same time.

The decomposition does not always lead to obtaining linear dynamic equations characteristic for Hammerstein and Wiener models. Such a case occurs if, for example, the general model is given by the following 1st-order equation:

$$\frac{\mathrm{d}y}{\mathrm{d}t} + y^2 = \frac{\mathrm{d}x}{\mathrm{d}t} + x^2 \tag{2.25}$$

Denoting the new variable as:

$$u_1 = x^2 \tag{2.26}$$

and introducing it into Eq. (2.25), we obtain the following:

$$\frac{\mathrm{d}y}{\mathrm{d}t} + y^2 = \frac{1}{2\sqrt{u_1}} \frac{\mathrm{d}u_1}{\mathrm{d}t} + u_1 \tag{2.27}$$

To make Eq. (2.27) statically ideal, we should introduce to it another variable:

$$u_2 = y^2 \tag{2.28}$$

which enables writing Eq. (2.27) in the following form:

$$\frac{1}{2\sqrt{u_2}} \frac{\mathrm{d}u_2}{\mathrm{d}t} + u_2 = \frac{1}{2\sqrt{u_1}} \frac{\mathrm{d}u_1}{\mathrm{d}t} + u_1 \tag{2.29}$$

that is nonlinear.

Linking equations (2.26), (2.29), and (2.28) in a chain, one obtains the decomposed model of the general equation (2.25) as the system of the following three equations:

$$u_1 = x^2 \tag{2.30}$$

$$\frac{1}{2\sqrt{u_2}} \frac{\mathrm{d}u_2}{\mathrm{d}t} + u_2 = \frac{1}{2\sqrt{u_1}} \frac{\mathrm{d}u_1}{\mathrm{d}t} + u_1 \tag{2.31}$$

$$y = \sqrt{u_2} \tag{2.32}$$

Everyone of them is nonlinear and, accordingly with the basic assumption, statically or dynamically ideal.

Taking into account that the signal reconstruction consist in calculation of the input signal estimate based on the estimate of the output signal, the order of solving the equations inverseto (2.30), (2.31) and (2.32) is as follows:

$$\hat{u}_2 = \hat{y}^2 \tag{2.33}$$

$$\frac{1}{2\sqrt{\hat{u}_1}} \frac{\mathrm{d}\hat{u}_1}{\mathrm{d}t} + \hat{u}_1 = \frac{1}{2\sqrt{\hat{u}_2}} \frac{\mathrm{d}\hat{u}_2}{\mathrm{d}t} + \hat{u}_2 \tag{2.34}$$

$$\hat{x} = \sqrt{\hat{u}_1} \tag{2.35}$$

The analysis of the reconstruction process from the error point of view let us to draw the conclusion that solutions of Eqs. (2.33) and (2.35) result in correction of the systematic static errors introduced by the nonlinear analog conversion modeled

by Eqs. (2.30) and (2.32), respectively. Correction of the dynamic error caused by the dynamic properties of the analog converter described by Eq. (2.31) is performed by solving Eq. (2.34) in relation to the signal $\hat{u}_1$.

As result of the presented considerations, after the decomposition, the analog conversions and the suitable partial reconstructions have to be treated jointly. For the model described recently, the partial models of the analog conversions and the suitable reconstruction algorithms create couples which are presented in Fig. 2.7.

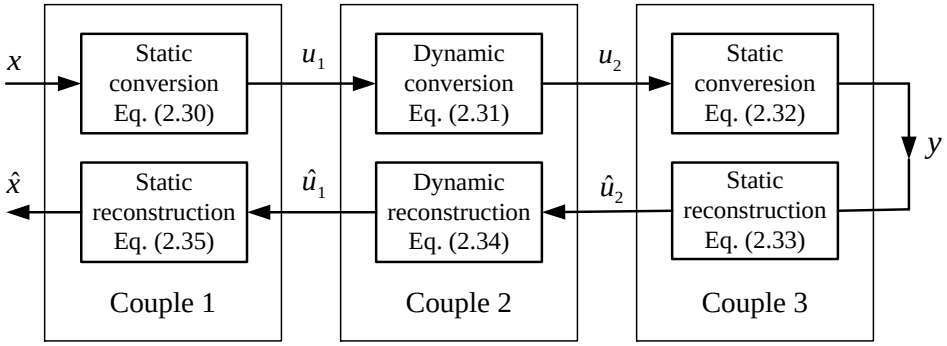

Fig. 2.7. Relations between analog conversions and reconstructions for the general model (2.29)

Accordingly with Fig. 2.7, the systematic errors that arise during the partial analog conversions are corrected by suitable reconstruction algorithms. If the reconstruction is ideal, the errors are eliminated from the measurement results. In the real sampling instrument these errors cannot be fully eliminated because on non-idealities both of partial conversion models and the suitable reconstruction algorithms. These properties of the reconstruction process cause the output estimate to be burden by rests of the not corrected systematic errors that are called the reconstruction errors and can be seen as resultant effects of partial analog conversions and suitable partial reconstructions. This means that from the error propagation point of view, every couple in Fig. 2.7 can be treated as one source of the specific error called the reconstruction error. Moreover, all random error that arise during the analog conversion can be described suitably as input error of the algorithm chain. Taking the above into account, one can conclude that the error analysis of the signal reconstruction can be considered by the prism of properties of the reconstruction algorithms that processes quantization results burdened by the errors arising in the analog part of the sampling instrument and the errors connected with non-ideal realization of the reconstruction algorithms.

2.3. Final remarks

The signal reconstruction consist in solving the inverse mathematical model to this one that describes the analog signal conversion in the sampling instrument. From the error analysis point of view, the inverse model should be decomposed into partial models describing static or dynamic properties of the analog conversion. The decomposition enables identification of specific static and dynamic errors, as well as description of the error propagation from the input to the output of the sampling instrument.

The sampling instrument is defined as the composition of tree parts performing the analog conversion, the AD conversion and digital reconstruction of samples of the input signal (see Chapter 1). It means that the output signal represents the reconstructed input signal in the discrete form, i.e. as a series of estimates of instantaneous values (samples) of the input signal. This book deals with the real-time work of the instrument, which means that it delivers at its output the reconstructed samples with a constant frequency. Such a work determines the necessity of performing the reconstruction algorithms in the time between succeeding sampling instants. This causes the reconstruction algorithms have to have as simpler form as possible with the assumption that the uncertainty of the reconstructed samples is at an acceptable level.

3. STATIC SIGNAL RECONSTRUCTION

Accordingly with considerations from Chapter 2, static reconstruction is defined as solving equations that describe an inverse model of static properties of all analog elements in the sampling instrument. Taking into account that all these elements are treated here as one whole, called the analog converter, the static properties of it are described by a static transfer function. It is one of two expressions creating the general Wiener or Hammerstein model, which differ from each other only in succession of occurrence static or dynamic partial transfer functions.

Independently of the general model, the static transfer function is generally described by the multidimensional equation (2.23) that is considered in this chapter in two forms: one-dimensional and two-dimensional.

The one-dimensional static characteristic is described by the equation:

$$y = S(x) \tag{3.1}$$

which is nonlinear in a general case. The static reconstruction consists in solving equation inverse to (3.1) on the basis of the measurement result of the output signal *y*. This operation can be written as:

$$\hat{x} = S^{-1}(\hat{y}) \tag{3.2}$$

where $\hat{x}$ and $\hat{y}$ are estimates of the input and output signals, respectively. Interdependence of both stages of the input signal processing, described by Eqs. (3.1) and (3.2), is presented in Fig. 3.1.

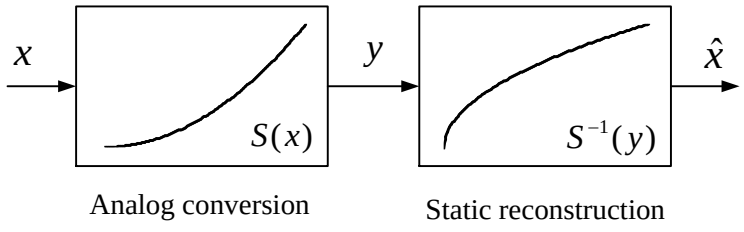

Fig. 3.1. Conception of static signal processing in the measuring chain with reconstruction

Accordingly with the scheme from Fig. 3.1, in the first stage of the processing, the analog input signal x is converted to the analog signal y that is measured. In the second stage, the reconstruction of the input signal value is performed, which consists in determining the estimate $\hat{x}$ of the input signal x on the basis of the inverse static characteristic of the analog converter and the measurement result $\hat{y}$.

The static characteristic of the analog converter has to be continuous, monotonic and the first derivative of this characteristic has to be continuous, too, and not equal to zero. For these properties, it is possible to determine the unequivocal inverse characteristic $S^{-1}(y)$ that is the basis of the determination of a static reconstruction algorithm that is performed by a processor as a program or by a neural network. Analytical form of the algorithm, consisting of calculations executed on measured data and coefficients stored in the processor memory, has to be prepared by a programmer, while a neural network builds the algorithm itself. It is done during a learning process on the basis of measurement data obtained as an effect of an identification of the static characteristic [R6, S7, O2, L4].

In practice, static characteristics of analog converters depend on quantities influenced their measurement properties. In such cases, the static characteristics of the analog converter are described by the multidimensional function, as a rule nonlinear. In this chapter, a two-dimensional static characteristic is considered, which can generally be described as:

$$y = S(x, \upsilon) \tag{3.3}$$

where υ denotes an influence quantity. In this case, the reconstruction consist in solving the inverse function:

$$\hat{x} = S^{-1}(\hat{y}, \hat{\upsilon}) \tag{3.4}$$

in which all dashed symbols are estimates (measurement results) of suitable quantities. This means that both the output signal and the influence quantities have to be measured with suitably low inaccuracy.

There are many mathematical tools which can be used to describe the inverse nonlinear static characteristics [M4] but the considerations in this chapter focus only on two methods of their approximation. The first one, analytical method, consist in application of the segmental linear approximation which best of all fulfills requirements specific for the signal reconstruction in real-time by using microcontrollers. The second method applies an artificial neural network to perform the reconstruction algorithm. The presented methods, selected as the numerically simplest, can be also seen as representative for all approximation methods of inverse static characteristics used for the reconstruction if one takes error analysis into account.

Generally, to determine an approximation of a static inverse characteristic for reconstruction purposes, one should first identify this characteristic. Next, based on identification results, one calculates parameters of the inverse approximation, which are stored in a microcontroller non-volatile memory. The quickest reconstruction algorithms are based on linear approximations, the parameters of which are stored in look-up tables [S4].

The inverse model can be given in an analytical form that is obtained as an effect of inversion of the analog conversion model or can be determined as a result of an identification process. Analytical or a neural approximation of the inverse model is the basis of the static reconstruction algorithm. Another way of obtaining these approximations consists in direct use of identification data to determine their parameters. Both ways are considered in this book.

3.1. Exemplary sampling instrument

To make further considerations closer to problems which happen in practice, the description and error analysis of the static reconstruction is presented on an example of the sampling instrument presented in Fig. 3.2.

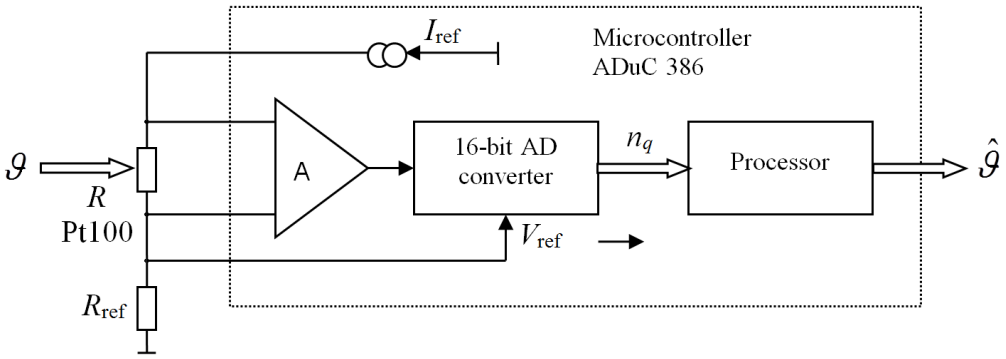

Fig. 3.2. Exemplary sampling instrument that applies the platinum sensor Pt100 and the micro-controller ADuC386 to perform reconstruction of the temperature signal

The input temperature ϑ changing in the range from 0 to 100°C is converted to the voltage V_R by the Pt100 sensor [Y4], the resistance of which is indicated as R. The sensor is connected in series with the reference resistor R_{ref}, the resistance of which at the nominal environmental temperature $\vartheta_{0env} = 25$°C is $R_{0ref} = 5.1253$ kΩ. Both resistors are supplied from the current source $I_{ref} = 400$ μA that is a part of the ADuC386 microcontroller [Y6]. The voltage drop across the resistor R_{ref} is used as the reference voltage V_{ref} of the 16-bit analog-to-digital converter (ADC), which

causes the drift of the I_{ref} does not influence the inaccuracy of the converter indications. The V_R voltage drop is introduced to the input of amplifier A working with the amplification coefficient $k_V = 32$. The amplifier output voltage is sampled and quantized by the AD converter which, together with the sensor and the amplifier, forms the analog converter. On the basis of the quantization results n_q and parameters of the inverse static characteristic, the estimate $\hat{\vartheta}$ of the input temperature is calculated accordingly with an one- or two-dimensional reconstruction algorithm. In this second case, the environmental temperature is measured using the additive AD converter of the microcontroller.

The characteristic of sensor Pt100 is nonlinear and it can be described by the polynomial:

$$R \cong R_0\left[1 + \alpha(\Delta\vartheta) + \beta(\Delta\vartheta)^2\right] \tag{3.5}$$

where R is the sensor resistance equal to $R_0 = 100.0\ \Omega$ at the input temperature $\vartheta_0 = 0^{\text{o}}\text{C}$, $\Delta\vartheta = \vartheta - \vartheta_0$, ϑ denotes the input temperature, α and β are constant coefficients, the values of which are [Y5]:

$$\alpha = 3.9083 \cdot 10^{-3\text{o}}\text{C}^{-1},\ \beta = -5.775 \cdot 10^{-7\text{o}}\text{C}^{-2} \tag{3.6}$$

With assumption that all elements of the analog converter are stable, i.e. their characteristics do not change in time, and they are not dependent on influence quantities, the static reconstruction problem can be treated as one-dimensional. It means that the reconstruction consists in solving the inverse model describing the relations between the indication n_q and the input temperature ϑ. The reconstruction procedures considered here are based on two approximations of the inverse characteristic: analytical and neural.

Properties of elements of real analog converters depend on influence quantities, mainly on the environmental temperature in which a sampling instrument works. In the case if only one influence quantity is taken into account, the reconstruction problem can be investigated as two-dimensional, which means that the inverse model must contain dependencies of the reconstructed quantity on the ADC indication and the influence quantity. For the exemplary converter, we assume that the reference resistor R_{ref} depends on the environmental temperature ϑ_{env}. In this case, the indication n_q and the temperature ϑ_{env} are the input quantities of the inverse model. Such a reconstruction problem is considered in Sections 3.4 and 3.5 for the analytical and the neural reconstruction, respectively.

3.2. One-dimensional analytical static reconstruction

3.2.1. Linear segmental approximation of static inverse characteristic of sensor

Properties of the linear segmental approximation are considered in this chapter for the Pt100 sensor applied in the exemplary instrument. The static characteristic (3.5) of the sensor can generally be written as $R = S(\vartheta)$; thus, the inverse characteristic of it is:

$$\vartheta = S^{-1}(R) \tag{3.7}$$

where ϑ is the reconstructed (input) temperature and R is the sensor resistance. After expanding the function (3.7) into the Maclaurin series for the temperature ϑ_p, we obtain the expression that for two initial terms takes the form:

$$\vartheta \cong \vartheta_\mathrm{p} + \frac{\partial S^{-1}(R)}{\partial R}\mathrm{d}R \cong \vartheta_\mathrm{p} + D\left(\vartheta_\mathrm{p}\right)\Delta R \tag{3.8}$$

With assumption that the series is determined only in selected points called nodes, the expression (3.8) describes the linear segment that approximates the inverse function (3.7) in any node. For node number N, the segment can be described as:

$$\vartheta_\mathrm{app} = \vartheta(N) + D(N)\cdot\left[R - R(N)\right] \tag{3.9}$$

where ϑ_app is the temperature calculated on the basis of the resistance value R. Parameters $\vartheta(N)$, $D(N)$ and $R(N)$ of the approximation are calculated for every node N on the basis of the static characteristic (3.5).

The exemplary characteristic inverse to (3.5) and approximated by 4 segments linking 5 nodes numbered from $N = 0$ to 4 is presented in Fig. 3.3.

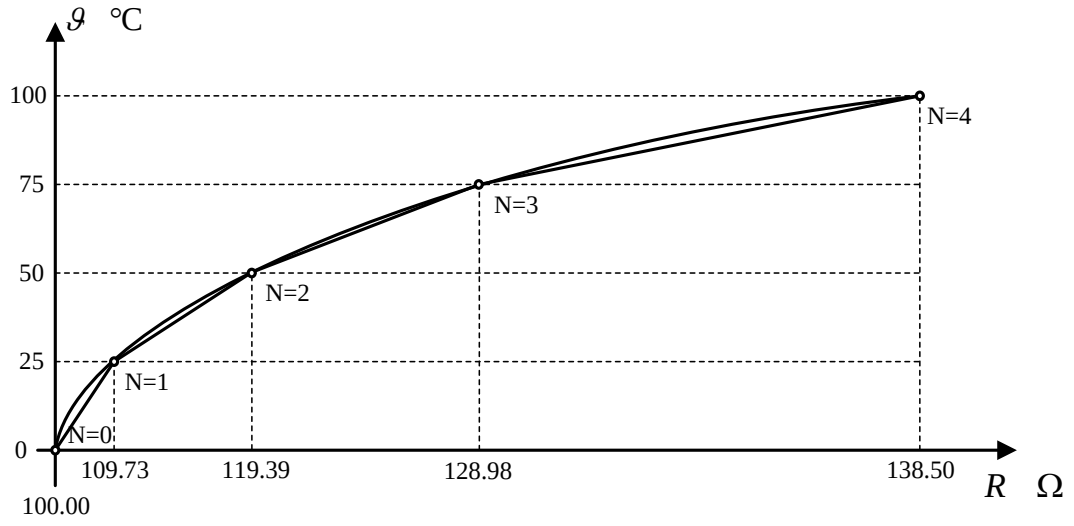

Fig. 3.3. Graphical presentation of the linear segmental approximation of the inverse characteristic of the Pt100 sensor

Some forms of the static reconstruction algorithm can be performed in a relatively short time if the distance between nodes is the same as it has been taken for the approximation presented in Fig. 3.3. For the distance $\Delta\vartheta$ equal to 25°C, the temperature in the nodes takes the values described by the expression:

$$\vartheta(N) = \vartheta(\Delta\vartheta \cdot N) = \vartheta(25 \cdot N) \quad \text{for } N = 0,1, ..., N_{\text{nod}} - 1 \tag{3.10}$$

where N_{nod} is the total number of nodes and $N_{\text{nod}} = 5$ in the case considered. As the resistance in node N is:

$$R(N) = R[\vartheta(N)] \tag{3.11}$$

the inclination coefficient of every segment is calculated as:

$$D(N) = \frac{\vartheta(N+1) - \vartheta(N)}{[R(N+1) - R(N)]} \tag{3.12}$$

The values of the approximation parameters, calculated on the basis of equations from (3.10) to (3.12), are contained in the Tab. 3.1.

Table 3.1

Parameters of the segments calculated for the 5-node linear approximation determined for the exemplary inverse characteristic of the sensor Pt100, N is the node number, $D(N)$ – the inclination coefficient (3.12)

N	0	1	2	3	4
$\vartheta(N)$°C	0	25	50	75	100
$R(N)$ Ω	100.0000	109.7347	119.3971	128.9874	138.5055
$D(N)$°C/Ω	2.568144	2.587330	2.606806	2.626576	

Experiment 3.1. Let us determine the distribution of the approximation error of the first segment described by the parameters contained in the Tab. 3.1. This error is defined as the difference between the input temperature ϑ and the temperature ϑ_{app} calculated on the basis of the equation (3.9). The histogram of the error values, obtained by using Monte Carlo method with the assumption that every value of the input temperature from 0 to 25°C is of the same probability, is shown in Fig. 3.4a.

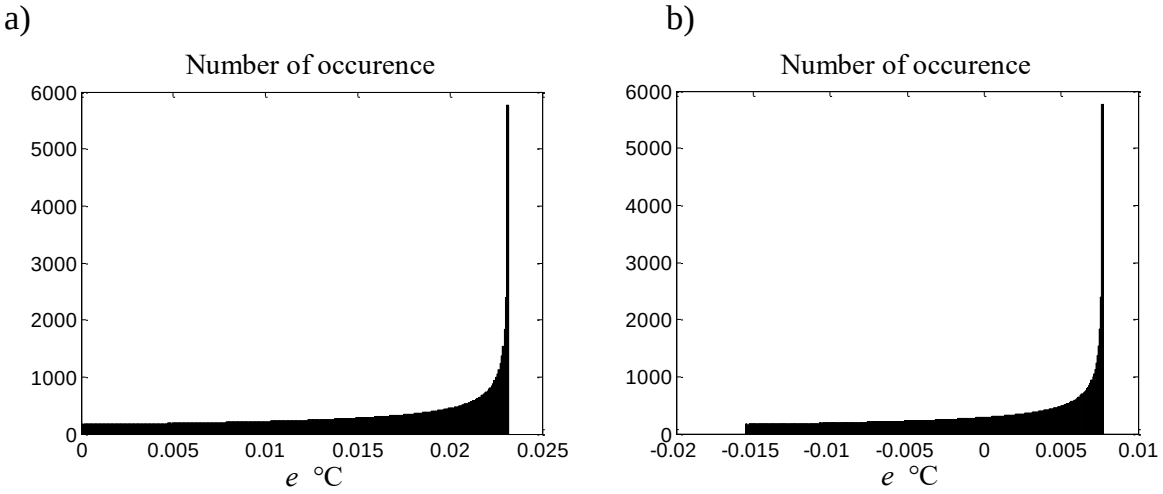

Fig. 3.4. Histograms of the approximation error of the first segment: a) the mean value of the error is equal to μ = -0.0154°C because it contains the systematic component, b) the systematic component is eliminated by adding the correction c_s = -0.0154°C to the reconstruction result, in this case μ = 0.0°C

The set of error values presented in Fig. 3.4a as the histogram contains the systematic component μ = - 0.0154°C that has been calculated as the mean value of the set. This component can be reduced to zero by subtracting this value from every error value. Accordingly with the error definition used in this book, this operation is equivalent to addition of this mean value to every value of the reconstructed temperature as a correction c_s. The histogram of the error obtained in the same way as in Experiment 3.1 but with using such a correction is shown in the Fig. 3.4b.

The values of the corrections c_s are different for all segments (nodes). They are calculated in the same way as described above and presented in the Tab. 3.2.

Table 3.2

Corrections of the reconstruction temperature, which are calculated as the mean values of the error distributions for the linear approximation of the exemplary sensor characteristic, N – node number

N	0	1	2	3	4
c_s°C	-0.0154	-0.0156	-0.0157	-0.0158	-

Adding the correction to the reconstructed result causes a suitable shifting of the approximating segment. As it results from the histogram presented in Fig. 3.4b, this operation decreases the error values about twice, which means that the shifting of the segments is the effective and simple manner of decreasing values of the approximation error. If all segments of the inverse characteristic are shifted accordingly with the values contained in Tab. 3.2, the global approximation error has a systematic component close to zero. This property is shown in Fig. 3.5 which

presents the deterministic characteristic of the global approximation error (a) and its distribution in the form of the histogram (b). This histogram has been obtained in the same way as described in Experiment 3.1 with the difference that the input temperature changes in the entire range from 0°C to 100°C.

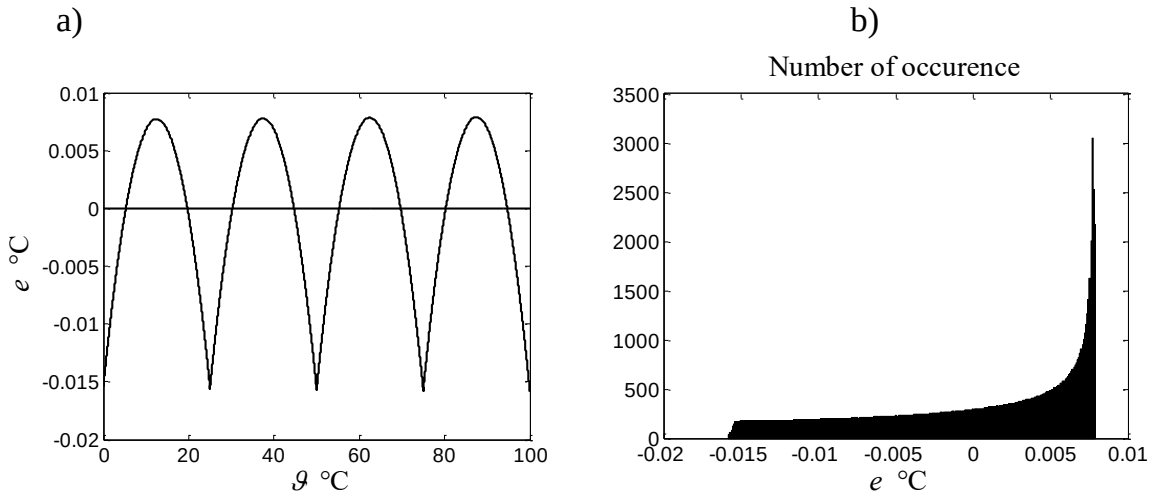

Fig. 3.5. a) Deterministic characteristic of the approximationerror of the inverse characteristic of the sensor as the function of the inputtemperature, b) histogram of the global approximation error, the standard deviation of which is $\sigma_{app} = 7.2 \cdot 10^{-3}$°C

3.2.2. One-dimensional static reconstruction algorithm

In the previous chapter, the principle of the linear segmental approximation considered in this book has been presented as an example of the inverse characteristic of the Pt100 sensor. To perform the static reconstruction using the exemplary instrument, it is necessary to approximate the inverse static characteristic of the whole analog converter as the part of the instrument. The converter consists of the sensor, the amplifier, and the AD converter; thus, the inverse characteristic is a relation between the quantization result n_q (the ADC indication) and the reconstructed input temperature. In this case, the reconstruction equation in the analytical form based on the linear segmental approximation (3.9) can generally be written as:

$$\hat{\vartheta} = a(N)\left[n_q - n_q(N)\right] + b(N) \tag{3.13}$$

where $\hat{\vartheta}$ denotes the estimate of the input temperature determined with the assumption that the mean value of the approximation error burdening the estimate is equal to 0. The inverse static characteristic in the form of Eq. (3.13) is made up of the set of $N_{seg} = N_{nod} - 1$ segments, N_{nod} is the number of all nodes, $n_q(N)$ is the indication, $a(N)$, $b(N)$ are constant coefficients in node N, $N = 0, 1, ..., N_{seg}$.

The determination of $a(N)$ and $b(N)$ has to be carried out beginning from the description of the indication n_q which is equal to the number of quanta obtained in the output of the AD converter. The value of the ADC quantum is generally given by the equation:

$$q = \frac{V_{\text{ref}}}{N_q} \tag{3.14}$$

where N_q is the maximum number of quanta which may occur in the ADC output, V_{ref} is the reference voltage obtained in the exemplary instrument using the reference resistor R_{ref}. Based on the scheme from Fig. 3.1, we have the following:

$$V_{\text{ref}} = I_{\text{ref}} R_{\text{ref}} \tag{3.15}$$

where I_{ref} is the current delivered by the reference source built-up in the microcontroller. Taking Eq. (3.15) into account, one can write Eq. (3.14) in the form:

$$q = \frac{I_{\text{ref}} R_{\text{ref}}}{N_q} \tag{3.16}$$

The voltage drop across the resistance R of the sensor is:

$$V_{\text{in}} = I_{\text{ref}} R \tag{3.17}$$

This voltage is introduced to the input of the amplifier, the amplification coefficient of which is denoted as k_V. The output voltage $k_V V_{\text{in}}$ of the amplifier is quantized by the AD converter, which means that, accordingly with Eq. (1.22), the number of quanta assigned to the quantized value is determined accordingly with the expression:

$$n_{\text{q}} = \text{ent}\left[\frac{k_V V_{\text{in}}}{q} + 0.5\right] \tag{3.18}$$

where the symbol “ent” denotes the function entier which is equal to the integer value of its argument. Based on Eqs. (3.18) and (3.17), one can write that the indication of the AD converter is described as:

$$n_{\text{q}} = \text{ent}\left[\frac{k_V I_{\text{ref}} R N_q}{I_{\text{ref}} R_{\text{ref}}} + 0.5\right] = \text{ent}\left[R\frac{k_V N_q}{R_{\text{ref}}} + 0.5\right] \tag{3.19}$$

which means that the input circuit of the instrument from Fig. 3.1 enables avoiding the influence of changes of the current I_{ref} on the quantization result.

Eq. (3.19) generally describes the dependence of the quantization result n_q on the resistance R of the sensor and the other parameters of the analog converter.

The amplification coefficient of the input amplifier is taken to be $k_V = 32$, the reference resistor $R_{ref} = 5.1253$ kΩ and the maximum number of quanta for the 16-bit ADC is $N_q = 2^{16}$. For these values, Eq. (3.19) takes the form:

$$n_q = \mathrm{ent}\left[\frac{R \cdot 32 \cdot 2^{16}}{5.1253 \cdot 10^3} + 0.5\right] = \mathrm{ent}\left[409.176R + 0.5\right] \tag{3.20}$$

where R depends on the input temperature ϑ accordingly with Eq. (3.5).

Eq. (3.20), together with the sensor characteristic, create the analytical model of analog and analog-to-digital conversions in the exemplary instrument. It is the basis for the determination of the inverse static characteristic in the form of linear segments. The node values of them are presented in Tab. 3.3 together with the mean values c_s of the approximation error, which are calculated separately for every segment in the following way.

Experiment 3.2. This experiment aims to determine the mean values c_s of the approximation error separately for each approximation segment. The input temperature is randomly changed in the ranges suitably for the nodes, the parameters of which are taken from Tab. 3.1. The nodal values of the inverse approximation and the obtained results are presented in Tab. 3.3.

Table 3.3

The nodal values of the linear approximation of the characteristic inverse to (3.20) and mean values of distributions of the approximation error, N is the node number

N	0	1	2	3	4
$\vartheta(N)$°C	0	25	50	75	100
n_q (N)	40918	44901	48854	52779	56673
$c_s(N)$°C	-0.0136	-0.0162	-0.0156	-0.0147	-

Based on the values from Tab. 3.3, one can determine the parameters of the approximating segments. Accordingly with Eq. (3.12), the inclinations are calculated as:

$$a(N) = \frac{\vartheta(N+1) - \vartheta(N)}{n_q(N+1) - n_q(N)} = \frac{25}{n_q(N+1) - n_q(N)} \tag{3.21}$$

while the shift coefficients are obtained from the equation:

$$b(N) = \vartheta(N) + c_s(N) \tag{3.22}$$

where $c_s(N)$ are the corrections taken from Tab. 3.3 equal to the mean values of the approximation error. The values of the parameters calculated for all nodes, accordingly with Eqs. (3.21) and (3.22), are placed in Tab. 3.4.

Table 3.4

Nodal values of the linear segmental approximation of the static inverse function of the exemplary analog converter, N is the node number

N	0	1	2	3	4
$\vartheta(N)$°C	0	25	50	75	100
$n_q\,(N)$	40918	44901	48854	52779	56673
$a(N)\cdot 10^{-3}$°C	6.2767	6.3243	6.3694	6.4201	
$b(N)$°C	-0.0136	24.9838	49.9844	74.9853	

The values in Tab. 3.4 are stored in a look-up-table created in the microcontroller non--volatile memory as the parameters of the exemplary linear approximation. On the basis of the AD converter indication and these parameters, the microcontroller performs the reconstruction algorithm in the following steps:

- The AD indication n_q is compared with all node values $n_q(N)$, $N = 0, 1, ..., 4$, which allows the determination of a suitable node number N.
- On the basis of the determined number N, the values of $a(N)$, $b(N)$ and $n_q\,(N)$ are read from the look-up table.
- Having known the parameters of the linear approximation, the estimate of the measured temperature is calculated using the equation (3.13).

The physical properties of the analog converter need that its model (3.20) should contain the random noise error e_{noi} that represents the influence of noises arising in all parts of the converter. In this case, Eq. (3.20) takes the form:

$$n_{\mathrm{q}} = \mathrm{ent}\left[409.176R + e_{\mathrm{noi}} + 0.5\right] \tag{3.23}$$

in which is the basis for the determination of the partial errors that burden the indication. It is used in simulative experiments aimed at obtaining distributions of the partial errors, such as the experiment described below.

Experiment 3.3. The input temperature of the exemplary instrument changes randomly in the range from 0 to 100°C according to the rectangular distribution. At every step of the experiment, first, the value of the suitable resistance R is determined according to Eq. (3.5). Next, the indication of the AD converter is calculated on the basis of Eq. (3.20) and the static reconstruction is performed by using the described algorithm. Finally, the reconstruction error is calculated and placed in the set, which after ending 100,000 steps of the experiment is presented as

the histogram in Fig. 3.6a. The histogram from Fig. 3.6b is determined in the same way, with this difference that the indications are calculated accordingly with Eq. (3.23) for the normal noise error N(0; 1).

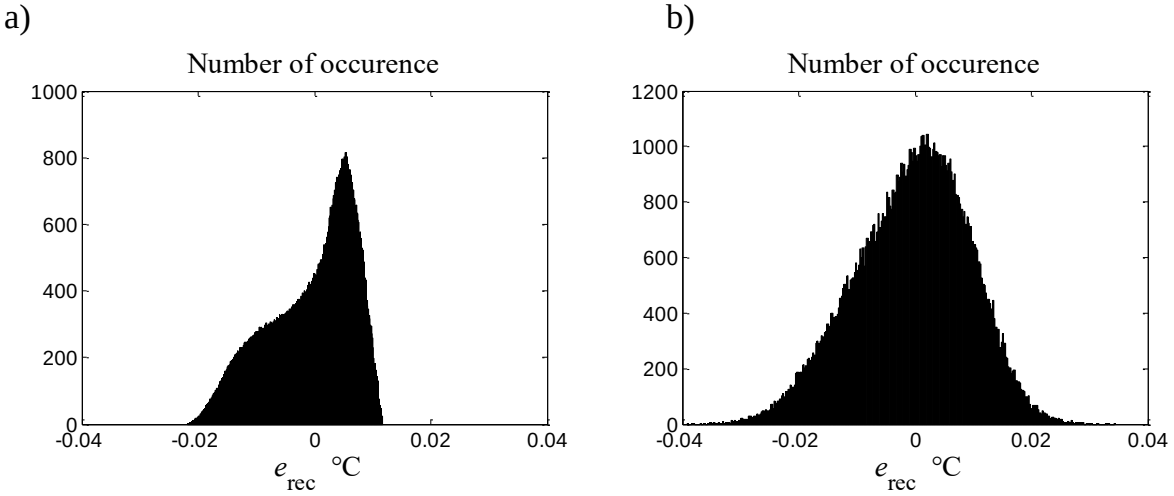

Fig. 3.6. Histograms of the reconstruction error composed: a) of the linear approximation error and the quantization error, the standard deviation of the reconstruction error is $\sigma_{rec} = 7.4 \cdot 10^{-3o}$C, b) of the same errors as previously, as well as of the noise error, $\sigma_{rec} = 9.8 \cdot 10^{-3o}$C in this case

Knowledge about the standard deviations of the total error and the partial errors enables the determination of the correlation coefficient between the partial errors. For the total error e_{tot} composed of two errors e_1 and e_2, it results from Eq. (1.53) that this coefficient is calculated from the expression:

$$c_{cor} = \frac{\sigma_{tot}^2 - \sigma_1^2 - \sigma_2^2}{2\sigma_1\sigma_2} \tag{3.24}$$

where σ_{tot}, σ_1 and σ_2 are standard deviations of errors, respectively.

Example 3.1. The standard deviations, obtained as effects of the simulative experiments for the errors presented in Figs. 3.5b and 3.6b, are: of the approximation error $\sigma_{app} = 7.2 \cdot 10^{-3o}$C and of the total error $\sigma_{rec} = 9.8 \cdot 10^{-3o}$C . The standard deviation of the quantization error can be determined analytically based on the quantum value q. Accordingly with Eq. (1.35), this error is of the rectangular distribution in the range from $-q/2$ to $q/2$ where q is equal to 1 at the output of the AD converter. Therefore, the standard deviation of the quantization error at the ADC output, the same as at the input of the static reconstruction algorithm, has the value [M2]:

$$\sigma_{q,in}^2 = \frac{q^2}{12} = \frac{1}{12} = 0.083 \tag{3.25}$$

The ADC indication is processed by the algorithm. It means that the errors which burden the indication must be transferred to the algorithm output to express them in values comparable with other errors of which the reconstruction error is composed. The transfer consists in multiplication of the input values by the coefficient which can be approximately determined as the inclination of the inverse static characteristic connecting its ending points. It is determined as the quotient:

$$S_{\text{stat}} = \frac{\vartheta_{\max} - \vartheta_{\min}}{n_{q\max} - n_{q\min}} = \frac{100 - 0}{56673 - 40918} = 6.35 \cdot 10^{-3}\ ^{\circ}\text{C} \tag{3.26}$$

the value of which is calculated accordingly with Tab. 3.3. Taking this into account, the variation of the quantization error in the output of the algorithm is as follows:

$$\sigma_{\text{q}}^2 = \left(\sigma_{\text{q,in}} S_{\text{stat}}\right)^2 = \left(\frac{1}{\sqrt{12}} 6.35 \cdot 10^{-3}\right)^2 = 3.36 \cdot 10^{-6}\ ^{\circ}\text{C}^2 \tag{3.27}$$

After introducing to Eq. (3.24) the standard deviations from Figs. 3.5b, 3.6b and described by Eq. (3.27), the correlation coefficient between the approximation error and the quantization error is obtained. It takes the value:

$$c_{\text{cor}} = \frac{\sigma_{\text{rec}}^2 - \sigma_{\text{app}}^2 - \sigma_{\text{q}}^2}{2\sigma_{\text{app}}\sigma_{\text{q}}} = \frac{7.4^2 - 7.2^2 - 3.36}{2 \cdot 7.2\sqrt{3.36}} = -0.016 \cong 0 \tag{3.28}$$

The result is close to zero, which means that these errors can be considered to be uncorrelated.

The standard deviation of the noise error $N(0; 1)$ is equal to 1 at the input of the algorithm. Accordingly with Eq. (3.27), at the algorithm output, the variance of this error takes the value:

$$\sigma_{\text{noi}}^2 = \left(\sigma_{\text{noi,in}} S_{\text{stat}}\right)^2 = \left(1 \cdot 6.35 \cdot 10^{-3}\right)^2 = 40.3 \cdot 10^{-6}\ ^{\circ}\text{C}^2 \tag{3.29}$$

Based on this value and the values from Figs. 3.6a and 3.6b, the correlation coefficient of the noise error in relation to the other errors contained in the reconstruction error can be calculated. One obtains the same result as for the quantization error, which means that the basis errors burdening the indication of the AD converter are uncorrelated.

3.2.3. Calibration of instrument with one-dimensional analytical static reconstruction

The static characteristics of real analog converters change over time, which is called the drift of the characteristic. This drift is caused by material changes occurring in amplifiers and in other analog elements used for signal conversion as well as by the influence of quantities such as the environmental temperature [J14, T1]. Errors connected with the drift should be taken into account in the error budget of an instrument if their values are within acceptable limits. If these limits are exceeded, the drift errors have to be reduced by calibrating a measuring instrument.

As the drift error changes over time, it is necessary to periodically check an instrument by introducing standards to its input and comparing the obtained indications with nominal values, for which a considered approximation of a static characteristic was determined [K1]. For the exemplary instrument, to check whether a calibration is necessary, one connects a standard resistor to the instrument input and the obtained indication is compared with this one suitable for the nominal characteristic. Such a checking procedure is described using the following example.

Example 3.2. The resistance of the standard resistor R_1 connected to input of the exemplary instrument is $R_1 = 138.5055\ \Omega$. The indication of ADC obtained at the instrument output is $\tilde{n}_{\mathrm{q}}(R_1) = 56689$, while the appropriate indication in the nominal conditions, that is for which the parameters of the linear approximation were determined, is $n_{\mathrm{q}}(R_1) = 56673$ (see Tab. 3.3 for $N = 4$)). The difference:

$$\tilde{n}_{\mathrm{q}}(R_1) - n_{\mathrm{q}}(R_1) = 56689 - 56673 = 16$$

is substantially greater than the acceptable value that is calculated as:

$$\left(\Delta n_{\mathrm{q}}\right)_{\mathrm{acp}} = \left(n_{\mathrm{qdr}} - n_{\mathrm{q}}\right)_{\max} = r\frac{n_{q\max} - n_{q\min}}{\vartheta_{\max} - \vartheta_{\min}} = 0.01\frac{56673 - 40918}{100 - 0} \cong 1.5$$

with assumption that the required resolution of the instrument is equal to $r = 0.01^{\mathrm{o}}\mathrm{C}$. This means that calibration of the instrument is necessary in this case.

A calibration consists in correction of an approximation parameters of a static characteristic on the basis of indications obtained for standards of an instrument input quantity. The necessary number of standards depends on a nonlinearity degree of the characteristic. The calibration of the exemplary instrument can be performed at two points because the nonlinearity of its characteristic is not strong. With

the assumption that the characteristic of the Pt100 sensor is stable [Y5], one can apply two standard resistors to calibrate the instrument instead of using two reference values of the input temperature. This is a much simpler method than using a reference temperature, which must be known with suitable low inaccuracy. On the basis of the indications and values of the resistors, one determines corrected parameters of the linear approximation, which replace, if necessary, these ones stored in the look-up table.

Let us apply the standard resistors R_1 and R_2, the values of which correspond to the input temperature values ϑ_1 and ϑ_2, respectively. For resistor R_1 connected to the input, one obtains the ADC indication n_{q1} and for R_2 the indication is n_{q2}. The nominal values of the indications, calculated for the resistances R_1 and R_2 on the basis of Eq. (3.20), are n_{q1nom} and n_{q2nom}, respectively. Therefore, the changes in the indications at the selected points that are caused by the drift are:

$$\Delta_1 = n_{q1} - n_{q1nom} \tag{3.30}$$

and

$$\Delta_2 = n_{q2} - n_{q2nom} \tag{3.31}$$

Based on these values, one can determine the equation which enables calculations of the corrections, which must be added to all nominal values of the indications. This equation has the following form:

$$\Delta = \Delta_1 + s \cdot (\vartheta - \vartheta_1) \tag{3.32}$$

where the inclination coefficient is defined as:

$$s = \frac{\Delta_2 - \Delta_1}{\vartheta_2 - \vartheta_1} \tag{3.33}$$

The modified ADC indications in the nodes, corresponding to the shifted characteristic, are determined as:

$$n_{qsh}(N) = n_q(N) + \Delta \tag{3.34}$$

where N is the node number. On the basis of the indications calculated by using Eq. (3.34), the corrected parameters of the segments are determined in the same way as described in the previous chapter.

The application of the described calibration procedure is presented in the next example.

Example 3.3. Calibration at two points is the most accurate if it is performed in extreme points of the characteristic. To carry out the calibration procedure for the exemplary instrument, one uses two standard resistors: $R_1 = 100.0\ \Omega$ corresponding to the input temperature $\vartheta_1 = 0^{\circ}\mathrm{C}$ and $R_2 = 138.5055\ \Omega$ for $\vartheta_2 = 100^{\circ}\mathrm{C}$. After completing the AD conversion for R_1 connected to the input, the indication is $n_{q1} = 40931$ and for R_2: $n_{q2} = 56689$. The next phases of the calibration are carried out in the following way:

- Having known indications n_{q1} and n_{q2}, one calculates the indication changes accordingly with Eqs. (3.30) and (3.31). One obtains:

  $$\Delta_1 = n_{q1} - n_{q1nom} = 40931 - 40918 = 13, \quad \Delta_2 = n_{q2} - n_{q2nom} = 56689 - 56673 = 16$$

  For these changes, the inclination coefficient (3.33) takes the value:

  $$s = \frac{\Delta_2 - \Delta_1}{\vartheta_2 - \vartheta_1} = \frac{16 - 13}{100 - 0} = 0.03\,^{\circ}\mathrm{C}^{-1}$$

- Using the calculated shift parameters, one corrects the nodal values of the characteristic accordingly with the equations (3.32) and (3.34). For the first node, the corrected indication is: $n_{qcal}(0) = n_{q1} = 40931$ and for the last, $n_{qcal}(4) = n_{q2} = 56689$.

  For the node number $N = 1$, one obtains:

  $$n_{qcal}(1) = n_q(1) + \Delta_1 + s \cdot (\vartheta(1) - \vartheta_1) = 44901 + 13 + 0.03 \cdot (25 - 0) = 44915$$

  For $N = 2$:

  $$n_{qcal}(2) = n_q(2) + \Delta_1 + s \cdot (\vartheta(2) - \vartheta_1) = 48854 + 13 + 0.03 \cdot (50 - 0) = 48869$$

  and for $N = 3$:

  $$n_{qcal}(3) = n_q(3) + \Delta_1 + s \cdot (\vartheta(3) - \vartheta_1) = 52779 + 13 + 0.03 \cdot (75 - 0) = 52794$$

- Based on the corrected nodal values, the inclinations from Tab. 3.3 are modified accordingly with Eq. (3.23), in which the nodal values from Tab. 3.3 are replaced by the corrected ones. The obtained inclinations are contained in the Tab. 3.5.

Table 3.5

Nodal values of the segmental linear approximation of the static inverse function, which are calculated on the basis of the calibration results, N is the node number

N	0	1	2	3	4
$\vartheta(N)$ °C	0	25	50	75	100
$n_{\text{qcal}}(N)$	40931	44915	48869	52794	56689
$a(N)\cdot 10^{-3}$ °C	6.2751	6.3227	6.3694	6.4185	-
$b(N)$ °C	-0.0136	24.9838	49.9844	74.9853	

The shift coefficients in Tab. 3.5 are the same as in Tab. 3.4, which can cause the mean value of the approximation error to differ substantially from 0. In this case, it is necessary to correct them in the same way, which was performed for determining these coefficient by using Eq. (3.24).

Based on the indications obtained during the calibration, one can determine the mathematical model of the analog converter valid for the measurement conditions under which the calibration is carried out. Generally, such a model is useful in error analysis, and, for the considered converter, it has the form:

$$\tilde{n}_q = \text{ent}\left[409.176\cdot R\cdot\left(1+\Delta_{\text{inc}}\right)+\Delta_{\text{sh}}+0.5\right] \tag{3.35}$$

obtained accordingly with Eq. (3.20) where Δ_{inc} is the relative change in the characteristic inclination and Δ_{sh} is the characteristic shift. Accordingly with this model and for the two considered results of the calibration, one obtains the system of two equations:

$$n_{\text{q1}} \cong 409.176\cdot R_1\cdot\left(1+\Delta_{\text{inc}}\right)+\Delta_{\text{sh}} \tag{3.36}$$

$$n_{\text{q2}} \cong 409.176\cdot R_2\cdot\left(1+\Delta_{\text{inc}}\right)+\Delta_{\text{sh}} \tag{3.37}$$

After solving them, one obtains values of the characteristic changes as is shown in the next example.

Example 3.4. For two calibration points: (R_1 = 100.0 Ω, n_{q1} = 40931) and (R_2 = 138.5055 Ω, n_{q2} = 56689), from Eqs. (3.36) and (3.37), we obtain the following results:

$$\Delta_{\text{inc}} = \frac{n_{\text{q2}}-n_{\text{q1}}}{409.176\cdot\left(R_2-R_1\right)}-1 = \frac{56689-40931}{409.176(138.5055-100.0)}-1 = 1.57\cdot 10^{-4} \tag{3.38}$$

and

$$\Delta_{\text{sh}} = n_{\text{q1}}-409.176\cdot R_1\cdot\left(1+\Delta_{\text{inc}}\right) = 40931-409.176\cdot 100.0\left(1+1.57\cdot 10^{-4}\right) = 7 \tag{3.39}$$

After introducing the values (3.38) and (3.39) into Eq. (3.35) and taking the noise into account, on obtains the model of the analog conversion that contains the drift parameters in the considered measurement conditions. It is of the form:

$$n_{\mathrm{qdr}} = \mathrm{ent}\left[409.176 \cdot R \cdot \left(1 + 1.57 \cdot 10^{-4}\right) + 7 + e_{\mathrm{noi}} + 0.5\right] \tag{3.40}$$

where e_{noi} is a realization of the normal noise error $N(0; 1)$.

Experiment 3.4. This experiment is carried out in the same way as Experiment 3.2 with these differences, that the indications are determined on the basis of the model (3.40), and the reconstruction is performed with using the parameters of the linear approximation contained in Tab. 3.5. The reconstruction error calculated in the case if the indications are determined accordingly with Eq. (3.40) is presented in Fig. 3.7b but if the noise in this equation is omitted in Fig. 3.7a.

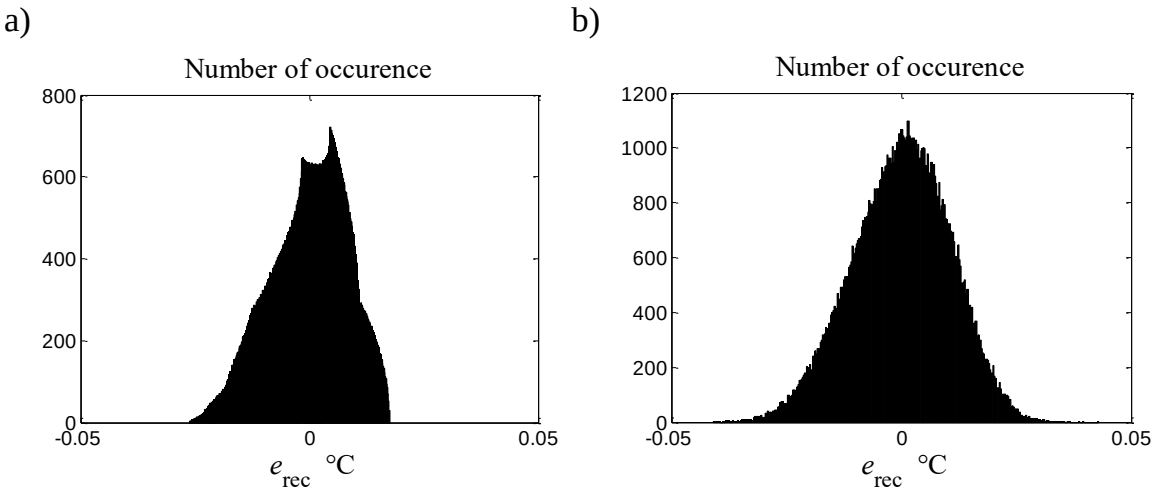

Fig. 3.7. Histograms of the static reconstruction error for the linear approximation parameters obtained as a result of the calibration: a) the reconstruction error is composed of the errors caused by the linear approximation, the calibration, and the quantization, the standard deviation of this error is $\sigma_{\mathrm{rec}} = 8.5 \cdot 10^{-3}$°C, b) the reconstruction error also contains the noise error, $\sigma_{\mathrm{rec}} = 10.6 \cdot 10^{-3}$°C

Based on data calculated for the histograms in Fig. 3.7, one can determinate the standard deviation of the calibration error. With the assumption that the partial errors are not correlated and accordingly with Eq. (1.53), the variance of the reconstruction error is the sum:

$$\sigma_{\mathrm{rec}}^2 = \sigma_{\mathrm{app}}^2 + \sigma_{\mathrm{q}}^2 + \sigma_{\mathrm{noi}}^2 + \sigma_{\mathrm{cal}}^2 \tag{3.41}$$

where the partial standard deviations represent: σ_{app} – the linear approximation error shown in Fig. 3.5b, σ_{q} – the quantization error, σ_{noi} – the noise error,

σ_{cal} – the calibration error. After rearranging the Eq. (3.41), we find that the standard deviation of the calibration error is expressed as:

$$\sigma_{\text{cal}} = \sqrt{\sigma_{\text{rec}}^2 - \sigma_{\text{app}}^2 - \sigma_{\text{q}}^2 - \sigma_{\text{noi}}^2} \tag{3.42}$$

After introducing the values from Figs. 3.5b, 3.7b and these given by Eqs. (3.27), (3.29), we have:

$$\sigma_{\text{cal}} = 10^{-3}\sqrt{10.6^2 - 7^2 - 3.36 - 40.3} = 4.44 \cdot 10^{-3}\ ^{\text{o}}\text{C} \tag{3.43}$$

As it results from comparison of standard deviations of the considered partial errors, their values are approximately at the same level. It means that such a simple calibration is accurate enough for the analog conversion performed in the exemplary instrument.

3.2.4. Identification of parameters of one-dimensional linear approximation

Generally, an identification of a static characteristic consists in measuring it in so many points as necessary to obtain such an approximation which fulfils accuracy requirements [G3, M8]. The number of points depends on the degree of nonlinearity of the characteristic and measurement conditions of the identification. From the reconstruction point of view, the identification should be carried out by direct determination of such a form of approximation which is applied in the reconstruction. It is possible to apply the other indirect way that is carried out in two stages. The first one consist in using the measurement results to calculate parameters of an initial analytical description of the static characteristic. The second stage aims to obtain the final approximation adapted to the reconstruction requirements on the basis of this initial description.

The direct identification of the static characteristic of the exemplary instrument considered in this chapter consists in determination parameters of the applied linear approximation on the basis of measurement results. Let us assume that every segment of the characteristic is identified in I points. At first, standard I resistors are connected to the instrument input instead of Pt100 sensor one after the other and the corresponding ADC indications $n_{\text{q}i}$, $i = 1,...,I$, are recorded. According to Eqs. (3.21) and (3.22), the parameters of the segment for the node N are calculated

with assumption that they minimize the following expression being the sum of the squared errors [L1]:

$$SM_{\text{err}}(N) = \sum_{i=1}^{I}\left[\vartheta_i(N) - \left(\hat{a}(N)n_{\text{qi}}(N) + \hat{c}(N)\right)\right]^2 \tag{3.44}$$

where the reference input temperature ϑ_i corresponds to resistance R_i according to the equation (3.5), $\hat{a}(N)$, $\hat{c}(N)$ are the estimates of the parameters describing the segment of node N. To determine these estimates, one equates to zero the first derivative of expression (3.44) in relation to $\hat{a}(N)$ and next to $\hat{c}(N)$. The obtained system of two equations enables determining the estimate of the segment inclination for node N as:

$$\hat{a}(N) = \frac{I\sum_{i=1}^{I}\vartheta_i(N)n_{qi}(N) - \left(\sum_{i=1}^{I}\vartheta_i(N)\right)\left(\sum_{i=1}^{I}n_{qi}(N)\right)}{I\sum_{i=1}^{I}n_{qi}^2(N) - \left(\sum_{i=1}^{I}n_{qi}(N)\right)^2} \tag{3.45}$$

The estimate of the beginning point of the segment is calculated as the mean value:

$$\hat{b}(N) = \frac{1}{I}\sum_{i=1}^{I}\left[\vartheta_i(N) - \hat{a}(N)n_{qi}(N)\right] = \frac{1}{I}\sum_{i=1}^{I}\vartheta_i(N) - \frac{1}{I}\hat{a}(N)\sum_{i=1}^{I}n_{qi}(N) \tag{3.46}$$

Let us take for example that the parameters of the linear approximation are identified in form of 4 segments the same as presented in Tab. 3.5. For every segment, 4 standard resistors, with nominal values R_i, $i = 1,\ldots,4$ are used. Introducing the resistor R_i into the instrument input is adequate to give the temperature ϑ_i to the sensor input accordingly with Eq. (3.5). The resolution of the resistors is 0.001 Ω, which corresponds to a temperature resolution equal to 0.001°C. The ADC indications obtained for the used standard resistors are determined on the basis of the analog conversion model (3.20). All values designated in the described identification process are presented in Tab. 3.6.

Table 3.6

ADC indications obtained for the selected standard resistors on the basis of Eq. (3.45), N is the number of the node, ϑ_i is the temperature responding the resistance R_i according to the characteristic (3.5) of the sensor, $i = 1, ..., I$, $I = 4$ is the total number of resistors used to identify the characteristic in one node

N	0	1	2	3
$R_1(N)$ Ω	100.000	109.856	119.424	129.035
$\vartheta_1(N)$°C	0	25.313	50.070	75.125
$n_{q1}(N)$	40917	44949	48866	52797
$R_2(N)$ Ω	102.454	112.130	121.651	131.435
$\vartheta_2(N)$ °C	6.285	31.180	55.859	81.411
$n_{q2}(N)$	41920	45882	49777	53782
$R_3(N)$ Ω	104.860	114.444	124.331	133.792
$\vartheta_3(N)$°C	12.458	37.161	62.838	87.596
$n_{q3}(N)$	42906	46829	50873	54744
$R_4(N)$ Ω	107.333	116.986	126.698	136.010
$\vartheta_4(N)$ °C	18.815	43.744	69.015	93.427
$n_{q4}(N)$	43918	47868	51843	55652

Based on the values contained in Tab. 3.6, one can calculate the parameters of 4 segments that approximate the exemplary inverse static characteristic. The segments are generally described by the following linear equation:

$$\hat{\vartheta} = \hat{a}(N) \cdot n_{\mathrm{q}} + \hat{c}(N), \quad N = 0, \ldots, 3 \tag{3.47}$$

where $\hat{a}(N)$ and $\hat{c}(N)$ are calculated accordingly with the equations (3.45) and (3.46), respectively.

Example 3.5. Let us calculate the approximation parameters for the first node ($N = 0$) on the basis of data from the first column of Tab. 3.6. Accordingly with Eq. (3.45), we obtain the estimate of the inclination equal to:

$$\hat{a}(0) = 6.2687 \cdot 10^{-3} \ ^{\circ}\mathrm{C}$$

The estimate of the shift coefficient from Eq. (3.47) is calculated as the mean value:

$$\hat{c}(0) = \frac{1}{4}\sum_{i=1}^{4} \vartheta_i(0) - \frac{\hat{a}(0)}{4}\sum_{i=1}^{4} n_{\mathrm{q}i}(0) = \frac{1}{4}\left(37.556 - 6.2687 \cdot 10^{-3} \cdot 169661\right) = -256.5 \ ^{\circ}\mathrm{C}$$

The coefficient $\hat{c}(N)$ describes the point on the vertical axis $\hat{\vartheta}$ for $n_q = 0$. For $N = 0$, the nodal value of the temperature $\vartheta(0) = 0^oC$. Taking this into account, the approximation segment begins from $\dot{n}_q(0)$, which can be determined on the basis of the equation (3.47) as:

$$\dot{n}_q(0) = -\frac{\hat{c}(0)}{\hat{a}(0)} = -\frac{-256.5}{6.2687 \cdot 10^{-3}} = 40917.57$$

To obtain the estimate $\hat{n}_q(0)$ of the indication in node 0, $\dot{n}_q(0)$ should be rounded as the indications take integer values. One obtains:

$$\hat{n}_q(0) = \text{ent}\left[\dot{n}_q(0) + 0.5\right] = \text{ent}(40917.57 + 0.5) = 40918$$

Based on the calculated values, the shift coefficient of the first segment is:

$$\hat{b}(0) = -\hat{a}(0)\left[\hat{n}_q(0) - \dot{n}_q(0)\right] = -6.2687 \cdot 10^{-3} \cdot (40918 - 40917.57)) = -0.003\,^oC$$

The values of the parameters obtained in Example 3.5 for node 0 are presented in the first column of Tab. 3.7. The remaining columns contain parameters of the other nodes, which are calculated in the same way as used for the first node. Distributions of the reconstruction errors are determined for the approximated parameters of Tab. 3.7 using Experiment 3.5.

Table 3.7

Node values of the segmental approximation of the inverse function identified on the basis of $I = 4$ points for every segment according to the equations (3.45) and (3.46), N is the node number

N	0	1	2	3	4
$\vartheta(N)$ °C	0	25.313	50.070	75.125	93.427
$\hat{n}_q(N)$	40918	44950	48866	52799	
$\hat{a}(N)\cdot 10^{-3}$ °C	6.2687	6.3146	6.3643	6.4123	
$\hat{b}(N)^oC$	-0.003	25.3147	50.0721	75.1270	

Experiment 3.5. This experiment aims to determine histograms of the reconstruction errors that contain the identification error. It is carried out in the same way as Experiment 3.2 with this difference that the estimates of the input temperature are calculated with using the parameters from Tab.3.7 obtained as a result of the direct identification. The ADC indications used for the reconstruction are determined on

the basis of Eq. (3.20) or (3.23) in the case if the indications are burdened by the normal noise $N(0; 1)$. The obtained histograms are presented in Figs. 3.8a and 3.8b, respectively.

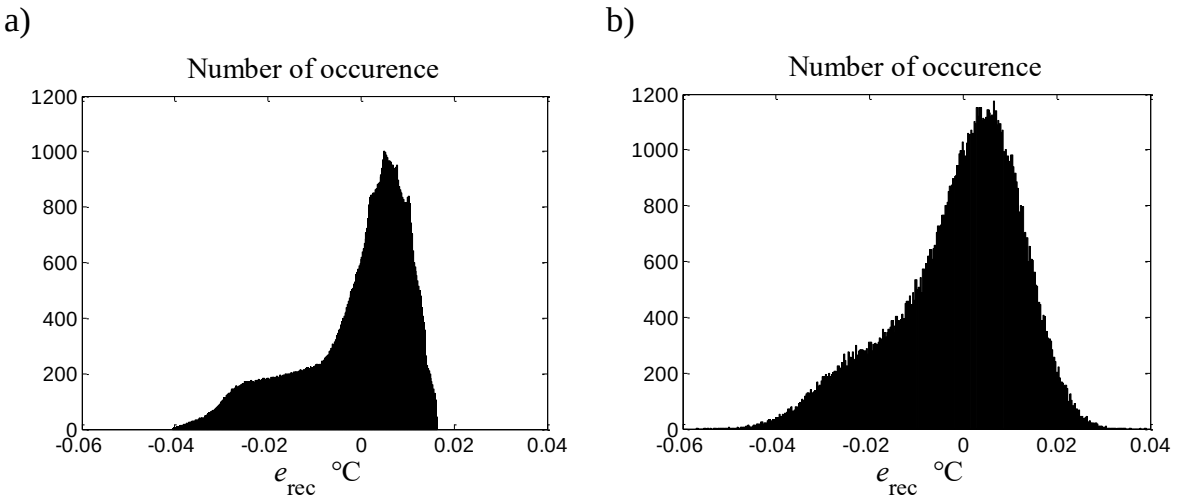

Fig. 3.8. Histograms of the reconstruction errors which are calculated for the linear approximated parameters from Tab. 3.7 obtained as a result of identification: a) the total error contains the approximation, identification, and quantization errors, $\sigma_{rec} = 11.8 \cdot 10^{-3}$°C, b) the total error additively contains the noise error, $\sigma_{rec} = 13.4 \cdot 10^{-3}$°C

Example 3.6. The reconstruction error from Fig. 3.8b is composed of the errors caused by: e_{app} – the linear approximation, e_q – the quantization, e_{noi} – the noise, and e_{id} – by the identification. If these errors are uncorrelated, the standard deviation of the identification error can be calculated in the same way as in Eqs. (3.41) and (3.42). One obtains:

$$\sigma_{id} = \sqrt{\sigma_{rec}^2 - \sigma_{app}^2 - \sigma_q^2 - \sigma_{noi}^2} \tag{3.48}$$

where σ_{rec} is the standard deviation of the reconstruction error described by the histogram in Fig. 3.8b, while the other standard deviations are the same as in Eq. (3.41). Based on these values, we have:

$$\sigma_{id} = 10^{-3}\sqrt{13.4^2 - 7^2 - 3.36 - 40.3} = 9.32 \cdot 10^{-3}\ ^{o}\text{C} \tag{3.49}$$

which means that, in the considered case, the identification error takes values comparable to the linear approximation error.

Identificationof a static characteristic of a sensor is generally a sophisticated problem from measurement point of view because it is necessary to use as many standards of an input quantity as identification points are chosen. For nonelectrical quantities, constructing of standards with suitable accuracy is difficult, and identification experiments need professional laboratory equipment. All these causes one strives to limit a number of identification points to a minimum. Tab. 3.8 contains standard

deviation values of the reconstruction error, which are determined for the number of identification points less than 4 for one segment. The parameters of the approximation are calculated on the basis of Eqs. (3.45) and (3.46).

Table 3.8

Standard deviations of the identification error in dependence on the number N_{ip} of identification points for one approximation segment, the number of segments $N_{seg} = 4$

N_{ip}	2	3	4
$\sigma_{id} \cdot 10^{-3}$°C	10.4	10.0	9.32

The values in Tab. 3.8 show that decreasing the identification points does not substantially influence the identification inaccuracy. This suggests that indirect identification enables more reduction of identification points. In the first step of such identification, one determines an inverse function as an analytical equation [A1].With the assumption that one uses the polynomial $\hat{\vartheta} = f(n_q)$ of the second order determined for $I = 16$ all identification points taken from Tab. 3.5 (4 points for each of the 4 segments), the function has the following form:

$$\hat{\vartheta} = -245.4200 + 5.7467 \cdot 10^{-3} \cdot n_q + 6.1444 \cdot 10^{-9} \cdot n_q^2 \qquad (3.50)$$

In the second step, one calculates the approximation coefficients in the same way as for the exemplary static characteristic (3.5). The obtained node values are presented in Table 3.9. Histograms of the reconstruction error determined in the case if this approximation is used are shown in Fig. 3.9.

Table 3.9

Nodal values of the linear segmental approximation of the inverse function (3.52) for the number of all identification points $I = 16$, N is the node number

N	0	1	2	3	4
$\hat{n}_q(N)$	40917	44949	48866	52797	55652
$\hat{a}(N) \cdot 10^{-3}$ °C	6.2680	6.3171	6.3655	6.4130	
$\hat{b}(N)$°C	-0.0015	25.2967	50.0644	75.1107	

Experiment 3.6. The reconstruction is performed using the parameters contained in Tab. 3.9, which are determined indirectly on the basis of Eq. (3.50). The histograms of the reconstruction errors obtained in the same way as used in Experiment 3.2 are shown in Fig. 3.9.

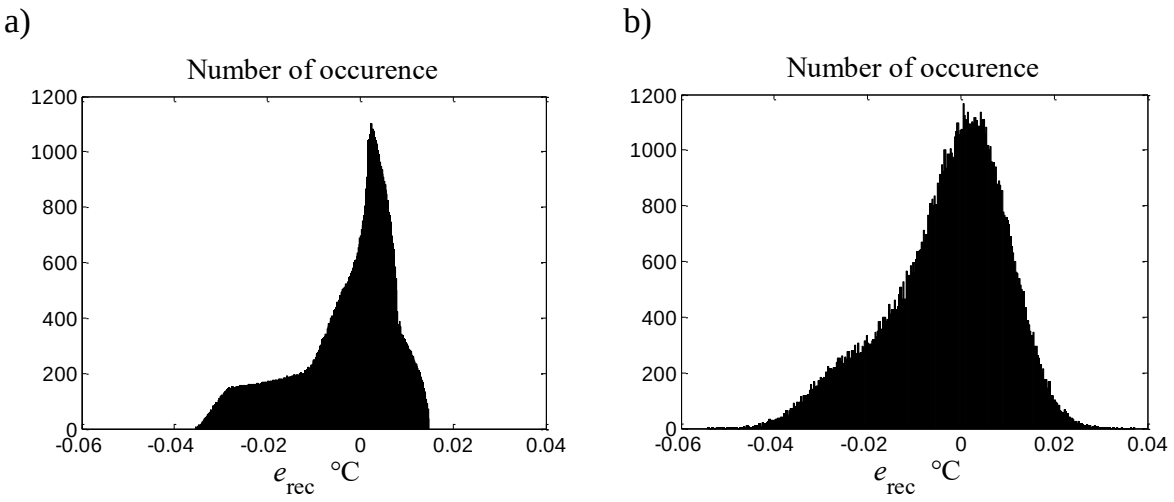

Fig. 3.9. Histograms of errors of the reconstruction performed indirectly using the linear approximation parameters from Tab. 3.9, which are determined on the basis of Eq. (3.50): a) the error contains both the approximation and the identification errors, as well as the quantization error, the standard deviation of the error is $\sigma_{rec} = 10.9 \cdot 10^{-3}$°C, b) the reconstruction error additively contains the noise error, $\sigma_{rec} = 12.6 \cdot 10^{-3}$°C

The standard deviation of the error due to indirect identification is determined from the equation.(3.48), the same as used for direct identification. On the basis of the histogram in Fig. 3.9b, one obtains:

$$\sigma_{id} = 10^{-3}\sqrt{12.6^2 - 7.2^2 - 3.36 - 40.3} = 7.95 \cdot 10^{-3}\ ^{o}\text{C} \qquad (3.51)$$

where the other values are the same as in Eq. (3.49). The values being calculated by using Eqs. (3.49) and (3.51) mean that the errors of direct and indirect identification are comparable for the same number of identification points I equal to 16. The data in Tab. 3.10 shows that decreasing the number of points used for indirect identification does not increase its inaccuracy. It means that the indirect identification of the parameters of the linear approximation enables using fever standards than the direct one. Therefore, it is more effective if one takes into account the number of standards applied.

Table 3.10

The standard deviations of the identification error in dependence on number I of identification points used for determination of the analytical function in the form (3.50) which is the basis of calculation of the segmental approximation parameters for $N = 5$ nodes

I	4	8	16
$\sigma_{id} \cdot 10^{3}$°C	7.33	7.5	8.13

3.2.5. Influence of non-linearity degree of static characteristic on number of nodes

From the linear approximation point of view, the number of nodes necessary to obtain the required accuracy is one of the basic properties of every class of approximated functions. The characteristic (3.5) of the exemplary Pt100 sensor belongs to the class of second-order polynomials. To consider the influence of the characteristic non-linearity on the necessary number of nodes, one can use an expression similar to Eq. (3.5) in the form:

$$R = R_0\left[1 + \alpha(\Delta\vartheta) + \beta(\Delta\vartheta)^2\right], \text{where} \beta = k \cdot 5{,}775 \cdot 10^{7}\ {}^{\circ}\text{C}^{-2}, k = 1, 10, 10^2, 10^3, 10^4 \quad (3.52)$$

where $R_0 = 100\ \Omega$, $\alpha = 3.9083 \cdot 10^{-3\circ}\text{C}^{-1}$, $\Delta\vartheta$ changes from 0 to 100°C. For $k = 1$, Eq. (3.52) describes the static characteristic of the Pt100 sensor. Taking into account that coefficient β forms the non-linearity degree of the sensor characteristic, the higher values of k cause the stronger non-linearity.

To evaluate the influence of the non-linearity of the static characteristic on the number of nodes N_n needed to achieve the allowable inaccuracy of the segmental linear approximation of the characteristic inverse to (3.52), the following experiment has been carried out.

Experiment 3.7. This experiment consists in looking, for $k = 1, 10, 10^2, 10^3$, the least number of nodes, for which the standard deviation of the approximation error is less than $\sigma_{app,max} = 10 \cdot 10^{-3\circ}\text{C}$. For every value of k, first, the parameters of the linear segmental approximation are determined for the number of nodes $N_n = 5$ and then, the approximation error is calculated in a simulative way. If the standard deviation of the error is higher than the allowable value $\sigma_{app,max} = 0.01^{\circ}\text{C}$, the number of nodes increases by 1 and all the procedure is repeated so long until the standard deviation is less than this value. The obtained minimal numbers of nodes are presented in Table 3.11.

Table 3.11

The least number of nodes $N_{n,min}$ necessary to obtain the allowable standard deviation of the approximation error $\sigma_{app,max} = 0.01^{\circ}\text{C}$ for the static characteristic (3.52) approximated by linear segments

K	1	10	10^2	10^3
$N_{n,min}$	5	11	25	46

The exemplary function (3.52) for $k = 10^2$ is presented in Fig. 3.10a. The histogram of the approximation error of this function that is approximated in $N_n = 11$ nodes by linear segments is shown in Fig. 3.10b.

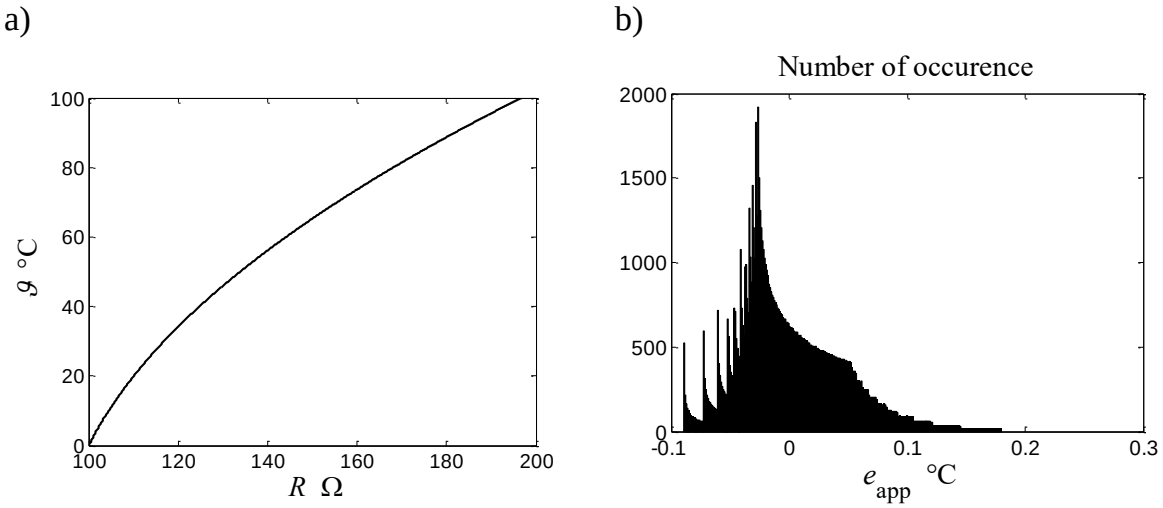

Fig. 3.10. a) Exemplary function (3.52) for $k = 10^2$, b) histogram of the linear approximation error of the function for the number of nodes $N_n = 11$

The results which are contained in Tab. 3.11 show that the number of nodes necessary to obtain allowable inaccuracy of the segmental linear approximation significantly grows with non-linearity increasing of the linearized function. It causes the number of coefficients which have to be stored in the non-volatile memory of the microcontroller to perform static reconstruction to be suitable large but this is not a problem if modern microcontrollers are applied [Y6].

3.3. Two-dimensional analytical static reconstruction

3.3.1. Two-dimensional static characteristic of exemplary sampling instrument

The output quantity y of the analog converter in a sampling instrument can be dependent not only on its input quantity x but also on other quantities that influence the analog conversion. Among the influence quantities, the environmental temperature, at which the instrument works, is most often taken into account. The considerations in this chapter focus on error analysis of the signal reconstruction of the exemplary instrument in the case where the ADC indications depend not only on the measured temperature but also on the environmental temperature.

The environmental temperature can influence many elements of the instrument but, to make the considerations simpler, only the temperature changes of the reference resistor R_{ref} (see Fig. 3.2) are considered. Denoting the environmental temperature as ϑ_{env}, the dependence of the resistance of R_{ref} on it can be described by the expression:

$$\tilde{R}_{\mathrm{ref}} = R_{\mathrm{ref}}\left[1+\left(\vartheta_{\mathrm{env}}-\vartheta_{0\mathrm{env}}\right)\varepsilon\right] = R_{\mathrm{ref}}\left[1+\Delta\vartheta_{\mathrm{env}}\cdot\varepsilon\right] = R_{\mathrm{ref}}+R_{\mathrm{ref}}\cdot\Delta\vartheta_{\mathrm{env}}\cdot\varepsilon = R_{\mathrm{ref}}+\Delta R_{\mathrm{ref}} \qquad (3.53)$$

where $\vartheta_{0,\mathrm{env}} = 25^{\mathrm{o}}\mathrm{C}$ is the nominal environmental temperature and R_{ref} is the value of the reference resistor at this temperature. The temperature drift coefficient ε is defined as the relative change of the resistor R_{ref} for the increase in the environmental temperature equal to $1^{\mathrm{o}}\mathrm{C}$. This resistor is a part of AD converter; therefore, the temperature drift of the resistor causes that the quantum value of the converter changes respectively. Denoting the fluent quantum as $\tilde{q}$ and based on Eq. (3.18), one can describe the ADC indication in this case as:

$$n_{\mathrm{q}} = \mathrm{ent}\left[\frac{k_V V_{\mathrm{in}}}{\tilde{q}}+0.5\right] = \mathrm{ent}\left[\frac{k_V I_{\mathrm{ref}} R(\vartheta)}{\frac{I_{\mathrm{ref}}\tilde{R}_{\mathrm{ref}}}{N_q}}+0.5\right] = \mathrm{ent}\left[\frac{R(\vartheta)}{\tilde{R}_{\mathrm{ref}}}k_V N_q+0.5\right] \qquad (3.54)$$

where $R(\vartheta)$ is the resistance of the Pt100 sensor, which depend on the input temperature ϑ accordingly with the equation (3.5). After introducing Eq. (3.53) to Eq. (3.54), one obtains the expression:

$$n_{\mathrm{q}} = \mathrm{ent}\left[\frac{R(\vartheta)}{\tilde{R}_{\mathrm{ref}}}k_V N_q+0.5\right] = \mathrm{ent}\left[k_V N_q\frac{R(\vartheta)}{R_{\mathrm{ref}}\left(1+\Delta\vartheta_{\mathrm{env}}\cdot\varepsilon\right)}+0.5\right] \qquad (3.55)$$

which is the analytical two-dimensional model composed of the analog and analog-to-digital parts of the exemplary instrument.

For the analysis of the properties of the model (3.55), another form of it is more usable. After rearranging the equation (3.53), this model takes the form:

$$n_{\mathrm{q}} = \mathrm{ent}\left[k_V\frac{R(\vartheta)N_q}{R_{\mathrm{ref}}+\Delta R_{\mathrm{ref}}}+0.5\right] \cong \mathrm{ent}\left[k_V\frac{R(\vartheta)N_q}{R_{\mathrm{ref}}}\left(1-\frac{\Delta R_{\mathrm{ref}}}{R_{\mathrm{ref}}}\right)+0.5\right] \qquad (3.56)$$

where it is taken into account that for $\Delta R_{\mathrm{ref}} << R_{\mathrm{ref}}$ we have: $\dfrac{1}{1+\dfrac{\Delta R_{\mathrm{ref}}}{R_{\mathrm{ref}}}} \cong 1-\dfrac{\Delta R_{\mathrm{ref}}}{R_{\mathrm{ref}}}$.

Example 3.7. Let us assume that the drift coefficient of the resistor R_{ref} is $\varepsilon = 30$ ppm/°C and the environmental temperature varies from 5°C to 45°C. This means that the maximum absolute value of the temperature deflection from its nominal value $\vartheta_{0\text{env}} = 25$°C is: $|\Delta\vartheta_{\text{env}}|_{\max} = 20$°C. Therefore, the maximum change of R_{ref} is of the value:

$$\left(\Delta R_{\text{ref}}\right)_{\max} = R_{\text{ref}} \cdot \left|\Delta\vartheta_{\text{env}}\right|_{\max} \cdot \varepsilon = R_{\text{ref}} \cdot 20 \cdot 30 \cdot 10^{-6} = R_{\text{ref}} \cdot 0.6 \cdot 10^{-3}\ \Omega \tag{3.57}$$

Omitting the quantization operation in Eq. (3.54), we can write it in the simplified form:

$$n_{\text{q}} \cong k_V \frac{R(\vartheta)N_q}{R_{\text{ref}}}\left(1 - \frac{\Delta R_{\text{ref}}}{R_{\text{ref}}}\right) = n_{\text{qnom}}\left(1 - \frac{\Delta R_{\text{ref}}}{R_{\text{ref}}}\right) = n_{\text{qnom}} - \Delta n_{\text{q}} \tag{3.58}$$

where n_{qnom} is the indication at the nominal temperature $\vartheta_{0,\text{env}} = 25$°C.

Accordingly with Eq. (3.58), one can determine the changes in the ADC indications caused by the influence of the environmental temperature on the resistor R_{ref}. The maximum value of these changes can be determined as:

$$\left(\Delta n_{\text{q}}\right)_{\max} = n_{\text{qnom}} \frac{\left(\Delta R_{\text{ref}}\right)_{\max}}{R_{\text{ref}}} \tag{3.59}$$

Based on this equation and taking into account the fact that the maximum number of quanta $(n_{\text{q}})_{\max} = 56673$ (see Tab. 3.3), we have:

$$\left(\Delta n_q\right)_{\max} = 56673 \cdot 0.6 \cdot 10^{-3} \cong 34 \tag{3.60}$$

In Example 3.2 it is calculated that the maximum acceptable change of the quantization result is $(\Delta n_{\text{q}})_{\text{acp}}$ if the input temperature resolution is $r = 0.01$°C. The change (3.60) is substantially higher than this acceptable, which means that it is necessary to correct the error caused by changes of the environmental temperature by applying a two-dimensional static reconstruction algorithm.

3.3.2. Algorithm of two-dimensional static reconstruction

As result of the analytical model (3.55), the indication of ADC depends on both the input temperature ϑ and the resistance of R_{ref}, which is influenced by the environmental temperature ϑ_{env}. Taking this into account, this model can be generally presented in the following form:

$$n_{\text{q}} = S(\vartheta, \vartheta_{\text{env}}) \tag{3.61}$$

In this case, the reconstruction is performed by solving Eq. (3.61) in relation to the input temperature ϑ. This operation can be written as:

$$\hat{\vartheta} = S^{-1}(n_{\mathrm{q}},\ \vartheta_{\mathrm{env}}) \tag{3.62}$$

where $\hat{\vartheta}$ is the estimate of the reconstructed input temperature, and ϑ_{env} is the environmental temperature. In the exemplary instrument, this temperature is converted by the inside sensor and measured by using the additional AD converter that is a part of the ADuC386 microcontroller [Y6].

By expanding the inverse function (3.62) in the Maclaurin series and taking only the initial terms into account, one obtains the following expression:

$$\begin{aligned}\hat{\vartheta} &\cong \vartheta_0 + \frac{\partial S^{-1}(n_{\mathrm{q}},\vartheta_{\mathrm{env}})}{\partial n_{\mathrm{q}}}\mathrm{d}n_{\mathrm{q}} + \frac{\partial S^{-1}(n_{\mathrm{q}},\vartheta_{\mathrm{env}})}{\partial \vartheta_{\mathrm{env}}}\mathrm{d}\vartheta_{\mathrm{env}} = \\ &= \vartheta_0 + \frac{\partial S^{-1}(n_{\mathrm{q}},\vartheta_{\mathrm{env}})}{\partial n_{\mathrm{q}}}\mathrm{d}n_{\mathrm{q}} + \frac{\partial S^{-1}(n_{\mathrm{q}},\vartheta_{\mathrm{env}})}{\partial n_{\mathrm{q}}}\frac{\partial n_{\mathrm{q}}}{\partial \vartheta_{\mathrm{env}}}\mathrm{d}\vartheta_{\mathrm{env}}\end{aligned} \tag{3.63}$$

Denoting:

$$\vartheta_0(N) \text{ as } b(N),\ \frac{\partial S^{-1}(n_{\mathrm{q}},\vartheta_{\mathrm{env}})}{\partial n_{\mathrm{q}}} \text{ as } a(N) \text{ and } \frac{\partial n_{\mathrm{q}}}{\vartheta_{\mathrm{env}}} \text{ as } c(N) \tag{3.64}$$

where N is the node number, and with assumption that:

$$\mathrm{d}n_{\mathrm{q}} \cong \Delta n_{\mathrm{q}} = n_{\mathrm{q}} - n_{\mathrm{q}}(N),\ \ \mathrm{d}\vartheta_{\mathrm{env}} \cong \Delta\vartheta_{\mathrm{env}} = \vartheta_{\mathrm{env}} - \vartheta_{0\mathrm{env}} \tag{3.65}$$

Eq. (3.63) can be written as:

$$\begin{aligned}\hat{\vartheta} &\cong b(N) + a(N)\left[n_{\mathrm{q}} - n_{\mathrm{q}}(N)\right] + a(N)c(N)(\vartheta_{\mathrm{env}} - \vartheta_{0\mathrm{env}}) = \\ &= b(N) + a(N)\left[n_{\mathrm{q}} - n_{\mathrm{q}}(N) + c(N)(\vartheta_{\mathrm{env}} - \vartheta_{0\mathrm{env}})\right]\end{aligned} \tag{3.66}$$

The coefficient $c(N)$ is interpreted as the inclination, in node N, of the linearized inverse characteristic in relation to the environmental temperature. Due to the non-linearity of the static characteristic, the inclination generally takes two values depending on the value of this temperature: c_+ for the value higher or equal to the nominal environmental temperature $\vartheta_{0\mathrm{env}}$ and c_- if the value is lower. The values of these inclinations are calculated as:

$$c_+(N) = \frac{n_{2,\mathrm{q}}(N) - n_{2,\mathrm{q}_+}(N)}{\Delta\vartheta_{\mathrm{env,max}}},\quad c_-(N) = \frac{n_{2,\mathrm{q}}(N) - n_{2,\mathrm{q}_-}(N)}{\Delta\vartheta_{\mathrm{env,min}}} \tag{3.67}$$

where $\Delta\vartheta_{\mathrm{env,min}}$, $\Delta\vartheta_{\mathrm{env,max}}$ are the minimum and maximum values of $\Delta\vartheta_{\mathrm{env}}$, $n_{2,\mathrm{q}+}$ and $n_{2,\mathrm{q}-}$ are the indications calculated for these extreme values, respectively.

The determination of the coefficients of the two-dimensional linear approximation is carried out on the basis of the nodal values. For the exemplary analog converter working in the given range of environmental temperature, the parameters of the nodes are the same as for the one-dimensional approximation. It means that the node number takes values $N = 0, ..., 4$, the amplification coefficient is $k_V = 32$ and the maximum number of ADC quanta $N_q = 2^{16}$. The nominal value of the reference resistor used in the instrument is $R_{\text{ref}} = 5.1253 \cdot 10^3\ \Omega$ and its temperature coefficient $\varepsilon = 30$ ppm/°C. The values of the environmental temperature change around its nominal value $\vartheta_{0\text{env}} = 25^{\text{o}}\text{C}$ from the maximum $\vartheta_{\text{env,max}} = 45°\text{C}$ to the minimum $\vartheta_{\text{env,min}} = 5°\text{C}$. On the basis of these values, one can calculate the dependencies of the ADC indications from values of the sensor resistance R for the extreme values of the environmental temperature. Taking into account the values of the described parameters, the indication (3.55) of the instrument working at the environmental temperature of 45°C is expressed as:

$$n_{\text{q+}}(N) = \text{ent}\left[32 \cdot 2^{16} \frac{R(N)}{5.1253 \cdot 10^3 \left[1 + 20 \cdot 30 \cdot 10^{-6}\right]} + 0.5\right] = \text{ent}\left[408.931 R(N) + 0.5\right] \quad (3.68)$$

and at the temperature 5°C:

$$n_{\text{q-}}(N) = \text{ent}\left[32 \cdot 2^{16} \frac{R(N)}{5.1253 \cdot 10^3 \left[1 - 20 \cdot 30 \cdot 10^{-6}\right]} + 0.5\right] = \text{ent}\left[409.422 R(N) + 0.5\right] \quad (3.69)$$

The minimum and maximum indications calculated for all nodes accordingly with Eqs. (3.68) and (3.69) are presented in Tab. 3.12.

Table 3.12

ADC indications determined on the basis of Eqs. (3.68), (3.69) and (3.5) in the nodes of two-dimensional exemplary inverse static characteristic including the influence of the environmental temperature, N is the node number, $n_{\text{q}}(N)$ – the indication in the nominal environmental temperature $\vartheta_{0\text{env}} = 25^{\text{o}}\text{C}$, $n_{\text{q+}}(N)$ in the temperature $\vartheta_{\text{env,max}} = 45°\text{C}$, $n_{\text{q-}}(N)$ in $\vartheta_{\text{env,min}} = 5°\text{C}$

N	0	1	2	3	4
$\vartheta(N)$°C	0	25	50	75	100
$R(N)$ Ω	100.0000	109.7347	119.3971	128.9874	138.5055
$n_{\text{q}}(N)$	40918	44901	48854	52779	56673
$n_{\text{q+}}(N)$	40893	44874	48825	52747	56639
$n_{\text{q-}}(N)$	40942	44928	48884	52810	56707

Accordingly with Eq. (3.67), the inclinations $c_{-}(N)$ and $c_{+}(N)$, calculated for an environmental temperature lower and higher than the nominal one, are:

$$c_{+}(N)=\frac{n_{q}(N)-n_{q+}(N)}{20}\frac{1}{^{o}C},\ c_{-}(N)=\frac{n_{q}(N)-n_{q-}(N)}{-20}\frac{1}{^{o}C} \tag{3.70}$$

Their values were obtained on the basis of data from Tab. 3.12 and they are presented in Tab. 3.13.

Table 3.13

Inclinations calculated accordingly with expressions (3.67), N is the node number

N	0	1	2	3	4
$c_{-}(N)$°C	1.2	1.35	1.5	1.55	–
$c_{+}(N)$°C	1.25	1.35	1.45	1.6	–

The inclinations of Tab. 3.13 have similar values, which means that only one inclination can be used for positive and negative variations of the $\Delta\vartheta_{env}$. For further considerations, the average value of the inclinations (3.70):

$$c(N)=\frac{c_{+}(N)+c_{-}(N)}{2} \tag{3.71}$$

is used. Values calculated on the basis of data from Tab. 3.13 are presented in the table 3.14 together with the rest of the parameters of the two-dimensional linear approximation, which are the same as for one-dimensional approximation (see Tab. 3.3).

Table 3.14

Parameters of the segments of the five-node two-dimensional linear approximation of the exemplary inverse characteristic calculated for model (3.55) based on the analytical description (3.5) of the sensor and Eq. (3.71), N is the node number

N	0	1	2	3	4
$R(N)$ Ω	100.0000	109.7347	119.3971	128.9874	138.5055
$n_q(N)$	40918	44901	48854	52779	56673
$a(N)\cdot10^{-3}$°C	6.2767	6.3243	6.3694	6.4201	
$b(N)$°C	-0.0140	24.9782	49.9833	74.9888	
$c(N)$°C	1.225	1.35	1.475	1.575	

The coefficients contained in Tab. 3.14 describe two-dimensional exemplary inverse characteristic created with using the segmental linear approximation, which is shown

in the graphical form in Fig. 3.11. The approximation coefficients are stored in the look-up table and applied in the algorithm of the two-dimensional static reconstruction described below.

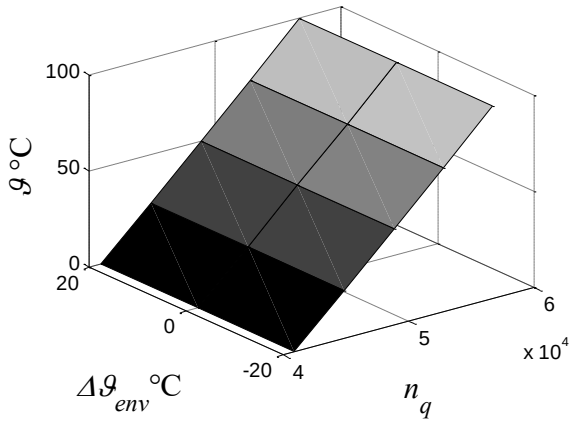

Fig. 3.11. Graphical view of the linear approximation of the exemplary two-dimensional inverse function

The two-dimensional reconstruction algorithm is performed in the following steps:

- The ADC indication n_q is compared with the node values $n_q(N)$, $N = 0, 1, ..., 4$, which allows the determination of suitable node number N.
- Based on the determined node number N, the suitable value of $c_2(N)$ is read from the look-up table and the correction $c(N)\cdot\Delta\vartheta_{env}$ is calculated, where $\Delta\vartheta_{env} = \hat{\vartheta}_{env} - \vartheta_{0env}$, $\hat{\vartheta}_{env}$ is the result of the environmental temperature measurement, $\vartheta_{0env} = 25^oC$.
- The calculated correction is added to the row result n_q, which enables obtaining the corrected result $\hat{n}_q$.
- The other parameters $a(N)$, $b(N)$ and $n_q(N)$ for the determined node number N are read from the look-up table.
- Based on the result $\hat{n}_q$ and read parameters, the input temperature estimate is calculated accordingly with Eq. (3.23), the same as used for the one-dimensional reconstruction equation.

Using the two-dimensional model (3.55), one can carry out experiments, which enable the determination of errors specific to the reconstruction. In real measurement conditions, the model should take noise errors into account, which causes the ADC indications in this case to be expressed as:

$$n_q = \mathrm{ent}\left[409.176\cdot\frac{R(\vartheta)}{1+\Delta\hat{\vartheta}_{env}\cdot\varepsilon} + e_{noi} + 0.5\right] \tag{3.72}$$

where in the performed experiments e_{noi} is the normal noise $N(0; 1)$. Moreover, this model has to be completed by the expression, which describes the result of the environmental temperature measurement. With the assumption that this temperature is measured with resolution 0.1°C, the estimate of its change is described by the following equation:

$$\Delta\hat{\vartheta}_{env} = \hat{\vartheta}_{env} - \vartheta_{0,env}, \quad \text{where} \quad \hat{\vartheta}_{env} = 0.1 \cdot \text{ent}\left(10 \cdot \vartheta_{env} + 0.5\right) \tag{3.73}$$

Experiment 3.8. Let us assume that the input temperature changes from 0 to 100°C and the environmental temperature changes from 5 to 45°C. At the beginning of every step of the experiment, two values are randomly taken: the input temperature and the environmental temperature – both in their ranges accordingly with suitable rectangular distributions. Next, two indications are determined. The first indication is calculated on the basis of Eq. (3.55), which does not include the noise error, and assuming that the environmental temperature is measured accurately. The second indication is calculated using Eqs. (3.72) and (3.73), i.e. for the indications containing all considered errors. For both kinds of indication, the reconstruction is performed accordingly with the described algorithm on the basis of the approximation parameters presented in Tab. 3.14. The distributions of the reconstruction errors are presented in the form of histograms in Fig. 3.12.

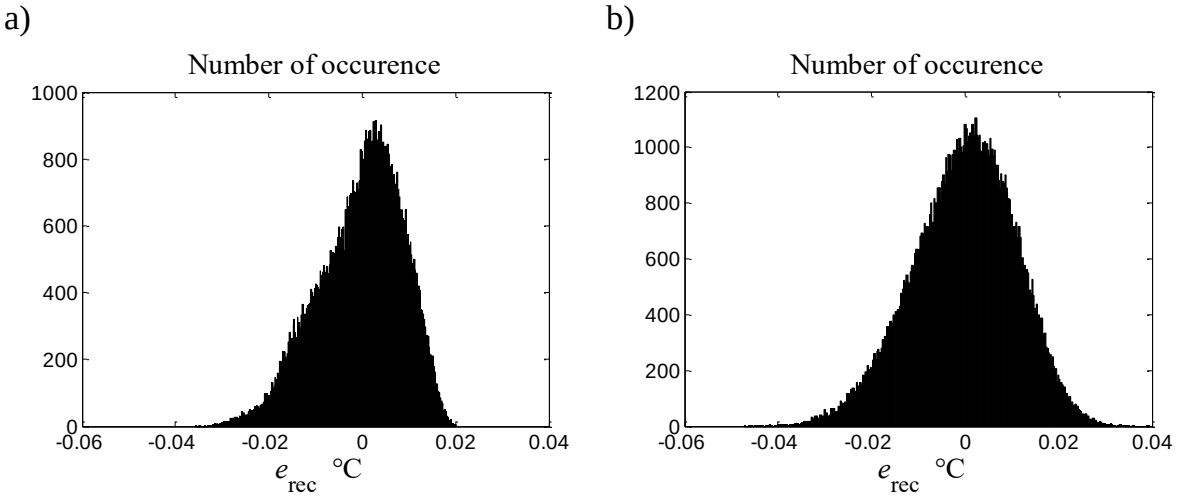

Fig. 3.12. Histograms of total errors of the two-dimensional static reconstruction: a) the reconstruction is performed on the basis of ADC indications burdened by the approximation error and the quantization error (values of the environmental temperatures are exactly known) accordingly with Eq. (3.55), the standard deviation of the reconstruction error is $\sigma_{rec} = 9.0 \cdot 10^{-3}$°C, b) indications are calculated accordingly with equations (3.72) and (3.73), which means that they are additively burdened by the noise errors and the measurement errors of the environmental temperature, $\sigma_{rec} = 11.1 \cdot 10^{-3}$°C

The histogram of the reconstruction error from Fig. 3.12a enables the determination of the standard deviation of the two-dimensional approximation error e_{app} because in this case it is:

$$\sigma_{app} = \sqrt{\sigma_{rec}^2 - \sigma_q^2} \tag{3.74}$$

where e_q is the quantization error with variance (3.39). After introducing the suitable values to Eq. (3.75), we obtain:

$$\sigma_{app} = 10^{-3}\sqrt{9^2 - 3.36} = 8.8 \cdot 10^{-3}\ ^{o}\text{C} \tag{3.75}$$

Having known the standard deviation σ_{app}, one can calculate the standard deviation σ_{env} of the error caused by the measurement of the environmental temperature, which is described by Eq. (3.74). For the histogram of Fig. 3.12b, we have:

$$\sigma_{env} = \sqrt{\sigma_{rec}^2 - \sigma_{app}^2 - \sigma_q^2 - \sigma_{noi}^2} \tag{3.76}$$

where σ_{noi} is the normal noise error $N(0; 1)$. Using these known values of the standard deviations, we obtain the following:

$$\sigma_{env} = 10^{-3}\sqrt{11.1^2 - 8.8^2 - 3.36 - 40.3} = 1.45 \cdot 10^{-3}\ ^{o}\text{C} \tag{3.77}$$

The value obtained is less than the other standard deviations, which means that the measurement of environmental temperature with resolution 0.1°C is accurate enough for the sampling instrument considered.

3.3.3. Calibration of instrument with two-dimensional analytical reconstruction

Taking into account that nonlinearity of the two-dimensional static characteristic of the analog converter is not great, one can carry out the calibration in the same way as applied for the one-dimensional characteristic, which is described in Section 3.2.3. It means that the calibration consists in measurements of the characteristic in the selected points and in modifying the approximation parameters on the basis of the obtained indications. As the environmental temperature can be one of the causes of the characteristic drift, the calibration must be performed at the nominal environmental temperature ϑ_{0env} = 25°C, which means that the indications obtained for this temperature are the same as in Tab. 3.4. The calibration procedure is presented in the following example.

Example 3.8. Two resistors: $R_1 = 100.0\ \Omega$ and $R_2 = 138.505\ \Omega$ are used to calibrate the instrument that performs the exemplary two-dimensional linear approximation. The resistor R_1 corresponds to the input temperature $\vartheta_1 = 0^{\circ}\mathrm{C}$ and R_2 – to the temperature $\vartheta_2 = 100^{\circ}\mathrm{C}$. The use of the resistor R_1 in the nominal environmental temperature $\vartheta_{0\mathrm{env}} = 25^{\circ}\mathrm{C}$ gives the indication $n_{\mathrm{qsh}}(0) = 40931$ but, if the resistor R_2 is connected to the input, the indication for the node number 4 is $n_{\mathrm{qsh}}(4) = 56689$. These indications are the same as in Example 3.6, which means that the constant component (3.27) of the correction is $\Delta_1 = 13$ and the inclination coefficient (3.30) is equal to $s = 0.03^{\circ}\mathrm{C}^{-1}$.

Based on the data presented, the other corrected indications in the nodes of the inverse two-dimensional static characteristic are calculated in the following way.

For node $N = 0$ one obtains:

$$n_{\mathrm{qsh}-}(0) = n_{q-}(0) + \Delta_1 + s \cdot (\vartheta(0) - \vartheta_1) = 40942 + 13 + 0.03 \cdot (0 - 0) = 44955$$
$$n_{\mathrm{qsh}+}(0) = n_{\mathrm{q}+}(0) + \Delta_1 + s \cdot (\vartheta(0) - \vartheta_1) = 40893 + 13 + 0.03 \cdot (0 - 0) = 40906$$

where the symbols ‘-‘ and ‘+’ denote the indications at the environmental temperatures $\vartheta_{\mathrm{env}} = 5^{\circ}\mathrm{C}$ and $\vartheta_{\mathrm{env}} = 45^{\circ}\mathrm{C}$, respectively.

For $N = 1$ we have:

$$n_{\mathrm{qsh}-}(1) = n_{q-}(1) + \Delta_1 + s \cdot (\vartheta(1) - \vartheta_1) = 44928 + 13 + 0.03 \cdot (25 - 0) = 44942$$
$$n_{\mathrm{qsh}+}(1) = n_{\mathrm{q}+}(1) + \Delta_1 + s \cdot (\vartheta(1) - \vartheta_1) = 44874 + 13 + 0.03 \cdot (25 - 0) = 44888$$

For $N = 2$:

$$n_{\mathrm{qsh}-}(2) = n_{q-}(2) + \Delta_1 + s \cdot (\vartheta(2) - \vartheta_1) = 48884 + 13 + 0.03 \cdot (50 - 0) = 48899$$
$$n_{\mathrm{qsh}+}(2) = n_{\mathrm{q}+}(2) + \Delta_1 + s \cdot (\vartheta(2) - \vartheta_1) = 48825 + 13 + 0.03 \cdot (50 - 0) = 48840$$

For $N = 3$:

$$n_{\mathrm{qsh}-}(3) = n_{q-}(3) + \Delta_1 + s \cdot (\vartheta(3) - \vartheta_1) = 52810 + 13 + 0.03 \cdot (75 - 0) = 52825$$
$$n_{\mathrm{qsh}+}(3) = n_{\mathrm{q}+}(3) + \Delta_1 + s \cdot (\vartheta(3) - \vartheta_1) = 52747 + 13 + 0.03 \cdot (75 - 0) = 52762$$

and for $N = 4$:

$$n_{\mathrm{qsh}-}(4) = n_{q-}(4) + \Delta_1 + s \cdot (\vartheta(4) - \vartheta_1) = 56707 + 13 + 0.03 \cdot (100 - 0) = 56723$$
$$n_{\mathrm{qsh}+}(4) = n_{\mathrm{q}+}(4) + \Delta_1 + s \cdot (\vartheta(4) - \vartheta_1) = 56639 + 13 + 0.03 \cdot (100 - 0) = 56655$$

The node values of indications are presented in the table 3.15. The parameters of he two-dimensional linear approximation, which are calculated on the basis of these indications in the way described in the previous chapter, are contained in Tab. 3.16.

Table 3.15

ADC indications determined by the effect of calibration

N	0	1	2	3	4
$\vartheta(N)$°C	0	25	50	75	100
$n_{q\text{sh}}(N)$	40931	44915	48869	52794	56689
$n_{q\text{sh-}}(N)$	40955	44942	48899	52825	56723
$n_{q\text{sh+}}(N)$	40906	44888	48840	52762	56655

Table 3.16

Parameters of the segments approximating the exemplary two-dimensional static characteristic obtained as the results of calculations performed on indications from Tab. 3.14, N is the node number

N	0	1	2	3	4
$a(N)\cdot 10^{-3}$°C	6.2750	6.3227	6.3703	6.4176	_
$b(N)$°C	-0.01533	24.98328	49.98341	74.98714	_
$c(N)$°C	1.2216	1.3441	1.4631	1.5785	

The error caused by the considered calibration can be determined by using the experiment in which the reconstruction error is calculated for the indications burdened by all the considered errors. These indications are determined by using the two-dimensional analytical model of the analog converter containing the influence of the drift. This model has the form:

$$n_{\text{q}} = \text{ent}\left[409.176\cdot\frac{R(\vartheta)}{1+\Delta\vartheta_{\text{env}}\cdot\varepsilon}\left(1+\Delta_{\text{inc}}\right)+\Delta_{\text{sh}}+e_{\text{noi}}+0.5\right] \tag{3.78}$$

that is obtained on the basis of Eqs. (3.35) and (3.75), where $R(\vartheta)$ is the resistance of the sensor dependent on the input temperature ϑ, Δ_{inc} – the drift coefficient of the static characteristic inclination, Δ_{sh} – the characteristic shift caused by the drift, $\Delta\vartheta_{\text{env}}$ – the environmental temperature, ε – the coefficient describing the influence of the environmental temperature on the characteristic, e_{noi} is the noise error.

The parameters of the linear approximation contained in Tab. 3.16 has been determined on the basis of the calibration results which enable calculation of values of the drift parameters in the nominal environmental temperature. For $\Delta\vartheta_{\text{env}} = 0$, one obtains: $\Delta_{\text{inc}} = 1.57\cdot 10^{-4}$, $\Delta_{\text{sh}} = 7$°C (see Eqs. (3.37) and (3.38)). For these values and for the environmental temperature coefficient $\varepsilon = 30$ ppm/°C, the model (3.78) takes the form:

$$n_{\mathrm{q}} = \mathrm{ent}\left[409.176 \cdot \frac{R(\vartheta)}{1 + \Delta\vartheta_{\mathrm{env}} \cdot 30 \cdot 10^{-6}} \left(1 + 1.57 \cdot 10^{-4}\right) + 7 + e_{\mathrm{noi}} + 0.5 \right] \qquad (3.79)$$

where e_{noi} is the error caused by the normal noise $N(0; 1)$.

Experiment 3.9. This experiment is aimed at determination of distributions of the reconstruction error for the parameters of the linear approximation from Tab. 3.16 and indications calculated accordingly with Eq. (3.79). One assumes that the input temperature ϑ varies randomly with the rectangular distribution in the range from 0 to 100°C changing the sensor resistance R accordingly with Eq. (3.5). The environmental temperature ϑ_{env} varies in the range from 5 to 45°C accordingly with the same kind of the distribution. The changes of this temperature are determined as: $\Delta\hat{\vartheta}_{\mathrm{env}} = \hat{\vartheta}_{\mathrm{env}} - \vartheta_{0\mathrm{env}}$ where $\hat{\vartheta}_{\mathrm{env}}$ is a measurement result of the environmental temperature obtained with the resolution 0.1°C as it is described by the equation (3.70). The reconstruction is carried out on the basis of the parameters from Tab. 3.16 with using the calculated values of both temperatures. The histogram of the reconstruction error is presented in Fig. 3.15b. The same operations are performed for the indications obtained with assumption that the noise does not occur and the environmental temperature is known exactly. The histogram of this error is shown in Fig. 3.13a.

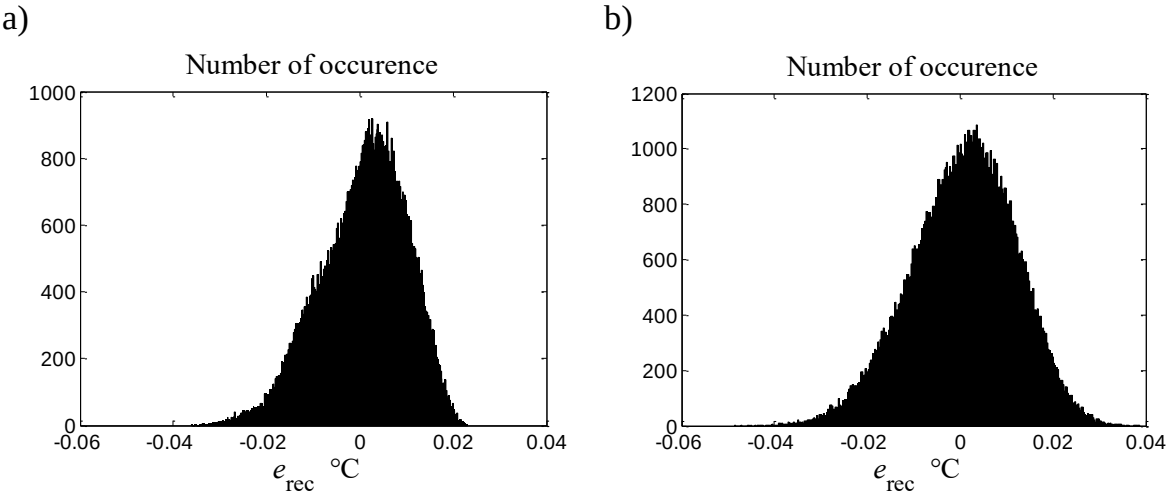

Fig. 3.13. Histograms of the reconstruction errors if the parameters of the two-dimensional static inverse characteristic are results of the calibration: a) the indications are burdened only by the quantization errors, $\sigma_{\mathrm{rec}} = 9.3 \cdot 10^{-3}$°C, b) the indications are burdened both by the quantization and the noise errors while the environmental temperature is measured with resolution 0.1, $\sigma_{\mathrm{rec}} = 11.3 \cdot 10^{-3}$°C

The reconstruction error e_{rec} from Fig. 3.13b is composed of the approximation error e_{app}, the quantization error e_{q}, the standard deviation of which is given by Eq. (3.39), the noise error e_{noi} with the standard deviation (3.40), the calibration error e_{cal} and the measurement error of the environmental temperature e_{env} described by Eq. (3.75).

Having known the distribution of the reconstruction error shown in Fig. 3.13b, one can calculate the standard deviation of the calibration error based on the expression:

$$\sigma_{\text{cal}} = \sqrt{\sigma_{\text{rec}}^2 - \sigma_{\text{app}}^2 - \sigma_{\text{q}}^2 - \sigma_{\text{noi}}^2 - \sigma_{\text{env}}^2} \tag{3.80}$$

After introducing the suitable values to Eq. (3.80), one obtains:

$$\sigma_{\text{cal}} = 10^{-3}\sqrt{11.3^2 - 8.8^2 - 3.36 - 40.3 - 1.57^2} = 2.12 \cdot 10^{-3}\ ^{\text{o}}\text{C} \tag{3.81}$$

which means that this error is of minor importance. Thus, the described calibration in two end points is relatively accurate in the measurement conditions for the exemplary instrument with the considered two-dimensional linear approximation of the static characteristic.

3.3.4. Identification of parameters of two-dimensional analytical reconstruction

In measurement practice, the key issue is to limit the number of an input quantity standards which are used for an identification of the static characteristic. As result of considerations in Section 3.2.4, the described indirect method requires the smallest number of standards for the identification of the inverse one-dimensional static characteristic approximated by linear segments. The results that are contained in the table 3.9 suggest that even three standards could be enough to determine the approximating polynomial with acceptable inaccuracy. The identification method described in this chapter is based on conclusions drawn in Section 3.2.4.

Let us take that the experiment of the considered identification is carried out for the environmental temperatures stabilized at $\vartheta_{\text{env-}} = 5^{\text{o}}\text{C}$, $\vartheta_{0\text{env}} = 25^{\text{o}}\text{C}$ and $\vartheta_{\text{env+}} = 45^{\text{o}}\text{C}$. At every temperature, the same 3 standard resistors are used: $R_{\text{std}}(I_{\text{id}})$, values of which are known with resolution 0.001 Ω, I_{id} is the identification point number, $I_{\text{id}} = 1,\ldots,3$. Using these values, the input temperature $\vartheta(I_{\text{id}})$ is determined accordingly with Eq. (3.5) with the assumption that the connection of one of the resistors $R_{\text{std}}(I_{\text{id}})$ to the instrument input is the equivalent to the placement of the Pt100 sensor at the corresponding temperature $\vartheta(I_{\text{id}})$.

The two-dimensional inverse characteristic of the exemplary instrument is approximated by linear segments connecting $N_{\text{nod}} = 5$ nodes. The first stage of the identification consists in carrying out the measurements for 3 values of the temperature inside the instrument housing stabilized at the $\vartheta_{\text{env}} = 5^{\text{o}}\text{C}$, 25^{o}C and

45°C. For every temperature, the 3 standard resistors $R_{\text{std}}(I_{\text{id}})$, the values of which are presented in Tab. 3.17, are connected in sequence to the instrument input. Measurements are repeated 5 times for every resistor to decrease the influence of the noise by averaging the obtained indications. The calculated average values: $\bar{n}_{q0}(I_{\text{id}})$, $\bar{n}_{q-}(I_{\text{id}})$ and $\bar{n}_{q+}(I_{\text{id}})$, where $I_{\text{id}} = 1, ..., 3$, are located in the Tab. 3.17 as the final identification results.

One should notice that during all the measurement experiments the standard resistors work in stable nominal temperature 25°C, while the instrument itself works in the 3 described environmental temperatures.

Table 3.17

Averaged indications determined for 3 standard resistors $R_{\text{st}}(I_{\text{id}})$, $I_{\text{id}} = 1, ..., 3$, during the identification performed, respectively, at 3 values of the environmental temperature: 5°C, 25°C and 45°C

I_{id}	1	2	3
$\vartheta(I_{\text{id}})$°C	0.155	52.513	101.211
$R_{\text{std}}(I_{\text{id}})$ Ω	100.061	120.364	138.965
$\bar{n}_{q-}(I_{\text{id}})$	40967	49280	56896
$\bar{n}_{q0}(I_{\text{id}})$	40943	49250	56861
$\bar{n}_{q+}(I_{\text{id}})$	40918	49221	56827

The second stage of the identification consists in the determination of 3 analytical forms of the inverse characteristic as the second order polynomial, respectively, for temperatures $\vartheta_{\text{env}} = 5$, 25 and 45°C. The general form of this polynomial is as follows:

$$\hat{\vartheta} = a_0 + a_1 n_q + a_2 n_q^2 \tag{3.82}$$

where a_0, a_1 and a_2 are constant coefficients determined on the basis of indications from Tab. 3.17 and presented in the Tab. 3.18.

Table 3.18

Polynomial coefficients that approximate the exemplary two-dimensional inverse static characteristic at environmental temperatures $\vartheta_{\text{env}} = 5$, 25, and 45°C accordingly with Eq. (3.82)

	a_0	$a_1 \cdot 10^{-3}$	$a_2 \cdot 10^{-9}$
$\vartheta_{\text{env}} = 5$°C	-245.72148	5.755326	6.01684
$\vartheta_{\text{env}} = 25$°C	-245.80685	5.761800	5.999101
$\vartheta_{\text{env}} = 45$°C	-245.63312	5.758227	6.076019

The third stage of the identification consists of calculation of the parameters of the segments approximating the exemplary two-dimensional static characteristic between equally distant 5 nodes in the same way as described in Chapter 3.2 for the one-dimensional approximation. The final results are presented in Tab. 3.19.

Table 3.19

Parameters of the segments approximating in 5 nodes the exemplary two-dimensional static characteristic obtained indirectly by using polynomials of the form (3.82), parameters of which are contained in Tab. 3.17, N is the node number

N	0	1	2	3	4
n_q (N)	40918	44901	48854	52779	56673
$a(N)\cdot 10^{-3}$°C	6.27664	6.32425	6.37151	6.41841	_
b (N)°C	-0.01718	24.9829	49.9829	74.9913	_
$c(N)$°C	1.2194	1.3359	1.4570	1.5827	

The reconstruction is performed on the basis of parameters from Tab. 3.19 accordingly with the algorithm described in Section 3.3.2. The histograms of the reconstruction errors obtained in the same way as described in Experiment 3.8 are presented in Fig. 3.14.

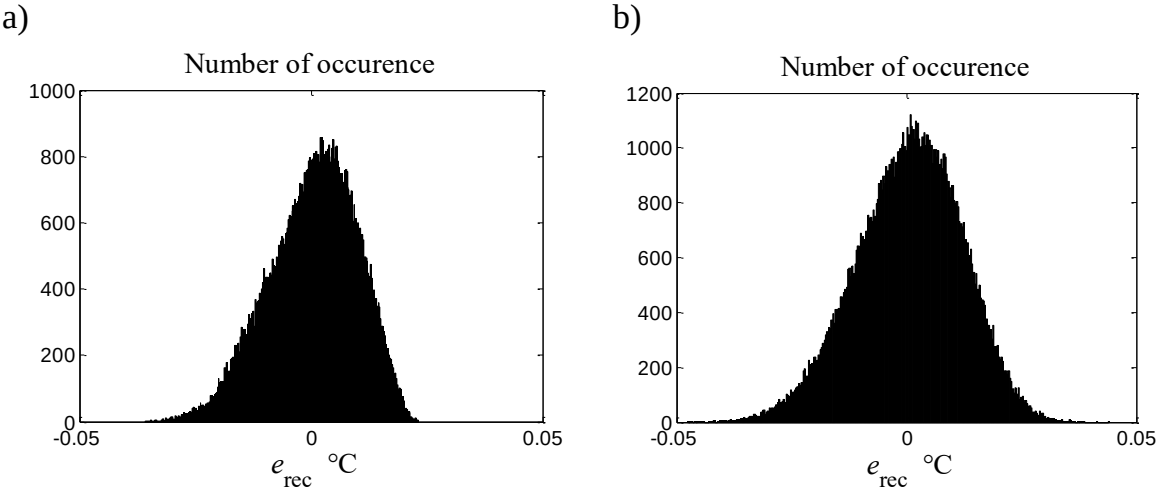

Fig. 3.14. Histograms of the reconstruction errors if the parameters of the two-dimensional static inverse characteristic are obtained as the results of the identification, the indications are burdened: a) by the identification, approximation, and quantization errors, $\sigma_{rec} = 9.5\cdot 10^{-3}$°C, b) additively by the noise error and error of the environmental temperature which is measured with resolution 0.1°C, $\sigma_{rec} = 11.5\cdot 10^{-3}$°C

The reconstruction error e_{rec} from Fig. 3.14b is the composition of the approximation error e_{app}, the quantization error e_q, the noise error e_{noi}, the measurement error of

the environmental temperature e_{env} and the identification error e_{id}. Taking this into account, the standard deviation of the identification error can be determined from the following equation:

$$\sigma_{\text{id}} = \sqrt{\sigma_{\text{rec}}^2 - \sigma_{\text{app}}^2 - \sigma_{\text{q}}^2 - \sigma_{\text{noi}}^2 - \sigma_{\text{env}}^2} \tag{3.83}$$

The standard deviation σ_{rec} is known from Fig. 3.14 and the values of the other standard deviations are the same as in the equation (3.77). For these values, we obtain the following:

$$\sigma_{\text{id}} = 10^{-3}\sqrt{11.5^2 - 8.8^2 - 3.36 - 40.3 - 1.45^2} = 3.0 \cdot 10^{-3}\ ^{\text{o}}\text{C} \tag{3.84}$$

which means that the identification error is comparable with the quantization error; thus, such a relatively simple identification procedure is accurate enough in the considered measurement conditions.

3.4. Basic properties of neural networks used for static reconstruction

Generally, neural static reconstruction can be considered as the task consisting in solving the inverse static characteristic modeled by an artificial neural network that approximates this characteristic [D1, H1]. The selected networks presented below meet the accuracy requirements of the reconstruction to a degree comparable with this achieved for the considered analytical algorithms.

An artificial neural network is composed of interconnected processing elements called neurons [A2, L4]. The general structure of a single neuron is shown in Fig. 3.15.

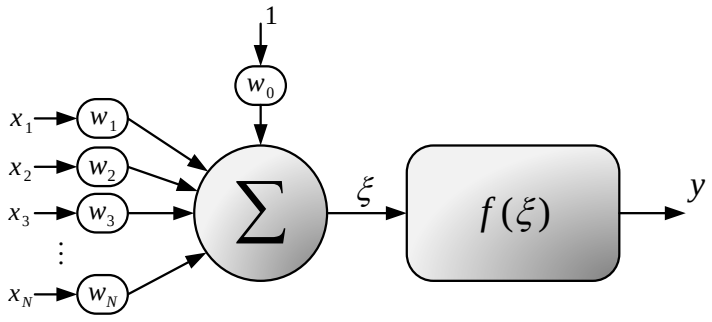

Fig. 3.15. General structure of an artificial neuron

The neuron consists of the two main elements seriously connected. The task of the first consists in summing of the signals obtained by multiplication of input signals x_j by suitably assigned weights w_j, $j = 1, \ldots, N$, N is the number of neuron inputs. Therefore, the output signal ξ of this element is given as the following linear combination:

$$\xi = \sum_{j=1}^{j=N} w_j x_j + w_0 \tag{3.85}$$

where w_0 is the threshold coefficient (bias). The procedure to determine values of these coefficients is called the learning process.

The weighted sum ξ is processed by the second element of the neuron accordingly with its transfer function $f(\xi)$, the form of which determines the properties of the neuron. The transfer functions of the sigmoidal type: unipolar and bipolar are the most commonly used in practice.

The unipolar transfer function is described by the relation:

$$f_{\mathrm{u}}(\xi) = \frac{1}{1 + \mathrm{e}^{-\beta\xi}} \tag{3.86}$$

where β is the parameter that shape the selected form of the function. In the learning process, it is necessary to know the first derivative of the transfer function [A2, A3]. The derivative of the function (3.87) is given by the equation:

$$\frac{\mathrm{d}f_{\mathrm{u}}(\xi)}{\mathrm{d}\xi} = \beta f_{\mathrm{u}}(\xi)\left(1 - f_{\mathrm{u}}(\xi)\right) \tag{3.87}$$

The bipolar transfer function is usually described by the expression:

$$f_{\mathrm{b}}(\xi) = \mathrm{tgh}(\beta\xi) \tag{3.88}$$

and its derivative has the form:

$$\frac{\mathrm{d}f_{\mathrm{b}}(\xi)}{\mathrm{d}\xi} = \beta\left(1 - f_{\mathrm{b}}^{2}(\xi)\right) \tag{3.89}$$

Diagrams of the considered sigmoidal transfer functions and their derivatives are shown in Fig. 3.16.

A set of neurons create an artificial neural network. The network composed of neurons with the sigmoidal transfer function, connected in this way that the signals propagate only in one direction from the input to the output of the network, is called feedforward sigmoidal neural network. The simplest structure of it, shown in Fig. 3.17a, consists of a single layer of neurons. It has small practical significance [A2] and is used in particular cases.

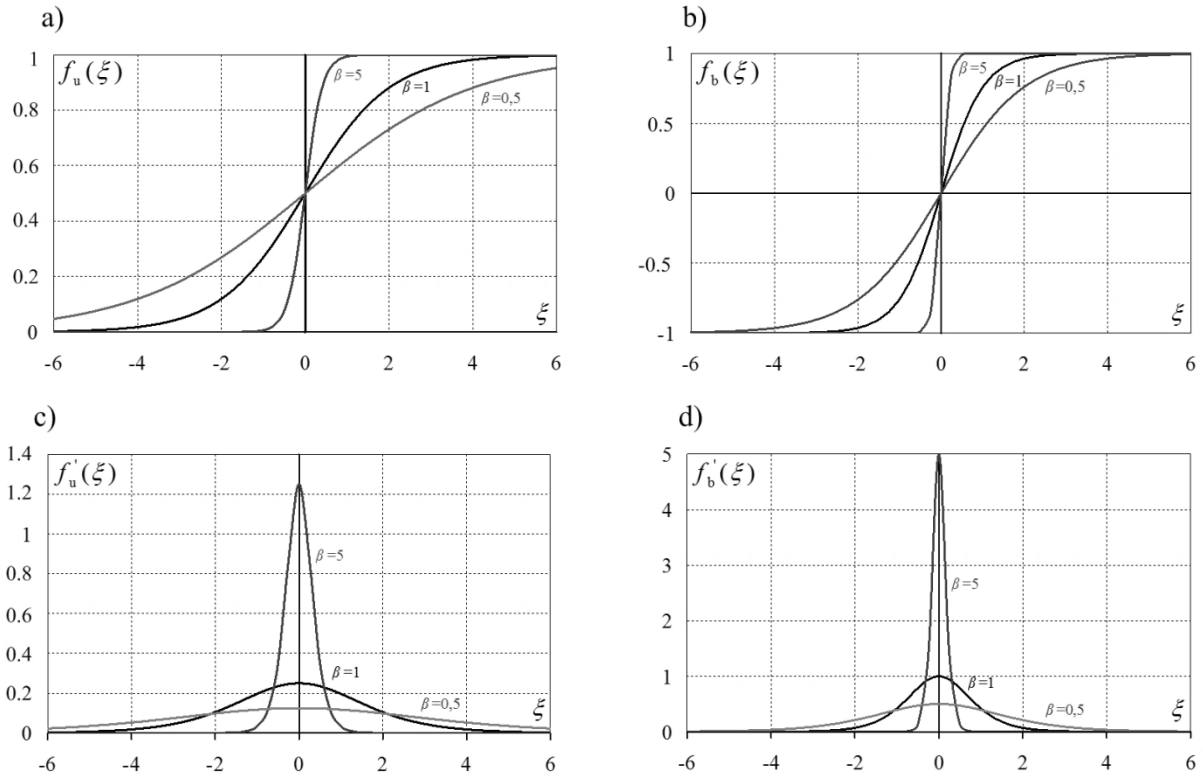

Fig. 3.16. Sigmoidal function diagrams for selected values of β coefficient: a) unipolar, b) bipolar, c) derivative of the unipolar function, d) derivative of the bipolar function

The feedforward multilayer network contains at least one hidden layer that transforms signals from the input layer to the output layer. The scheme of this network is shown in Fig. 3.17b.

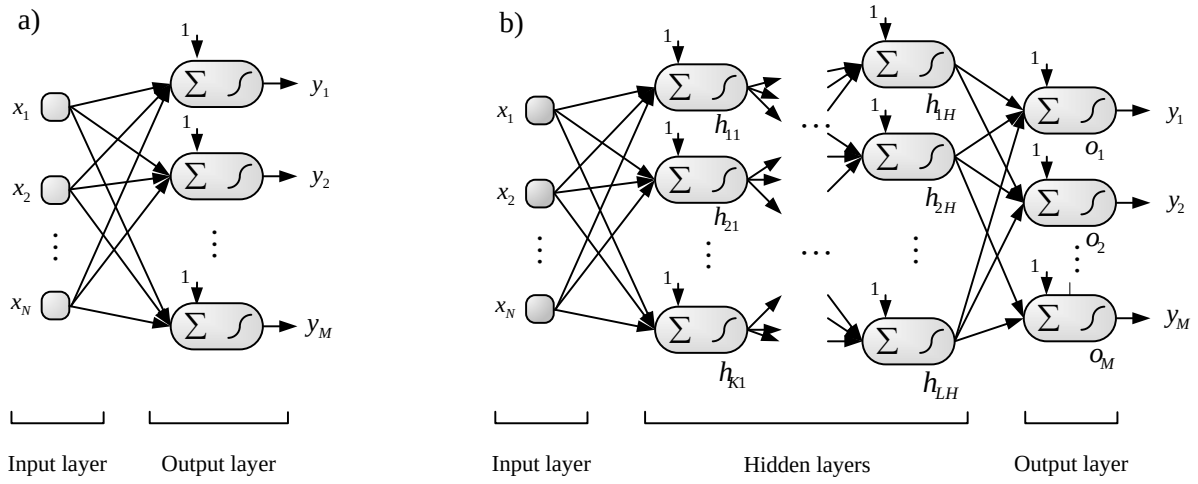

Fig. 3.17. The general structure of the feedforward sigmoidal neural network: a) single layer network, b) multilayer network, N is the number of network inputs, K – the number of neurons in the first hidden layer, L – the number of neurons in the H-th hidden layer, M – number of output neurons

The function implemented by the network with one hidden layer is of the form:

$$\boldsymbol{y} = f_{\mathrm{O}}\left[\boldsymbol{w}_{\mathbf{O}}\, f_{\mathrm{H}}\left(\boldsymbol{w}_{\mathbf{H}}\boldsymbol{x} + \boldsymbol{w}_{\mathbf{H0}}\right) + \boldsymbol{w}_{\mathbf{O0}}\right] \tag{3.90}$$

where: $\boldsymbol{x}$, $\boldsymbol{y}$ are vectors of the network input and output signals, respectively, $\boldsymbol{w}_{\mathbf{H}}$, $\boldsymbol{w}_{\mathbf{O}}$ – weight matrices of hidden and output layers, $\boldsymbol{w}_{\mathbf{H0}}$, $\boldsymbol{w}_{\mathbf{O0}}$ – bias vectors, f_{H}, f_{O} – sigmoidal transfer functions.

The input layer is usually applied for a pre-treatment of the input signals (e.g. normalization, coding) and their transfer to the first hidden layer. Neurons in the hidden and output layers perform processing accordingly with the taken sigmoidal functions. The connections between layers are formed in such a way that every neuron of the preceding layer is connected to every neuron of the next layer.

The feedforward multilayer sigmoidal neural network is usually called a Multi-Layer Perceptron or a Feed-Forward Neural Network as well as a Back-Propagation Neural Network. Networks of this type are most often described in the literature [A2] and used in practical applications. The main reason for this is the development of effective methods of their learning, numerous modifications and improvements.

A feedforward neural network performs mathematical operations on the input signals represented in discrete forms by numerical data. These operations depend on both the structure of the network itself and the values of the weight coefficients of the neurons. Taking this into account, we can treat the exemplary expression (3.93) as an approximation of a real dependence between the output and the input data. Assuming that the network structure and the neuron transfer functions do not change, the approximation properties of the network are fixed by the weight coefficients.

The corresponding values of the network coefficients are determined in the process of network learning which can generally be divided into supervised and unsupervised learning [B3]. In this book only the first method is applied for learning networks that perform static reconstruction. Using the supervised learning for the feedforward sigmoidal networks, one assumes application of a network learning set which consists of the input data vector and a corresponding output data vector. Elements of the learning input data vector are processed by the network, and the results obtained in the output of the network are compared with the output learning vector. The error, which is the difference between the compared values, is the primary parameter used to adjust the weights. It is the basis of the error backpropagation algorithm [L4], which is a generalization of the so-called delta rule that allows learning of multilayer neural networks. The operations performed accordingly with this algorithm consist of

optimizing the cost function by using a gradient method. The gradient of the cost function indicates the direction of the fastest growth and, by changing the sign, the direction of steepest descent. Therefore, it is possible to minimize the cost function by changing values of its variables, i.e. the weighting factors, in the direction of the steepest descent function in proportion to the gradient.

Using a neural network for static reconstruction requires preparing an appropriate set of learning patterns in the identification process, which consist of numbers representing the input and output static signals, respectively. The size of this set can influence, among others, on the network structure, and more specifically on the number of neurons in the hidden layer. The results of the simulation studies, described in [R5], show some regularity, which, in short, can be formulated in the following way: the more numerous is the set of learning data the more neurons in the hidden layer may be applied, providing, as a rule, a more accurate static reconstruction.

Evaluation of the neural approximation accuracy takes place in the process of network testing, wherein the set of testing data should be much larger than the set of learning data. This means that, in the simplest case, the identification results of the static characteristic should be divided into two separable sets: learning and testing. However, in practice, obtaining a suitably numerous set of measurement results of the static characteristic is difficult to carry out, time-consuming and costly, especially for nonelectrical quantities. Therefore, another approach is applied, which consists first in determiningan analytical approximation of the static characteristic on the basis of data obtained during the identification [M9]. Next, this approximation is used to calculate as numerous learning and testing sets as necessary [A2, A4]. One should emphasize that for the neural network working in the sampling instrument, testing consists in determination and analysis of distributions of the reconstruction errors by using Monte Carlo method [K4].

3.5. One-dimensional neural static reconstruction

3.5.1. One-dimensional neural approximation of the sensor inverse characteristic

As result of the analysis presented in [R5], a feedforward neural network with one hidden layer performs static reconstruction with a good enough accuracy. For the Pt100 sensor, the characteristic of which is nonlinear in a small degree,

the simplest structure 1-3-1 (one input, 3 neurons in hidden layer, one output) of this kind of network can be applied. The scheme describing mathematical operations performed by this network is shown in Fig. 3.20.

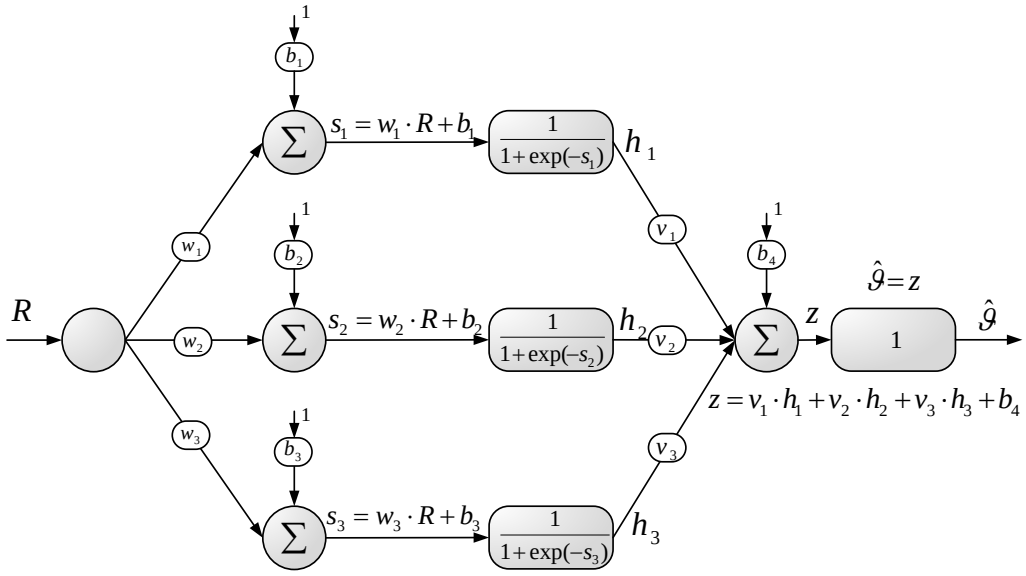

Fig. 3.18. Detailed structure of the 1-3-1 feedforward neural network applied for the static reconstruction of the input signal of the exemplary Pt100 sensor

The scheme shown in Fig. 3.18 can be interpreted as the graphical form of the reconstruction algorithm implemented by the neural network. The coefficients of this algorithm are determined on the basis of the analytical equation (3.5) that describes the static characteristic of the sensor. The network process the input value, which is the resistance R of the sensor, to the estimate $\hat{\vartheta}$ of the reconstructed temperature. Taking into account that the output layer is reduced to one neuron realizing function $\hat{\vartheta} = z$, the general equation (3.91) is transformed into the expression:

$$\hat{\vartheta} = \sum_{i=1}^{3} v_i \, f_{\mathrm{H}}\left(w_i R + b_i\right) + b_4 \tag{3.91}$$

where f_{H} is the sigmoidal transfer function (3.87) with $\beta = 1$.

The the network learning considered in this book is performed by using Lavenberg-Marquard method [W3]. For the network in Fig. 3.18, the set of learning data consists of two vectors: the input vector $\boldsymbol{R} = [R(1), R(2), ..., R(P)]$, wherein P is the number of the learning patterns, and the output vector $\vartheta = [\vartheta(1), \vartheta(2), ..., \vartheta(P)]$. The graphical illustration of the network learning process is presented in Fig. 3.19.

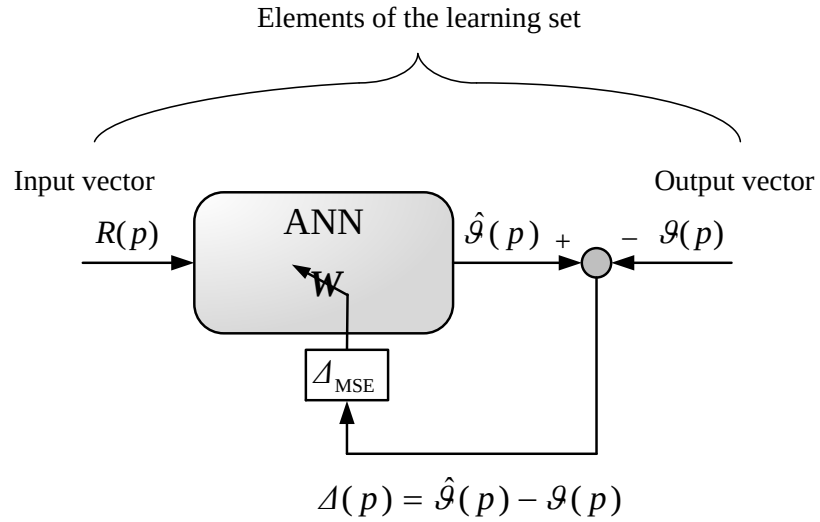

Fig. 3.19. Illustration of a supervised learning process of the exemplary neural network with one input and one output, p is the current number of the learning step $p = 1, \ldots, P$

One learning cycle (epoch) consists in comparing successive responses $\hat{\vartheta}(p)$ of the network withthe values of the input vector to determine the difference:

$$\Delta(p) = \hat{\vartheta}(p) - \vartheta(p) \tag{3.92}$$

where $\vartheta(p)$ is the postulated true value (pattern) of the response, $p = 1, \ldots, P$. After realization of the whole cycle of learning, the differences obtained are used to calculate the mean square error accordingly with the expression:

$$\Delta_{\text{MSE}} = \frac{\sum_{p=1}^{p=P} [\Delta(p)]^2}{P} \tag{3.93}$$

The value of the mean square error Δ_{MSE} is interpreted as a current measure of learning quality [B3] during the whole learning process and is used to modify the weighting coefficients $\boldsymbol{W}$ of the network in a manner dependent on the applied learning algorithm. After that, Δ_{MSE} is compared with the acceptable value and if it is greater than this value, the described procedure is repeated. The learning process is carried out until the calculated value of Δ_{MSE} is less than its taken value.

Example 3.9. The characteristic of the Pt100 sensor is described by Eq. (3.5). The neural network from Fig. 3.18 is dedicated to representing the inverse static characteristic of this sensor, The network is learned by using data set $\{R(P), \vartheta(P), P = 5\}$

which is created on the basis of the values from Tab. 3.1 and shown in Fig. 3.20. Every pattern in the set consists of two values: the first value is the sensor resistance, while the second is the input temperature.

$$\{100.0 \quad 0\}_{p=1}, \{109.7347 \quad 25\}_{p=2}, \{119.3971 \quad 50\}_{p=3}, \{128.9874 \quad 75\}_{p=4}, \{138.5055 \quad 100\}_{p=5}$$

Fig. 3.20. Data set used for learning the exemplary network, *p* is the current number of the pattern

Values of the network coefficients obtained after the selected step numbers of the learning process are presented in Tab. 3.19. At each step, all data from the set of patterns are used successively.

Table 3.20

Dependence of values of the network coefficients shown in Fig. 3.20 on the number of cycles used to learn the network by using the set from Fig. 3.22

Learning cycles	w_1 w_2 w_3	b_1 b_2 b_3	v_1 v_2 v_3	b_4	Δ_{MSE}
8	8.027609 6.571468 0.367789	-60.3751 52.08052 -43.6316	11.87466 11.31855 12.4188	12.22235	1093.97
16	4.766387 18.00239 -0.0736	-60.3952 52.15988 8.798834	43.41665 36.02665 -160.671	51.4009	2.44343
32	-2.90368 -6.75304 0.038204	-60.462 -51.9444 -4.60223	-0.56514 36.27894 282.8482	-88.5475	0.194
64	-1.80717 17.81642 0.022277	-60.4609 52.1508 -2.72876	-0.73434 -121.974 473.3286	-56.5376	0.023
128	-4.8623 13.83558 0.01363	-60.4709 52.11928 -1.74102	-0.3695 -163.086 768.6503	-149.416	0.0033
1000	-2.59298 7.645763 -0.0044	-60.4605 -52.1179 0.882913	-0.6474 759.7593 -2438.51	725.1683	4.23E-05

The exemplary learning progress is graphically presented in Fig. 3.21. The values of the learning quality measure Δ_{MSE}, which determines the inaccuracy of the learning process, are shown in this figure as a function of the number of the learning cycles.
The process is stopped after reaching the taken value of Δ_{MSE} equal to 10^{-6}. The final values of the coefficients are shown in the scheme of the neural network presented in Fig. 3.22.

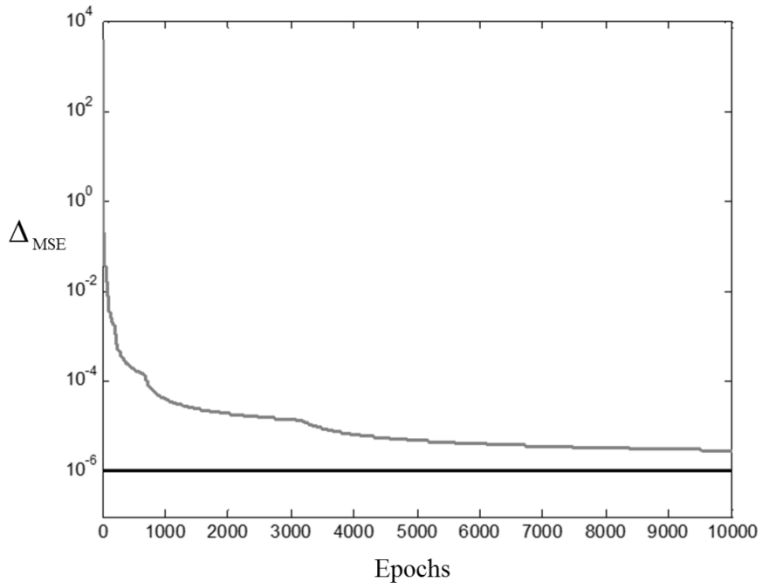

Fig. 3.21. Dependence of the learning quality measure Δ_{MSE} from the number of learning cycles (Epochs) in the case if the set from Fig. 3.20 is used to learn the network from Fig. 3.19

As in from Fig. 3.21, the learning process can be ended much earlier if one takes $\Delta_{MSE} = 10^{-4}$ for example. But one should notice that this value could not be acceptable because the final decision about ending this process must be made on the basis of knowledge about the reconstruction error distribution.

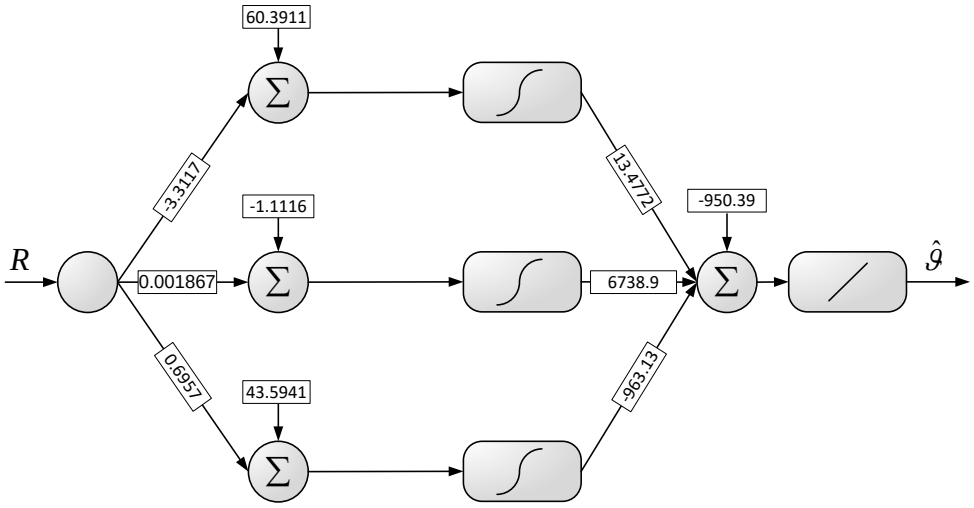

Fig. 3.22. Values of the weight coefficients of the neural network, which are obtained as a result of the learning process performed on the basis of data presented in Fig. 3.20

The scheme in Fig. 3.22 presents the structure of the neural network approximating the inverse characteristic of the Pt100 sensor and the values of its parameters. The approximation error of this network is presented in analytical form in Fig. 5.23a. From another point of view, the scheme from Fig. 3.22 can be treated as a specific neural description of the algorithm which performs the static reconstruction of the sensor input signal on the basis of values of its resistance.

After the learning process, it is necessary to evaluate the final inaccuracy of the network as the performer of the static reconstruction. This is done by testing the network with using a suitable numerous set of the input data and a corresponding set of the output data, both have to be known with a suitable accuracy. One should notice that the testing in the case if a network is used for realizing the signal reconstruction consists in determining the reconstruction error distribution by using the Monte Carlo method in the same way as for the analytical reconstruction.

Experiment 3.10. After learning, the network of Fig. 3.22 is tested in the simulative way in 100,000 steps. At each step, the true values of the input temperature ϑ are taken randomly from the range 0 to 100°C according to the rectangular distribution. After introducing this value into Eq. (3.5), one obtains the resistance R, on the basis of which the estimate of the input temperature is determined by using the considered network. Both values are subtracted and the resultis treated as the value of the approximation error, which is located at the set of error values. After finishing all steps, the approximation error is presented in the form of histogram shown in Fig. 3.23b. The standard deviations of this error and other errors that influence inaccuracy of the reconstruction are compared to evaluate whether the reconstruction error takes values comparable to the other errors.

a) b)

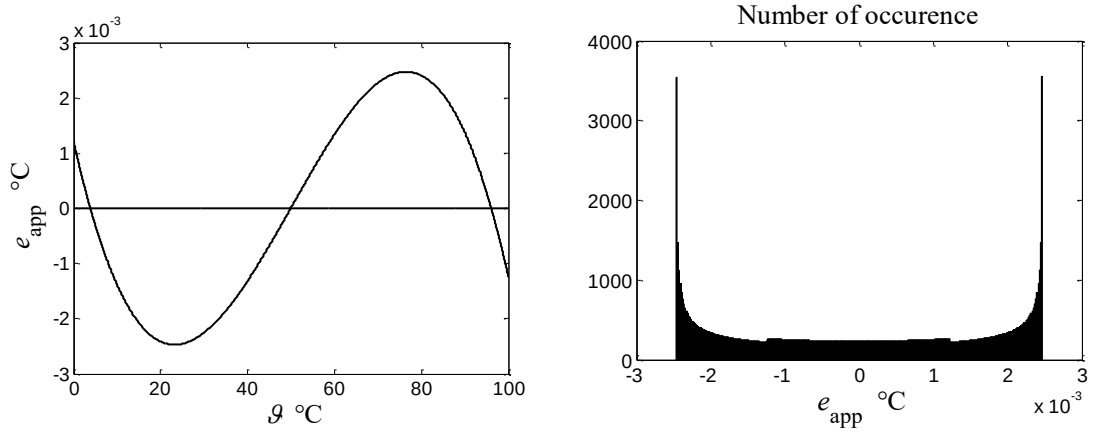

Fig. 3.23. a) Dependence of the approximation error on the input temperature for the neural network of Fig. 3.22, which is learned in 5 points accordingly with the set from Fig. 3.20, b) histogram of this error obtained by using Experiment 3.10, $\sigma_{app} = 1.71 \cdot 10^{-3}$ °C

As it results from comparing figures 3.5b and 3.23b, the error of the neural approximation is less than that of the approximation composed of the linear segments, despite the fact that the network from Fig. 3.22 is of the very simple structure. This feature is connected with a relatively low nonlinearity of the sensor characteristic. For stronger nonlinearities, one can suppose that more neurons in the hidden layer should be used. To check how the approximation error depends on the number of neurons in the hidden layer and the number of points in the learning set, the simulation experiments were carried out in the same way as described in Experiment 3.10. The results are presented in the Tab. 3.21.

Table 3.21

Standard deviations of the approximation error in dependence of the parameters of neural network from Fig. 3.22

$\sigma_{napp} \cdot 10^3$ °C		Number P of elements in learning set			
		5	8	12	16
Number of neurons in the hidden layer	3	1.71	1.40	1.32	1.28
	5	1.71	1.40	0.0224	0.0320
	7	1.71	1.40	0.0190	0.0372
	9	1.71	1.41	0.0119	0.0408
	11	1.75	1.40	0.00373	0.0127

The basic conclusion which one can draw from the results contained in Tab. 3.21 is that the approximation error of the network with one hidden layer can be significantly less than the error of the linear segmental approximation determined under comparable conditions. The error decreases with increasing the number of learning points, but only if one uses a suitable number of neurons in the hidden layer. This property may be important for the static characteristics of sensors with relatively strong nonlinearity, while 3 neurons in this layer are a sufficient number for the considered characteristic.

3.5.2. One-dimensional static neural reconstruction in exemplary instrument

As considered in Section 3.2, the static reconstruction of the input signal of the exemplary instrument is performed on the basis of the inverse model of the analog converter and the ADC indication. Such a model is obtained as an approximation of the static characteristic inverse to Eq. (3.20). In the case of the analytical

reconstruction, the model takes the form of linear segments, while for the neural reconstruction, it is approximated by a structure and coefficients of the neural network, which is created as effect of the learning process.

Let us use the same nodal values for determination of the neural network parameters as applied in the case of the linear approximation of the inverse static characteristic. Based on the data from Tab. 3.3, one obtains the learning set presented in Fig. 3.24. The scheme of the exemplary neural network, parameters of which are obtained after learning the network with using this set, is shown in Fig. 3.25.

$$\{40918 \quad 0\}_{p=1}, \{44901 \quad 25\}_{p=2}, \{48854 \quad 50\}_{p=3}, \{52779 \quad 75\}_{p=4}, \{56673 \quad 100\}_{p=5}$$

Fig. 3.24. Data set used for learning the exemplary network from Fig. 3.25, where p is the current number of the learning pattern

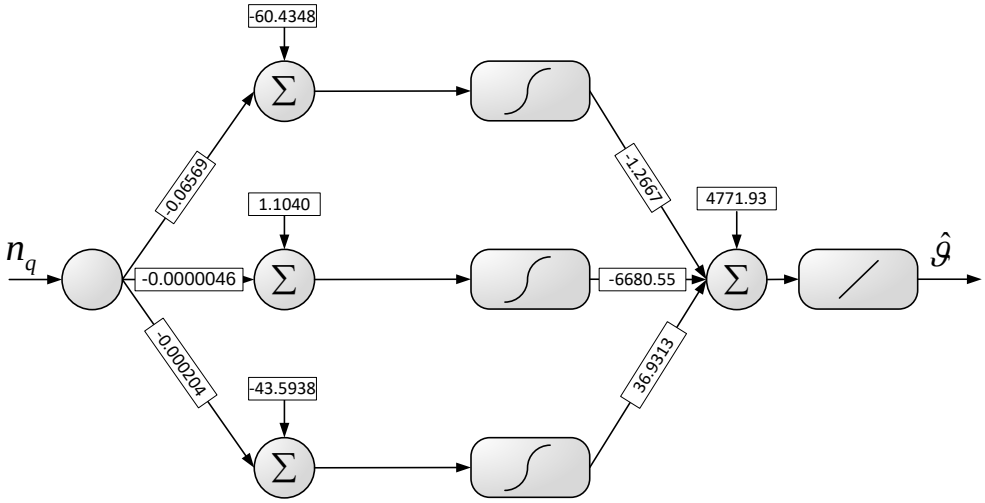

Fig. 3.25. Values of the weight coefficients of the exemplary neural network obtained as a result of the learning process using the set from Fig. 3.24

Determination of metrological properties of the neural reconstruction is carried out by testing the network with using two sets: the first one contains the true values of the input quantity, the second – the reconstruction results obtained on the basis of indications suitable for these values. In practice, the indications are burdened at least by the quantization errors, and usually by the noise errors, too. The next experiment is devoted to determination of the reconstruction errors if the network from Fig. 3.25 is applied.

Experiment 3.11. The input temperature value is randomly taken from the range 0 to 100°C with the rectangular distribution; after that the sensor resistance is calculated accordingly with the equation (3.5). On the basis of the obtained resistance value, two indications are calculated: accordingly with Eq. (3.20) and Eq. (3.22). The indications obtained are processed by the network from Fig. 3.25, which results in determining

the suitable estimates of the input temperature. The differences between the true value of the temperature and its estimatesare located in two sets of the reconstruction error values, which are presented in the form of histograms in Fig. 3.26 after the end of the experiment.

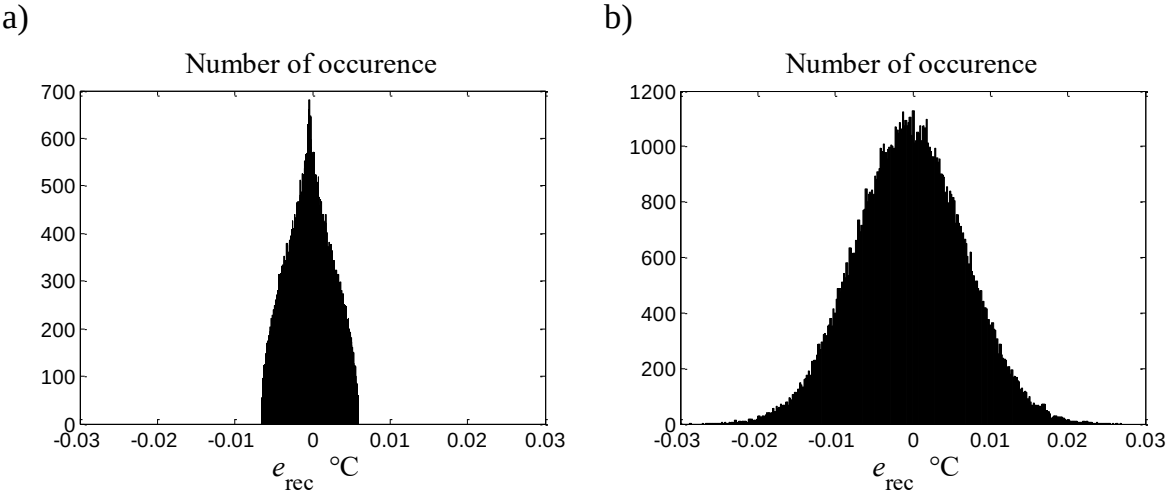

Fig. 3.26. Histograms of the reconstruction error of the network shown in Fig. 3.25 if the indications are burdened by: a) the quantization error, $\sigma_{rec} = 2.87 \cdot 10^{-3}$ °C, b) the quantization error and the noise error, $\sigma_{rec} = 6.97 \cdot 10^{-3}$ °C

The histograms obtained allow for the determination of the standard deviation of the neural approximation error σ_{app}. Using the relationship between the standard deviations of uncorrelated errors, one can write that:

$$\sigma_{app} = \sqrt{\sigma_{rec}^2 - \sigma_q^2 - \sigma_{noi}^2} \tag{3.94}$$

where σ_{rec} is the standard deviation of the reconstruction error given by Fig. 3.30b and σ_q, σ_{noi} are given by Eqs. (3.39) and (3.40), respectively. Based on these values, we have:

$$\sigma_{app} = 10^{-3}\sqrt{6.97^2 - 3.36 - 40.3} = 2.22 \cdot 10^{-3}\ ^{\circ}\mathrm{C} \tag{3.95}$$

Thus, this error takes values less than the approximation error of the linear approximation. This means that the considered neural approximation of the static characteristic is more accurate under the same conditions than the one composed of the linear segments.

The occurrence of noises in an analog converter allows us to suppose that errors caused by them could be filtered during the learning process. To verify this hypothesis, 5 standard resistors connected sequentially to the instrument input are used. For every resistor, 4 indications are determined accordingly with Eq. (3.22), which means that

they are burdened both by the quantization and the noise errors. The input temperature values corresponding to the selected values of the resistors are presented in Fig. 3.27 in 4 rows.

$$\{40917 \quad 0.000\}_{p=1},\ \{43917 \quad 18.815\},\ \{47869 \quad 43.744\},\ \{51842 \quad 69.015\},\ \{55650 \quad 93.427\}_{p=5}$$
$$\{40919 \quad 0.000\}_{p=6},\ \{43919 \quad 18.815\},\ \{47866 \quad 43.744\},\ \{51841 \quad 69.015\},\ \{55652 \quad 93.427\}_{p=10}$$
$$\{40917 \quad 0.000\}_{p=11},\ \{43918 \quad 18.815\},\ \{47868 \quad 43.744\},\ \{51843 \quad 69.015\},\ \{55651 \quad 93.427\}_{p=15}$$
$$\{40917 \quad 0.000\}_{p=16},\ \{43917 \quad 18.815\},\ \{47868 \quad 43.744\},\ \{51843 \quad 69.015\},\ \{55654 \quad 93.427\}_{p=20}$$

Fig. 3.27. Data set used for learning the 1-3-1 exemplary network obtained for the same 5 standard resistors, on the basis of which the corresponding input temperatures are calculated and pointed as the second element in brackets, all indications are burdened by the quantization and noise errors

The 1-3-1 network shown in Fig. 3.25 is learned successively by using the data from Fig. 3.27 starting from first row. After every learning process, the standard deviation of the reconstruction error is determined in the simulation way by using the Monte Carlo method, and the results are presented in the table 3.22.

Table 3.22

Dependence of the standard deviations of the reconstruction error for the number N_{rep} of rows from Fig. 3.31 used for the network learning

N_{rep}	1	2	3	4
$\sigma_{rec}\cdot 10^{-3}$ °C	5.27	3.29	2.84	1.53

It results from values contained in Tab. 3.22, an increasing number of ADC indications used for the network learning enables a decrease in the reconstruction error, which means that noise errors are filtered in the learning process.

Based on the histogram presented in Fig. 3.26, one can draw the conclusion that the simple network 1-3-1 that is learned by using 5 patterns approximates accurately enough the inverse static characteristic of the exemplary analog converter. This feature enables us to take the fact that the considered neural approximation is acceptable for further considerations.

3.5.3. Identification of a network for one-dimensional neural reconstruction

The neural network from Fig. 3.25 has been determined on the basis of the analytical description (3.20) of the exemplary analog converter. In practice, such knowledge of a static characteristic is relatively seldom; thus, it is identified in a measurement

process using standards of the sensor input quantity, the number of which should be minimized. As it results from the table 3.10, the indirect identification using the polynomial (3.49) can be performed with application of 4 standards only.

To compare properties of the analytical and neural approximations determined indirectly in this way, the learning set composed of 5 patterns is determined on the basis of the polynomial (3.49) and presented in Fig. 3.28. The parameters of the exemplary network 1-3-1 obtained for this set are shown in Fig. 3.29. The histograms of the errors of the reconstruction performed using the network are presented in Fig. 3.30.

$$\{0.00468 \quad 40917\}_{p=1},\ \{25.3026 \quad 44949\}_{p=2},\ \{50.0704 \quad 48866\}_{p=3},$$
$$\{75.1162 \quad 52797\}_{p=4},\ \{93.4254 \quad 55652\}_{p=5}$$

Fig. 3.28. Learning set obtained on the basis of the polynomial (3.49)

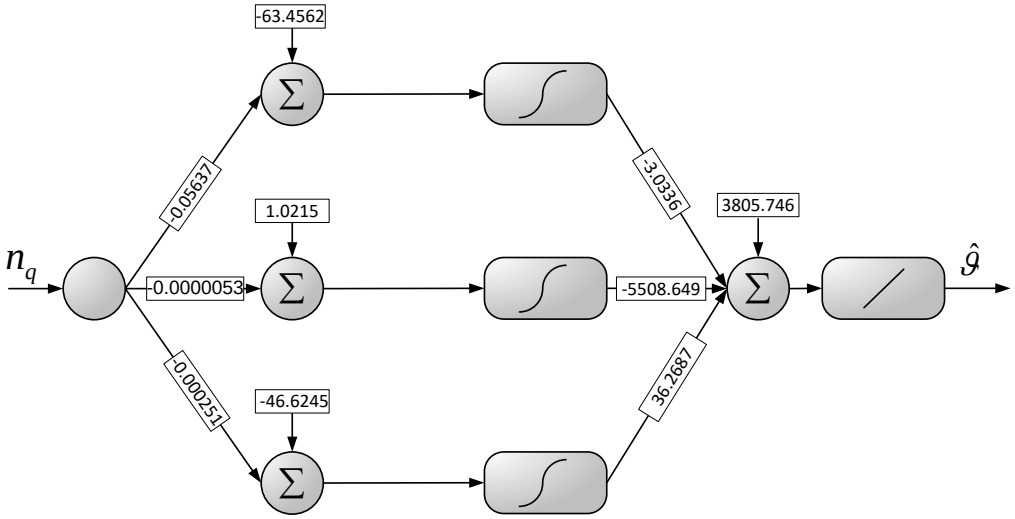

Fig. 3.29. Scheme and values of the weight coefficients of the exemplary neural network obtained as a result of the learning process by using the data from Fig. 3.28

Experiment 3.12. This experiment is carried out in the same way as Experiment 3.11. It is aimed at determining the distribution of the reconstruction errors in the case if the network is learned on the basis of the set that is obtained indirectly accordingly with the polynomial (3.49) and presented in Fig. 3.28. The histogram shown in Fig. 3.30a is determined for the indications calculated based on Eq. (3.20), while this from Fig. 3.30b on the basis of Eq. (3.22).

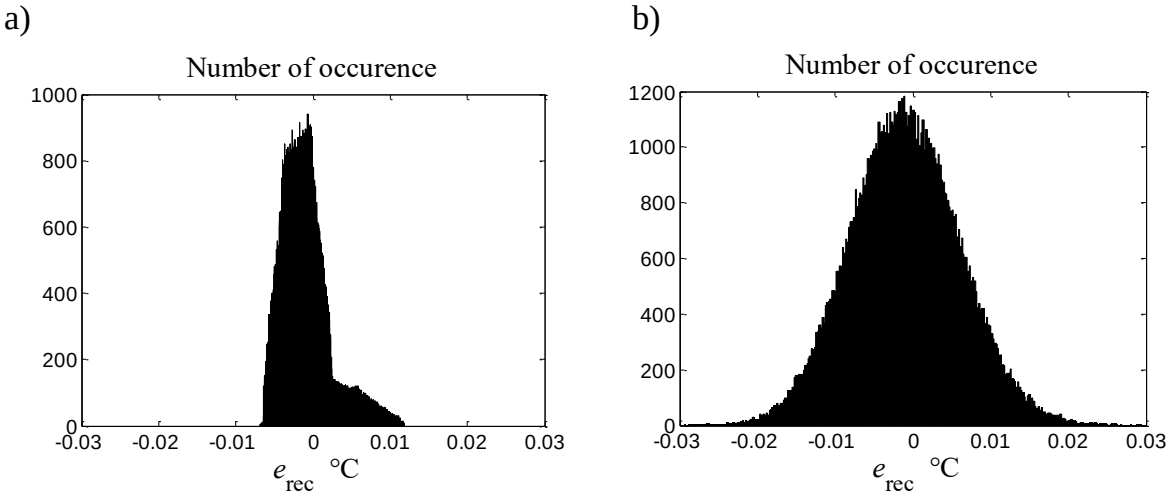

Fig. 3.30. Histograms of the reconstruction error of the network from Fig. 3.29, the parameters of which are obtained on the basis of the data presented in Fig. 3.28, which are determined accordingly with the polynomial (3.49); the ADC indications are burdened by: a) the quantization errors, $\sigma_{rec} = 3.16 \cdot 10^{-3}$ °C, b) by the quantization and noise errors, $\sigma_{rec} = 7.11 \cdot 10^{-3}$ °C

The reconstruction error e_{rec} from Fig. 3.30b is composed of the approximation error e_{app}, the identification error e_{id}, the quantization error e_q, and the noise error e_{noi}. Knowledge of the suitable standard deviation of these errors allows calculation of the standard deviation of the approximation error as:

$$\sigma_{id} = \sqrt{\sigma_{rec}^2 - \sigma_{app}^2 - \sigma_q^2 - \sigma_{noi}^2} \tag{3.96}$$

where σ_{rec} is the standard deviation of the reconstruction error with distribution presented in Fig. 3.30b, σ_{app} is calculated using Eq. (3.92) and σ_q, σ_{noi} are given by Eqs. (3.39) and (3.40), respectively. Using these values, we have:

$$\sigma_{id} = 10^{-3}\sqrt{7.11^2 - 2.22^2 - 3.36 - 40.3} = 1.4 \cdot 10^{-3} \text{ °C} \tag{3.97}$$

Having known the polynomial (3.49), one can calculate as many patterns in the learning set as necessary. In Tab. 3.23, dependencies of the standard deviations of the reconstruction errors are presented on the number of patterns determined indirectly on the basis of polynomial (3.49).

Table 3.23

Standard deviations of the reconstruction errors of the neural reconstruction that is performed by the 1-3-1 network in relation to number P of elements in the learning set obtained on the basis of Eq. (3.49), σ_1 is the standard deviation obtained if indications are burdened by the quantization error only, σ_2 – if they are burdened both by quantization error and the noise error $N(0; 1)$

P	5	8	12	16
$\sigma_1 \cdot 10^{-3}$ °C	3.16	3.33	3.34	3.31
$\sigma_2 \cdot 10^{-3}$ °C	7.11	7.18	7.18	7.17

As it results from values presented in Tab. 3.23, the reconstruction errors do not depend on the number of patterns obtained indirectly. It means that one can take, for the described kind of identification, the same number of identification points as used for the linear approximation, i.e.: 5. One may notice that the identification error in the case if the neural network approximates one-dimensional inverse static characteristic is suitably less than this error for the analytical approximation.

3.5.4. Calibration of instrument with one-dimensional neural reconstruction

As is analyzed in Section 3.2.3, the changes in time of the static characteristic cause its approximation should be periodically modified by using the calibration. In the case of a neural network, the network coefficients cannot be modified as is done for the analytical approximation. Therefore, the calibration consists in identifying, i.e. in determining these coefficients for the changed operating conditions of the sampling instrument, which requires the use of a sufficiently large number of the input quantity standards. However, it is possible to indicate another method, which requires only two standards for a characteristic with a small nonlinearity. It consists in modifying the segmental linear approximation coefficients as shown in Section 3.2.3, and then the modified nodal values should be determined, which become learning patterns for the modified network.

To present properties of such a kind of calibration, the determined nodal values of the linear approximation contained in Tab. 3.5 are used to learn the network. The learning set is presented in Fig. 3.31, and the parameters obtained for the 1-3-1 exemplary network are shown in Fig. 3.32. The execution of Experiment 3.13 enables the determination of the distributions of the reconstruction errors for the instrument after the calibration.

$$\{40931 \quad 0\}_{p=1},\ \{44915 \quad 25\}_{p=2},\ \{48869 \quad 50\}_{p=3},\ \{52794 \quad 75\}_{p=4},\ \{56689 \quad 100\}_{p=5}$$

Fig. 3.31. The learning set obtained on the basis of the calibration results from Tab. 3.4

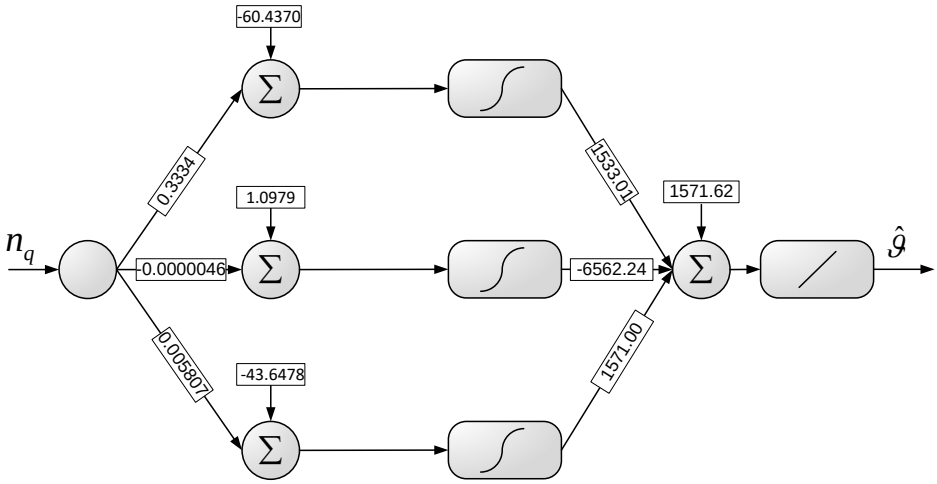

Fig. 3.32. Weight coefficients of the exemplary neural network being learned up using the data from Fig. 3.31, which are obtained on the basis of the calibration results from Tab. 3.4

Experiment 3.13. This experiment is aimed at the determination of distributions of the reconstruction errors in the case if the exemplary network is learned on the basis of data from Fig. 3.31 obtained as a result of the exemplary instrument calibration at two points. The course of the experiment is the same as in Experiment 3.11. The histogram shown in Fig. 3.33a is determined for the indications calculated based on of Eq. (3.20), while this from Fig. 3.33b one the basis of Eq. (3.22).

a) b)

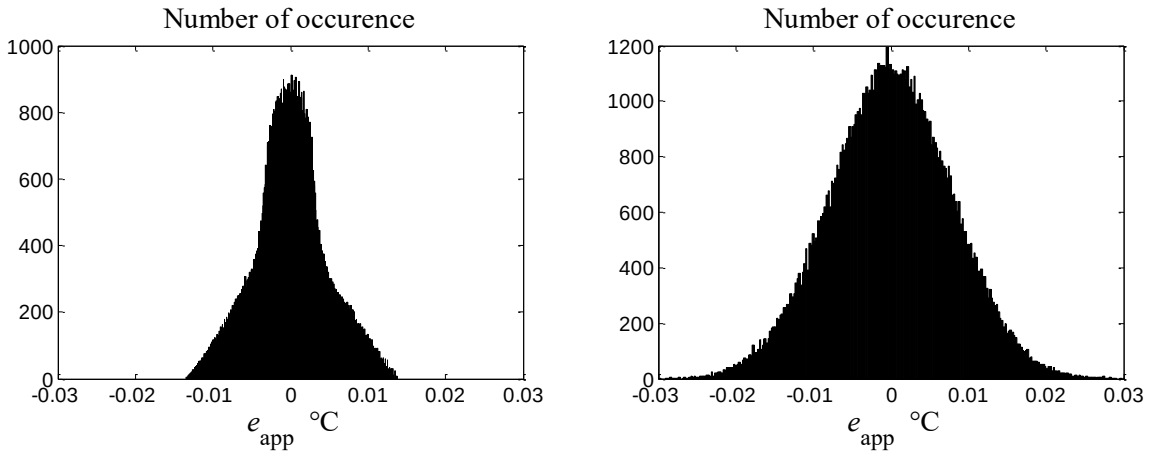

Fig. 3.33. Histograms of the reconstruction error of the network from Fig. 3.32, the parameters of which are obtained as the results of the two-point calibration, the ADC indications are burdened by: a) the quantization errors, $\sigma_{app} = 4.69 \cdot 10^{-3}$°C, b) by the quantization and the noise errors, $\sigma_{app} = 7.91 \cdot 10^{-3}$°C

Knowledge of the standard deviation σ_{rec} of the reconstruction error presented in Fig. 3.33b enables the determination of the standard deviation σ_{cal} of the error caused by the considered calibration of the exemplary instrument. It is:

$$\sigma_{\text{cal}} = \sqrt{\sigma_{\text{rec}}^2 - \sigma_{\text{app}}^2 - \sigma_{\text{q}}^2 - \sigma_{\text{noi}}^2} \tag{3.98}$$

where σ_{app} is calculated using Eq. (3.92) and σ_{q}, σ_{noi} are given by Eqs. (3.39) and (3.40), respectively. Based on these values, we have:

$$\sigma_{\text{cal}} = 10^{-3}\sqrt{7.91^2 - 2.22^2 - 3.36 - 40.3} = 3.74 \cdot 10^{-3}\ ^{\text{o}}\text{C} \tag{3.99}$$

which means that the calibration error takes values comparable with the other errors of the sampling instrument in the considered measurement conditions.

3.6. Two-dimensional neural static reconstruction

3.6.1. Structure of neural network used for two-dimensional static reconstruction

As it results from consideration presented in Section 3.3, the linear approximation of the inverse one-dimensional static characteristic may be enhanced in the simple way to the two-dimensional one. The same approach can be used if the neural approximation is applied. For further considerations, a neural network with 3 neurons in the hidden layer and two inputs, shown in Fig. 3.34, is used.The detailed structure of the network is shown in Fig. 3.35.

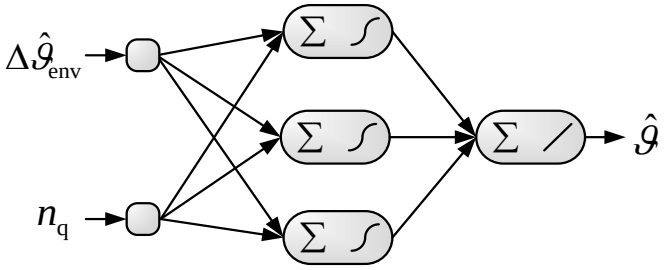

Fig. 3.34. General scheme of the neural network applied for the two-dimensional static reconstruction of the exemplary instrument, n_{q} is the indication in the AD converter output, $\Delta\hat{\vartheta}_{\text{env}}$ – the estimate of the environmental temperature change in relation to the reference temperature, $\hat{\vartheta}$ – the reconstructed input temperature

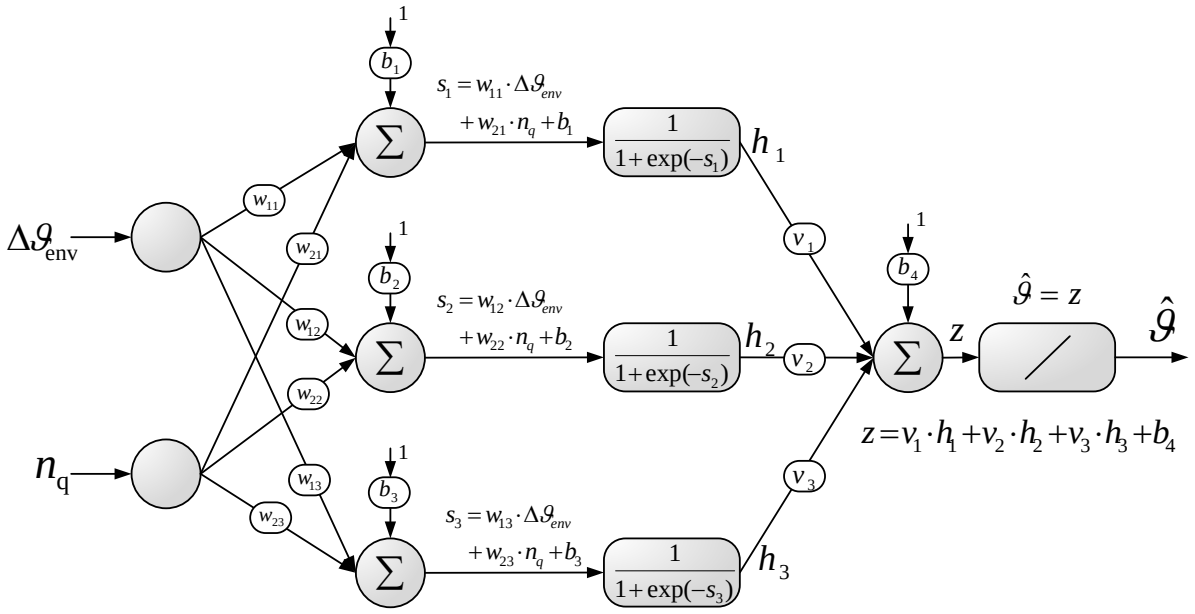

Fig. 3.35. Detailed structure of the neural network 2-3-1 from Fig. 3.34 applied for two-dimensional static reconstruction of the exemplary instrument

From Fig. 3.35, it results that the static reconstruction algorithm performed by the network can be written in the analytical form as:

$$\hat{\vartheta} = f_{\mathrm{O}}\left(\sum_{i=1}^{3} v_i \, f_{\mathrm{H}}\left(w_{1i}\Delta\vartheta_{env} + w_{2i}n_q + b_i\right) + b_4\right) \tag{3.100}$$

where: w_{ij}, v_{i} are appropriately weight coefficients of the hidden and the output layers, b_{i} are the biases, f_{H}, f_{O} – are the transfer functions, respectively, of the hidden and the output layers.

For this type of neural network, the learning data set consists of P elements, each of them is composed of 3 values, as shown in Fig. 3.36.

$$\left\{\begin{matrix}\Delta\hat{\vartheta}_{env}(1) \\ n_q(1)\end{matrix}\quad \vartheta(1)\right\},\ \left\{\begin{matrix}\Delta\hat{\vartheta}_{env}(2) \\ n_q(2)\end{matrix}\quad \vartheta(2)\right\},\ \ldots,\ \left\{\begin{matrix}\Delta\hat{\vartheta}_{env}(P) \\ n_q(P)\end{matrix}\quad \vartheta(P)\right\}$$

Fig. 3.36. General structure of the data set used for learning of the neural network from Fig. 3.35

In Table 3.12, indications are contained calculated accordingly with the analytical model of the exemplary two-dimensional static characteristic, on the basis of which the learning set shown in Fig. 3.37 is created. The parameters of the exemplary neural network obtained by using the set from this figure are presented in Fig. 3.38.

$$\begin{Bmatrix} -20 \\ 0 \\ 40942 \end{Bmatrix}_{p=1} \begin{Bmatrix} -20 \\ 25 \\ 44928 \end{Bmatrix}_{p=2} \begin{Bmatrix} -20 \\ 50 \\ 48884 \end{Bmatrix}_{p=3} \begin{Bmatrix} -20 \\ 75 \\ 52810 \end{Bmatrix}_{p=4} \begin{Bmatrix} -20 \\ 100 \\ 56707 \end{Bmatrix}_{p=5}$$

$$\begin{Bmatrix} 0 \\ 0 \\ 40918 \end{Bmatrix}_{p=6} \begin{Bmatrix} 0 \\ 25 \\ 44901 \end{Bmatrix}_{p=7} \begin{Bmatrix} 0 \\ 50 \\ 48854 \end{Bmatrix}_{p=8} \begin{Bmatrix} 0 \\ 75 \\ 52779 \end{Bmatrix}_{p=9} \begin{Bmatrix} 0 \\ 100 \\ 56673 \end{Bmatrix}_{p=10}$$

$$\begin{Bmatrix} 20 \\ 0 \\ 40893 \end{Bmatrix}_{p=11} \begin{Bmatrix} 20 \\ 25 \\ 44874 \end{Bmatrix}_{p=12} \begin{Bmatrix} 20 \\ 50 \\ 48825 \end{Bmatrix}_{p=13} \begin{Bmatrix} 20 \\ 75 \\ 52747 \end{Bmatrix}_{p=14} \begin{Bmatrix} 20 \\ 100 \\ 56639 \end{Bmatrix}_{p=15}$$

Fig. 3.37. The data used to learn the neural network from Fig. 3.39, p is the current number of the element in the learning set, $p = 1, \ldots, P$, $P = 15$

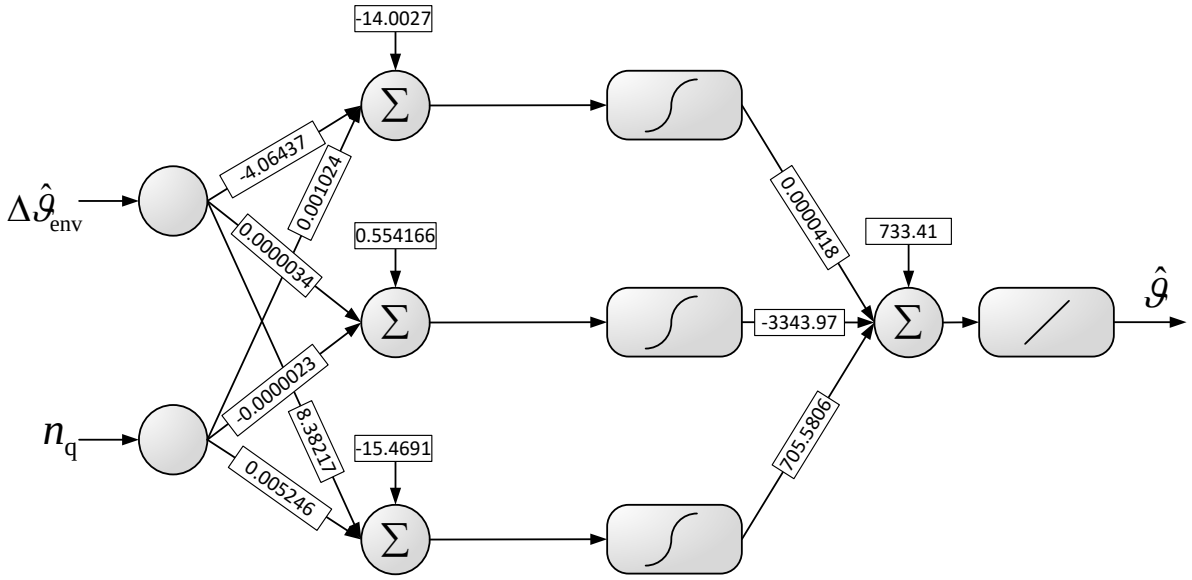

Fig. 3.38. The values of the weight coefficients of the exemplary network from Fig. 3.35, which are obtained on the basis of the learning data from Fig. 3.37 for the network performing neural approximation of the exemplary two-dimensional inverse static characteristic

Experiment 3.14. This experiment aims at determination of distributions of errors burdening the two-dimensional reconstruction performed by the network from Fig. 3.38 with the assumption that the input and the environmental temperatures change randomly with the rectangular distributions: the input temperature varies in the range from 0 to 100°C and the environmental temperature in the range from 5 to 45°C. The histogram of the reconstruction error shown in Fig. 3.39a is determined for the indications burdened only by the quantization errors and with the assumption that values of the environmental temperature are known accurately. The histogram from

Fig. 3.39b is obtained for indications burdened additively by noise and for the environmental temperature measured with resolution 0.1°C accordingly with Eq. (3.76).

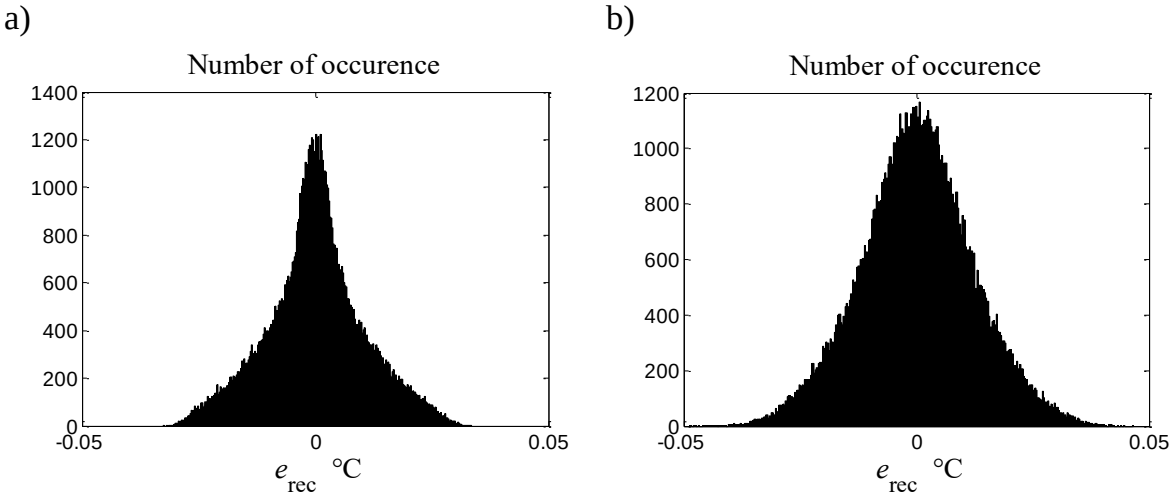

Fig. 3.39. Histograms of the two-dimensional static reconstruction errors for the network in Fig. 3.38 that is created by using the learning data obtained analytically: a) the reconstruction is performed based on the indications of the ADC with assumption that the indications are burdened by the quantization errors, the values of the environmental temperature are exactly known; the standard deviation of static reconstruction errors is $\sigma_{rec} = 10.2 \cdot 10^{-3}$°C, b) the indications are additively burdened by the noise errors, moreover, the environmental temperature values contain errors connected with the measurement resolution equal to 0.1°C, $\sigma_{rec} = 12 \cdot 10^{-3}$°C

The histograms from Fig. 3.39 enable determining the standard deviation of the approximation error. The reconstruction error shown in Fig. 3.39a contains the approximation and the quantization errors. Therefore, the standard deviation σ_{app} of the two-dimensional neural approximation error can be calculated as:

$$\sigma_{app} = \sqrt{\sigma_{rec}^2 - \sigma_q^2} \tag{3.101}$$

in which σ_{rec} is the standard deviation of the reconstruction error, the value of which is taken from Fig. 3.39a, σ_q – the standard deviationof the quantization error given by Eq. (3.39). After introducing the suitable values to Eq. (3.101), we obtain:

$$\sigma_{app} = 10^{-3}\sqrt{10.2^2 - 3.36} = 10 \cdot 10^{-3}\ ^{o}\text{C} \tag{3.102}$$

The value (3.102) is comparable to the approximation error of the two-dimensional linear approximation (see Eq. (3.75). It means that the considered structure 2-3-1 of the neural network is accurate enough for the assumed level. If necessary, this error can be reduced by extending the network with additional neurons in the hidden layer.

3.6.2. Calibration of instrument with two-dimensional neural reconstruction

The assumptions taken for the calibration of the instrument performing the static two-dimensional neural reconstruction can be the same as for the calibration described in Section 3.4.4. As result from the considerations presented there, the calibration can be carried out in two endpoints of the static characteristic with the use of two resistor standards. The indications obtained are applied to determine the shifted values of the static characteristic, which are used to create the learning set. Such a set composed of the same nodal values as used to determine the parameters of the two-dimensional linear approximation is presented in Fig. 3.40. The network obtained on the basis of this learning set is shown in Fig. 3.41 while the histograms of the reconstruction errors determined for this network using the Experiment 3.15 in Fig. 3.42.

$$\left\{\begin{matrix}-20\\0\\40955\end{matrix}\right\}_{P=1}\left\{\begin{matrix}-20\\25\\44942\end{matrix}\right\}_{P=2}\left\{\begin{matrix}-20\\50\\48899\end{matrix}\right\}_{P=3}\left\{\begin{matrix}-20\\75\\52825\end{matrix}\right\}_{P=4}\left\{\begin{matrix}-20\\100\\56723\end{matrix}\right\}_{P=5}$$

$$\left\{\begin{matrix}0\\0\\40931\end{matrix}\right\}_{P=6}\left\{\begin{matrix}0\\25\\44915\end{matrix}\right\}_{P=7}\left\{\begin{matrix}0\\50\\48869\end{matrix}\right\}_{P=8}\left\{\begin{matrix}0\\75\\52794\end{matrix}\right\}_{P=9}\left\{\begin{matrix}0\\100\\56723\end{matrix}\right\}_{P=10}$$

$$\left\{\begin{matrix}20\\0\\40906\end{matrix}\right\}_{P=11}\left\{\begin{matrix}20\\25\\44888\end{matrix}\right\}_{P=12}\left\{\begin{matrix}20\\50\\48840\end{matrix}\right\}_{P=13}\left\{\begin{matrix}20\\75\\52762\end{matrix}\right\}_{P=14}\left\{\begin{matrix}20\\100\\56655\end{matrix}\right\}_{P=15}$$

Fig. 3.40. The learning set obtained on the basis of nodal values from Tab. 3.14, which is used to calibrate the exemplary instrument performing the two-dimensional neural static reconstruction

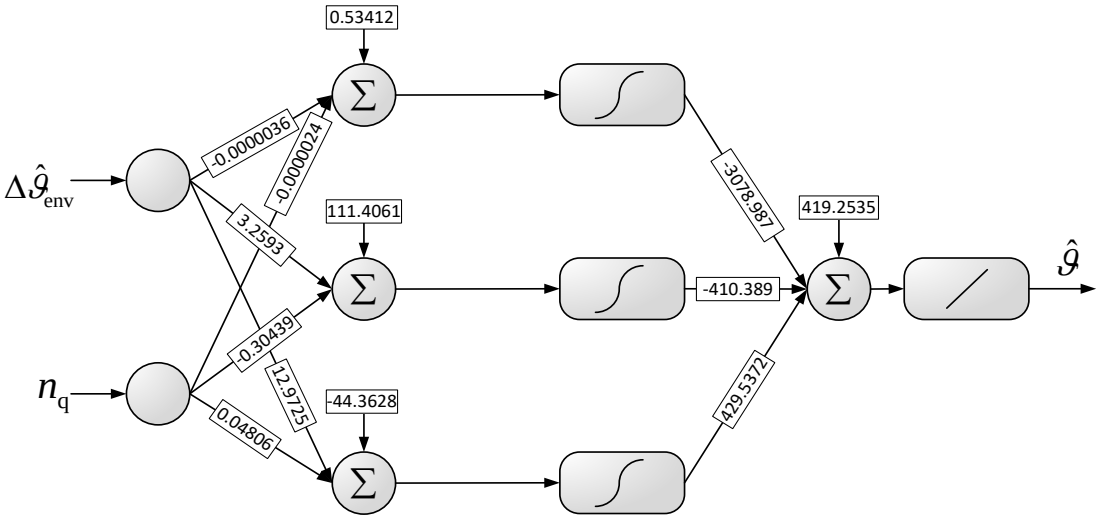

Fig. 3.41. Values of the weight coefficients of the 2-3-1 exemplary neural network determined by using the learning set from Fig. 3.40

Experiment 3.15. This experiment is carried out with the same assumptions as Experiment 3.14 with this difference that the exemplary neural network has been learned by using the data obtained as results of the two-point calibration described in Section 3.3.3. The histograms obtained for the reconstruction errors are presented in Fig. 3.42 a) and b).

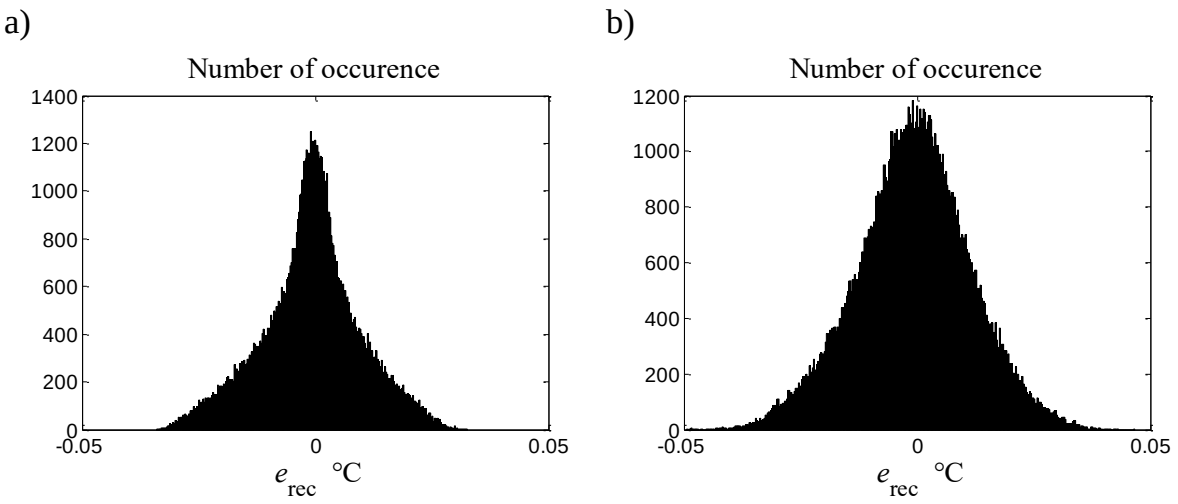

Fig. 3.42. Histograms of the two-dimensional static reconstruction error for the network in Fig. 3.41 obtained after calibration: a) the reconstruction is performed based on the indications (3.49) of the ADC, which are burdened by the quantization error, moreover, the values of the environmental temperature are exactly known, $\sigma_{rec} = 10.54 \cdot 10^{-3}$°C, b) the indications are burdened additively by the noise errors, and the values of the environmental temperature contain errors connected with the resolution of this temperature equal to 0.1°C, $\sigma_{rec} = 12.31 \cdot 10^{-3}$°C

The standard deviations of the errors presented in Fig. 3.42 enable determining the standard deviation σ_{cal} of the error connected with the calibration of the instrument performing the static neural approximation. For the partial errors forming the total reconstruction error from Fig. 3.51a, we have the following:

$$\sigma_{cal} = \sqrt{\sigma_{rec}^2 - \sigma_{app}^2 - \sigma_q^2} \tag{3.103}$$

where σ_{rec} is the standard deviation of the reconstruction error, σ_{app} – of the approximation error given by Eq. (3.102) and σ_q by Eq. (3.39). On the basis of these values, one obtains:

$$\sigma_{cal} = 10^{-3}\sqrt{10.54^2 - 10.3^2 - 3.36} = 1.28 \cdot 10^{-3}\ ^{o}\text{C} \tag{3.104}$$

which means that such a simple calibration does not introduce a significant error to the error budget of the instrument.

3.6.3. Identification of a neural network for two-dimensional static reconstruction

As shown in Section 3.2.2, the most effective way of an identification of the parameters of the two-dimensional linear approximation is carried out indirectly in two stages. At first, the polynomials are determined for three standards, respectively, which correspond to the extreme values of the environmental temperatures: 5ºC, 45ºC, and to the nominal temperature 25ºC. If the neural reconstruction is applied, the second stage consists in calculating elements of the learning set and determination of the network weighs in the learning process. The set from Fig. 3.43 is determined on the basis of the polynomials, the coefficients of which are contained in Tab. 3.17. The weights of the obtained neural network are shown in Fig. 3.44, while the errors burdened the reconstruction results in the output of the exemplary instrument, which applies this neural network, are presented in Fig. 3.45.

$$\left\{\begin{matrix}-20\\0.155\\40967\end{matrix}\right\}_{P=1}\left\{\begin{matrix}-20\\26.233\\45124\end{matrix}\right\}_{P=2}\left\{\begin{matrix}-20\\52.513\\49280\end{matrix}\right\}_{P=3}\left\{\begin{matrix}-20\\76.776\\53088\end{matrix}\right\}_{P=4}\left\{\begin{matrix}-20\\101.211\\56896\end{matrix}\right\}_{P=5}$$

$$\left\{\begin{matrix}0\\0.155\\40943\end{matrix}\right\}_{P=6}\left\{\begin{matrix}0\\26.233\\45097\end{matrix}\right\}_{P=7}\left\{\begin{matrix}0\\52.513\\49250\end{matrix}\right\}_{P=8}\left\{\begin{matrix}0\\76.776\\53056\end{matrix}\right\}_{P=9}\left\{\begin{matrix}0\\101.211\\56861\end{matrix}\right\}_{P=10}$$

$$\left\{\begin{matrix}20\\0.155\\40918\end{matrix}\right\}_{P=11}\left\{\begin{matrix}20\\26.233\\45070\end{matrix}\right\}_{P=12}\left\{\begin{matrix}20\\52.513\\49211\end{matrix}\right\}_{P=13}\left\{\begin{matrix}20\\76.776\\53024\end{matrix}\right\}_{P=14}\left\{\begin{matrix}20\\101.211\\56827\end{matrix}\right\}_{P=15}$$

Fig. 3.43. The learning set obtained on the basis of the polynomials determined in the first stage of the identification described in Section 3.2.3

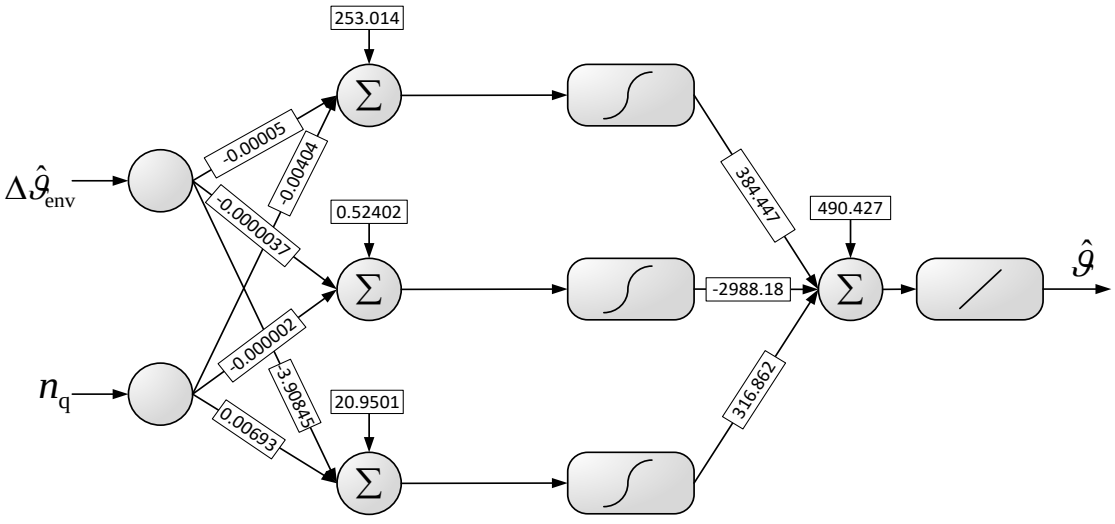

Fig. 3.44. Values of the weight coefficients of the 2-3-1 exemplary neural network determined for the learning data from Fig. 3.43

Experiment 3.16. This experiment is carried out to determine histograms of the reconstruction errors of the network, the weights of which are determined indirectly in the identification process on the basis of polynomials approximating the inverse static characteristic for three values of the environmental temperature: 5°C, 25°C and 45°C. The course of this experiment is the same as in Experiment 3.9. The histograms obtained for the reconstruction errors are presented in Fig. 3.45.

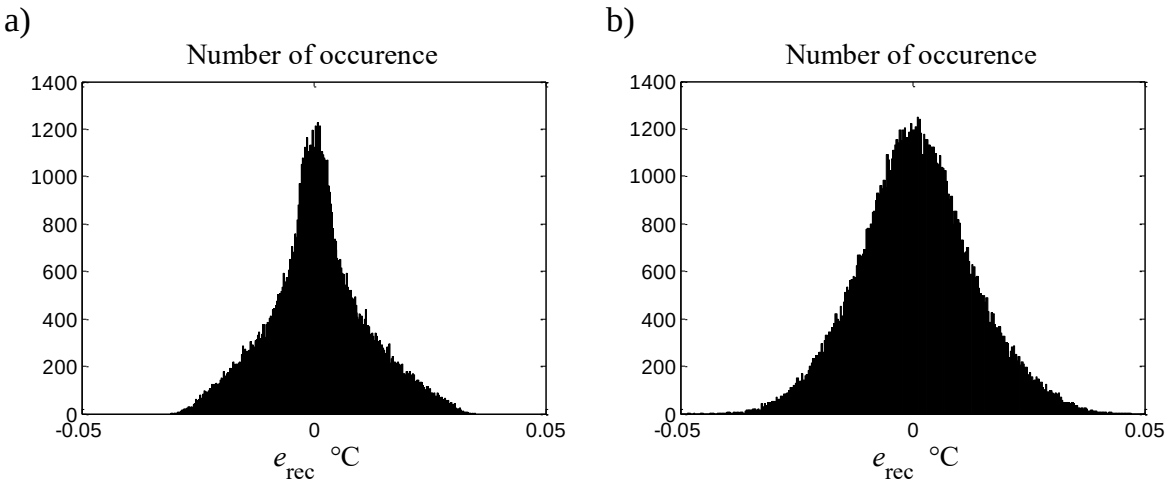

Fig. 3.45. Histograms of the two-dimensional static reconstruction error for the network from Fig. 3.44 obtained as a result of the identification: a) the reconstruction is performed on the basis of the ADC indications burdened by the quantization errors (Eq. 3.71) with the assumption that the environmental temperature is exactly known, $\sigma_{rec} = 10.5 \cdot 10^{-3}$°C, b) indications are burdened by both quantization errors and the noise errors (Eq. 3.72), plus, the estimates of the environmental temperature contain errors connected with the measurement resolution equal to 0.1°C (Eq. 3.73), $\sigma_{rec} = 12.3 \cdot 10^{-3}$°C

Using the standard deviations of the reconstruction error from Fig. 3.45 one can determine the standard deviation of the identification error. Based on the error from Fig. 3.45b, one can write that the standard deviation of the error connected with the identification can be calculated as

$$\sigma_{id} = \sqrt{\sigma_{rec}^2 - \sigma_{app}^2 - \sigma_q^2 - \sigma_{noi}^2 - \sigma_{env}^2} \tag{3.105}$$

Having given the standard deviation σ_{rec} of the error from Fig. 3.45a and the standard deviation σ_{app} of the neural approximation given by Eq. (3.102), we obtain the following value:

$$\sigma_{id} = 10^{-3}\sqrt{12.5^2 - 10^2 - 3.36 - 40.3 - 1.45^2} = 3.24 \cdot 10^{-3}\ ^{o}\text{C} \tag{3.106}$$

which is approximately the same as the identification error of the linear approximation.

3.7. Final remarks

The basis of the static reconstruction is knowledge about the inverse characteristic of the analog converter being the beginning part of a sampling instrument. In order to perform the reconstruction in the real-time by a microcontroller, it is necessary to use an approximation of the characteristic, the form of which enables minimizing of necessary arithmetical operations. In this chapter, two ways of obtaining such an approximation were considered. The first one consists in using analytical description in the form of the segmental linear approximation, the parameters of which have to be calculated and introduced to a non-volatile microcontroller memory as a look-up table. The second method applies artificial neural networks that can create the approximation themselves on the basis of learning data.

The considered analytical approximation needs very numerically simple algorithms for both one-dimensional and two-dimensional signal reconstruction independently of nonlinearity degree of the static characteristic. If the nonlinearity is stronger, the number of parameters necessary to store in a microcontroller memory increases, but it is not a problem for the modern microcontrollers. In the case of neural approximation, the stronger nonlinearity may implies using a network with a larger number of neurons in the hidden layer, but the general structure of the network does not change, and it is still very simple.

The inverse static characteristic can be approximated on the basis of known static characteristic of the analog converter and the analog-to-digital converter or it can be identified as the effect of the identification process, which consists in determining the characteristic in selected points by using standards of the reconstructed input quantity. The approximation can be done directly by using identification results or indirectly by determining a polynomial describing the inverse characteristic. This second way consists in calculating on the basis of this polynomial either parameters of the linear approximation or the learning data. As it results from the presented investigations, indirect identification is more effective than direct because it needs less number of standards to be used.

The static characteristic changes in time, which causes the sampling instrument have to be periodically calibrated. The calibration consists in modification of parameters of the linear approximation stored in a microcontroller memory on the basis of measurements in selected point of the characteristic. In the case of a neural network performing the reconstruction, the calibration needs learning up it by using

the data obtained on the basis of the measurements. For the considered exemplary sampling instrument, the calibration needs only measurements at two end points of the characteristic both in the case of the one- and two-dimensional approximation.

The inaccuracy of the static reconstruction is described in this chapter by standard deviations of the reconstruction errors, which are at the level of 0.01°C for the exemplary instrument. These errors can be decreased if one increases the number of nodes of the linear approximation or the number of neurons in the case of the neural approximation. The main limitation of this is the level of noise appearing in analog converters of sampling instruments.

4. DYNAMIC SIGNAL RECONSTRUCTION

The dynamic properties of the analog converter cause its output signal to depend on time variations of the input signal [L1, Z2]. The output signal component that occurs for vary over time input signal can be considered as a dynamic error [J1, J16, M10, R2, R7]. For this reason, the dynamic reconstruction consists in elimination of the dynamic error from the output signal of the converter. Taking into account that the basic dynamic model of an analog converter is a differential equation, the dynamic reconstruction is performed by solving the inverse dynamic model, that is by solving the differential equation in relation to the input signal.

The dynamic reconstruction algorithm is an element of the chain of partial algorithms, which, as a whole, perform the input signal reconstruction. Partial algorithms are obtained as the effect of the decomposition described in Chapter 1. One of the fundamental models from the decomposition point of view is known as the Wiener model, which is treated as the basis for further considerations. The first element in this model is a linear differential equation, which describes dynamic properties of the analog converter, while the second is a static equation. Taking into account that the partial reconstructions are performed in inverse order to this one in which the partial models are situated, the dynamic reconstruction makes calculation on the results of the static reconstruction. These results are burdened by errors propagated from the instrument input, errors related to the static properties of the converter and errors caused by the static reconstruction. This chapter is devoted to the description of these errors and analyzing their influence on accuracy of the result of the dynamic reconstruction.

4.1. Significance of dynamic error for accuracy of analog conversion

The dynamic error of an analog converter depends both on the variability of the input signal and the dynamic properties of the converter; therefore, the analysis of this error must be carried out for standard signals. Among them, the sinusoidal signal is

commonly used because the analytical description of the dynamic errors is relatively simple for this signal. For changes of its frequency, one can analyse dynamic properties of the converter and compare dynamic errors with other errors from the point of view of its influence on the accuracy of the signal processing. The essentiality of this analysis is presented graphically in Fig. 4.1.

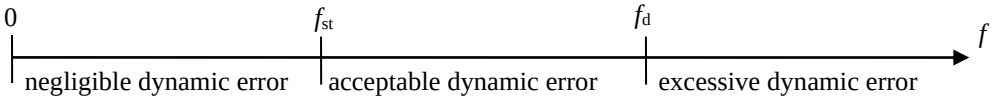

Fig. 4.1. General relation between errors of an analog converter in dependence on the frequency of its input signal

Three ranges of the input signal frequency f can be separated. In the first, for the frequency from 0 to f_{st}, the dynamic error is negligible small in relation to the static errors, which means that the signal is processed accordingly with the converter static transfer function. Therefore, this frequency range can be called static for the converter considered.

In the second range, for the frequency from f_{st} to f_d, the dynamic error is comparable to other errors of the converter; thus, it must be contained by the error budget of the converter. For the frequency greater than f_d, values of the dynamic error become essentially big and it is necessary to decrease them to an acceptable level. Elimination of excessive dynamic error from measurement results is called dynamic correction [J9, J12, R2, R9,] that can be performed on principle of the signal reconstruction.

The simplest form of description of dynamic properties of the analog converter is the 1-st order linear differential equation:

$$\tau \frac{\mathrm{d}u(t)}{\mathrm{d}t} + u(t) = Sx(t) \tag{4.1}$$

where τ is the time constant, x and u are the input and output signals, respectively, t denotes time, S is the static transfer function that describes the properties of the converter if the input signal does not change, that is, for the signal frequency $f \to 0$. If the input signal is sinusoidal, Eq. (4.1) can be written in the frequency domain as [L2]:

$$\tau \, \mathrm{j}\omega U(\mathrm{j}\omega) + U(\mathrm{j}\omega) = SX(\mathrm{j}\omega) \tag{4.2}$$

where $X(j\omega)$, $U(j\omega)$ are transforms of the input and output signals, $\omega = 2\pi/f$. For the sinusoidal signal, the dynamic properties of the converter are given by the transfer function:

$$S(j\omega) = \frac{U(j\omega)}{X(j\omega)} = \frac{S}{1 + j\omega\tau} \tag{4.3}$$

The dynamic error is defined as the difference between the output signal of the real converter and the reference converter with transmittance S_{ref}, the output signal of which is taken as dynamically ideal. As the reference, the converter working in the static state is used [M1, J12], the transmittance of which is equal to S. Taking this into account, the dynamic error of the converter that is described by Eq. (4.3) may be written as :

$$e_{dyn}(j\omega) = X(j\omega)[S_{ref} - S(j\omega)] = X(j\omega)\left[S - \frac{S}{1 + j\omega\tau}\right] = SX(j\omega)\frac{j\omega\tau}{1 + j\omega\tau} \tag{4.4}$$

For the purpose of error analysis, the dynamic transfer function (4.3) can often be expressed in the following form:

$$S(j\omega) = \frac{S}{1 + j\dfrac{f}{f_b}} \tag{4.5}$$

where $f = \omega/(2\pi)$, $f_b = 1/(2\pi\tau)$ is the cutoff frequency [M2] of the converter bandwidth defined as the frequency for which we have:

$$\left|S(j\omega)\right|_{f=f_b} = \frac{S}{\sqrt{2}} \tag{4.6}$$

Based on Eq. (4.5) and taking into account that the module of the signal spectral transform is equal to the signal amplitude, we may describe the amplitude of the error (4.4) using the expression:

$$\left|e_{dyn}(j\omega)\right| = S\left|X(j\omega)\right|\left|\frac{j\dfrac{f}{f_b}}{1 + j\dfrac{f}{f_b}}\right| = S\left|X(j\omega)\right|\frac{\dfrac{f}{f_b}}{\sqrt{1 + \left(\dfrac{f}{f_b}\right)^2}} \tag{4.7}$$

For the $f << f_b$, the expression (4.7) can be written as:

$$\left|e_{dyn}(j\omega)\right| \cong S\left|X(j\omega)\right|\frac{f}{f_b} = A_{out}\frac{f}{f_b} \tag{4.8}$$

where $A_{out} = S\left|X(j\omega)\right|$ is the amplitude of the output signal.

Example 4.1. The static transfer function S of an amplifier is called the amplification coefficient and is denoted as k_V. The dynamic properties of the amplifier applied in the exemplary microcontroller presented in Section 3.1 are described by the 1-st order equation (4.5), and, for $k_V = 1$, its bandwidth is $f_b = 1$ MHz. To evaluate the significance of the dynamic error in relation to other errors of the analog converter, one can compare the A_{out} amplitude of this error in the amplifier output with the total error described by the uncertainty U. If we want the dynamic error to be significantly less than the total error, the dynamic error amplitude must be at least 3 times less than U (such a relation causes the ariance of the dynamic error to be about 10 times less than the variance of the total error, which means that it can be omitted in the error budget). Taking this into account, one can determine the limit of the static working range f_{st} defined in Fig. 4.1. Based on Eq. (4.8), we have:

$$\left|e_{dyn}(j\omega)\right| \cong A_{out}\frac{f_{st}}{f_b} \le \frac{U}{3}$$

If we take: $U/A_{out} = 10^{-3}$, the range calculated from this expression take the value:

$$f_{st} = \frac{f_b}{3}\frac{U}{A_{out}} = \frac{10^6}{3}10^{-3} = 333\ \text{Hz}$$

which means that the dynamic error introduced by the amplifier can be neglected for the signal frequency f in the range from 0 to 333 Hz,.

In the bandwidth from f_{st} to f_d, the dynamic error takes the values acceptable from the total uncertainty point of view, which means that the uncertainty of this error cannot significantly exceed U. For this assumption, the limit f_d is determined on the basis of the expression:

$$\left|e_{dyn}(j\omega)\right| \cong A_{out}\frac{f_d}{f_b} \le U$$

from which we have:

$$f_d = f_b\frac{U}{A_{out}} = 10^6 \cdot 10^{-3} = 1\ \text{kHz}$$

As in Fig. 4.1, for the frequency $f > f_d = 1$ kHz, the dynamic error exceeds the acceptable values and should be corrected.

Example 4.2. For the concrete construction of the measuring amplifier, the product of its amplification coefficients and the bandwidth takes a constant value [M1]; thus, it is:

$$k_{V1} \cdot f_{b1} = k_{V2} \cdot f_{b2}$$

where f_{b1} is the bandwidth for the coefficient k_{V1} and f_{b2} for k_{V2}. For $k_{V1} = 1$,we have:

$$f_{b2} = \frac{f_b}{k_{V2}}$$

which means that the bandwidth decreases as many times as the amplification coefficients increases. The amplifier in the exemplary microcontroller works with $k_{V2} = 32$, which causes the limit values of frequencies that determine the bandwidths of the amplifier to be:

$$f_{s2} = \frac{f_s}{32} = \frac{333}{32} \cong 10\,\text{Hz}, \quad f_{d2} = \frac{f_d}{32} = \frac{1000}{32} \cong 31\,\text{Hz}$$

From the above calculations, it results that the amplifier works in the static state for the input signal frequencies from 0 to 10 Hz. If the frequency is greater than 31 Hz, the dynamic error of the exemplary amplifier should be corrected, which can be performed using the dynamic reconstruction algorithm.

Example 4.3. Let us assume that the dynamic properties of the exemplary Pt100 sensor, if it measures the temperature of the air flowing in a ventilation duct with a constant speed, can be described by the 1-st order equation (3.11). In these measurement conditions, the sensor time constant is $\tau = 2$ s, which means that the sensor bandwidth is: $f_b = 1/(2\pi \cdot 2) = 0.08$ Hz. Moreover, let us take the air temperature should be measured with uncertainty not greater than $U = 0.1$°C. This temperature varies from 0°C at night to 40°C at day, and can be described as sinusoidal signal with the amplitude $A_{in} = (40 - 0)/2 = 20$°C. If we want the dynamic error to be significantly less than the total error described by the uncertainty U, its amplitude (4.6) must be at least three times less than U. Taking this into account and based on Eq. (4.8), one can determine the limit frequency f_{st} of the static bandwidth from expression:

$$A_{out} \frac{f_{st}}{f_b} \cong A_{in} \frac{f_{st}}{f_b} \le \frac{U}{3}$$

because, for a relatively small dynamic error, the amplitudes of the input and the output signals are approximately equal for the dynamic model used as the basis of the dynamic reconstruction (see Eq. (2.16)). Therefore, one obtains the following:

$$f_{st} = \frac{U}{3} \frac{f_b}{A_{in}} = \frac{0.1}{3} \frac{0.08}{20} = 0.13 \cdot 10^{-3}\,\text{Hz}$$

The maximum frequency of the bandwidth, in which the dynamic error is acceptable, is calculated as:

$$f_{\mathrm{d}} = U\frac{f_{\mathrm{b}}}{A_{\mathrm{in}}} = 0.1\frac{0.08}{20} = 0.4\cdot 10^{-3}\ \mathrm{Hz}$$

The obtained values mean that, for the frequency from $f = 0$ to $f_{\mathrm{s}} = 0.27\cdot 10^{-3}$ Hz, the dynamic error of the sensor is negligible small, thus the sensor works in the static state. From $f_{\mathrm{s}} = 0.27\cdot 10^{-3}$ Hz to $f_{\mathrm{d}} = 0.4\cdot 10^{-3}$ Hz, the values of the dynamic error are comparable with other sensor errors and this error should be taken into account in the error budget. For $f > f_{\mathrm{d}} = 0.4\cdot 10^{-3}$ Hz the dynamic error exceeds the acceptable value and it should be decreased by using a dynamic reconstruction algorithm.

As resultof the presented examples, the amplifier used in the exemplary instrument works in a static state because its limit of static bandwidth $f_{\mathrm{s2}} = 10$ Hz is significantly greater than the frequency $f_{\mathrm{d}} = 0.4\cdot 10^{-3}$ Hz of the sensor. Therefore, there is no need for the general dynamic model of the exemplary analog converter to include the amplifier description.

4.2. Dynamic models of analog conversion

4.2.1. Analog model of conversion

The analog model describes the relations between analog signals at the output and the input of the considered conversion. A signal is called analog if it is represented by a continuous function of the continuous time [L1]. In this book, it is taken that all elements of the measuring chain that perform the conversion are treated as a whole, i.e., as a single analog converter, the dynamic properties of which are generally described by the analog model being *n*-order linear ordinary differential equation:

$$a_n u^{(n)} + a_{n-1} u^{(n-1)} + \ldots + a_1 \dot{u} + u = x \tag{4.9}$$

where x and u are varying over the time input and output signals of the dynamic model (4.9), a_n, ..., a_1 are constant coefficients. For further considerations, two basic forms of the model (4.9), most often used in measurement practice [L1], are taken into account.

These are:

- The 1-st order model described by the equation:

$$a_1\dot{u} + u = x \tag{4.10}$$

where a_1 is equal to the time constant τ of the converter (see Eq. 4.1).

- The 2-nd order model given by the expression:

$$a_2 \frac{\mathrm{d}^2 u}{\mathrm{d}t^2} + a_1\dot{u} + u = x \tag{4.11}$$

which is often presented in the form [H3, R9, Z2]:

$$\frac{\mathrm{d}^2 u}{\mathrm{d}t^2} + 2b\omega_0 \frac{\mathrm{d}u}{\mathrm{d}t} + \omega_0^2 u = \omega_0^2 x \tag{4.12}$$

where ω_0 is the natural frequency of the converter, b is its dumping coefficient.

Most frequently for analysis of dynamic properties of the converter, one uses two kinds of the input signal: the step-change signal and the sinusoidal signal. To simplify considerations, the expressions presented below are determined for unitary step change signal occurring at time $t = 0$. For this assumption, the output signal of the 1-st order converter has the form:

$$u(t) = 1 - \mathrm{e}^{-\frac{t}{\tau}} \tag{4.13}$$

The response of the 2-nd order converter to the unitary step change signal depends on the value of the damping coefficient b [H3]. For:

- $b < 1$, the output signal is given by the equation:

$$u(t) = 1 - \frac{e^{-b\omega_0 t}}{\sqrt{1-b^2}} \sin\left(\sqrt{1-b^2}\,\omega_0 t + \operatorname{arctg}\frac{\sqrt{1-b^2}}{b}\right) \tag{4.14}$$

- $b = 1$, it is:

$$u(t) = 1 - (1 + \omega_0 t)e^{-\omega_0 t} \tag{4.15}$$

- The value of $b > 1$ occurs in the case if the converter can be described as two 1-st order elements connected one after the other. Therefore, as a whole, they can be described by the two equation system. The first equation is the following:

$$\tau_1 \frac{\mathrm{d}u_1(t)}{\mathrm{d}t} + u_1(t) = x(t) \tag{4.16}$$

and the second:

$$\tau_2 \frac{\mathrm{d}u(t)}{\mathrm{d}t} + u(t) = u_1(t) \tag{4.17}$$

where τ_1 and τ_2 are the time constants of the selected converters, respectively. Combining Eqs. (4.16) and (4.17), we obtain the equation:

$$\tau_1\tau_2 \frac{\mathrm{d}^2u(t)}{\mathrm{d}t^2} + (\tau_1 + \tau_2)\frac{\mathrm{d}u(t)}{\mathrm{d}t} + u(t) = x(t) \tag{4.18}$$

that describes the both converters as one whole.

The response of the conversion that is modeled by Eq. (4.18) to the unitary step change of the input signal at $t = 0$ has the form:

$$u(t) = 1 - \frac{1}{\tau_1 - \tau_2}\left(\tau_1 \mathrm{e}^{-\frac{t}{\tau_1}} - \tau_2 \mathrm{e}^{-\frac{t}{\tau_2}}\right) \tag{4.19}$$

For sinusoidal signals, the dynamic properties of the converter in the frequency domain are described as a spectral transmittance. In this case, the output signal of a dynamic converter for the input signal with amplitude equal to 1, i.e., $x(t) = \sin\omega t$, is expressed as:

$$u(t) = |S(\mathrm{j}\omega)|\sin(\omega t + \varphi) \tag{4.20}$$

The spectral transmittance $S(\mathrm{j}\omega)$ of the 1-st order converter (4.10) is given by Eq. (4.3) with $S = 1$. According to this, the module of its transmittance is:

$$|S(\mathrm{j}\omega)| = \frac{1}{\sqrt{1 + (\omega\tau)^2}} \tag{4.21}$$

and the phase shift:

$$\varphi = -\arctan\omega\tau \tag{4.22}$$

The transmittance of the 2-nd order converter (4.12) is given by the expression:

$$S(\mathrm{j}\omega) = \frac{U(\mathrm{j}\omega)}{X(\mathrm{j}\omega)} = \frac{\omega_0^2}{(\mathrm{j}\omega)^2 + \mathrm{j}2b\omega + \omega_0^2} = \frac{1}{1 + \mathrm{j}2b\dfrac{\omega}{\omega_0} - \left(\dfrac{\omega}{\omega_0}\right)^2} \tag{4.23}$$

Thus, its module is described as:

$$|S(\mathrm{j}\omega)| = \frac{1}{\sqrt{\left[1 - \left(\dfrac{\omega}{\omega_0}\right)^2\right]^2 + \left(2b\dfrac{\omega}{\omega_0}\right)^2}} \tag{4.24}$$

and the phase shift takes the form:

$$\varphi = \arctan \frac{2b}{\frac{\omega}{\omega_0} - \frac{\omega_0}{\omega}} \tag{4.25}$$

4.2.2. Discrete model of analog conversion

The basis of a dynamic reconstruction algorithm that is considered in this book is such a discrete model of the conversion, which enables solving differential equation (4.9) in real time. This model can be built using the transformation of this equation to the form of state equations [M12, O1]. In the beginning, we need write Eq. (4.9) as:

$$u^{(n)} + d_{n-1}u^{(n-1)} + \ldots + d_1\dot{u} + d_0 u = d_0 x \tag{4.26}$$

where it is: $d_0 = 1/a_{(n-1)}$, $d_1 = a_{(1)}/a_{(n-1)}$ and so on. In the next step, Eq. (4.26) is transformed to the form of n state equations after introducing new variables that are succeeding derivatives of the output signal:

$$\begin{aligned} \dot{u}_1 &= u_2 \\ \dot{u}_2 &= u_3 \\ &\vdots \\ \dot{u}_{n-1} &= u_n \\ \dot{u}_n &= -d_{n-1}u_n - \ldots - d_0 u_1 + d_0 x \end{aligned} \tag{4.27}$$

where u_1, ..., u_n are state variables and $u_1 = u$, which means that the output signal u is treated as one of the state variables.

The system of equations (4.27) can be written in matrix form:

$$\dot{\mathbf{u}} = \mathbf{F}\mathbf{u} + \mathbf{G}x \tag{4.28}$$

where:

$$\mathbf{u} = \begin{bmatrix} u_1 \\ u_2 \\ \vdots \\ u_{n-1} \\ u_n \end{bmatrix}, \ \mathbf{F} = \begin{bmatrix} 0 & 1 & 0 & \ldots & 0 \\ 0 & 0 & 1 & \ldots & 0 \\ \vdots & \vdots & \vdots & \vdots & \vdots \\ 0 & 0 & 0 & \ddots & 1 \\ -d_0 & -d_1 & -d_2 & \ldots & -d_{n-1} \end{bmatrix}, \ \mathbf{G} = \begin{bmatrix} 0 \\ 0 \\ \vdots \\ 0 \\ d_0 \end{bmatrix} \tag{4.29}$$

After solving Eq. (4.28) for the time between instants t_k and t_{k+1}, k is the current number of the instant, $k = 0, 1, ...$, one obtains [M12]:

$$\mathbf{u}(t_{k+1}) = \mathrm{e}^{\mathbf{F}T_\mathrm{s}}\mathbf{u}(t_k) + \int_{t_k}^{t_{k+1}} \mathrm{e}^{\mathbf{F}T_\mathrm{s}} \mathrm{e}^{-\mathbf{F}\tau}\mathbf{G}x(\tau)\mathrm{d}\tau \tag{4.30}$$

where: $t_{k+1} - t_k$ is the time distance between the instants at which the state variables are discretized. This time distance is equal to the sampling period T_s, since, at the discretization instants, the described signal is sampled, and therefore, it is: $t_k = kT_\mathrm{s}$. Because $T_\mathrm{s} = \text{const.}$, one can simplify the notation of the variables by putting $u(t_k) = u(k)$ and so on. Taking this into account and assuming that the state variables change only in the discretization instants, which means that the state variables are taken as constant between them [M12], Eq. (4.28) can be written in discrete form:

$$\mathbf{u}(k+1) = \mathbf{\Phi}\mathbf{u}(k) + \mathbf{\Psi}x(k) \tag{4.31}$$

where:

$$\mathbf{y}(k) = \begin{bmatrix} y_1(k) \\ \vdots \\ y_n(k) \end{bmatrix}, \ \mathbf{\Phi} = \begin{bmatrix} \varphi_{11} & \cdots & \varphi_{1n} \\ \vdots & \ddots & \vdots \\ \varphi_{n1} & \cdots & \varphi_{nn} \end{bmatrix}, \ \mathbf{\Psi} = \begin{bmatrix} \psi_1 \\ \vdots \\ \psi_n \end{bmatrix} \tag{4.32}$$

For constant sampling period T_s, the elements of the matrixes $\mathbf{\Phi}$ and $\mathbf{\Psi}$ have constant values and can be calculated on the basis of Eq. (4.30) as:

$$\mathbf{\Phi} = \mathrm{e}^{\mathbf{F}T_\mathrm{s}}, \tag{4.33}$$

$$\mathbf{\Psi} = \left[\int_0^{T_\mathrm{s}} \mathrm{e}^{-\mathbf{F}(T_\mathrm{s}-\tau)}\mathrm{d}(\tau)\right]\mathbf{G} \tag{4.34}$$

For the 1-st order converter, the matrix equation (4.31) takes the scalar form:

$$u(k+1) = \varphi u(k) + \psi x(k) \tag{4.35}$$

for which the matrices (4.32) reduce to the coefficients determined accordingly with Eqs. (4.33) and (4.34). They are expressed as:

$$\varphi = \mathrm{e}^{FT_\mathrm{s}} = \mathrm{e}^{-d_0 T_\mathrm{s}} = \mathrm{e}^{-\frac{T_\mathrm{s}}{\tau}}, \ \psi = 1 - \mathrm{e}^{-\frac{T_\mathrm{s}}{\tau}} = 1 - \varphi \tag{4.36}$$

where τ is the time constant of the analog converter.

Example 4.4. The time constant of the 1-st order sensor Pt100 from Example 4.3 is equal $\tau = 2$ s. For the discretization period $T_s = 0.2$ s, the parameters of the dynamic discrete sensor model, according to Eq. (4.36), take the following values:

$$\varphi = \mathrm{e}^{-\frac{T_s}{\tau}} = e^{-\frac{0.2}{2}} = 0{,}9048, \quad \psi = 1 - \varphi = 1 - 0.9048 = 0.0952$$

Moreover, let us assume that at the instant number $k = 0$ the step change of the input temperature from 0 to $\vartheta_{ran} = 100^{o}$C occurs, which means that $\vartheta(k) = 100^{o}$C for instants $k = 0, 1, \ldots$. The discrete model enables the calculation of the of the sensor wire temperature at the succeeding discretization instants. Taking into account that the sensor output signal $u(0) = 0^{o}$C and based on Eq. (4.35), one obtains:

$$\vartheta(1) = \varphi u(0) + \psi x(0) = 0.9048 \cdot 0 + 0.0952 \cdot 100 = 9.52\ ^{o}\mathrm{C}$$
$$\vartheta(2) = \varphi u(1) + \psi x(1) = 0.9048 \cdot 9.52 + 0.0952 \cdot 100 = 18.13\ ^{o}\mathrm{C}$$
$$\vdots$$

and so on for the succeeding instants. On should notice that this model has the recurrent form because, to calculate the output temperature at any instant, one should know the previous one.

The values of the output temperature, calculated in the described way for 10 succeeding instants, are presented in Tab. 4.1 and Fig. 4.2b.

Table 4.1

The output signal values of the 1-st order exemplary converter calculated in Example 4.4 for the step change of the input signal on the basis of the discrete model, k is the number of the discretization instant

k	0	1	2	3	4	5	6	7	8	9
$u(k)^{o}$C	0	9.52	18.13	25.92	32.98	39.36	45.13	50.35	55.08	59.35

In Fig. 4.2a, one can see the response of the converter in the analytical form described by the expression:

$$u(t) = \vartheta_{ran}\left(1 - \mathrm{e}^{-\frac{t}{\tau}}\right) = 100\left(1 - \mathrm{e}^{-0.5t}\right)\ ^{o}\mathrm{C} \tag{4.37}$$

which is the solution of the differential equation (4.10) for the step change of the input signal ϑ from 0 to $\vartheta_{ran} = 100^{o}$C at $t = 0$.

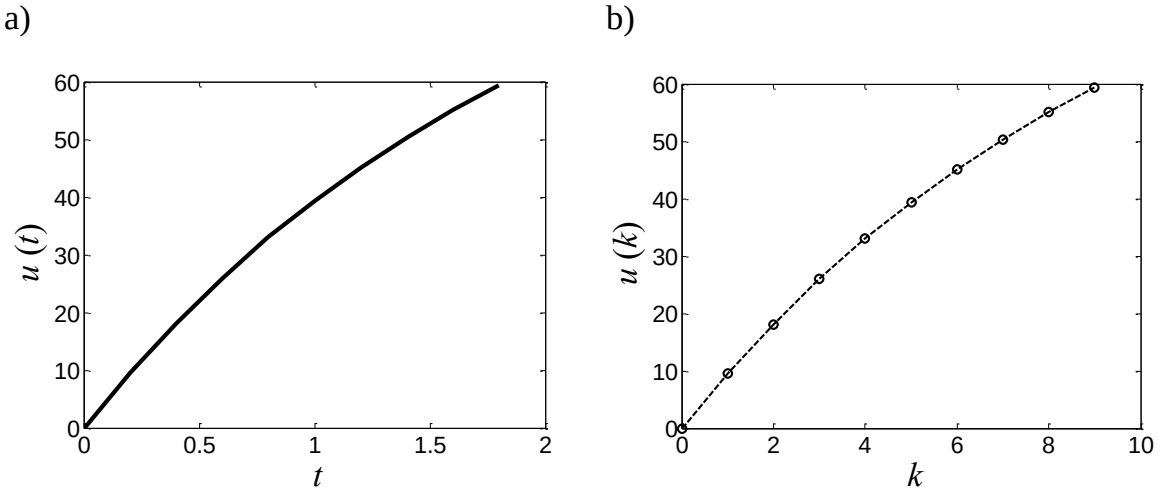

Fig. 4.2. Step response of the exemplary converter described by 1-st order differential equation (4.10) obtained on the basis of: (a) the analog model, (b) the discrete model for 10 beginning instants

For converters described by differential equations of the order higher than the first, the matrix equation (4.31) can be written in the form of the system of n discrete state equations:

$$\begin{aligned} u_1(k+1) &= \varphi_{11}u_1(k) + \ldots + \varphi_{1n}u_n(k) + \psi_1 x(k) \\ &\vdots \\ u_n(k+1) &= \varphi_{n1}u_1(k) + \ldots + \varphi_{nn}u_n(k) + \psi_n x(k) \end{aligned} \tag{4.38}$$

where $x(k)$ is the input signal sample, $u_1(k)$, ..., $u_n(k)$ are the values of the state variables at k instant, $k = 0, 1, ...$, and it is $u_1(k) = u(k)$, because, accordingly with Eq. (4.27), the output signal u is treated as the state variable u_1.

The dynamic model in the general discrete form (4.38) is of recurrent form because, for the determination of the output signal $u(k+1)$, it is necessary to know both the input signal and the state variables of the previous instant k. It means that at every step of the calculations, the determined values of the state variables must be stored to use them in the next step. Moreover, to start the calculations, the beginning values of the state variables should be known. If these values cannot be determined, the calculation algorithm begins its activity in a transient state that ends after a number of the steps dependently on parameters of the model and properties of the input signal [M12].

The 2-nd order dynamic converter is described generally by differential equation (4.11), which, based on Eqs. (4.12) and (4.13), can be written as two state equations:

$$\begin{aligned} \dot{u} &= u_2 \\ \dot{u}_2 &= -2b\omega_0 u_2 - \omega_0^2 u + \omega_0^2 x \end{aligned} \tag{4.39}$$

Presenting Eq. (4.39) in the matrix notation (4.28), we obtain the following forms of the matrices:

$$\mathbf{u}=\begin{bmatrix} u \\ u_2 \end{bmatrix},\ \mathbf{F}=\begin{bmatrix} 0 & 1 \\ -\omega_0^2 & -2b\omega_0 \end{bmatrix},\ \mathbf{G}=\begin{bmatrix} 0 \\ \omega_0^2 \end{bmatrix} \tag{4.40}$$

After discretization of the state equations (4.39) in the described way, one obtains the discrete matrix equation: $\mathbf{u}(k+1)=\mathbf{\Phi u}(k)+\mathbf{\Psi}x(k)$ where it is:

$$\mathbf{y}(k)=\begin{bmatrix} y(k) \\ y_2(k) \end{bmatrix},\ \mathbf{\Phi}=\begin{bmatrix} \varphi_{11} & \varphi_{12} \\ \varphi_{21} & \varphi_{22} \end{bmatrix},\ \mathbf{\Psi}=\begin{bmatrix} \psi_1 \\ \psi_2 \end{bmatrix} \tag{4.41}$$

This means that the discrete state equations take in this case the following form of two equations:

$$u(k+1)=\varphi_{11}u(k)+\varphi_{12}u_2(k)+\psi_1 x(k) \tag{4.42}$$

$$u_2(k+1)=\varphi_{21}u(k)+\varphi_{22}u_2(k)+\psi_2 x(k) \tag{4.43}$$

Elements of the matrix $\mathbf{\Phi}$ can be calculated on the basis of Eq. (4.33) as $\mathbf{\Phi}=\mathrm{e}^{\mathbf{F}T_s}$, while elements of $\mathbf{\Psi}$ can be obtained on the basis of them if one takes static properties of the converter into account. In the converter static state, i.e. when the state variables are not changing over time, it is:

$$u(k+1)=u(k) \tag{4.44}$$

and the values of the first derivative of the output signal take the value:

$$u_2(k+1)=u_2(k)=0 \tag{4.45}$$

Moreover, the static properties of the converter dynamic model are ideal (see Section 2.2), which means that at every instant of the static state $x(k)=u(k)$. Taking above into account, one obtains from Eq. (4.42) that:

$$\psi_1=1-\varphi_{11} \tag{4.46}$$

From Eq. (4.43), we have the following:

$$\psi_2=-\varphi_{21} \tag{4.47}$$

To start calculations of the output signal values, it is necessary to know the beginning values of the input signal $x(k)$, the output signal $u(k)$, and the state variable $u_2(k)$ that is the first derivative of the output signal. Having given them, the values of the output signal $u(k+1)$ are calculated for the subsequent instant $k+1$ accordingly with Eqs. (4.42), (4.43). After that, the value of the state variable $u_2(k+1)$ is determined to be stored and used in next step of calculations, that is, for the instant $k+2$. Next, all this procedure is repeated for the subsequent instants $k+2$, $k+3$,... .

Example 4.5. Let us assume that the parameters of the 2-nd order converter described by Eq. (4.11) have values: $\omega_0 = 1$ and $b = 0.7$, which means that this equation takes the form:

$$\frac{\mathrm{d}^2 u}{\mathrm{d}t^2} + 1.4\frac{\mathrm{d}u}{\mathrm{d}t} + u = x$$

According to Eq. (4.31), this expression can be written as two state equations:

$$\dot{u} = u_2$$
$$\dot{u}_2 = -1.4u_2 - u + x$$

This means that the matrix **F** has the form:

$$\mathbf{F} = \begin{bmatrix} 0 & 1 \\ -1 & -1.4 \end{bmatrix}$$

Based on this matrix, the matrix $\mathbf{\Phi}$ is calculated. According to Eq. (4.33) $\mathbf{\Phi} = \mathrm{e}^{\mathbf{F}T_\mathrm{s}}$, which means that one can use Maclaurin's sequence to determine the values of this matrix [M12]. One obtains the following sequence:

$$\mathbf{\Phi} = 1 + \mathbf{F}T_\mathrm{s} + \frac{1}{2}\left[\mathbf{F}T_\mathrm{s}\right]^2 + \ldots$$

For the determined matrix **F** and the sampling period $T_\mathrm{s} = 0.5$ s, we have:

$$\mathbf{\Phi} = \begin{bmatrix} \varphi_{11} & \varphi_{12} \\ \varphi_{21} & \varphi_{22} \end{bmatrix} = \begin{bmatrix} 0.9017 & 0.3449 \\ -0.3449 & 0.4188 \end{bmatrix}$$

Based on Eqs. (4.46) and (4.47), values of the coefficients of the matrix $\mathbf{\Psi}$ can be calculated according to Eqs. (4.46) and (4.47) as follows:

$$\psi_1 = 1 - \varphi_{11} = 0.0983,\ \psi_2 = -\varphi_{21} = 0.3449$$

To start the calculations accordingly with the discrete model (4.42), (4.43) of the converter, one can take the starting values $u(k) = 0$ and $u_2(k) = 0$. Taking into account that, for the unitary step change, $x(0) = 1$, one can calculate the discrete values of the output signal at the succeeding instants in the following recurrent way (the values of u_2 are determined to use them in the next step of the calculations):

$$u(1) = \varphi_{11}u(0) + \varphi_{12}u_2(0) + \psi_1 x(0) = 0.9017 \cdot 0 + 0.3449 \cdot 0 + 0.0983 \cdot 1 = 0.0983$$
$$u_2(1) = \varphi_{21}u(0) + \varphi_{22}u_2(0) + \psi_2 x(0) = -0.3449 \cdot 0 + 0.4188 \cdot 0 + 0.3449 \cdot 1 = 0.3449$$
$$u(2) = \varphi_{11}u(1) + \varphi_{12}u_2(1) + \psi_1 x(1) = 0.9017 \cdot 0.0983 + 0.3449 \cdot 0.3449 + 0.0983 \cdot 1 = 0.3059$$
$$u_2(2) = \varphi_{21}u(1) + \varphi_{22}u_2(1) + \psi_2 x(1) = -0.3449 \cdot 0.0983 + 0.4188 \cdot 0.3449 + 0.3449 \cdot 1 = 0.4554$$
$$\vdots$$

The obtained values were placed in Tab. 4.2 and presented in Fig. 4.3b. In Fig. 4.3a, the output signal of the converter is shown in the analog form as the expression:

$$u(t) = 1 - \frac{e^{-0.7t}}{\sqrt{1-0.7^2}} \sin\left(\sqrt{1-0.7^2}\, t + \operatorname{arctg} \frac{\sqrt{1-0.7^2}}{0.7} \right) = 1 - 1.4e^{-0.7t} \sin\left(0.714t + \operatorname{arctg} 1.02\right)$$

determined on the basis of Eq. (4.14) for the exemplary values of the 2-nd order converter, the parameters of which are: for $\omega_0 = 1$ and $b = 0.7$.

Table 4.2

The output signal values of the exemplary 2-nd order converter calculated on the basis of the discrete model for unitary step change of the input signal, sampling period $T_s = 0.5$ s, k is the number of the instant for which the values are determined

k	0	1	2	3	4	5	6	7	8	9
$u(k)$	0	0.0983	0.3059	0.5313	0.7257	0.8706	0.9653	1.0185	1.0416	1.0458

a) b)

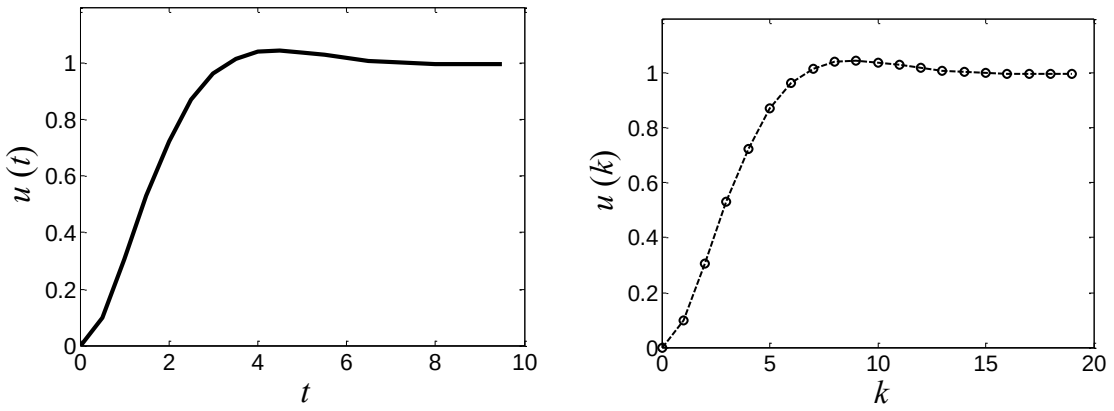

Fig. 4.3. Step responses of the 2-nd order converter from Example 3.5, which are obtained on the basis of the analog (a) and discrete (b) models

Example 4.6. Let us assume that the input signal of the 2-nd order converter from Example 4.5 has the form: $x(t) = \sin\omega t$, $\omega = 1\ s^{-1}$. For the beginning values $u(k) = u_2(k) = 0$ of the state variables, the use of the discrete model in the form of equations (4.42) and (4.42) to calculate the output signal values of the exemplary converter causes the appearance of transient state shown in Fig. 4.4b. The duration of this state depends on the properties of the input signal and parameters of the discrete model. In Fig. 4.4a, the analog form of the signal calculated for correct beginning values is presented.

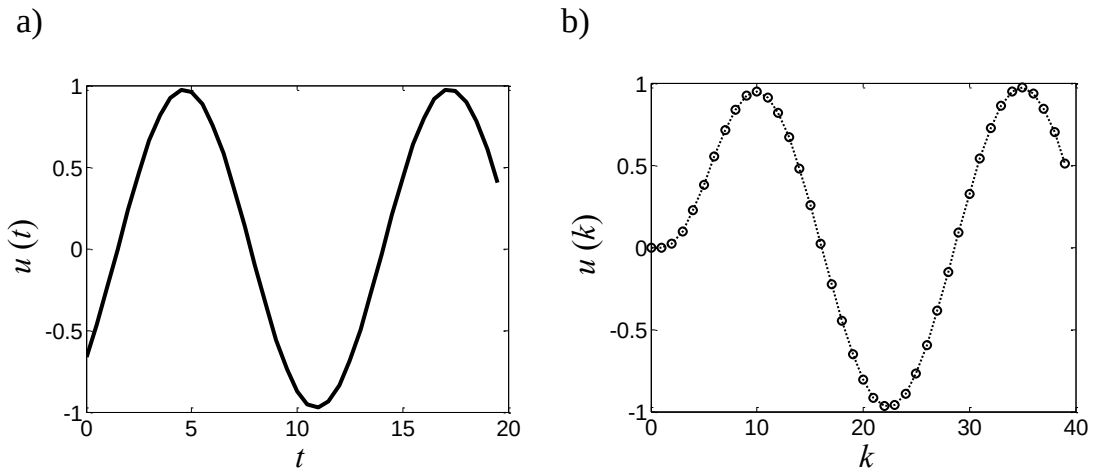

Fig. 4.4. Exemplary responses of the 2-nd order converter from Example (4.6) to the sinusoidal signal: in the analog form (a) obtained on the basis of Eqs. (4.20), (4.24) and (4.25), in the discrete form (b) calculated for zeroed beginning values of the state variables

4.2.3. Discretization error

Coefficients of the discrete model of the converter are calculated with the assumption that the input signal does not change between discretization (sampling) instants, which is necessary to present Eq. (4.26) in its discrete form (4.31). This assumption is fulfilled only for step change input signals. For other signals, the discrete model gives results which differs from these exact ones. These differences are described by the discretization error:

$$e_{\mathrm{dis}}(k) = u(k) - u_{\mathrm{dis}}(k) \tag{4.48}$$

where $u(k)$ is the instantaneous value of the analog output signal determined for the instant k and $u_{\mathrm{dis}}(k)$ is the response of the discrete model calculated for the same instant.

The discretization error describes generally imperfection of the discrete dynamic model in its representation of the analog dynamic model, as it is illustrated by the next example.

Example 4.7. Let us determine the waveform of the discretization error of the exemplary 1-st order converter from Example 4.4 for the input signal $x(t) = 50+50\sin\omega t$°C. Accordingly with Eqs. (4.48) and (4.20), the error value at instant k is described as:

$$e_{\mathrm{dis}}(k) = X\left[\left|S(\mathrm{j}\omega)\right|\sin\left(\frac{2\pi k T_{\mathrm{s}}}{T} + \varphi\right) - u_{\mathrm{dis}}(k)\right]$$

where $k = 0, 1, ...$, $T_s = 0.2$ s is the sampling (discretization) period, $\omega = 2\pi f$, the signal amplitude is $X = 50^oC$, its frequency $f = 0.01$ Hz, $u_{dis}(k)$ is the sample in the converter output calculated using the discrete model in the way described in Example 4.4 for the given samples $x(k)$ of the converter input signal.

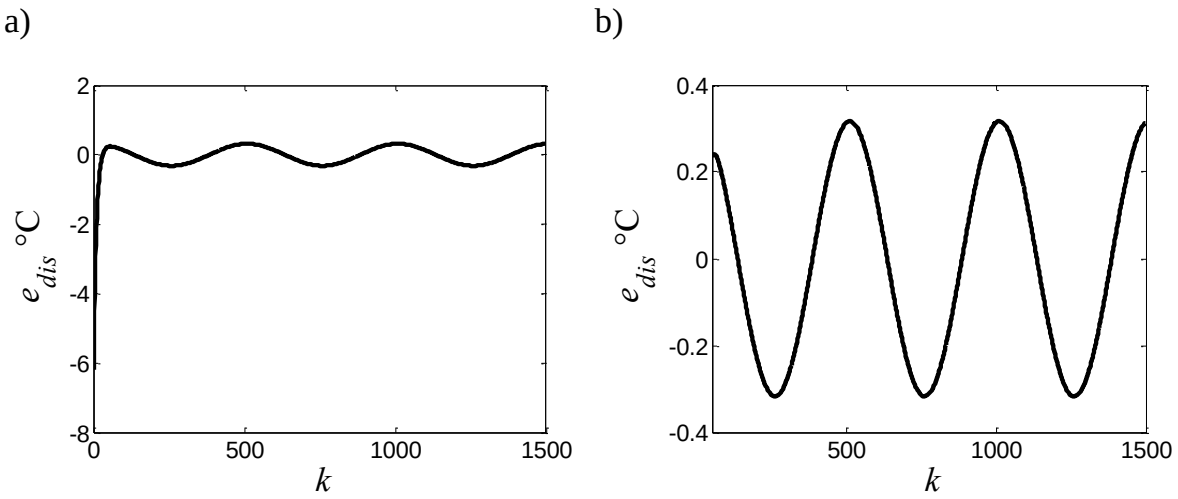

Fig. 4.5. Waveforms of the discretization error determined for the sinusoidal input signal of the 1-st order converter with amplitude $X = 50^oC$ and frequency $f = 0.01$ Hz calculated for the initial values equal to 0 (a), and for accurate initial values (b)

As in Fig. 4.5, the discretization error changes sinusoidal for the sinusoidal input signal (excluding the transient state in Fig. 4.5a). The amplitude E_{dis} of the error depends on the number of discretization points (samples) in the signal period. In Tab. 4.3, there are presented values of the discretization error in relation to the number of samples for the exemplary converter described in Example 4.4.

Table 4.3

The amplitude E_{dis} of the discretization error of the exemplary 1-st order converter in relation to the number of samples N_{sam} in the period T of the input signal, $N_{sam} = T/T_s$, T_s is the sampling period, E_{dis} is calculated for the amplitude of the input signal $X = 50^oC$

N_{sam}	20	50	100	200	500
$E_{dis}{}^oC$	2.4208	1.9876	1.3523	0.7618	0.3169

It results from Tab. 4.3 that the discretization error increases if the number N_{sam} decreases. Taking this into account that this number is related to the signal period, the assumption of the maximum acceptable value of this error imposes a maximum value of the signal frequency.

Comparing the results from Tab. 4.2, obtained on the basis of the discrete converter model, with the results calculated for the analog model, one can find that

they are the same at the sampling instants. Thus, that the discrete model is accurate for the step input signal, which means that it enables the calculation of accurate output signal samples for this signal.

For the step change of the input signal, the zeroed beginning values of the state variables are correct, and the transient state does not appear in the response of the converter as can be seen in Fig. 4.5b. For other input signals, a transient state occurs in the output signal as shown in Fig. 4.5a for the sinusoidal signal.

4.3. Analytical dynamic reconstruction

4.3.1. Recurrent form of reconstruction algorithm

The dynamic reconstruction algorithm is constructed on the basis of the dynamic discrete model of the analog converter. According to the general consideration presented in Chapter 2, the reconstruction algorithm is a specific solution of an inverse model. Taking into account that the considered dynamic model of the converter has the form of *n* discrete state equations (4.38), the dynamic reconstruction consists in solving these equations in relation to the input signal. Based on the first equation from the system (4.38), the instantaneous value $x(k)$ of this signal is calculated accordingly with equation:

$$\hat{x}(k)=\frac{1}{\psi_1}\left[-\varphi_{11}\hat{u}(k)-\varphi_{12}\hat{u}_2(k)-\ldots-\varphi_{1n}\hat{u}_n(k)+\hat{u}(k+1)\right] \tag{4.49}$$

All quantities in this equation are estimates of the quantities, being state variables of the dynamic model (4.38) in this sense that all errors that burden the estimates, are random and are deprived of systematic components, as it is discussed in Chapter 1. The input signal is one of these variables, the rest are determined by using the system of the following *n* - 1 equations as:

$$\begin{aligned}\hat{u}_2(k+1)&=\varphi_{21}\hat{u}(k)+\varphi_{22}\hat{u}_2(k)+\ldots+\varphi_{2n}\hat{u}_n(k)+\psi_2\hat{x}(k)\\ &\vdots\\ \hat{u}_n(k+1)&=\varphi_{n1}\hat{u}(k)+\varphi_{n2}\hat{u}_2(k)+\ldots+\varphi_{nn}\hat{u}_n(k)+\psi_n\hat{x}(k)\end{aligned} \tag{4.50}$$

The estimates obtained accordingly with equations (4.50) are used in Eqs. (4.49) and (4.50) in the next step of algorithm realization, which means that the algorithm is performed recurrently.

One can point a substantial difference between the estimates $\hat{u}(k), \hat{u}(k+1)$, which are given directly since they are quantized samples of the converter output signal, or they are obtained as results of the static reconstruction algorithm performed previously, while the other estimates $\hat{u}_2(k), \ldots, \hat{u}_n(k)$ are calculated indirectly on the basis of other estimates using equations (4.50).

From the measurement point of view, the current instant number $k = 0, 1,...$ is interpreted as the pointer of the beginning of the measurement window shown in Fig. 2.1 that contains all measurement results necessary to calculate one reconstruction result. For the recurrent form of the dynamic reconstruction algorithm, the width of the window is equal to 2 because two measurement (quantization) results $\hat{u}(k), \hat{u}(k+1)$ are used.

As it results from the above considerations, the dynamic reconstruction algorithm is performed in two steps. At each current instant k one must dispose 2 samples $\hat{u}(k), \hat{u}(k+1)$ of the output signal and $n - 1$ values of the state variables $\hat{u}_2(k), \ldots, \hat{u}_n(k)$ which are calculated in the previous instant $k - 1$ and stored to use them in the current instant k. The first step consists in calculating the estimate of the input signal $\hat{x}(k)$ accordingly with Eq. (4.49), while, during the second step, estimates of the state variables $\hat{u}_2(k), \ldots, \hat{u}_n(k)$ are determined and stored to use them in the next step of the algorithm realization.

To start the algorithm, it is necessary to have given 2 samples of the output signal and the beginning values of the rest state equations, i.e. $\hat{u}_2(0), \ldots, \hat{u}_n(0)$. They can be taken as equal to 0, which causes the transient state of the algorithm (the real values usually differ from 0) but after several steps all values of the state variables take the values close enough to the real ones. This is a general property of stable dynamic models [O1], which is illustrated in Example 4.6.

The dynamic model of the 1-st order converter is given by Eq. (4.35), the coefficients of which are described by expressions (4.36). Solving Eq. (4.35) in relation to the input quantity, one obtains the reconstruction algorithm in the form:

$$\hat{x}(k) = \frac{1}{\psi}\left[\hat{u}(k+1) - \varphi\hat{u}(k)\right] = \frac{1}{1-\varphi}\left[\hat{u}(k+1) - \varphi\hat{u}(k)\right] \tag{4.51}$$

This algorithm has not recurrent form because to calculate the sample of the input signal x, only 2 samples of the output signal u are needed. The specificity of calculations performed accordingly with this algorithm is illustrated in the following example.

Example 4.8. As it results from expressions (4.36), to perform 1-st order dynamic reconstruction algorithm, it is necessary to know one parameter φ of the discrete model. Its value, calculated in Example 4.4 for the exemplary analog converter, is: $\varphi = 0.9048$. Based on the samples of the converter response to the step change of the input signal contained in Tab. 4.1, we obtain the following input signal samples reconstructed on the basis of Eq. (4.51):

$$\hat{x}(0) = \frac{1}{1-0.9048}\left[\hat{u}(1) - 0.9048\,\hat{u}(0)\right] = 10.50 \cdot (9.52 - 0.9048 \cdot 0) = 100.0\ ^{\circ}\mathrm{C}$$

$$\hat{x}(1) = 10.50\left[\hat{u}(2) - 0.9048\,\hat{u}(1)\right] = 10.50\left[18.13 - 0.9048 \cdot 9.52\right] = 100.0\ ^{\circ}\mathrm{C}$$

$$\vdots$$

The reconstruction results for 10 beginning samples are shown in Fig. 4.6.

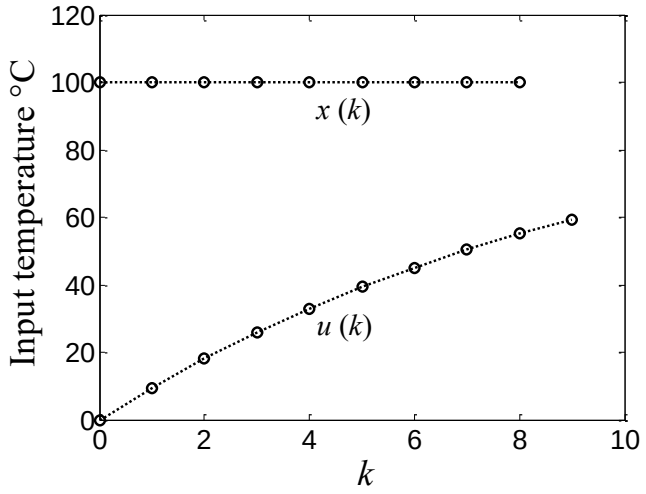

Fig. 4.6. Exemplary reconstruction results of the 1-st order exemplary converter, which are calculated for the step change of the input signal, $u(k)$ denotes samples of the output signal of the dynamic converter

For the 2-nd order converter, the first part of the reconstruction algorithm, described by Eq. (4.49), takes the form:

$$\hat{x}(k) = \frac{1}{1-\varphi_{11}}\left[\hat{u}(k+1) - \varphi_{11}\hat{u}(k) - \varphi_{12}\hat{u}_2(k)\right] \tag{4.52}$$

while the second part, obtained on the basis of the first equation of the system (4.50), is described by the expression:

$$\hat{u}_2(k+1) = \varphi_{21}\hat{u}(k) + \varphi_{22}\hat{u}_2(k) - \varphi_{21}\hat{x}(k) \tag{4.53}$$

which aimes at calculation of the estimate of the state variable $\hat{u}_2$, the value of which is stored to use it in the next step of calculations. Both parts of the algorithm create the loop, characteristic for the recurrent form of the reconstruction algorithm, shown in Fig. 4.7.

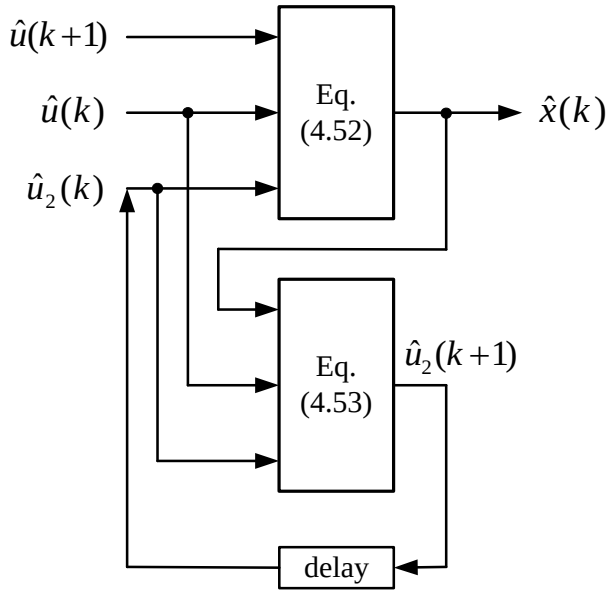

Fig. 4.7. Block diagram of the algorithm performing the dynamic reconstruction of the 2-nd order converter, "delay" denotes the operation of storing the value for one sampling period

To start activity of the reconstruction algorithm in the form of the equations (4.52) and (4.53), the beginning value of the state variable $\hat{u}_2(0)$ is necessary. If the reconstructed signal is step-changed at the instant $k = 0$, the beginning value is equal to 0; therefore, starting the algorithm with this value does not cause appearance of the transient state. Exemplary reconstruction of the step change input signal using 2-nd order algorithm is described in the following example.

Example 4.9. Let us apply the algorithm in the form of Eqs. (4.52) and (4.53) for the reconstruction of the input signal based on the samples of its output signal that are contained in Tab. 4.2. The algorithm has the same coefficients values as calculated in Example 4.5:

$$\varphi_{11} = 0.9017, \quad \varphi_{12} = 0.3449, \quad \varphi_{21} = -0.3449, \quad \varphi_{22} = 0.4188$$

The estimates obtained for the following instants take the values:

$$\hat{x}(0)=\frac{1}{1-\varphi_{11}}\left[\hat{u}(1)-\varphi_{11}\hat{u}(0)-\varphi_{12}\hat{u}_2(0)\right]=10.173\cdot\left(0.0983-0.9017\cdot 0-0.3449\cdot 0\right)=1.0000$$

$$\hat{u}_2(1)=\varphi_{21}\hat{u}(0)+\varphi_{22}\hat{u}_2(0)-\varphi_{21}\hat{x}(0)=-0.3449\cdot 0+0.4188\cdot 0+0.3449\cdot 1.000=0.3449$$

$$\hat{x}(1)=\frac{1}{1-\varphi_{11}}\left[\hat{u}(2)-\varphi_{11}\hat{u}(1)-\varphi_{12}\hat{u}_2(1)\right]=10.173\cdot\left(0.3059-0.9017\cdot 0.0983-0.09316\cdot 0.3449\right)=1.0001$$

$$\hat{u}_2(2)=\varphi_{21}\hat{u}(1)+\varphi_{22}\hat{u}_2(1)-\varphi_{21}\hat{x}(1)=-0.3449\cdot 0.0983+0.4188\cdot 0.3449+0.3449\cdot 1.0000=0.4555$$

$$\vdots$$

The calculated values are presented in the graphical form in Fig. 4.8.

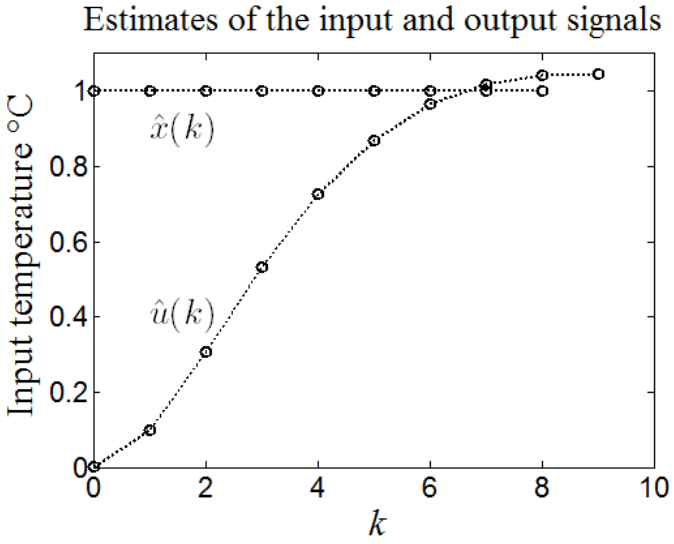

Fig. 4.8. Beginning 10 reconstructed samples $\hat{x}(k)$ of the unitary step change input signal of the exemplary 2-nd order converter, $\hat{u}(k)$ is the estimate of the output signal, k is the current number of the reconstruction instant

Application of the algorithm to the sinusoidal signal reconstruction causes it to be necessary to know the beginning value $\hat{u}_2(0)$ to start the calculations. If this value is not correct, the transient state occurs as illustrated by the next example.

Example 4.10. The input signal of the exemplary 2-nd order converter from Example 4.6 is: $x(t) = \sin\omega t$, $\omega = 1\ s^{-1}$. On the basis of the samples of the output signal, which are calculated accordingly with Eqs. (4.20), (4.24) and (4.25), the input signal estimates reconstructed by using Eq. (4.52) and (4.53) are presented in Fig. 4.9 for the correct and not-correct beginning value $\hat{u}_2(0)$.

a) b)

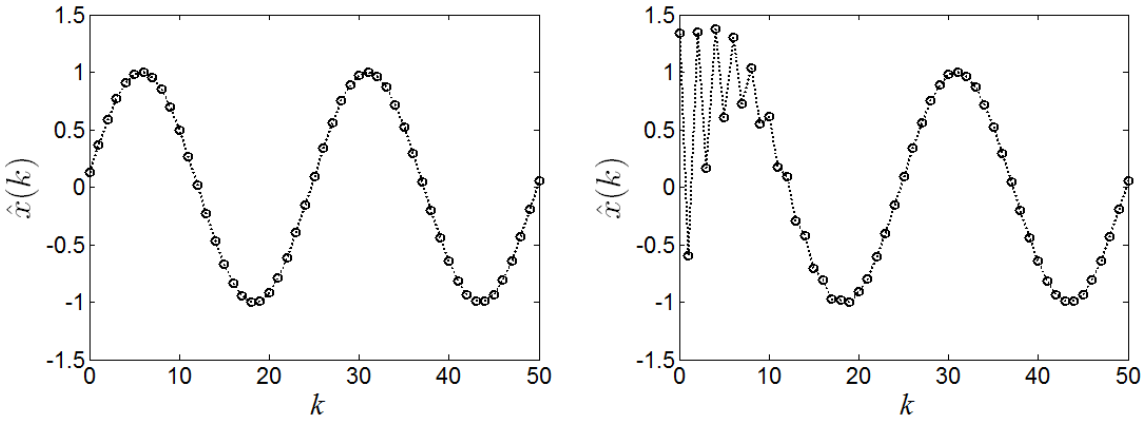

Fig. 4.9. Reconstruction of a sinusoidal input signal of the exemplary 2-nd order converter for: a) correct beginning value $\hat{u}_2(k) = 0.346$, b) incorrect beginning value $\hat{u}_2(k) = 0$

The recurrent form of the reconstruction algorithm enables its realization in minimally short time, which is necessary if the algorithm is applied in a measuring and control system working in real-time. The current window contains only 2 samples of the output signal, however, one should point out that many previous samples have their participation in the value of the state variable $\hat{u}_2$ and, therefore, in the reconstructed sample. Although, as it results from Eq. (4.51), the algorithm for the 1-st order converter is not recurrent, it also needs 2 samples.

4.3.2. Non-recurrent form of algorithm

Signal reconstruction can be performed in batch mode on the basis of recorded measuring data by using a non-recurrent form of the reconstruction algorithm, such as described in [B4]. For the considered algorithm, the non-recurrent form can be obtained on the basis of Eqs. (4.49) and (4.50). This form is very usable for analysis of the error propagation, since it enables the determination of the influence of errors burdening the succeeding samples of the output signal on the reconstructed samples of the input signal. The method of transformation of the recurrent form to its non-recurrent form is presented on an example of the reconstruction algorithm determined for 2-nd order converter as the system of equations (4.52) and (4.53).

The recurrent form of the algorithm can be transformed to a sequence in succeeding steps consisting in decreasing by 1 the number of the running instant and introducing the obtained expressions suitably to the previous equations. Based on (4.52), the estimate of the state variable at the instant *k* takes the form:

$$\hat{u}_2(k) = \varphi_{21}\hat{u}(k-1) + \varphi_{22}\hat{u}_2(k-1) + \psi_2\hat{x}(k-1) \tag{4.54}$$

Introducing (4.53) into (4.52) yields the following:

$$\begin{aligned}\hat{x}(k) &= \frac{1}{\psi_1}\left[\hat{u}(k+1) - \varphi_{11}\hat{u}(k) - \varphi_{12}\left[\varphi_{21}\hat{u}(k-1) + \varphi_{22}\hat{u}_2(k-1) + \psi_2\hat{x}(k-1)\right]\right] = \\ &= \frac{1}{\psi_1}\left[\hat{u}(k+1) - \varphi_{11}\hat{u}(k) - \varphi_{12}\varphi_{21}\hat{u}(k-1) - \varphi_{12}\varphi_{22}\hat{u}_2(k-1) - \varphi_{12}\psi_2\hat{x}(k-1)\right]\end{aligned} \tag{4.55}$$

Moreover, from Eq. (4.53), it results that:

$$\hat{x}(k-1) = \frac{1}{\psi_1}\left[\hat{u}(k) - \varphi_{11}\hat{u}(k-1) - \varphi_{12}\hat{u}_2(k-1)\right] \tag{4.56}$$

Based on Eq. (4.54), we can write Eq. (4.56) as:

$$\begin{aligned}\hat{x}(k) &= \frac{1}{\psi_1}\left\{\hat{u}(k+1) - \varphi_{11}\hat{u}(k) - \varphi_{12}\varphi_{21}\hat{u}(k-1) - \varphi_{12}\varphi_{22}\hat{u}_2(k-1) - \right. \\ &\left. - \frac{\varphi_{12}\psi_2}{\psi_1}\left[\hat{u}(k) - \varphi_{11}\hat{u}(k-1) - \varphi_{12}\hat{u}_2(k-1)\right]\right\} = \\ &= \frac{1}{\psi_1}\left\{\hat{u}(k+1) - \left[\varphi_{11} + \frac{\varphi_{12}\psi_2}{\psi_1}\right]\hat{u}(k) - \left[\varphi_{12}\varphi_{21} - \frac{\varphi_{11}\varphi_{12}\psi_2}{\psi_1}\right]\hat{u}(k-1) - \right. \\ &\left. - \left[\varphi_{12}\varphi_{22} - \frac{\varphi_{12}^2\psi_2}{\psi_1}\right]\hat{u}_2(k-1)\right\}\end{aligned} \tag{4.57}$$

Using relations (4.46), (4.47) and denoting:

$$H = \frac{\varphi_{12}\varphi_{21}}{1-\varphi_{11}} \tag{4.58}$$

one can write Eq. (4.57) in the following form:

$$\hat{x}(k) = \frac{1}{1-\varphi_{11}}\left[\hat{u}(k+1) + (H-\varphi_{11})\hat{u}(k) - H\hat{u}(k-1) - \varphi_{12}(\varphi_{22}+H)\hat{u}_2(k-1)\right] \tag{4.59}$$

After applying of the presented procedure for the previous moments: $k-1$, $k-2$ …, $k-m$ using the relations (4.56) and (4.57), one obtains the reconstruction algorithm in the form of the sequence:

$$\begin{aligned}\hat{x}(k) = \frac{1}{1-\varphi_{11}}[&\hat{u}(k+1) + (H-\varphi_{11})\hat{u}(k) + \\ &+ H(H+\varphi_{22}-1)\hat{u}(k-1) + \\ &+ H(H+\varphi_{22}-1)(H+\varphi_{22})\hat{u}(k-2) + \\ &\vdots \\ &+ H(H+\varphi_{22}-1)(H+\varphi_{22})^{m-1}\hat{u}(k-m) + \\ &\vdots\end{aligned} \tag{4.60}$$

which is the linear combination of constant coefficients and estimates of the samples at instants $k+1$, k, $k-1$, ..., $k-m$, ... Denoting the coefficients in Eq. (4.60) as:

$$\begin{aligned} A_{k+1} &= \frac{1}{1-\varphi_{11}} \\ A_k &= \frac{H-\varphi_{11}}{1-\varphi_{11}} \\ A_{k-1} &= \frac{H(H+\varphi_{22}-1)}{1-\varphi_{11}} \\ &\vdots \\ A_{k-m} &= \frac{H(H+\varphi_{22}-1)}{1-\varphi_{11}}(H+\varphi_{22})^{m-1} \\ &\vdots \end{aligned} \tag{4.61}$$

expression (4.60) can be written as the sequence:

$$\hat{x}(k) = A_{k+1}\hat{u}(k+1) + A_k\hat{u}(k) + A_{k-1}\hat{u}(k-1) + \ldots + A_{k-m}\hat{u}(k-m) + \ldots \tag{4.62}$$

which describes the reconstruction algorithm in the non-recurrent form.

Example 4.11. The coefficients of the discrete model of the 2-nd order converter from Example 4.5 have values:

$$\varphi_{11} = 0.9017, \quad \varphi_{12} = 0.3449, \quad \varphi_{21} = -0.3449, \quad \varphi_{22} = 0.4188$$

which causes, accordingly with Eq.(4.58), that we have:

$$H = \frac{\varphi_{12}\varphi_{21}}{1-\varphi_{11}} = \frac{0.3449 \cdot (-0.3449)}{1-0.0917} = -1.21$$

Based on these values, one obtains the following values of the coefficients (4.61):

$$A_{k+1} = \frac{1}{1-\varphi_{11}} = \frac{1}{1-0.9017} = 10.17$$

$$A_k = \frac{H-\varphi_{11}}{1-\varphi_{11}} = \frac{-1.21-0.9017}{1-0.9017} = -21.48$$

$$A_{k-1} = \frac{H\left(H+\varphi_{22}-1\right)}{1-\varphi_{11}} = \frac{-1.21\left(-1.21+0.4188-1\right)}{1-0.9017} = 22.05$$

$$\vdots$$

Ten starting values of the coefficients obtained in this way are presented in Tab. 4.4.

Table 4.4

Ten starting values of the coefficients (4.61) of the sequence (4.62) determined for the exemplary 2-nd order converter

A_{k+1}	A_k	A_{k-1}	A_{k-2}	A_{k-3}	A_{k-4}	A_{k-5}	A_{k-6}	A_{k-7}	A_{k-8}
10.17	-21.48	22.05	-17.45	13.80	-10.92	8.64	-6.84	5.41	-4.28

As it results from Eq. (4.61), the coefficients of the sequence (4.62), beginning from the third element, create the geometrical sequence with the quotient:

$$q_A = H + \varphi_{22} \tag{4.63}$$

which causes that the sum:

$$S = \left(A_{k-1} + \ldots + A_{k-m}\right)\Big|_{m\to\infty} = \frac{H\left(H+\varphi_{22}-1\right)}{\left(1-\varphi_{11}\right)\left(1-H-\varphi_{22}\right)} = \frac{H}{\varphi_{11}-1} \tag{4.64}$$

Taking Eq. (4.64) into account, one obtains that the sum of all coefficients (4.61) is:

$$A_{k+1} + A_k + S = \frac{H\left(H+\varphi_{22}-1\right)}{\left(1-\varphi_{11}\right)\left(1-H-\varphi_{22}\right)} = \frac{1}{1-\varphi_{11}} + \frac{H-\varphi_{11}}{1-\varphi_{11}} + \frac{-H}{1-\varphi_{11}} = 1 \tag{4.65}$$

if the number of sequence terms (4.61) comes to infinity. It means that the 2-nd recurrent algorithm in the general form of equations (4.52) and (4.53) is stable, because it can be described as the sequence with elements having finite sum (the measurement results have always finite values).

The finite sum of the geometrical sequence means that the quotient $|q_A| < 1$, which results in decreasing the values of the coefficients (4.61) with increasing of m. This causes the participations of succeeding measurements in the reconstruction result to decrease, too, and for some value of $m = m_{\lim}$ the remaining elements can be neglected

from the reconstruction accuracy point of view. This means that the reconstruction algorithm can be considered in the form of the sequence (4.62) containing finite $m_{\text{lim}} = m_{\text{min}} + 2$ elements.

The properties of the algorithm described above in the form of the sequence can be generalized for all dynamic reconstruction algorithms that are stable. It means that every recurrent algorithm may be analyzed in two manners from the measurement window point of view. The window determines the number of measurement data (estimates of the output samples), which are used to obtain one estimate of the input signal sample and, for the current window, this number is equal to 2 (see beginning considerations in Section 4.3.1). But, for the algorithm in the form of the described sequence, the number of measurements necessary to calculate one output sample is at least equal to $K = m_{\text{min}}$. Therefore, from the reconstruction accuracy point of view, the length of the algorithm measurement window is equal to $KT_{\text{s}} = m_{\text{min}}T_{\text{s}}$, T_{s} is the sampling period.

Let us analyze how many elements of the reconstruction algorithm in the form of sequence (4.62) are necessary for calculation of the input signal sample with error less than e_{max}. The sum of all omitted terms of sequence (4.62) must be equal or less than e_{max}, dependently on the acceptable inaccuracy of the reconstruction. As it results from Tab. 4.5, the terms of the sequence take positive and negative values alternately. Thus, to determine m_{min}, sequence (4.62) should be replaced by sequence the terms of which are the sum of two successive terms described by expressions (4.61). The quotient of this sequence is positive and equal: $-H-\varphi_{22}$, which means that the i-th term of it is expressed as:

$$\begin{aligned}&\frac{H\left(H+\varphi_{22}-1\right)}{1-\varphi_{11}}\left[\left(-H-\varphi_{22}\right)^{i}-\left(-H-\varphi_{22}\right)^{i+1}\right]=\\&=\frac{H\left(H+\varphi_{22}-1\right)\left(1+H+\varphi_{22}\right)}{1-\varphi_{11}}\left(-H-\varphi_{22}\right)^{i}\end{aligned} \tag{4.66}$$

Beginning from m_{min}, the sum of the terms have to fulfil the condition:

$$\sum_{i=m_{\text{min}}+1}^{\infty}\frac{H\left(H+\varphi_{22}-1\right)\left(H+\varphi_{22}+1\right)}{1-\varphi_{11}}\left(-H-\varphi_{22}\right)^{m_{\text{min}}}\left(-H-\varphi_{22}\right)^{i}\le e_{\text{max}} \tag{4.67}$$

The expression in (4.67) creates the geometrical sequence, which means that it is:

$$\frac{H\left(H+\varphi_{22}-1\right)\left(H+\varphi_{22}+1\right)\left(H+\varphi_{22}\right)^{m_{\text{min}}}}{\left(1-\varphi_{11}\right)}\frac{1}{1-\left(-H-\varphi_{22}\right)}\le e_{\text{max}} \tag{4.68}$$

From Eq. (4.68), we obtain the following:

$$m_{\min} \geq \frac{\log \dfrac{e_{\max}(1-\varphi_{11})}{H(H+\varphi_{22}-1)}}{\log(-H-\varphi_{22})} \tag{4.69}$$

Example 4.12. Let us take $e_{\max} = 0.001$. For the exemplary 2-nd order algorithm from Example 4.11, it is: H = -1.21. Based on the expression (4.66), we have:

$$m_{\min} \geq \frac{\log \dfrac{0.001 \cdot (1-0.9017)}{-1.21 \cdot (-1.21+0.4188-1)}}{\log(1.21-0.4188)} = \frac{-4.34}{-0.102} = 42.5$$

This means that the number K of samples in the measurement window, which is the minimum number of terms representing the reconstruction algorithm in the form of the sequence, is:

$$K = m_{\min} + 2 = 43 + 2 = 45$$

As it results from Eq. (4.51), the reconstruction algorithm of the 1-st order converter has only the non-recurrent form:

$$\hat{x}(k) = \frac{1}{1-\varphi}\left[\hat{u}(k+1) - \varphi\hat{u}(k+1)\right] = \frac{1}{1-\varphi}\hat{u}(k+1) + \frac{-\varphi}{1-\varphi}\hat{u}(k) \tag{4.70}$$

Accordingly with Eq. (4.62), the general form of the sequence (4.51) reduces in this case to 2 elements:

$$\hat{x}(k) = A_{k+1}\hat{u}(k+1) + A_k\hat{u}(k) \tag{4.71}$$

The coefficients of this expression have the forms:

$$A_{k+1} = \frac{1}{1-\varphi}, \quad A_k = \frac{-\varphi}{1-\varphi} \tag{4.72}$$

The sum of both coefficients is:

$$A_{k+1} + A_k = \frac{1}{1-\varphi} + \frac{-\varphi}{1-\varphi} = 1 \tag{4.73}$$

which means that static sensitivity of the dynamic algorithm is equal 1, the same as obtained for the 2-nd order reconstruction algorithm accordingly with Eq. (4.65). This property is the same as results from the basic decomposition assumptions described in Chapter 2.

Example 4.13. The coefficient φ of the discrete model of the 1-st order converter from Example 4.2 has the value: $\varphi = 0{,}9048$. On the basis of expressions (4.72), the coefficients of the sequence (4.71), calculated for this value, are:

$$A_{k+1} = \frac{1}{1-\varphi} = \frac{1}{1-0.9048} = 10.50, \quad A_k = \frac{-\varphi}{1-\varphi} = \frac{-0.9048}{1-0.9048} = -9.50$$

4.3.3. Description of dynamic reconstruction in frequency domain

From an error analysis point of view, every reconstruction algorithm can be presented as such an element of the sampling instrument, which both introduces inside errors and propagates the input errors to the output. Inside errors are connected with the fact that the basis of the dynamic reconstruction algorithm is the discrete model of the analog converter described in Section 4.2.2. The use of this model causes the samples of the reconstructed signal to be burdened by the discretization error that is immanently connected with the mathematical conditions of the discretization of the analog model. One can say that the discretization error is the same kind of error as the approximation error of the static reconstruction, because both errors describe imperfection of the reconstruction, static and dynamic, respectively.

The reconstruction consists in realizing mathematical operations on the samples that are burdened by errors. It means that the same operations are performed on the input samples as on their errors, which causes that the output samples contain error dependent on properties both of the input errors and the mathematical operation specific for the algorithm. Transmission of an error from the algorithm input to its output is generally called an error propagation and described by a propagation equation that consist of relations between realizations of the output and the input errors. The propagation is described in the following chapters for two basic input errors that arise during the physical realization of digitalization of the input signal, which is made up of the signal sampling and the quantization of the obtained samples.

The parameters of the discrete state equation (4.31) are determined with the assumption that the input signal does not vary between discretization instants, which is not true. This assumption causes that dynamic reconstruction algorithm to be inaccurate because it is the inverse solution of the inaccurate discrete model of the analog converter. This results in the appearance of the error in the output of the reconstruction algorithm, which is called the dynamic discretization error. The nature of this error is connected with nonideality of the reconstruction caused by application of the discrete model.

The dynamic discretization error depends on both the parameters of the model and the properties of the reconstructed signal. Taking this into account, the error analysis should be carried out for selected signals. The sinusoidal signal is commonly used because for it, the analysis of the reconstruction algorithm gives essential information and is relatively simple.

For the sinusoidal signal, the dynamic properties of the algorithm are described by the spectral transmittance that is its transfer function in the frequency domain ω [L2]. Based on the sequence form (4.62) of the algorithm and taking into account that the estimates $\hat{u}(k+1),\hat{u}(k),\ldots,\hat{u}(k+m)+\ldots$ represent samples of the algorithm input signal, we can write the spectral form $\hat{X}(\mathrm{j}\omega)$ of the reconstructed signal as the expression:

$$\hat{X}(\mathrm{j}\omega)=\left(A_{k+1}e^{\mathrm{j}\omega T_\mathrm{s}}+A_k+A_{k-1}e^{-\mathrm{j}\omega T_\mathrm{s}}+\ldots+A_{k-m}e^{-\mathrm{j}m\omega T_\mathrm{s}}+\ldots\right)\hat{U}(\mathrm{j}\omega) \tag{4.74}$$

where $\hat{U}(\mathrm{j}\omega)$ denotes the spectral form of the output signal of the analog converter, and T_s is the sampling (discretization) period. To obtain this equation, the theorem is used, according to which rotation of the vector by the angle $m\omega T_\mathrm{s}$ on the complex plane corresponds to the sample shift in the time domain by m sampling periods T_s [L2]. Based on Eq. (4.74), we obtain the spectral transfer function (transmittance) of the dynamic algorithm in the form of the sequence:

$$A(\mathrm{j}\omega)=\frac{\hat{X}(\mathrm{j}\omega)}{\hat{U}(\mathrm{j}\omega)}=A_{k+1}e^{\mathrm{j}\omega T_\mathrm{s}}+A_k+A_{k-1}e^{-\mathrm{j}\omega T_\mathrm{s}}+\ldots+A_{k-m}e^{-\mathrm{j}m\omega T_\mathrm{s}}+\ldots \tag{4.75}$$

From the dynamic error analysis point of view, the reconstruction algorithm should be considered as the second of two elements from the couple shown in Fig. 4.10. One can interpret the dependence between these elements in this manner so that the dynamic error arising during the analog signal conversion is eliminated (decreased) by the dynamic reconstruction, which works as the dynamic error corrector. The transfer function of the reconstruction algorithm is the basis of determination of its efficiency as the corrector of the dynamic error.

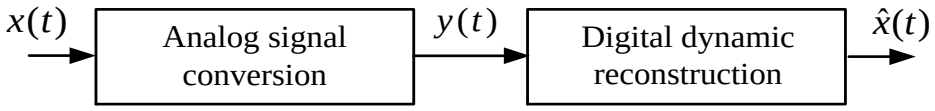

Fig. 4.10. Dynamic reconstruction chain composed of the analog conversion and the digital reconstruction described in the time domain

The dynamic properties of the analog converter, being the first element of the chain of Fig. 4.10, are modeled by the transfer function $S(\mathrm{j}\omega)$, while the dynamic reconstruction algorithm by the transmittance $A(\mathrm{j}\omega)$ described by Eq. (4.75). Based on the scheme from Fig. 4.10, the relation between the input signal $X(\mathrm{j}\omega)$, and its reconstructed form $\hat{X}(\mathrm{j}\omega)$ can be written as follows:

$$\hat{X}(\mathrm{j}\omega) = \frac{\hat{X}(\mathrm{j}\omega)}{\hat{U}(\mathrm{j}\omega)} \frac{U(\mathrm{j}\omega)}{X(\mathrm{j}\omega)} X(\mathrm{j}\omega) = A(\mathrm{j}\omega) S(\mathrm{j}\omega) X(\mathrm{j}\omega) \tag{4.76}$$

with the assumption that the estimation errors of the signal $U(\mathrm{j}\omega)$ is neglected; therefore, $U(\mathrm{j}\omega) = \hat{U}(\mathrm{j}\omega)$. Based on Eq. (4.76), one can describe the transmittance of the chain from Fig. 4.10 as the whole:

$$S_{\mathrm{rec}}(\mathrm{j}\omega) = \frac{\hat{X}(\mathrm{j}\omega)}{X(\mathrm{j}\omega)} = A(\mathrm{j}\omega) S(\mathrm{j}\omega) \tag{4.77}$$

presented graphically in Fig. 4.11.

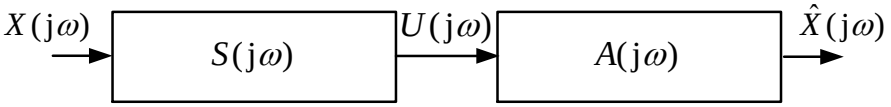

Fig. 4.11. Dynamic reconstruction chain described in the frequency domain

Accordingly with Eq. (4.51), the transmittance the reconstruction algorithm for the 1-st order converter consists of two terms, which means that the sequence (4.75) is described in this case by the expression:

$$A(\mathrm{j}\omega) = A_{k+1} e^{\mathrm{j}\omega T_{\mathrm{s}}} + A_k \tag{4.78}$$

The transmittance $S(\mathrm{j}\omega)$ of the 1-st order converter is described by Eq. (4.3). Taking into account that the static sensitivity of the converter $S = 1$ and based on Eqs. (4.77) and (4.78), one can write the transmittance of the 1-st order reconstruction chain in the form:

$$S_{\mathrm{rec}}(\mathrm{j}\omega) = A(\mathrm{j}\omega) S(\mathrm{j}\omega) = \left(A_{k+1} e^{\mathrm{j}\omega T_{\mathrm{s}}} + A_k\right) \frac{1}{1 + \mathrm{j}\omega\tau} \tag{4.79}$$

After introducing the expressions (4.72) to (4.79), one obtains the following:

$$S_{\mathrm{rec}}(\mathrm{j}\omega) = \frac{1}{1 + \mathrm{j}\omega\tau} \left(\frac{1}{1-\varphi} e^{\mathrm{j}\omega T_{\mathrm{s}}} - \frac{\varphi}{1-\varphi} \right) = \frac{1}{1-\varphi} \frac{\cos\omega T_{\mathrm{s}} - \varphi + \mathrm{j}\sin\omega T_{\mathrm{s}}}{1 + \mathrm{j}\omega\tau} \tag{4.80}$$

The transmittance of the reconstruction chain generally describes the relation between the complex forms of the input and the reconstructed signals. Accordingly

with Eqs. (4.80) and (4.77), the relation between amplitudes of these signals for the 1-st order reconstruction chain can be written as:

$$\frac{\left|\hat{X}(\mathrm{j}\omega)\right|}{\left|X(\mathrm{j}\omega)\right|}=\left|S_{\mathrm{rec}}(\mathrm{j}\omega)\right|=\left|\frac{1}{1-\varphi}\,\frac{\cos\omega T_{\mathrm{s}}-\varphi+\mathrm{j}\sin\omega T_{\mathrm{s}}}{1+\mathrm{j}\omega\tau}\right|=\frac{1}{1-\varphi}\sqrt{\frac{(\cos\omega T_{\mathrm{s}}-\varphi)^2+\sin^2\omega T_{\mathrm{s}}}{1+(\omega\tau)^2}} \quad (4.81)$$

One can point to another way of determining the module of the reconstruction chain transmittance. Accordingly with Eq. (4.77), this transmittance can be described in the following form:

$$\left|S_{\mathrm{rec}}(\mathrm{j}\omega)\right|=\left|\frac{\hat{X}(\mathrm{j}\omega)}{X(\mathrm{j}\omega)}\right|=\left|A(\mathrm{j}\omega)S(\mathrm{j}\omega)\right|=\left|A(\mathrm{j}\omega)\right|\left|S(\mathrm{j}\omega)\right| \quad (4.82)$$

Considering the 1-st order algorithm, one obtains that the module of its transmittance accordingly with Eq. (4.78) is described by the expression:

$$\left|A(\mathrm{j}\omega)\right|=\left|A_{k+1}e^{\mathrm{j}\omega T_{\mathrm{s}}}+A_k\right|=\left|\frac{1}{1-\varphi}e^{\mathrm{j}\omega T_{\mathrm{s}}}-\frac{\varphi}{1-\varphi}\right|=\frac{\sqrt{(\cos\omega T_{\mathrm{s}}-\varphi)^2+\sin^2\omega T_{\mathrm{s}}}}{1-\varphi} \quad (4.83)$$

The module of the 1-st order converter is described by Eq. (4.21); therefore, based on Eqs. (4.82) and (4.83), the expression (4.83) takes the form:

$$\left|S_{\mathrm{rec}}(\mathrm{j}\omega)\right|=\frac{1}{\sqrt{1+(\omega\tau)^2}}\,\frac{\sqrt{(\cos\omega T_{\mathrm{s}}-\varphi)^2+\sin^2\omega T_{\mathrm{s}}}}{1-\varphi} \quad (4.84)$$

the same as (4.80).

Example 4.14. The time constant of the 1-st order converter from Example 4.4 is $\tau = 2$ s. The frequency of the sinusoidal input signal is $f = 0.01$ Hz. The signal is sampled with the period $T_{\mathrm{s}} = 0.2$ s, which means that the coefficient $\varphi = 0.9048$ and $\omega T_{\mathrm{s}} = 2\cdot\pi\cdot f\cdot T_{\mathrm{s}} = 2\cdot\pi\cdot 0.01\cdot 0.2 = 12.56\cdot 10^{-3}$. For these assumptions, the module of the converter transmittance (4.3) takes the following value:

$$\left|S(\mathrm{j}\omega)\right|=\frac{1}{\sqrt{1+(\omega\tau)^2}}=\frac{1}{\sqrt{1+(2\pi\cdot 0.01\cdot 2)^2}}=0.9922$$

The module of the 1-st order reconstruction algorithm (4.83) is:

$$\left|A(\mathrm{j}\omega)\right|=\frac{\sqrt{(\cos\omega T_{\mathrm{s}}-\varphi)^2+\sin^2\omega T_{\mathrm{s}}}}{1-\varphi}=\frac{\sqrt{1-2\varphi\cos\omega T_{\mathrm{s}}+\varphi^2}}{1-\varphi}=$$

$$=\frac{\sqrt{1-2\cdot 0.9048\cdot\cos\left(12.56\cdot 10^{-3}\right)+0.9048^2}}{1-0.9048}=1.00784$$

Thus, the module of transmittance of the reconstruction chain has the value:

$$|S_{\text{rec}}(\text{j}\omega)| = |A(\text{j}\omega)||S(\text{j}\omega)| = 0.9922 \cdot 1.00784 = 0.99998$$

which means that it is close to the ideal one equal to 1.

As in Example 4.14, the efficiency of the dynamic reconstruction can be considered on the basis of the transmittances of the reconstruction chain. But the better way to do such considerations seems to be an analysis of dynamic errors, which enables to compare these errors with other reconstruction errors. According to the general definition (1.50), the dynamic error of the sinusoidal output signal of the converter described by the statically ideal transmittance $S(\text{j}\omega)$ (its static transfer function $S = 1$) is defined as:

$$e_{\text{dyn}}(\text{j}\omega) = X(\text{j}\omega) - Y(\text{j}\omega) = X(\text{j}\omega)\left[1 - \frac{Y(\text{j}\omega)}{X(\text{j}\omega)}\right] = [1 - S(\text{j}\omega)]X(\text{j}\omega) \qquad (4.85)$$

where $X(\text{j}\omega)$ and $Y(\text{j}\omega)$ are spectral transforms of the input and output signal, respectively.

The reconstruction chain can be considered as such a converter which aims at minimalization of the dynamic error at its output by using a suitable reconstruction algorithm. The basic error of this chain is connected with the discrete form of the reconstruction algorithm. This error is called the discretization error and, accordingly with Eq. (4.85), it is described in the frequency domain as:

$$e_{\text{dis}}(\text{j}\omega) = X(\text{j}\omega) - \hat{X}(\text{j}\omega) = X(\text{j}\omega)\left[1 - \frac{\hat{X}(\text{j}\omega)}{X(\text{j}\omega)}\right] = [1 - S_{\text{rec}}(\text{j}\omega)]X(\text{j}\omega) \qquad (4.86)$$

where $\hat{X}(\text{j}\omega)$ is the spectral form of the reconstructed signal.

The transmittance of the 1-st order reconstruction chain is described by Eq. (4.79), thus, the discretization error (4.86) takes the following form:

$$e_{\text{dis}}(\text{j}\omega) = [1 - S_{\text{rec}}(\text{j}\omega)]X(\text{j}\omega) = \left[1 - \frac{1}{1 + \text{j}\omega\tau}\left(A_{k+1}e^{\text{j}\omega T_{\text{s}}} + A_k\right)\right]X(\text{j}\omega) \qquad (4.87)$$

from which one obtains that the amplitude of the error is:

$$|e_{\text{dis}}(\text{j}\omega)| = |X(j\omega)|\left|1 - \frac{1}{1 + \text{j}\omega\tau}\left(A_{k+1}e^{\text{j}\omega T_{\text{s}}} + A_k\right)\right| = |X(j\omega)|\frac{\left|1 + \text{j}\omega\tau - A_{k+1}e^{\text{j}\omega T_{\text{s}}} - A_k\right|}{|1 + \text{j}\omega\tau|} \qquad (4.88)$$

where $X|(j\omega)|$ is the amplitude of the input signal. Based on Eq. (4.80), the numerator of expression (4.88) can be written as:

$$1+\mathrm{j}\omega\tau - A_{k+1}e^{\mathrm{j}\omega T_\mathrm{s}} - A_k = 1+\mathrm{j}\omega\tau - \frac{e^{\mathrm{j}\omega T_\mathrm{s}}}{1-\varphi} + \frac{\varphi}{1-\varphi} = \frac{1-\cos\omega T_\mathrm{s}}{1-\varphi} + \mathrm{j}\left(\omega\tau - \frac{\sin\omega T_\mathrm{s}}{1-\varphi}\right)$$

(4.89) which means that the amplitude of the discretization error (4.88) is expressed in the form:

$$E_\mathrm{dis} = \left|e_\mathrm{dis}(\mathrm{j}\omega)\right| = \left|X(j\omega)\right|\sqrt{\frac{\left(\frac{1-\cos\omega T_\mathrm{s}}{1-\varphi}\right)^2 + \left(\omega\tau - \frac{\sin\omega T_\mathrm{s}}{1-\varphi}\right)^2}{1+(\omega\tau)^2}} \tag{4.90}$$

Reconstruction reduces the dynamic error introduced by the analog converter to the discretization error. Taking this into account, the discretization error can be interpreted as the effect of non-ideal elimination of the dynamic error by the reconstruction algorithm. The degree of this reduction may be determined by using the reduction coefficient generally defined as:

$$k_\mathrm{Dred} = \frac{E_\mathrm{dyn}}{E_\mathrm{dis}} \tag{4.91}$$

where E_dyn is amplitude of the dynamic error in the input of the reconstruction algorithm and E_dis is the amplitude of the output error resulting from non-ideal reconstruction of the input signal by the discrete algorithm.

The transmittance of the 1-st order converter is given by Eq. (4.3) (with $S = 1$). In this case, the dynamic error (4.85) takes the form:

$$e_\mathrm{dyn}(\mathrm{j}\omega) = [1-S(\mathrm{j}\omega)]X(\mathrm{j}\omega) = \left[1-\frac{1}{1+\mathrm{j}\omega\tau}\right]X(\mathrm{j}\omega) = \frac{\mathrm{j}\omega\tau}{1+\mathrm{j}\omega\tau}X(\mathrm{j}\omega) \tag{4.92}$$

which means that the amplitude of this error is:

$$E_\mathrm{dyn} = \left|e_\mathrm{dyn}(\mathrm{j}\omega)\right| = \frac{\omega\tau}{\sqrt{1+(\omega\tau)^2}}\left|X(\mathrm{j}\omega)\right| \tag{4.93}$$

Therefore, on the basis on Eqs.(4.91) and (4.93), the reduction coefficient (4.91) for the 1-st order converter is described by the expression:

$$k_\mathrm{Dred} = \frac{E_\mathrm{dyn}}{E_\mathrm{dis}} = \frac{\omega\tau}{\sqrt{\left(\frac{1-\cos\omega T_\mathrm{s}}{1-\varphi}\right)^2 + \left(\omega\tau - \frac{\sin\omega T_\mathrm{s}}{1-\varphi}\right)^2}} \tag{4.94}$$

The considered errors calculated for the exemplary 1-st order converter in dependence of the input signal frequency are shown in Fig. 4.12, while the selected values of these errors and the reduction coefficient are presented in Tab. 4.5.

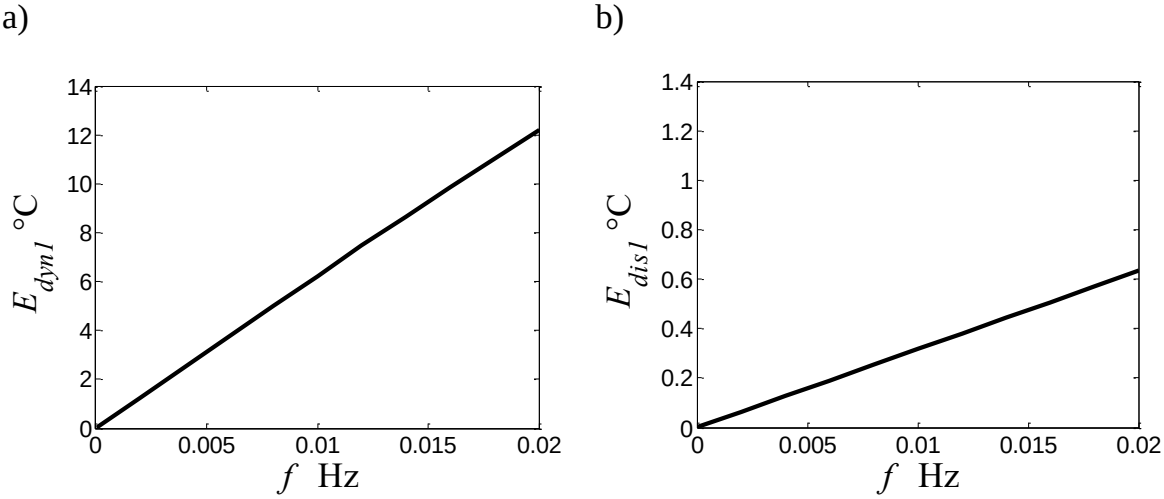

Fig. 4.12. Dependences of the amplitudes: a) of the dynamic error, b) of the discretization error as the function of frequency $f = \omega/2\pi$ of the input temperature signal $\vartheta(t) = x(t) = 50+50\sin\omega t$°C determined for the exemplary 1-st order converter, both amplitudes are expressed in relation to the signal amplitude equal to 50°C

Table 4.5

Values of amplitudes of the dynamic errors of the exemplary 1-st order converter in dependence of the frequency f of the sinusoidal signal $\vartheta(t) = x(t) = 50+50\sin\omega t$°C, E_{dyn} is the amplitude of the converter dynamic error, and E_{dis} is the amplitude of the discretization error, both amplitudes are expressed in relation to the signal amplitude equal to 50°C

f Hz	0.001	0.002	0.005	0.01	0.02
E_{dyn1}	0.628	1.256	3.135	6.234	12.19
E_{dis1}	0.0317	0.0634	0.158	0.317	0.634
k_{Dred1}	19.8	19.8	19.8	19.7	19.2

On the basis of results presented in Tab. 4.5, one can state that for the exemplary 1-st order converter the dynamic error is reduced about 20 times in result of application of the dynamic reconstruction although, starting of some signal frequency, the efficiency of the reconstruction diminishes.

The transmittance of the reconstruction algorithm of the 2-nd order converter can be written as the expression:

$$A(\mathrm{j}\omega) = A_{k+1}e^{\mathrm{j}\omega T_s} + A_k + \frac{A_{k-1}}{1 - q_A e^{-\mathrm{j}\omega T_s}} \tag{4.95}$$

which is obtained basing on the fact that, beginning from 3-rd element, the terms in Eq. (4.75) create the geometrical complex sequence with the quotient $q_A e^{-j\omega T_s}$, where the coefficient q_A is given by Eq. (4.63). Introducing the algorithm coefficients (4.61) to Eq. (4.95), we have:

$$A(j\omega) = \frac{1}{1-\varphi_{11}}\left[e^{j\omega T_s} + H - \varphi_{11} + \frac{H(H+\varphi_{22}-1)}{1-(H+\varphi_{22})e^{-j\omega T_s}} \right] \tag{4.96}$$

where H is given by Eq. (4.58).

The module $|A(j\omega)|$ of the transmittance of the 2-nd order reconstruction algorithm can be determined on the basis of Eq. (4.86) but the numerically simpler way consists in calculation of the real and imaginary parts of the transmittance in the form of the sequence (4.75). Eq. (4.96) as the sequence is of the form:

$$\begin{aligned} A(j\omega) = {} & A_{k+1}(\cos\omega T_s + j\sin\omega T_s) + A_k + A_{k-1}(\cos\omega T_s - j\sin\omega T_s) + \ldots \\ & + A_{k-m}(\cos m\omega T_s - j\sin m\omega T_s) + \ldots \end{aligned} \tag{4.97}$$

After splitting expression (4.97), one obtains its real part as:

$$\mathrm{Re}\{A(j\omega)\} = A_{k+1}\cos\omega T_s + A_k + A_{k-1}\cos\omega T_s + \ldots + A_{k-m}\cos m\omega T_s + \ldots \tag{4.98}$$

while the imaginary part is:

$$\mathrm{Im}\{A(j\omega)\} = A_{k+1}\sin\omega T_s - A_{k-1}\sin\omega T_s + \ldots + A_{k-m}\sin m\omega T_s + \ldots \tag{4.99}$$

Generally, the algorithm transmittance can be written in the form:

$$A(j\omega) = |A(j\omega)|e^{j\varphi_A} \tag{4.100}$$

where the module is expressed as:

$$|A(j\omega)| = \sqrt{\mathrm{Re}\{A(j\omega)\}^2 + \mathrm{Im}\{A(j\omega)\}^2} \tag{4.101}$$

and the phase shift is:

$$\varphi_A = \arctan\frac{\mathrm{Im}\{A(j\omega)\}}{\mathrm{Re}\{A(j\omega)\}} \tag{4.102}$$

Having calculated the algorithm transmittance accordingly with the presented equations, one can determine the amplitude of the reconstructed signal on the basis of Eq. (4.76) as:

$$|\hat{X}(j\omega)| = |S_{\mathrm{rec}}(j\omega)||X(j\omega)| = |S(j\omega)||A(j\omega)||X(j\omega)| \tag{4.103}$$

Example 4.15. Let us take that the parameters of the 2-nd order converter are the same as in Example 4.5, and the coefficients of the reconstruction algorithms are taken from Example 4.11. The sinusoidal input signal: $x(t) = \sin\omega t$, $\omega = 2\pi f$, $f = 0.1$ Hz, is sampled with period $T_s = 0.5$ s. For these parameters, the module of the converter transmittance (4.24) is as follows:

$$|S(\mathrm{j}\omega)| = \frac{1}{\sqrt{\left[1-\left(\frac{\omega}{\omega_0}\right)^2\right]^2 + \left(2b\frac{\omega}{\omega_0}\right)^2}} = \frac{1}{\sqrt{\left[1-\left(\frac{2\pi\cdot 0.1}{1}\right)^2\right]^2 + \left(\frac{2\cdot 0.7\cdot 0.1}{1}\right)^2}} = 0.93656$$

In Example 4.12, 45 elements of the sequence (4.97) are calculated to be necessary to obtain the inaccuracy at the level of 0.001. In this case, accordingly with Eqs. (4.98) and (4.99), the real and imaginary parts of the reconstruction algorithm have the values:

$$\mathrm{Re}\{A(\mathrm{j}\omega)\} = 0.46226 \qquad \text{and} \qquad \mathrm{Im}\{A(\mathrm{j}\omega)\} = 0.96685$$

Based on these values, the module of the reconstruction is calculated as:

$$|A(\mathrm{j}\omega)| = \sqrt{\mathrm{Re}\{A(\mathrm{j}\omega)\}^2 + \mathrm{Im}\{A(\mathrm{j}\omega)\}^2} = \sqrt{0.46226^2 + 0.96685^2} = 1.0717$$

Thus, on the basis of Eq. (4.103), the amplitude of the reconstructed signal takes the value:

$$\left|\hat{X}(\mathrm{j}\omega)\right| = |S_2(j\omega)||A_2(j\omega)||X(j\omega)| = 0.93656\cdot 1.0717\cdot 1 = 1.0037$$

The errors calculated in the way presented in Example 4.15 for this exemplary 2-nd order converter in dependence of the input signal frequency are shown in Fig. 4.13. The selected values of these errors and the reduction coefficient k_{Dred} are presented in Tab. 4.6.

a) b)

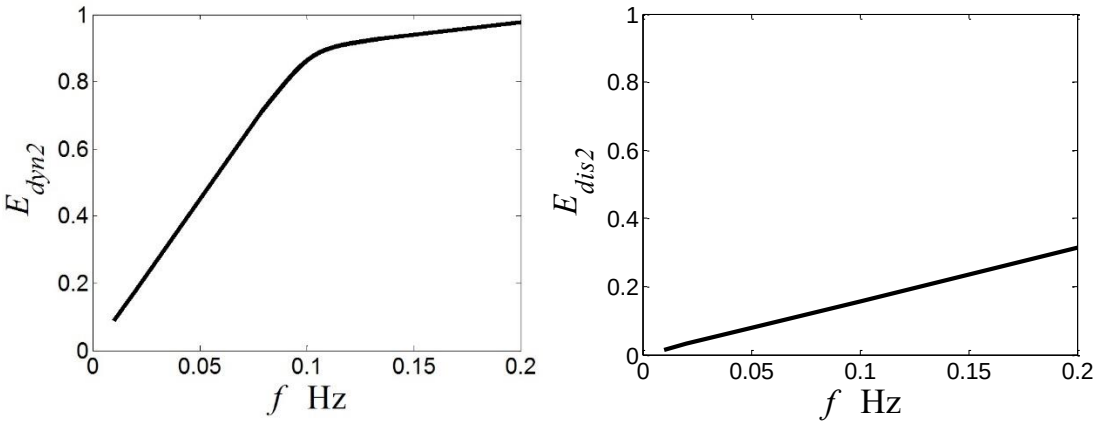

Fig. 4.13. Dependences of the dynamic error (a) and the discretization error (b) determined for the exemplary 2-nd order converter as a function of the frequency $f = \omega/2\pi$ of the sinusoidal input signal with the amplitude equal to 1, both amplitudes are expressed in relation to the signal amplitude

Table 4.6

Values of the amplitudes of the dynamic errors of the exemplary 2-nd order converter in dependence of the frequency f of the sinusoidal signal with the amplitude equal to 1, E_{dyn} is the amplitude of the converter dynamic error while E_{dis} is the amplitude of the discretization error, k_{Dred} is the reduction coefficient defined by Eq. (4.91)

f Hz	0.01	0.02	0.05	0.1	0.2
E_{dyn}	0.0881	0.1767	0.4495	0.9030	0.9767
E_{dis}	0.0152	0.0313	0.0781	0.1568	0.3153
k_{Dred}	5.7921	5.6400	5.7517	5.7580	3.0974

Based on results presented in Tab. 4.6, one can state that, for the exemplary 2-nd order converter, the dynamic error is reduced about 6 times as a result of application of the dynamic reconstruction algorithm although, starting of some signal frequency, the efficiency of the reconstruction diminishes.

4.4. Identification of parameters of dynamic algorithms

4.4.1. Identification of first-order algorithm

In practice, the coefficients of the dynamic model are determined in a measurement experiment, which means that they are identified on the basis of measurement data burdened by errors. This causes the obtained values of the model coefficients to be inaccurate, which results in occurrence of a specific error of the reconstruction algorithm called the identification error.

One of the simplest ways of the dynamic model identification consists in stimulation of the converter input by a well-determined reference signal and carrying out measurements of the response at the converter output [K2]. To obtain a satisfactory identification accuracy, it is necessary to reduce errors that burden the measured results. Such a reduction can be achieved if one uses step-changing reference signal [M8], because for this signal, the discretization error is equal to zero (see Fig. (4.6)).

For 1-st order converter, the relation between samples of the input and output signal is described by Eq. (4.35). Based on Eq. (4.36), one can write that, for the unitary step change of the input signal, that is, for $x(k) = 1$, $k = 0, 1, ...$, it is:

$$\frac{1}{1-\varphi}\left[\hat{u}(k+1)-\varphi\hat{u}(k)\right]=x(k)=1 \tag{4.104}$$

According to this equation, the estimate of the reconstruction algorithm coefficient that is determined for k instant is obtained as:

$$\hat{\varphi}(k) = \frac{1-\hat{u}(k+1)}{1-\hat{u}(k)} \tag{4.105}$$

Expression (4.105) enables the calculation of coefficient φ basing on 2 subsequent samples of the output signal. Taking into account that the samples are burdened by random errors, inaccuracy of the identified coefficient can be decreased if we determine its estimate as the average value of partial identification results. If one uses K beginning samples of the same response, the estimate is calculated as:

$$\hat{\varphi}(K) = \frac{1}{K}\sum_{k=0}^{K-1}\hat{\varphi}(k) = \frac{1}{K}\sum_{k=0}^{K-1}\frac{1-\hat{u}(k+1)}{1-\hat{u}(k)} \tag{4.106}$$

In measurement practice, the sensor input signal is converted both by its static and dynamic part, which means that the output signal used for the identification is burdened by static and dynamic errors. The sensor applied in the exemplary instrument is described by the Wiener model; therefore, the dynamic input signal is converted at first by the dynamic linear part of the sensor; and then, by the static nonlinear part. This means that, before performing the identification of the dynamic properties of the sensor, it is necessary to correct static nonlinearity errors, i.e., to perform the static reconstruction.

Example 4.16. Let us determine the coefficient φ of the 1-st order dynamic reconstruction algorithm applied in the exemplary sampling instrument for the step input temperature signal changed from ϑ = 0°C to 100°C at time instant t = 0 (k = 0). The sensor output signal is sampled with the period T_s = 0.2 s and statically corrected using the algorithm (3.13). According to Fig. 3.6b, the total static reconstruction error can be described as normal noise $N(0; 0.01)$°C (its standard deviation is equal to 0.01°C). Taking this into account, the estimates $\hat{u}(k)$, $k = 0, 1, ...,$ can be determined in a simulative way as samples of the output signal of the dynamic sensor with the time constant τ = 2 s, which are burdened by the noise error $N(0; 0.01)$°C. The beginning 9 output samples are presented in the table 4.7.

Table 4.7

Beginning samples of the response of the 1-st order sensor applied in the exemplary instrument to the step input signal from ϑ = 0°C to 100°C, k is the number of the sample

k	0	1	2	3	4	5	6	7	8
$\hat{u}(k)$°C	0.015	9.509	18.131	25.916	32.979	39.336	45.119	50.347	55.078

Based on the results from Tab. 4.7, the estimates $\hat{\varphi}$ are calculated accordingly with Eq. (4.106) with such a difference that the estimate for the instant k is calculated as:

$$\hat{\varphi}(k) = \frac{100 - \hat{u}(k+1)}{100 - \hat{u}(k)} \tag{4.107}$$

because the step change of the input signal is 100°C in the case considered. The obtained estimates are contained in Tab. 4.8 together with the E_{tot} amplitude of the total dynamic error calculated for every estimate $\hat{\varphi}(k)$ accordingly with the expression:

$$E_{\text{tot}}(k) = |X(j\omega)| \sqrt{\frac{\left(\frac{1-\cos\omega T_{\text{s}}}{1-\hat{\varphi}(k)}\right)^2 + \left(\omega\tau - \frac{\sin\omega T_{\text{s}}}{1-\hat{\varphi}(k)}\right)^2}{1+(\omega\tau)^2}} \tag{4.108}$$

obtained on the basis of Eq. (4.90) for:

$$|X(j\omega)| = 50\ ^{\circ}\text{C},\ \omega = 2\cdot\pi\cdot f,\ f = 0.02\ \text{Hz},\ T_{\text{s}} = 0.2\ \text{s},\ \tau = 2\ \text{s}$$

Table 4.8

Estimates of the coefficient φ of the 1-st order dynamic reconstruction algorithm used in the exemplary instrument, which are calculated on the basis of Eqs. (4.106) and (4.107), K is the number of samples used to obtain a single estimate, E_{tot} is the amplitude of the error at the output of the dynamic reconstruction algorithm for the input sinusoidal signal with the amplitude 50°C, the exact value of φ is 0.90484

K	2	3	4	5	6	7	8	9	10
$\hat{\varphi}(K)$	0.90489	0.90489	0.90483	0.90490	0.90486	0.90484	0.90483	0.90481	0.90484
$E_{\text{tot}}(K)$°C	0.645	0.646	0.638	0.647	0.642	0.640	0.637	0.636	0.639

The error e_{tot}, the amplitude of which is denoted as E_{tot}, is determined as the discretization error in the case if the coefficient φ is calculated by effect of its identification as the estimate $\hat{\varphi}$. It means that the error e_{tot} is a composition of the discretization error e_{dis} calculated for the exact value of φ and the additive error connected with the difference between φ and its estimate $\hat{\varphi}$. The amplitude of the error e_{dis} is $E_{\text{dis}} = 0.639$°C in the considered conditions. $E_{\text{tot}}(K)$ values do not differ essentially from E_{dis}, which means that the coefficient φ determined on the basis of 2 samples of the step response is accurate enough in the experimental conditions.

4.4.2. Identification of the second-order algorithm in the analytical form

The reconstruction algorithm for the 2-nd order analog converter consists of 2 equations (4.52) and (4.53). The simplest way to identify the algorithm coefficients consists in measuring beginning values of the converter response u to unitary step change and in calculating estimates of the coefficient on the basis of the description of the algorithm [M8].

For the step change of the input signal, the beginning values of the state variables are:

$$u(0)= u_2(0) = 0 \tag{4.109}$$

of the input signal x from 0 to 1. The instantaneous values of the input signal that change from 0 to 1 at instant $k = 0$ are: $x(k) = 1$ for $k = 0,1,...$, which means that Eq. (4.53) for $k = 0$ takes the form:

$$x(0) = \frac{1}{1-\varphi_{11}}\left[\hat{u}(1) - \varphi_{11}\hat{u}(0) - \varphi_{12}\hat{u}_2(0)\right] = \frac{\hat{u}(1)}{1-\varphi_{11}} = 1 \tag{4.110}$$

from which one obtains:

$$\hat{\varphi}_{11} = 1 - \hat{u}(1) \tag{4.111}$$

Having known $\hat{\varphi}_{11}$, one can calculate $\hat{\varphi}_{12}$ on the basis of Eq. (4.53). For $k = 1$, we have:

$$x(1) = \frac{1}{1-\hat{\varphi}_{11}}\left[\hat{u}(2) - \varphi_{11}\hat{u}(1) - \varphi_{12}\hat{u}_2(1)\right] = 1 \tag{4.112}$$

from which, it is:

$$\hat{\varphi}_{12} = \frac{\hat{u}(2) - 1 + \hat{\varphi}_{11}\left[1 - \hat{u}(1)\right]}{\hat{u}_2(1)} = \frac{\hat{u}(2) - 1 + \hat{\varphi}_{11}^2}{\hat{u}_2(1)} \tag{4.113}$$

As it results from Eq. (4.113), to identify the coefficient $\hat{\varphi}_{12}$, it is necessary to know the value of the state variable $u_2(1)$ that is the first derivative of the output signal (see Eq.(4.27)). This variable can be approximated by samples of the output signal u as the mean value of its two successive estimates:

$$\hat{u}_2(k+1) \cong \frac{\dfrac{\hat{u}(k+1) - \hat{u}(k)}{T_s} + \dfrac{\hat{u}(k+2) - \hat{u}(k+1)}{T_s}}{2} = \frac{\hat{u}(k+2) - \hat{u}(k)}{2T_s} \tag{4.114}$$

where T_s is the sampling period. According to this equation, the value $u_2(1)$ of the state variable may be determined as:

$$\hat{u}_2(1) \cong \frac{\hat{u}(2)-\hat{u}(0)}{2T_s} = \frac{\hat{u}(2)}{2T_s} \tag{4.115}$$

where it is taken into account that, accordingly with (4.108), $u(0) = 0$. After introducing Eq. (4.115) to (4.113), one obtains the following:

$$\varphi_{12} = \frac{\hat{u}(2)-1+\hat{\varphi}_{11}^2}{\frac{\hat{u}(2)}{2T_s}} = 2T_s \frac{\hat{u}(2)-1+\hat{\varphi}_{11}^2}{\hat{u}(2)} \tag{4.116}$$

As result of Example 4.5, we have:

$$\hat{\varphi}_{21} = -\hat{\varphi}_{12} \tag{4.117}$$

This relation can be used to calculate the last coefficient. For k =1 and $x(k)$ =1, Eq. (4.53) takes the form:

$$\hat{u}_2(2) = \hat{\varphi}_{21}\hat{u}(1) + \hat{\varphi}_{22}\hat{u}_2(1) - \hat{\varphi}_{21} \tag{4.118}$$

on the basis of which and Eq. (4.117), we obtain the following:

$$\varphi_{22} = \frac{\hat{u}_2(2) - \hat{\varphi}_{12}[1-\hat{u}(1)]}{\hat{u}_2(1)} = \frac{\hat{u}_2(2) - \hat{\varphi}_{12}\hat{\varphi}_{11}}{\hat{u}_2(1)} \tag{4.119}$$

Accordingly with Eq. (4.113), it is:

$$\hat{u}_2(2) \cong \frac{\hat{u}(3)-\hat{u}(1)}{2T_s} \tag{4.120}$$

Based on Eqs. (4.115) and (4.119), Eq.(4.120) can be written in the following form:

$$\varphi_{22} = \frac{\frac{\hat{u}(3)-\hat{u}(1)}{2T_s} - \hat{\varphi}_{12}\hat{\varphi}_{11}}{\frac{\hat{u}(2)}{2T_s}} = \frac{\hat{u}(3)-\hat{u}(1)-2T_s\hat{\varphi}_{12}\hat{\varphi}_{11}}{\hat{u}(2)} \tag{4.121}$$

The main problem connected with the determination of the estimate of the state variable u_2 is that it is physically the first derivative of the output signal of the analog converter. Using Eqs. (4.114) and (4.119) causes u_2 to be calculated as the inclination of the straight line connecting two points of the converter response, which differs significantly from the real value of the derivative. This causes the errors that burden the estimates of the coefficients to be determined on the basis of the equations (4.115), (4.116) and (4.118). Application of such inaccurate coefficients in the reconstruction

algorithm entails that its results differ significantly from these obtained using the exact values of the coefficient determined on the basis of the definition (4.33). The next example illustrates this problem.

Example 4.17. The beginning four samples of the output response to the step input signal in Tab. 4.2 are: $u(k) = 0$, $u(1) = 0.0983$, $u(2) = 0.3059$, $u(3) = 0.5313$. These values were obtained for the 2-nd order exemplary converter, the output signal of which is sampled with the period $T_s = 0.5$ s. Using them to calculate the coefficients of the dynamic reconstruction algorithm according to Eqs. (4.111), 4.116), (4.117) and (4.121), respectively, gives the results:

$$\hat{\varphi}_{11} = 1 - u(1) = 1 - 0.0983 = 0.9017$$

$$\hat{\varphi}_{12} = 2T_s \frac{u(2) - 1 + \hat{\varphi}_{11}^2}{u(2)} = 2 \cdot 0.5 \frac{0.3059 - 1 + 0.9017^2}{0.3059} = 0.3889$$

$$\hat{\varphi}_{21} = -\hat{\varphi}_{12} = -0.3889$$

$$\hat{\varphi}_{22} = \frac{u(3) - u(1) - 2T_s \hat{\varphi}_{12} \hat{\varphi}_{11}}{u(2)} = \frac{0.5313 - 0.0983 - 2 \cdot 0.5 \cdot 0.3889 \cdot 0.9017}{0.3059} = 0.2691$$

To compare the calculated values with these exact, they are located together with the other coefficients in Tab. 4.9.

Table 4.9

Exact and estimated values of the coefficients of the exemplary 2-nd order dynamic reconstruction algorithm

Coefficient	φ_{11}	φ_{12}	φ_{21}	φ_{22}
Estimated values	0.9017	0.3889	-0.3889	0.2691
Exact values	0.9017	0.3449	-0.3449	0.4188

The amplitude of the discretization error calculated for the sinusoidal signal frequency $f = 0.02$ Hz by using the exact values is $E_{dis} = 0.0313$, while for the estimated values this error substantially exceeds 1. This means that the simple method applied to identify the coefficients is useless in practice.

As it results from the presented example, the key issue in the coefficient identification is an accurate enough calculation of the first derivative of the output signal. One can do it determining the analytical form of the step response (4.14) on the basis of known discrete samples of it and then calculating the derivatives in the suitable points. Such a way is mathematically complicated, so, in practice, simpler methods should be taken into account. In the following example, the results of application of polynomials to approximate the step response are presented in order to calculate the derivative of this signal.

Example 4.18. To measure samples of the step response of the exemplary 2-nd order converter, the 16-bit AD converter is used, which works in the range from 0 to 1. It is assumed that the quantized signal is disturbed by the normal noise $N(0; q)$, q is the quantum value. The 5 beginning samples of the response measured with the sampling period $T_s = 0.5$ s are presented in the table 4.10. They are calculated accordingly with the equation:

$$\hat{u}(k) = q \cdot \mathrm{ent}\left\{\frac{1}{q}\left[1 - \frac{e^{-b\omega_0 kT_s}}{\sqrt{1-b^2}}\sin\left(\sqrt{1-b^2}\,\omega_0 kT_s + \mathrm{arctg}\frac{\sqrt{1-b^2}}{b}\right)\right] + e_{noi} + 0.5\right\} \quad (4.122)$$

obtained on the basis of Eq. (4.14), with the assumption that $b = 0.7$ and $\omega_0 = 1$, and the number k of the sample takes values: $k = 0, ..., 4$.

Table 4.10

Beginning samples of the response to the unitary step change of the input signal of the exemplary 2-nd order converter obtained on the basis of Eq. (4.122)

k	0	1	2	3	4
$\hat{u}(k)$	0	0.098312	0.305954	0.531265	0.725708

In the following table, there are presented values of the coefficients calculated on the basis of the results from Tab. 4.10 with the assumption that the state variable u_2 is determined using polynomials of the order 3 and 4. The last column contains values of the amplitude of the discretization error calculated for the suitable values of the coefficients.

Table 4.11

Results of identification of the coefficients of the exemplary 2-nd order algorithm on the basis of the samples of the step response from Tab. 4.10 using polynomials of 3-rd and 4-th order to calculate the state variable u_2, the exact values, determined from definition, are taken from Example 4.5

Polynomial	φ_{11}	φ_{12}	φ_{21}	φ_{22}	E_{dis}
3rd order	0.9017	0.3647	-0.3647	0.3909	0.73
4th order	0.9017	0.3462	-0.3462	0.4195	0.030
Exact values	0.9017	0.3449	-0.3449	0.4188	0.031

The amplitudes of the discretization error E_{dis} presented in the last column show that using the polynomial of the forth order gives approximately the same results as obtained for the exact values of the coefficient. This means that the identification using this polynomial does not introduce a significant error.

In practice, the identification of the parameters of the dynamic model is realized on the basis of measurement results that are obtained at the output of the analog converter. These results are burdened by several errors; among them is the static error connected with nonlinearity of the sensor characteristic, which occurs dependently on the general model of the analog converter. In the Hammerstein model (see Chapter 1), the first element is static and nonlinear, while the second is dynamic and linear. This means that the step input signal changes its value after propagation through the first static element, which must be taken into account during the identification. If the Wiener model is used, the first element is dynamic, while the second is static, which causes the nonlinearity error introduced by it to be corrected before making the identification of the dynamic parameters. This means that the static reconstruction error must be taken into account in the budget of identification errors.

4.5. Neural dynamic reconstruction

Accordingly with Eqs. (4.49) and (4.50), the estimate of the reconstructed sample $\hat{x}(k)$ is the linear combination of the estimates of the state variables and the constant coefficients. This means that the neural implementation of these equations takes the form of network composed of the linear neurons that consists of n neurons described generally as the system of the recurrent equations, which can be written in the following form:

$$\hat{x}(k) = \sum_{i=2}^{i=n} w_{1i}\hat{u}_i(k) + w_{11}\hat{u}(k) + w_{10}\hat{u}(k+1) \tag{4.123}$$

and

$$\begin{aligned} \hat{u}_2(k+1) &= \sum_{i=2}^{i=n} w_{2i}\hat{u}_i(k) + w_{21}\hat{u}(k) + w_{20}\hat{x}(k) \\ &\vdots \\ \hat{u}_n(k+1) &= \sum_{i=2}^{i=n} w_{ni}\hat{u}_i(k) + w_{n1}\hat{u}(k) + w_{n0}\hat{x}(k) \end{aligned} \tag{4.124}$$

where $\hat{u}(k)$ and $\hat{u}(k+1)$ are estimates of samples of the output signal, $\hat{u}_i(k), i = 2, ..., n$ are estimates of the state variables, and w_{ij} are constant coefficients.

The network composed of neurons performing operations described by equations (4.123) and (4.124) is graphically presented in Fig. 4.14.

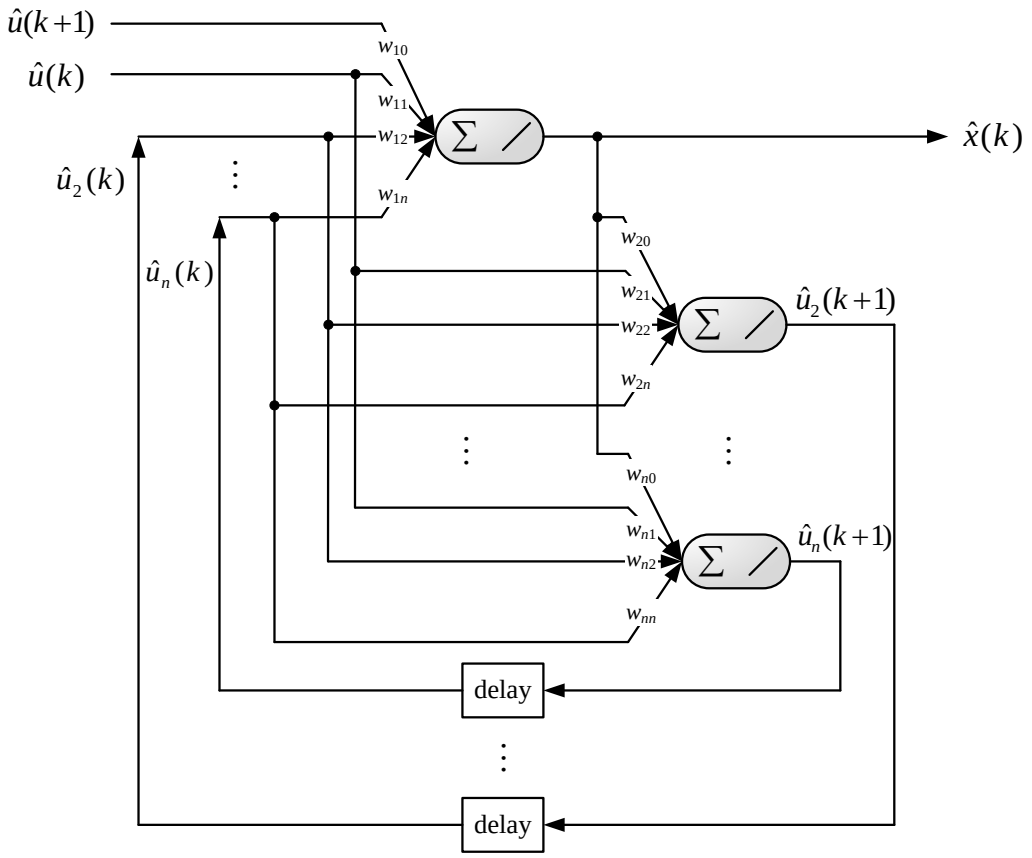

Fig. 4.14. The scheme of the neural network that perform dynamic reconstruction according to equations (4.123) and (4.124), "delay" denotes the operation of storing the sample for one sampling period of the reconstructed signal

The arithmetical operations performed by the network from Fig. 4.14 are repeated at every cycle of the reconstruction between two succeeding sampling instants k and k+1, k = 0, 1, ... To carry out the reconstruction, the two measurement results $\hat{u}(k),\hat{u}(k+1)$ of the output signal should be known, which means that the reconstruction is realized with the delay equal to the sampling period T_s. Moreover, it is necessary to give in the network input the state variables $\hat{u}_2(k),\ldots,\hat{u}_n(k)$, which are calculated in the previous cycle and stored to use them in the next cycle. This causes that to start activity the network, the initial values $\hat{u}_2(0),\ldots,\hat{u}_n(0)$ of the state variables are required. These values can be estimated or taken as zero. Assuming the initial values to be different from the real ones results in appearance of a transient state of the same kind as shown in Fig. 4.9b. This state disappears after a certain number of cycles from the beginning of the reconstruction.

4.5.1. Identification of coefficients of first-order network

For the 1-st order dynamic converter, the system of equations (4.123) and (4.124) reduces to the one expression that is the linear combination of the two measuring results $\hat{u}(k)$ and $\hat{u}(k+1)$ multiplied by constant coefficients w_1 and w_2. Thus, the input sample estimate is determinedby one linear neuron that realizes the following equation:

$$\hat{x}(k) = w_1\hat{u}(k) + w_2\hat{u}(k+1) \tag{4.125}$$

in which, accordingly with Eq. (4.72), the coefficients take the forms:

$$w_1 = A_k = -\frac{\varphi}{1-\varphi}, \quad w_2 = A_{k+1} = \frac{1}{1-\varphi} \tag{4.126}$$

where φ is given by Eq. (4.36).

The neuron described by expression (4.124) is graphically presented in Fig. 4.15.

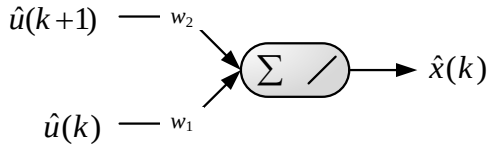

Fig. 4.15. Linear neuron realizing the dynamic reconstruction of one input signal sample of a first-order dynamic converter

The simplest way of determining the coefficients of the neuron from Fig. 4.15 consist in calculating them by using Eq. (4.126). Such values are named in the Table 4.12 as “exact values” because they are determined from the definition on the basis of the known parameters of the dynamic analog converter. Another way can be applied if the responses of the converter to the step input signal are known [S5]. This way is described in the next example.

Example 4.19. Let us consider the sampling instrument presented in Example 4.16, which works under the described conditions. Two beginning samples of the responses to the step input signal are measured in three cases: for the input step from ϑ = 0°C to 100°C, from ϑ = 0°C to 50°C and from ϑ = 100°C to 0°C. The estimates of the output samples, obtained with the assumption that they are burdened by the normal noise $N(0; 0.01)$°C, are presented in Fig. 4.16. The learning data presented in Fig. 4.17, the same as in Fig. 4.16, were used to learn the 1-st order neural network from Fig. 4.15.

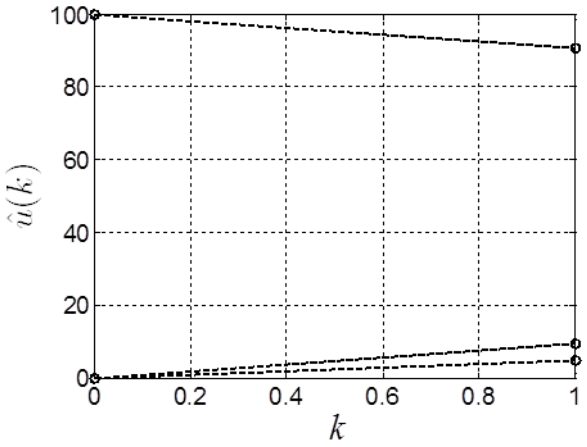

Fig. 4.16. The results used to obtain the learning set presented in Fig. 4.17

$$\left\{\begin{matrix}\hat{u}(0)_1 = 0 \\ \\ \hat{u}(1)_1 = 9.5163\end{matrix}\right.\quad \begin{matrix} \\ x(0)_1 = 100 \\ \\ \end{matrix}\left.\right\},\ \left\{\begin{matrix}\hat{u}(0)_2 = 0 \\ \\ \hat{u}(1)_2 = 4.7581\end{matrix}\right.\quad \begin{matrix} \\ x(0)_2 = 50 \\ \\ \end{matrix}\left.\right\},\ \left\{\begin{matrix}\hat{u}(0)_3 = 100 \\ \\ \hat{u}(1)_3 = 90.4837\end{matrix}\right.\quad \begin{matrix} \\ x(1)_3 = 0 \\ \\ \end{matrix}\left.\right\}$$

Fig. 4.17. The learning set used to learn the neuron from Fig. 4.15

The values of the neuron coefficients obtained after 3 learning steps using the set from Fig. 4.17 are presented in the table 4.12. They are the same as the exact values that are calculated on the basis of parameters of the exemplary 1-st order dynamic converter.

Table 4.12

Exact and estimated values of the weight coefficients of the neuron from Fig. 4.15

Coefficients	w_1	w_2	*Bias*
Exact values	-9.5083	10.5083	0
Estimated values	-9.5083	10.5083	$3.6858 \cdot 10^{-10}$

4.5.2. Identification of coefficients of second-order network

For the 2-nd order converter, the reconstruction algorithm in the form of the expressions (4.122) and (4.123) is deribed as two recurrent equations:

$$\hat{x}(k) = w_1\hat{u}(k+1) + w_2\hat{u}(k) + w_3\hat{u}_2(k) \tag{4.127}$$

$$\hat{u}_2(k+1) = v_1\hat{u}(k) + v_2\hat{u}_2(k) + v_3\hat{x}(k) \tag{4.128}$$

wherein the coefficients w_1, w_2, w_3 and v_1, v_2, v_3 have constant values. Accordingly with the scheme of Fig. (4.14), the structure of the neural network that performs the operations described by the equations (4.127) and (4.128) can be presented as in Fig. 4.18.

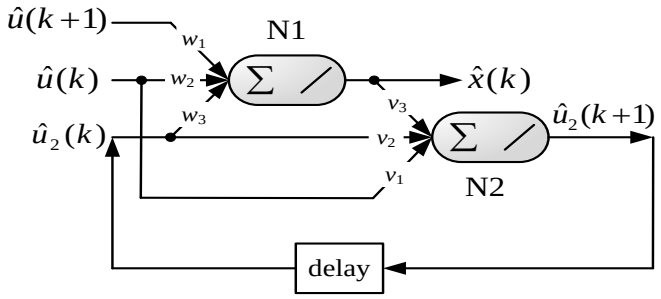

Fig. 4.18. The scheme of the network described by the recurrent equations (4.127) and (4.128), "delay" denotes operation of storing the sample for 1 sampling period of the reconstructed signal

The coefficients of the network from Fig. 4.18 can be calculated on the basis of parameters of the equations (4.52) and (4.53), which describe the analytical form of the dynamic reconstruction algorithm of the 2-nd order. Taking into account that accordingly with Eqs. (4.46) and (4.47) we have: $\psi_1 = 1 - \varphi_{11}$ and $\psi_2 = -\varphi_{21}$, one obtains the following expressions describing the coefficients of Eq. (4.127) and (4.128) in relation to the parameters of Eqs. (4.52) and (4.53):

$$w_1 = \frac{1}{1-\varphi_{11}}, \quad w_1 = -\frac{\varphi_{11}}{1-\varphi_{11}}, \quad w_1 = -\frac{\varphi_{12}}{1-\varphi_{11}} \tag{4.129}$$

$$v_1 = \varphi_{21}, \quad v_2 = \varphi_{22}, \quad v_3 = -\varphi_{21} \tag{4.130}$$

The values that are calculated accordingly with Eqs. (4.129) and (4.130) on the basis of the parameters of the exemplary 2-nd order converter taken in Example 4.5 are called here as "exact values". They are contained in Tables 4.13 and 4.14 together with the values estimated as the results of the identification that is considered in the following sections of the text.

Table 4.13

Exact and estimated values of the weight coefficients of the N1 neuron of the network shown in Fig. 4.18

Coefficients	w_1	w_2	w_3	*Bias*
Exact values	10.1701	-9.1701	-3.5077	0
Estimated values	10.1506	-9.1514	-3.4982	$2.8675 \cdot 10^{-4}$

Table 4.14

Exact and estimated values of the weight coefficients of the N2 neuron of the network presented in Fig. 4.18

Coefficients	v_1	v_2	v_3	*Bias*
Exact values	0.3449	0.4188	-0.3449	0
Estimated values	0.3452	0.4184	-0.3451	$-6.0937\cdot10^{-5}$

The identification needs the measurement data of the output responses to 3 different step input signals. The estimates of the output samples used to identify the parameters of the exemplary 2-nd order converter are described by the following expressions:

$$\hat{u}(k)_1 = q \cdot \mathrm{ent}\left\{\frac{1}{q}(1-u(k)) + e_{\mathrm{noi}} + 0.5\right\} \tag{4.131}$$

$$\hat{u}(k)_2 = q \cdot \mathrm{ent}\left\{\frac{0.5}{q}(1-u(k)) + e_{\mathrm{noi}} + 0.5\right\} \tag{4.132}$$

$$\hat{u}(k)_3 = q \cdot \mathrm{ent}\left\{\frac{1}{q}u(k) + e_{\mathrm{noi}} + 0.5\right\} \tag{4.133}$$

where $k = 0, 1, \ldots$, e_{noi} is the normal noise N(0; 1), and accordingly with Eq. (4.14), it is:

$$u(k) = 1 - \frac{e^{-b\omega_0 kT_s}}{\sqrt{1-b^2}}\sin\left(\sqrt{1-b^2}\,\omega_0 kT_s + \mathrm{arctg}\frac{\sqrt{1-b^2}}{b}\right) \tag{4.134}$$

The learning data includes the values of the first derivative $u_2(k)$ of the response. These values can be calculated on the basis of the derivative of the expression (4.134), but the numerically simpler way seems to be to use a polynomial for this purpose. As considered in Section 4.4.2, use of the 5-th order polynomial leads to obtaining exact enough values of estimated parameters. In Fig. 4.19a, 6 discrete values of 3 responses to the step input signals are presented, which are calculated using Eqs. (4.131), (4.132), and (4.133). On the basis of these values, the polynomial is determined and the discrete values of its derivatives are calculated in the points presented in Fig. 4.19b.

a) b)

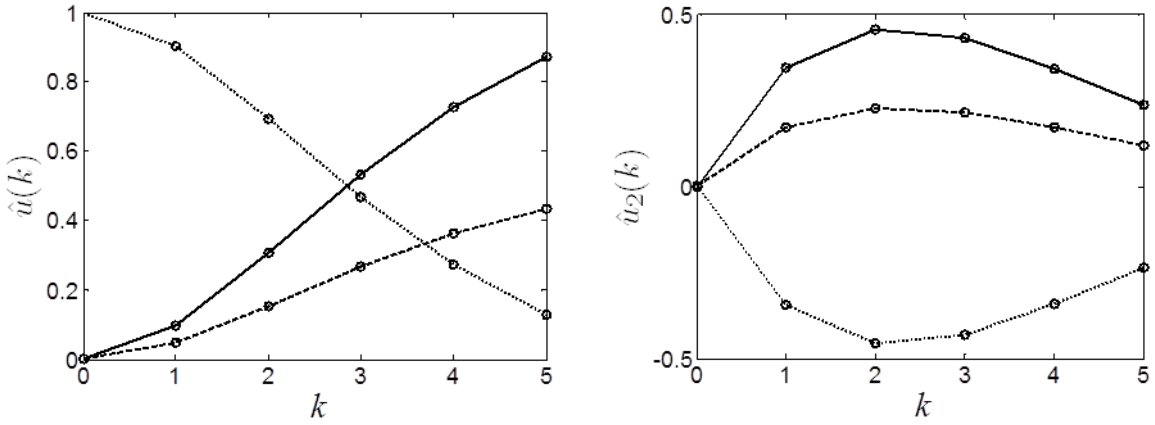

Fig. 4.19. a) Samples of the responses to the step input signals (4.31), (4.132), and (4.133), b) the first derivatives of the these responses

The learning data consist of the elements that, according to the scheme of the network in Fig. 4.18, have the general form presented in Fig. 4.20.

$$\left\{\begin{matrix} u(k+1) \\ u(k) \\ u_2(k) \end{matrix} \quad x(k)\right\}^{\mathrm{N1}}_{k,n} \qquad \left\{\begin{matrix} x(k) \\ \hat{u}_2(k) \\ u(k) \end{matrix} \quad \hat{u}_2(k+1)\right\}^{\mathrm{N2}}_{k,n}$$

Fig. 4.20. The general form of the elements of the data used to learn the network from Fig. 4.18, $k = 0,1,\ldots$ is the number of the output sample, $n = 1, 2, 3$ is the number of the response, N1 and N2 denote the learning data of neurons from this figure

As in Fig. 4.18, both neurons are learned separately. For the N1 neuron, the learning data containing 4 samples from Fig. 4.19 are presented in Fig. 4.21. After 4 steps of the learning process, the obtained coefficients of the neuron do not substantially change their values as presented in Tab. 4.15.

$$\left\{\begin{matrix} 0.0983 \\ 0 \\ -0.0005 \end{matrix} \quad 1\right\}_{0,1} \left\{\begin{matrix} 0.3059 \\ 0.0983 \\ 0.3450 \end{matrix} \quad 1\right\}_{1,1} \left\{\begin{matrix} 0.5313 \\ 0.3059 \\ 0.4554 \end{matrix} \quad 1\right\}_{2,1} \left\{\begin{matrix} 0.7257 \\ 0.5313 \\ 0.4301 \end{matrix} \quad 1\right\}_{3,1}$$

$$\left\{\begin{matrix} 0.0492 \\ 0 \\ -0.0004 \end{matrix} \quad 0.5\right\}_{0,2} \left\{\begin{matrix} 0.1530 \\ 0.0492 \\ 0.1725 \end{matrix} \quad 0.5\right\}_{1,2} \left\{\begin{matrix} 0.2656 \\ 0.1530 \\ 0.2277 \end{matrix} \quad 0.5\right\}_{2,2} \left\{\begin{matrix} 0.3629 \\ 0.2656 \\ 0.2150 \end{matrix} \quad 0.5\right\}_{3,2}$$

$$\left\{\begin{matrix} 0.9017 \\ 1 \\ 0.0005 \end{matrix} \quad 0\right\}_{0,3} \left\{\begin{matrix} 0.6941 \\ 0.9017 \\ -0.3450 \end{matrix} \quad 0\right\}_{1,3} \left\{\begin{matrix} 0.4687 \\ 0.6941 \\ -0.4554 \end{matrix} \quad 0\right\}_{2,3} \left\{\begin{matrix} 0.2743 \\ 0.4687 \\ -0.4301 \end{matrix} \quad 0\right\}_{3,3}$$

Fig. 4.21. The data used to learn the N1 neuron from Fig. 4.18

Table 4.15

Values of the coefficients of the N1 neuron from Fig. 4.18, which are obtained in dependence of the number of the learning steps N_{ls}

N_{ls}	1	2	3	4
MSE	0.00383	6.7e-006	1.4e-007	1.4e-007
w_1	6.9257	10.0166	10.1501	10.1506
w_2	-6.3727	-9.0359	-9.1510	-9.1514
w_3	-2.0993	-3.4401	-3.4980	-3.4982
Bias	0.1922	0.0083	3.2e-004	2.9e-004

The data used to learn the N2 neuron from Fig. 4.18, are presented in Fig. 4.22. The values of the coefficients obtained in the succeeding steps of the learning processare presented in the table 4.16.

$$\begin{Bmatrix} 1 \\ -0.0005 & 0.3450 \\ 0 \end{Bmatrix}_{0,1} \quad \begin{Bmatrix} 1 \\ 0.3450 & 0.3450 \\ 0.0983 \end{Bmatrix}_{1,1} \quad \begin{Bmatrix} 1 \\ 0.4554 & 0.4301 \\ 0.3059 \end{Bmatrix}_{2,1} \quad \begin{Bmatrix} 1 \\ 0.4301 & 0.3419 \\ 0.5313 \end{Bmatrix}_{3,1}$$

$$\begin{Bmatrix} 0.5 \\ -0.0004 & 0.1725 \\ 0 \end{Bmatrix}_{0,2} \quad \begin{Bmatrix} 0.5 \\ 0.1725 & 0.2277 \\ 0.0492 \end{Bmatrix}_{1,2} \quad \begin{Bmatrix} 0.5 \\ 0.2277 & 0.2150 \\ 0.1530 \end{Bmatrix}_{2,2} \quad \begin{Bmatrix} 0.5 \\ 0.2150 & 0.1710 \\ 0.2656 \end{Bmatrix}_{3,2}$$

$$\begin{Bmatrix} 0 \\ 0.005 & -0.3450 \\ 1 \end{Bmatrix}_{0,3} \quad \begin{Bmatrix} 0 \\ -0.3450 & -0.4554 \\ 0.9017 \end{Bmatrix}_{1,3} \quad \begin{Bmatrix} 0 \\ -0.4554 & -0.4301 \\ 0.6941 \end{Bmatrix}_{2,3} \quad \begin{Bmatrix} 0 \\ -0.4301 & -0.3419 \\ 0.4687 \end{Bmatrix}_{3,3}$$

Fig. 4.22. Data used for learning the neuron N2 from Fig. 4.18.

Table 4.16

Values of coefficients of the N2 neuron from Fig. 4.18 in dependence of the number of the learning steps N_{ls}

N_{ls}	1	2	3
MSE	1.2e-007	6.3e-009	6.3e-009
v_1	0.3437	0.3452	0.3452
v_2	0.4197	0.4184	0.4184
v_3	-0.3462	-0.3451	-0.3451
Bias	0.0011	-6.0e-005	-6.1e-005

As it results from Tabs. 4.13 and 4.14, the values of the coefficients estimated in the learning process are very close to these calculated as the exact values. To evaluate the accuracy of the estimated values, the amplitudes of the reconstruction error

composed of the discretization error and the identification error are determined depending on the frequency of reconstructed signal. They are presented in Tab. 4.17 together with the discretization error. Comparing these values leads to the conclusion that the identification error is negligibly small in relation to the discretization error, which means that the considered method of identification is effective from accuracy of the reconstruction point of view.

Table 4.17

Values of amplitudes of the dynamic errors of the exemplary 2-nd order converter in dependence of the frequency f of the sinusoidal signal with the amplitude equal to 1, E_{rec} is the amplitude of the reconstruction error obtained for the network from Fig. 4.18, E_{dis} is the amplitude of the discretization error determined for the exact values of the coefficients

f Hz	0.01	0.02	0.05	0.1	0.2
E_{rec}	0.0159	0.0315	0.0786	0.1574	1.9675
E_{dis}	0.0158	0.0315	0.0787	0.1571	1.9682

4.6. Final remarks

Summing up the considerations presented in this chapter, one can state that realization of the dynamic reconstruction algorithm is an effective way of the correction of the error which arises when a varying over time signal is converted by the sensor modeled by a differential equation. As result of the presented examples, the correction effectiveness depends on relationships between parameters of the sensor model and the frequency of the input signal, as well as on the discretization (sampling) period. This means that the choice of these relationships should be preceded by the metrological analysis of the applied algorithm.

The characterized relationships result from the fact that the signal conversion and the suitable reconstruction create the couple, the property of which should be considered together. In particular, this couple has to be treated as one specific error source connected with non-ideal realization of the reconstruction. For the dynamic algorithm, this error is caused by the step approximation of the varying in time signal, and it is called the discretization error. It should be noticed that for the step-changing signal this approximation is made exactly; therefore, the dynamic algorithm does not introduce any error in this case (see Example 5.9).

Such a coupling of the analog conversion and the digital reconstruction causes that description of the error propagation through the sampling instrument can be limited to the algorithms since its elements performing analog and analog-to-digital conversions can be treated as sources of errors conveyed at the input of the first algorithm. This enables treating the error propagation in the instrument entirely from the considered algorithms point of view.

The main advantage of neural network applications to signal reconstruction is self--building of the inverse model based directly on the measurement results obtained during the identification. In the case of dynamic reconstruction, this advantage is not important because it is necessary to use polynomials to obtain learning patterns, and the complexity of the learning process means that the easiest way is to obtain network coefficients based on the parameters of the analytical algorithm.

5. PROPAGATION OF ERRORS IN SAMPLING INSTRUMENT

A sampling instrument delivers estimates, which are sufficiently accurate instantaneous values (digital samples) of its input signal representing a varying over time measured quantity. Samples occur in the instrument output periodically with frequency determined by the sampling frequency. An inaccuracy of this instrument is described by the uncertainty of the error burdening the reconstructed samples. This erroris a combination of many partial errors that arise in elements of the instrument and propagate to its output. Arising and propagation of errors are strictly connected with specificity of the signal processing that is performed by three main parts of the instrument shown in Fig. 1.1, which realize the analog conversion, the digitalization and the digital reconstruction.

As it results from the scheme presented in Fig. 2.3, the reconstruction is realized by the chain of partial reconstruction algorithms created as the effect of the decomposition of the analog conversion. According to Fig. 2.2, every algorithm processes samples from its measurement window that contains K samples of the input signal. With the assumption that the algorithm realizes operation on true values of samples, its output result, according to the model of the measurement result (1.18), can be generally written as:

$$\hat{x}(k) + e_{\text{out}}(k) = a_0\left[\hat{y}(k) + e_{\text{in}}(k)\right] + \ldots + a_{K-1}\left[\hat{y}(k+K-1) + e_{\text{in}}(k+K-1)\right] \qquad (5.1)$$

where a_0, ..., $a_{K\text{-}1}$ are coefficients of the algorithm, $\hat{y}(k)$ and $\hat{x}(k)$ are estimates of the samples in its input and output, respectively, $e_{\text{in}}(k)$, $e_{\text{out}}(k)$ are realizations of input and output errors, k is interpreted both as the number of the first sampling instant in the window and the number of the current measurement window, $k = 0, 1, \ldots$.

According to the considerations presented in Section 1.4, two expressions can be extracted from Eq. (5.1). The first one:

$$\hat{x}(k) = a_0\hat{y}(k) + \ldots + a_{K-1}\hat{y}(k+K-1) \qquad (5.2)$$

describes numerical operations performed by a reconstruction algorithm on estimates of the input samples to obtain the estimate of the output sample. The second expression:

$$e_{\text{out}}(k) = a_0 e_{\text{in}}(k) + \ldots + a_{K-1} e_{\text{in}}(k + K - 1) \tag{5.3}$$

determines propagation of the input errors to the algorithm output.

In Eqs. (5.2) and (5.3), the arithmetical operation performed on the estimates and the errors are the same, but, in the case of the errors, a value of the output error depends on both the coefficients of the applied algorithm and the properties of the input errors. It causes the error propagation should be described in at least three categories: separately for static, dynamic, and random errors.

Every algorithm performs its task only approximately, which causes that Eq. (5.3) should be supplemented by the inside error of the algorithm, which is the difference between the results obtained at the outputs: of the ideal model and the real form of the algorithm. Taking this into account, one can write Eq. (5.3) in the form:

$$e_{\text{out}}(k) = a_0 e_{\text{in}}(k) + \ldots + a_{K-1} e_{\text{in}}(k + K - 1) + e_{\text{rec}}(k) \tag{5.4}$$

where $e_{\text{rec}}(k)$ is the inside error of the algorithm caused by non-ideal realization of the reconstruction.

The decomposition of the general model of the analog conversion causes the reconstruction to be realized as a chain of algorithms performed in series. In the case where the chain of the algorithm consists of I elements, the general model of the error propagation takes the form presented in Fig. 5.1.

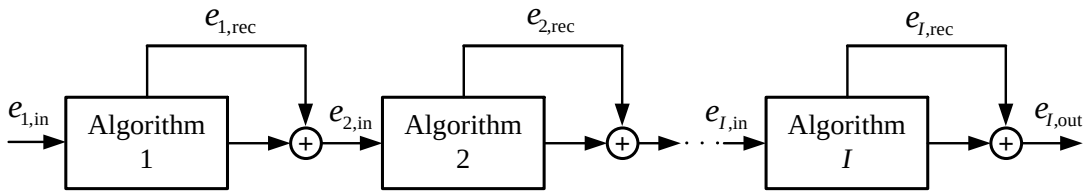

Fig. 5.1. General scheme of error propagation in the sampling instrument

As in Fig. 5.1, every algorithm transforms a realization of the input error e_{in} into the output and introduces its inside reconstruction error e_{rec}. The error at the output of the last algorithm is the total error of the sampling instrument, and it is a composition of all errors which propagate from the input to the output of the algorithm chain.

5.1. General error model of exemplary sampling instrument

5.1.1. Signal processing in exemplary instrument

The further considerations are carried out for the exemplary instrument, for which the Wiener model is applied suitable for physical properties of the converters used in the instrument described in Section 3.1. One should emphasize that although the presented error analysis is focused on the reconstruction using the Wiener model, the applied methods are of universal character and can be used for whichever model of the sampling instrument, the input signal of which is reconstructed.

Accordingly with the Wiener model presented in Fig. 2.5, the signal processingin the exemplary sampling instrument may be presented, from the reconstruction point of view, in the graphical form, as in Fig. 5.2.

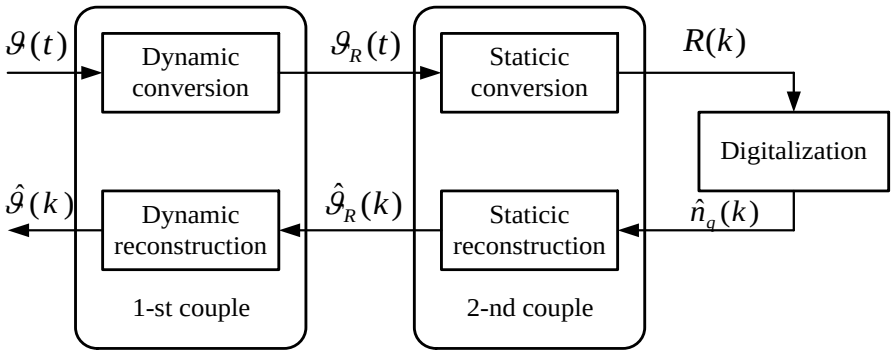

Fig. 5.2. Scheme of signal processing in the exemplary instrument, *k* is the number of the reconstructed sample (number of the measurement window)

According to the physical properties of the Pt100 sensor, the reconstructed temperature $\vartheta(t)$ varying over time is converted to the temperature $\vartheta_R(t)$ of the sensor wire causing changes of its resistance $R(t)$. This resistance is converted to the voltage, which is sampled at instant *k*, and the sample is quantized by the AD converter. The quantization result $\hat{n}_q(k)$ is the estimate of the quantized voltage sample expressed as a number of quanta hat is assigned to the sample value. On the basis of the quantization result, the estimate of the temperature sample $\hat{\vartheta}_R(k)$ of the wire is calculated accordingly with the static reconstruction algorithm. Finally, based on the results of the static reconstruction, the estimate of the input temperature $\hat{\vartheta}_R(k)$ is determined using the dynamic reconstruction algorithm.

As result of considerations presented in Chapter 2, the partial analog conversions and the suitable digital reconstructions can be described as couples. On the basis of this property, one can state that the error propagation model of the sampling

instrument can be constructed taking into account only properties of the reconstruction algorithms, which are performed in series. The result of this is that all input errors of the instrument and errors arising in the analog conversion as well as during the digitalization are contained by the quantization result. Thus, these errors can be modeled as the input errors of the first element of chain of the algorithms, which is the static algorithm in the case considered. This means that, for the exemplary instrument and from the error propagation point of view, the scheme from Fig. 5.2 can be reduced to two elements shown in Fig. 5.3.

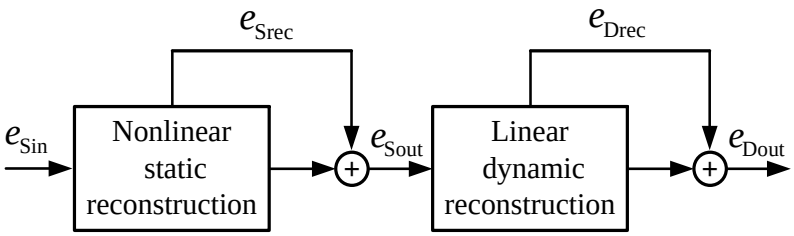

Fig. 5.3. General form of the error propagation model in the exemplary instrument

The scheme from Fig. 5.3 is universal in this sense that it can be used for all sampling instruments, the analog part of which is described by the Wiener model. In the case where the Hammerstein model is applied, the order of the static and the dynamic reconstruction is reverse to that in this figure.

The error propagation model from Fig. 5.3 consists of two elements. The first represents numerical operations performed on the input error e_{Sin} accordingly with equations that describe the static reconstruction. Realization of these operations causes the propagation of the error e_{Sin} to the algorithm output, which results in the occurrence of the error e_{Sprop}. The second element models properties of the dynamic algorithm performing calculations on the static output error e_{Sout}, which is the sum of the error e_{Sprop} and e_{Srec} that is the error introduced by the static algorithm itself. The output error e_{Dout} of the dynamic algorithm is also the total error e_{tot} in the output of the sampling instrument. This error is a composition of the errors which propagate throughout the chain, as well as the errors e_{Srec} and e_{Drec} arising as effects of non-ideal realizations of the reconstruction algorithms, static and dynamic, respectively. As it is proved in this chapter, all composed errors can be described as the sum of uncorrelated and correlated partial errors.

The input error e_{Sin} is the composition of the errors introduced to the input of the instrument, the errors arising during the analog conversion and the errors caused by digitalization of the analog signal, i.e., connected with sampling of the signal and

quantization of the obtained samples. All these errors burden the digital data processed by the algorithms, which means that all errors must be transformed to the input of the chain of algorithms and expressed in quanta.

5.1.2. Mathematical description of error propagation

Dependently on the algorithm kind, the reconstruction of one input sample needs one or more quantization results, the number of which is determined by the suitable measurement window. If the static algorithm is applied, a single quantization result is used to obtain the reconstruction result. Accordingly with Eq. (3.13), the temperature estimate $\hat{\vartheta}_R(k)$ that is obtained at the output of the static reconstruction algorithm is described as the following linear approximation:

$$\hat{\vartheta}_R(k) = a(N)\left[\hat{n}_{\mathrm{q}}(k) - n_{\mathrm{q}}(N)\right] + b(N) \tag{5.5}$$

where $a(N)$ and $b(N)$ are coefficients dependent on the working point in the inverse static characteristic, N is the number of the approximation node, $\hat{n}_{\mathrm{q}}(k)$ is the estimate of the indication of the ADC and $n_{\mathrm{q}}(N)$ is the indication suitable for node N. Based on the taken error definition (1.23), one can describe the input error as:

$$e_{\mathrm{Sin}} = \dot{n}_{\mathrm{q}}(k) - \hat{n}_{\mathrm{q}}(k) \tag{5.6}$$

where $\dot{n}_{\mathrm{q}}(k)$ denotes the accurate (ideal) quantization result that could be obtained if $q \to 0$. According to Fig. 5.3, the output error of the static algorithm is the sum of two errors:

$$e_{\mathrm{Sout}} = \vartheta_R(k) - \hat{\vartheta}_R(k) = e_{\mathrm{Sprop}} + e_{\mathrm{Srec}} \tag{5.7}$$

where $\vartheta_R(k)$ is the instantaneous true value of the temperature of the sensor wire.

Connection of equations (5.5), (5.6) and (5.7) yields:

$$e_{\mathrm{Sout}} = \vartheta_R(k) - a(N)\left[\dot{n}_{\mathrm{q}}(k) - e_{\mathrm{Sin}} - n_{\mathrm{q}}(N)\right] - b(N) = e_{\mathrm{Sprop}} + e_{\mathrm{Srec}} \tag{5.8}$$

After splitting Eq. (5.8) to two parts, one obtains description of the error that propagate from the input to the output of the static algorithm as:

$$e_{\mathrm{Sprop}}(k) = a(N)e_{\mathrm{Sin}}(k) \tag{5.9}$$

and the expression describing the static reconstruction error:

$$e_{\mathrm{Srec}} = \vartheta_R(k) - a(N)\left[\dot{n}_{\mathrm{q}}(k) - n_{\mathrm{q}}(N)\right] - b(N) = e_{\mathrm{app}} \tag{5.10}$$

which is identical to the error e_{app} of the linear segmental approximation described by Eq. (5.5) and used to calculate the estimate $\hat{\vartheta}_R(k)$ of the temperature of the wire. If the neural network is applied for the static reconstruction, e_{app} is the error connected with the neural approximation described in Section 3.4.

The inclination $a(N)$ in Eq. (5.9) depends on the value of the quantization result, but it is possible using one constant coefficient k_S to describe the transfer of errors from the input to the output of the static algorithm. This coefficient is determined as the mean value of the inclinations of the segments approximating the inverse static characteristic. For the number N_{node} of the nodes, the relation between the input and the output errors may be written as:

$$e_{Sout}(k) = k_S e_{Sin}(k),\ k_S = \frac{1}{N_{node}} \sum_{N=1}^{N_{node}} a(N) \tag{5.11}$$

According to Eq. (3.26), the static transfer coefficient can be approximately calculated as the inclination of the segment linking the endpoints of the inverse static characteristic:

$$k_S = \frac{\vartheta_{max} - \vartheta_{min}}{n_{q,max} - n_{q,min}} \tag{5.12}$$

This approximation is universal in this sense that it can be applied both for the programmed and the neural static reconstruction. As shown in Chapter 3, the coefficient (5.12) enables the description of relations between errors accurately enough.

Introducing Eq. (5.9) into (5.7), we obtain the general error model of the static algorithm in the form:

$$e_{Sout}(k) = e_{Srec}(k) + k_S e_{Sin}(k) \tag{5.13}$$

For the exemplary instrument, the distribution of the total static input error e_{Sin} is the same in the successive sampling instants. Whereas, the static reconstruction error depends on the working point in the nonlinear static characteristic, which means that its values change in the sampling instants for signals varying over time.

Example 5.1. The inverse static characteristic of the exemplary instrument is approximated by using 4 segments. Based on the values of Tab. 3.4, the transfer coefficient (5.11) takes the value:

$$k_S = \frac{1}{4} \sum_{N=0}^{3} a(N) = \frac{1}{4}(6.2767 + 6.3243 + 6.3694 + 6.4201) \cdot 10^{-3} = 6.35 \cdot 10^{-3}\ ^{o}\text{C}$$

The second way of determination of this coefficient is based on the data from Tab. 3.4. According to them, the range of the input temperature is from $\vartheta_{\min} = 0^{o}$C to $\vartheta_{\max} = 100^{o}$C, and the extreme indications are: $n_{q,\min} = 40918$, $n_{q,\max} = 56673$. For these values, we have:

$$k_S = \frac{100 - 0}{56673 - 40918} = 6.35 \cdot 10^{-3} \ ^{o}\text{C}$$

The second algorithm in the chain presented in Fig. 5.3 realizes dynamic reconstruction. As result of the considerations presented in Section 4.3.2, this algorithm must be written for the analysis of errors in the non-recurrent form (4.61).Taking into account that the measurand, for the dynamic algorithm, is the single sample of sensor resistance $\vartheta_R(k)$ and basing on considerations presented in Chapter 1.4, one can present the algorithm in the form of two equations. The first:

$$\hat{\vartheta}(k) = A_{k+1}\left[\hat{\vartheta}_R(k+1)\right] + A_k\left[\hat{\vartheta}_R(k)\right] + \ldots + A_{K-m}\left[\hat{\vartheta}_R(k-m)\right] \tag{5.14}$$

is the linear combination of constant coefficients $A_{k+1}, A_k, ..., A_{k-m}$ and estimates of the samples $\hat{\vartheta}_R(k+1), \hat{\vartheta}_R(k), \ldots, \hat{\vartheta}_R(k-m)$ which are the results of the static algorithm realization (see Fig. 5.3). The second equation:

$$e_{\text{Dprop}}(k) = A_{k+1}e_{\text{Din}}(k+1) + A_k e_{\text{Din}}(k) + \ldots + A_{K-m}e_{\text{Din}}(k-m) \tag{5.15}$$

describes the same arithmetical operations as in Eq. (5.14) but on realizations of the input error $e_{\text{Din}}(k)$, the result of which is the realization of the input error $e_{\text{Dprop}}(k)$.

Eq. (5.15) can be written in matrix form as:

$$e_{\text{Dprop}}(k) = \mathbf{A}^{\text{T}}\mathbf{e}_{\text{Din}}(k) \tag{5.16}$$

where T is the symbol of the vector transposition, and it is denoted:

$$\mathbf{A} = \begin{bmatrix} A_{k+1} \\ A_k \\ \vdots \\ A_{k-m} \end{bmatrix}, \quad \mathbf{e}_{\text{Din}}(k) = \begin{bmatrix} e_{\text{Din}}(k+1) \\ e_{\text{Din}}(k) \\ \vdots \\ e_{\text{Din}}(k-m) \end{bmatrix} \tag{5.17}$$

Accordingly with Fig. (5.3), the error at the output of the dynamic algorithm is the sum of the dynamic reconstruction error $e_{\text{Drec}}(k)$ and the propagated error $e_{\text{Dprop}}(k)$:

$$e_{\text{Dout}}(k) = e_{\text{Drec}}(k) + e_{\text{Dprop}}(k) \tag{5.18}$$

After introducing Eq. (5.16) into it, Eq.(5.18) takes the form:

$$e_{\mathrm{Dout}}(k) = \mathbf{A}^{\mathrm{T}}\mathbf{e}_{\mathrm{Din}}(k) + e_{\mathrm{Drec}}(k) \tag{5.19}$$

As in Fig. (5.3), every output error of the static algorithm is introduced to the input of the dynamic algorithm; therefore, taking Eq. (5.13) into account, we have:

$$e_{\mathrm{Din}}(k) = e_{\mathrm{Sout}}(k) = k_{\mathrm{S}}e_{\mathrm{Sin}} + e_{\mathrm{Srec}}(k) \tag{5.20}$$

Based on this relation, one can present the vector of the input error described by expressions (5.17) as:

$$\mathbf{e}_{\mathrm{Din}}(k) = \begin{bmatrix} k_{\mathrm{S}}e_{\mathrm{Sin}}(k+1) + e_{\mathrm{Srec}}(k+1) \\ k_{\mathrm{S}}e_{\mathrm{Sin}}(k) + e_{\mathrm{Srec}}(k) \\ \vdots \\ k_{\mathrm{S}}e_{\mathrm{Sin}}(k-m) + e_{\mathrm{Srec}}(k-m) \end{bmatrix} = k_{\mathrm{S}}\mathbf{e}_{\mathrm{Sin}}(k) + \mathbf{e}_{\mathrm{Srec}}(k) \tag{5.21}$$

where it is:

$$\mathbf{e}_{\mathrm{Srec}}(k) = \begin{bmatrix} e_{\mathrm{Srec}}(k+1) \\ e_{\mathrm{Srec}}(k) \\ \vdots \\ e_{\mathrm{Srec}}(k-m) \end{bmatrix} \tag{5.22}$$

Combining Eqs. (5.19) and (5.21), one obtains the general error model that describes the error propagation from the input to the output for the chain of the algorithms presented in Fig. 5.3. This model has the matrix form:

$$e_{\mathrm{Dout}}(k) = \mathbf{A}^{\mathrm{T}}\left[k_{\mathrm{S}}\mathbf{e}_{\mathrm{Sin}}(k) + \mathbf{e}_{\mathrm{Srec}}(k)\right] + e_{\mathrm{Drec}}(k) \tag{5.23}$$

For the 1-st order dynamic converter, the dynamic reconstruction algorithm is reduced to 2 beginning terms (see Eq. 4.71). In this case, the equation (5.23) of the error propagation takes the scalar form:

$$e_{\mathrm{Dout}}(k) = A_{k+1}\left[k_{\mathrm{S}}e_{\mathrm{Sin}}(k+1) + e_{\mathrm{Srec}}(k+1)\right] + A_k\left[k_{\mathrm{S}}e_{\mathrm{Sin}}(k) + e_{\mathrm{Srec}}(k)\right] + e_{\mathrm{Drec}}(k) \tag{5.24}$$

5.1.3. Decomposition of general error model

In general, the following three types of input errors can be distinguished if the physical properties of errors are taken into account:

- static errors, values of which do not change in the measurement window,

- dynamic errors that have sinusoidal values for the form of the input signal taken in this book,
- random – values of these errors are described in the probabilistic categories.

According to the general error model (1.50), the input error can be written as the sum of partial errors:

$$e_{\mathrm{Sin}} = e_{\mathrm{Sstat,in}} + e_{\mathrm{Sdyn,in}} + e_{\mathrm{Sran,in}} \tag{5.25}$$

where $e_{\mathrm{Sstat,in}}$, $e_{\mathrm{Sdyn,in}}$ and $e_{\mathrm{Sran,in}}$ are static, dynamic and random errors, respectively. Moreover, every algorithm can introduce its inside errors of the described kinds. This means that the total reconstruction error of the static algorithmis:

$$e_{\mathrm{Srec}} = e_{\mathrm{Sstat,rec}} + e_{\mathrm{Sdyn,rec}} + e_{\mathrm{Sran,rec}} \tag{5.26}$$

and, for the dynamic algorithm, we have:

$$e_{\mathrm{Drec}} = e_{\mathrm{Dstat,rec}} + e_{\mathrm{Ddyn,rec}} + e_{\mathrm{Dran,rec}} \tag{5.27}$$

Introducing Eqs. (5.26), (5.27) and (5.22) in (5.24), one obtains the general error model in the form:

$$\begin{aligned} e_{\mathrm{Dout}}(k) = \mathbf{A}^{\mathrm{T}}\left[k_{\mathrm{S}}\mathbf{e}_{\mathrm{stat,in}}(k) + k_{\mathrm{S}}\mathbf{e}_{\mathrm{dyn,in}}(k) + k_{\mathrm{S}}\mathbf{e}_{\mathrm{ran,in}}(k) + \mathbf{e}_{\mathrm{Sstat,rec}}(k) + \mathbf{e}_{\mathrm{Sdyn,rec}}(k) + \mathbf{e}_{\mathrm{Sran,rec}}(k)\right] + \\ + e_{\mathrm{Dstat,rec}}(k) + e_{\mathrm{Ddyn,rec}}(k) + e_{\mathrm{Dran,rec}}(k) \end{aligned} \tag{5.28}$$

Describing the output error as the sum of three partial errors of the considered kinds, we have the following:

$$e_{\mathrm{Dout}} = e_{\mathrm{Dstat,out}} + e_{\mathrm{Ddyn,out}} + e_{\mathrm{Dran,out}} \tag{5.29}$$

After introducing Eq. (5.29) in (5.28) and splitting the obtained expression into three parts, one obtains the equations that describe the propagation of the extracted errors. It is:

- for the static error:

$$e_{\mathrm{Dstat,out}}(k) = \mathbf{A}^{\mathrm{T}}\left[k_{\mathrm{S}}\mathbf{e}_{\mathrm{Sstat,in}}(k) + \mathbf{e}_{\mathrm{Sstat,rec}}(k)\right] + e_{\mathrm{Dstat,rec}}(k) \tag{5.30}$$

- for the dynamic error:

$$e_{\mathrm{Ddyn,out}}(k) = \mathbf{A}^{\mathrm{T}}\left[k_{\mathrm{S}}\mathbf{e}_{\mathrm{Sdyn,in}}(k) + \mathbf{e}_{\mathrm{Sdyn,rec}}(k)\right] + e_{\mathrm{Ddyn,rec}}(k) \tag{5.31}$$

- and for the random error:

$$e_{\mathrm{Dran,out}}(k) = \mathbf{A}^{\mathrm{T}}\left[k_{\mathrm{S}}\mathbf{e}_{\mathrm{Sran,in}}(k) + \mathbf{e}_{\mathrm{Sran,rec}}(k)\right] + e_{\mathrm{Dran,rec}}(k) \tag{5.32}$$

The static algorithm does not introduce dynamic errors as well as the dynamic algorithm the static errors. Moreover, one can omit the random errors generated by the static and dynamic algorithms. These errors arise as effects of rounding of numbers

during arithmetical operations. The reconstruction algorithms considered here, both the static and the dynamic, are numerically simple, which means that the errors caused by rounding take values much less than the quantization errors even if 16-bit representation of numbers is used as in the exemplary sampling instrument. Analysis of the rounding errors can be carried out using Monte Carlo method [K4].

If errors discussed above are omitted in Eqs. (5.30), (5.31) and (5.32), they take the forms of the following expressions:

$$e_{\mathrm{Dstat,out}}(k) = \mathbf{A}^{\mathrm{T}}\left[k_{\mathrm{S}}\mathbf{e}_{\mathrm{Sstat,in}}(k) + \mathbf{e}_{\mathrm{Sstat,rec}}(k)\right] \tag{5.33}$$

$$e_{\mathrm{Ddyn,out}}(k) = \mathbf{A}^{\mathrm{T}}k_{\mathrm{S}}\mathbf{e}_{\mathrm{Sdyn,in}}(k) + e_{\mathrm{Ddyn,rec}}(k) \tag{5.34}$$

$$e_{\mathrm{Dran,out}}(k) = \mathbf{A}^{\mathrm{T}}k_{\mathrm{S}}\mathbf{e}_{\mathrm{Sran,in}}(k) \tag{5.35}$$

The equations (5.33), (5.34) and (5.35) can be written in more clear forms if one takes into account the sequence of the algorithms in the chain presented in Fig. 5.3. The first algorithm is static, which means that errors at its input are the input errors of the chain; thus, the symbol *S* in their indexes can be omitted. Similar principle can be used for the errors in the output of the dynamic algorithm, which are the errors in the output of the chain. This means that all symbols *S* and *D* that denote the kind of the algorithm in the symbols of errors can be omitted. Thus, Eqs. (5.33), (5.34) and (5.35) can be written in the more communicative forms as:

$$e_{\mathrm{stat,out}}(k) = \mathbf{A}^{\mathrm{T}}\left[k_{\mathrm{S}}\mathbf{e}_{\mathrm{stat,in}}(k) + \mathbf{e}_{\mathrm{stat,rec}}(k)\right] \tag{5.36}$$

$$e_{\mathrm{dyn,out}}(k) = k_{\mathrm{S}}\mathbf{A}^{\mathrm{T}}\mathbf{e}_{\mathrm{dyn,in}}(k) + e_{\mathrm{dyn,rec}}(k) \tag{5.37}$$

$$e_{\mathrm{dran,out}}(k) = k_{\mathrm{S}}\mathbf{A}^{\mathrm{T}}\mathbf{e}_{\mathrm{ran,in}}(k) \tag{5.38}$$

The presented above equations describe three kinds of errors that together compose to the output error e_{out} at the output of the chain of algorithms, which is also the total error e_{tot} of the estimate delivered by the sampling instrument. Therefore, Eq. (5.29) may be written in the form:

$$e_{\mathrm{tot}}(k) = e_{\mathrm{out}}(k) = e_{\mathrm{stat,out}}(k) + e_{\mathrm{dyn,out}}(k) + e_{\mathrm{ran,out}}(k) \tag{5.39}$$

Eqs. (5.36), (5.37), (5.38) and (5.39) describe the partial errors of a single reconstructed sample at the instant *k*. These equations create together the model of error propagation in the chain of the reconstruction algorithms used in the exemplary sampling instrument accordingly with the Wiener model. This error model, shown in the graphical form in Fig. 5.4, has the decomposed form, which enables separate analysis of the propagation of different kinds of error and linking the obtained partial errors to determine descriptions of all kinds of errors at every stage of the propagation.

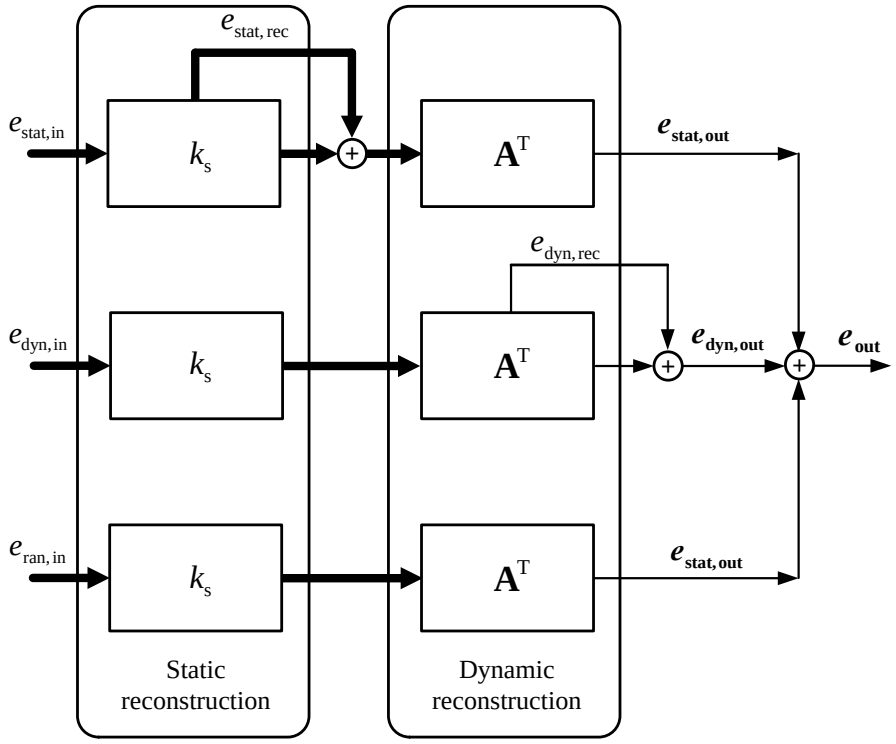

Fig. 5.4. Decomposed general model of error propagation in the exemplary sampling instrument

To compare the results of the error analysis that is carried out using the general error model, it is necessary to take two basic assumptions. The first is related to the fact that many of the errors depend on changes in the input signal. For the further considerations, it is taken that the input signal changes sinusoidal in the suitable temperature range with the frequency dependent on properties of the analysed errors. The second assumption is connected with using probabilistic descriptions of all analysed errors in the form of probability density functions that are mainly described by histograms. The histograms are obtained as the effect of realization of probabilistic experiments by using Monte Carlo method with assumption that the measurement window is selected randomly in the signal period with rectangular distribution. On the basis of obtained histograms, the probabilistic parameters of errors are determined, mainly standard deviations and uncertainties, which are applied in comparison of the analyzed errors.

The analysis is carried out in the same way for both kinds of reconstruction algorithms: analytical and neural, because the differences between errors specific for these algorithms are of minor importance. In these cases, for which these differences are important, the errors are analysed using suitable examples.

5.2. Propagation of static errors

5.2.1. Propagation of input static errors by reconstruction chain

From the definition, the static error does not change its values in the measurement window, which means that $e_{\text{stat,in}}(k+1) = e_{\text{stat,in}}(k) = ... = e_{\text{stat,in}}(k\text{-}m)$. Taking this into account, one may write the static propagation equation (5.36) in the form:

$$e_{\text{stat,out}}(k) = k_{\text{S}}\left(A_{k+1} + A_k + \ldots + A_{k-m}\right)e_{\text{stat,in}}(k) + \mathbf{A}^{\text{T}}\mathbf{e}_{\text{stat,rec}}(k) \tag{5.40}$$

Accordingly with Eq. (4.65), the sum of the coefficients of the dynamic algorithm is equal to 1; thus, Eq. (5.40) takes the following form:

$$e_{\text{stat,out}}(k) = k_{\text{S}}e_{\text{stat,in}}(k) + \mathbf{A}^{\text{T}}\mathbf{e}_{\text{stat,rec}}(k) \tag{5.41}$$

The propagation of the static reconstruction error $e_{\text{stat,rec}}$ is described in Section 5.2.2. After omitting this error in Eq. (5.41), one obtains the expression:

$$e_{\text{stat,out}}(k) = k_{\text{S}}e_{\text{stat,in}}(k) \tag{5.42}$$

which means that every realization of the output static error is calculated by multiplying the input error value by the constant coefficient k_{S} defined in Example 5.1. The graphical description of the propagation of the static errors from the input to the output of the reconstruction chain is presented in Fig. 5.5.

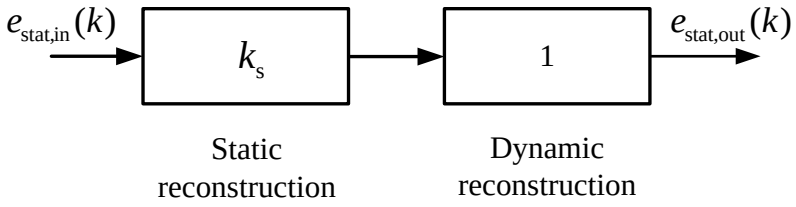

Fig. 5.5. Propagation of the input static errors by the reconstruction chain

The basic input static errors are connected with the thermal and temperature drift of the characteristic of the static conversion [J14,V1]. These factors influence on the shift and the inclination of the characteristic, which means that the total input static error can be described as the sum of these two partial errors:

$$e_{\text{stat,in}}(k) = e_{\text{sh,in}}(k) + e_{\text{inc,in}}(k) \tag{5.43}$$

where $e_{\text{sh,in}}$ is the input error caused by the shift of the characteristic, while $e_{\text{inc,in}}$ by changes in the characteristic inclination.

Accordingly with Eqs. (5.42) and (5.43), the static output error is in this case the sum of partial errors described as:

$$e_{\text{stat,out}}(k) = k_{\text{S}} e_{\text{sh,in}}(k) + k_{\text{S}} e_{\text{inc,in}}(k) = e_{\text{sh,out}}(k) + e_{\text{inc,out}}(k) \tag{5.44}$$

The following experiment is aimed at determination of histograms both of the considered partial errors and their total error in the output of the reconstruction chain.

Experiment 5.1. Let us take that the shift error $e_{\text{sh,in}}$ of the static characteristic, which arises in the exemplary instrument is described as random in the range from -2 to 2 with the rectangular distribution.The inclination error is expressed as: $e_{\text{inc,in}} = n_{\text{q}} \cdot \varepsilon_{\text{inc}}$, wherein n_{q} is the quantization result and the inclination coefficient ε_{inc} changes accordingly with the rectangular distribution in the range from $-5 \cdot 10^{-5}$ to $5 \cdot 10^{-5}$. The input signal of the instrument changes sinusoidal in the input range from 0 to 100°C, that is, it is described as: $x(t) = 50\sin\omega t + 50$°C, $\omega = 2 \cdot \pi \cdot f$, f is frequency and it is taken that $f = 0.01$ Hz. This signal is converted by the sensor Pt100 to the resistance R in accordance with Eq. (3.5) and; next, to the voltage. To avoid the influence of the quantization error on the analyzed errors, it is assumed that the quantization is ideal, which means that it is performed with the quantum value $q \to 0$. This assumption causes that Eq. (3.20) describing the quantization result takes the form:

$$\dot{n}_{\text{q}} = 409.176R \tag{5.45}$$

At every step, after random determination of the sampling instant in the signal period $T = 1/f$ accordingly with the rectangular distribution, the voltage value is calculated in three cases, i.e., for the voltage burdened by:

- the input shift error $e_{\text{sh,in}}$,
- the input inclination error $e_{\text{inc,in}}$,
- both the input shift error and the inclination error.

The obtained values of the errors are multiplied by the coefficient k_{S} accordingly with the propagation model from Fig. 5.5 and the output values of these errors are located in the suitable sets. The histograms of the partial errors are presented in Figs. 5.6a and 5.6b, whereas the error that is composition of them in Fig. 5.7. For every set of the error, the suitable standard deviation is calculated.

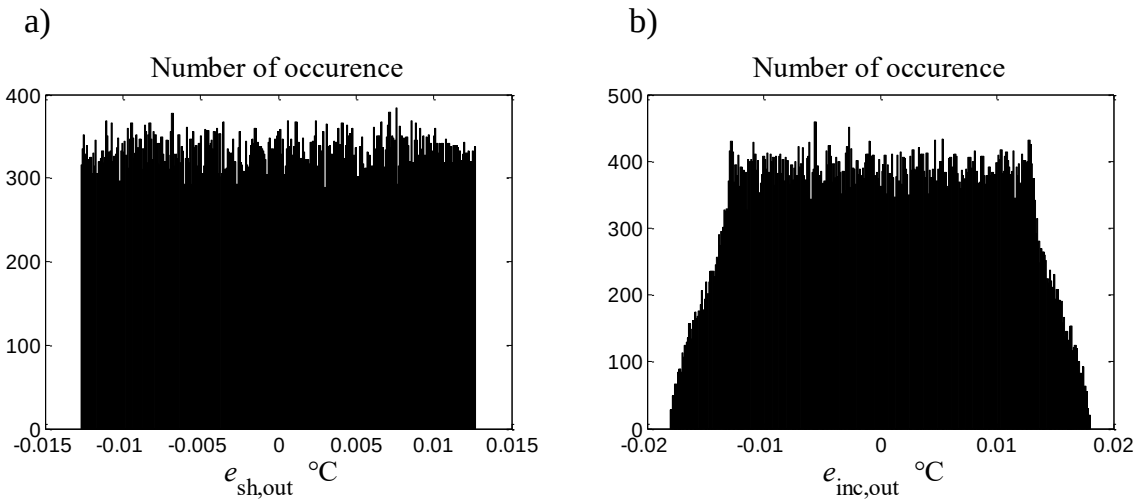

Fig. 5.6. Histograms of the static errors in the output of the reconstruction chain: a) the shift error, its standard deviation is $\sigma_{sh,out} = 7.3 \cdot 10^{-3o}$C, b) the inclination error, the standard deviation $\sigma_{inc,out} = 9 \cdot 10^{-3o}$C

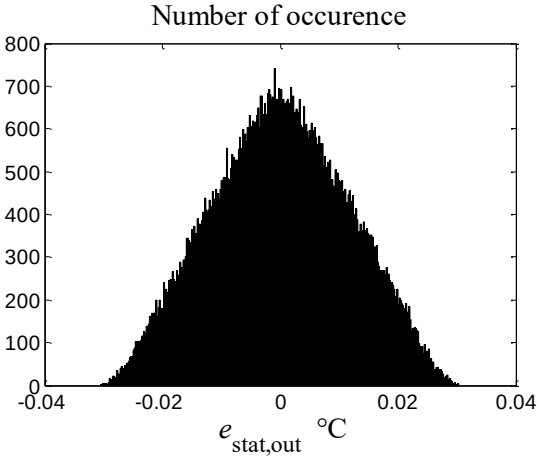

Fig. 5.7. Histogram of the output error composed of the shift error and the inclination error, the distributions of which are presented in Fig. 5.6 as histograms, the standard deviation $\sigma_{stat,out} = 11.6 \cdot 10^{-3o}$C

For the total error is described as a sum of partial errors, it is necessary, from the error propagation point of view, to determine the correlation coefficients describing codependences between the partial errors. In Experiment 5.1, the standard deviations of the drift errors are calculated, which are: $\sigma_{sh,out} = 7.3 \cdot 10^{-3o}$C, $\sigma_{inc,out} = 9 \cdot 10^{-3o}$C for the partial errors, and $\sigma_{stat,out} = 11.6 \cdot 10^{-3o}$C for the error composed of them. On the bases of these values and accordingly with Eq. (3.24), we obtain the following correlation coefficient of the partial drift errors:

$$c_{cor,dr} = \frac{\sigma_{stat,out}^2 - \sigma_{sh,out}^2 - \sigma_{inc,out}^2}{2\sigma_{sh,out}\sigma_{inc,out}} = \frac{11.6^2 - 7.3^2 - 9^2}{2 \cdot 7.3 \cdot 9} 10^{-3} = 0.002 \cong 0 \qquad (5.46)$$

which means that they are not correlated. Therefore, their standard deviations can be composed with others accordingly with Eq. (1.52).

5.2.2. Propagation of static reconstruction errors by dynamic algorithm

The static reconstruction error arises as the effect of both the approximation of the real static characteristic and the identification of the parameters of the inverse model. Thus, this error can be described as the sum of the error e_{Sapp} connected with the linear or neural approximation of the inverse static characteristic and the identification error e_{Sid}. It is:

$$e_{\mathrm{stat,rec}}(k) = e_{\mathrm{Sapp}}(k) + e_{\mathrm{Sid}}(k) \tag{5.47}$$

The approximation errors depend on the working point in the static characteristic, which means that, for the sinusoidal input signals, values of these errors change in time. Processing such errors by the dynamic reconstruction algorithm causes the output error depends both on the frequency and the amplitude of the signal. On the basis of Eqs. (5.41) and (5.47), the propagation of the static approximation error by the dynamic algorithm can be described as:

$$e_{\mathrm{stat,out}}(k) = \mathbf{A}^{\mathrm{T}}\mathbf{e}_{\mathrm{stat,rec}}(k) = \mathbf{A}^{\mathrm{T}}\left[\mathbf{e}_{\mathrm{Sapp}}(k) + \mathbf{e}_{\mathrm{Sid}}(k)\right] = e_{\mathrm{Sapp,out}}(k) + e_{\mathrm{Sid,out}}(k) \tag{5.48}$$

For the 1-st order dynamic reconstruction algorithm, the partial output errors in Eq. (5.48) take the following forms:

$$e_{\mathrm{Sapp,out}}(k) = \mathbf{A}^{\mathrm{T}}\mathbf{e}_{\mathrm{Sapp}}(k) = A_{k+1}e_{\mathrm{Sapp}}(k+1) + A_k e_{\mathrm{Sapp}}(k) \tag{5.49}$$

$$e_{\mathrm{Sid,out}}(k) = \mathbf{A}^{\mathrm{T}}\mathbf{e}_{\mathrm{Sid}}(k) = A_{k+1}e_{\mathrm{Sid}}(k+1) + A_k e_{\mathrm{Sid}}(k) \tag{5.50}$$

The succeeding experiments are intended to show the relation between the input and the output errors described by Eqs. (5.49) and (5.50) for the programmed and neural realization of the static reconstruction in the case if the dynamic reconstruction is performed by using the exemplary the 1-st order algorithm.

Experiment 5.2. This experiment aims to determine the histograms of the input and output errors connected with linearization for the sinusoidal input signal with the amplitude $X = 50^{\mathrm{o}}\mathrm{C}$ and the frequency $f = 0.01$ Hz, which is sampled with period $T_{\mathrm{s}} = 0.2$ s. The propagation of the linearization error e_{Sapp} to the output of the dynamic algorithm is described by Eq. (5.49). The experiment is carried out in the same way and with the same assumptions as taken in Experiment 5.1 with this difference that the ideal indications are processed by the static reconstruction algorithm (3.13) and; next, by the of the 1-st order dynamic algorithm (4.51).The value of the error e_{Sapp} in the input of the dynamic algorithm is calculated as the difference between the true

value $\vartheta_R(k)$ of the sensor resistance (see Fig. 5.2), while the output error on the basis of Eq. (5.49). The obtained histograms are presented in Figs. 5.8a and 5.8b, respectively.

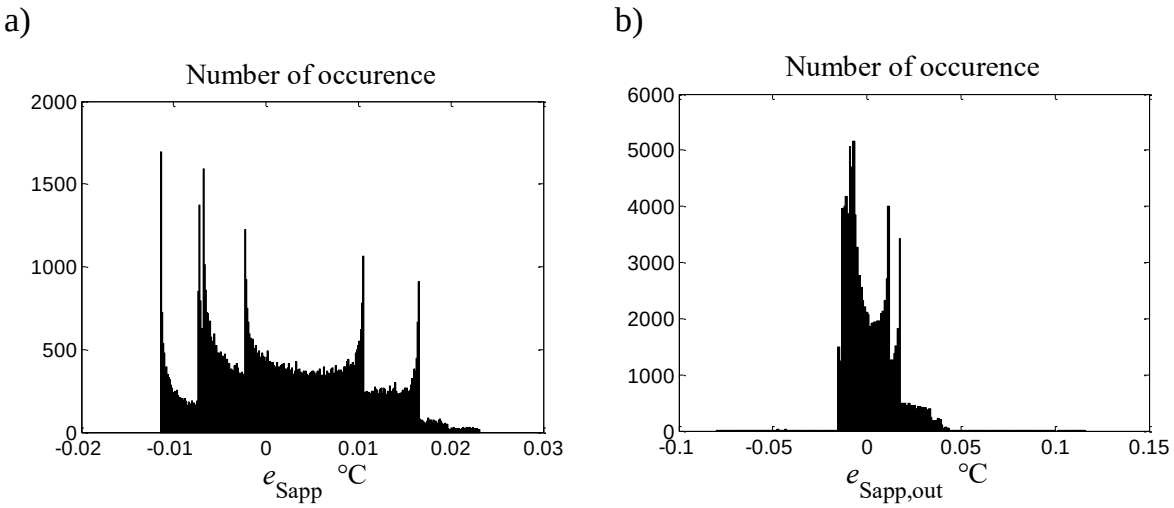

Fig. 5.8. Histograms of the linear approximation error e_{Sapp} obtained for the sinusoidal signal under the measurement conditions described in Experiment 5.2: a) at the input of the of the 1-st order dynamic algorithm, $\sigma_{Sapp} = 8.2 \cdot 10^{-3}$°C, b) at its output, $\sigma_{Sapp,out} = 14 \cdot 10^{-3}$°C

As it results from Fig. 5.8, propagation of the approximation error by the dynamic algorithm changes the distribution of this error, which can be expressed as the error propagation coefficient. It is generally defined as the ratio of the standard deviations:

$$k_D = \frac{\sigma_{Dout}}{\sigma_{Din}} \tag{5.51}$$

where σ_{Dout} is determined for the same error at the output of the dynamic algorithm and σ_{Din} at the algorithm input. For the approximation error e_{Sapp} that propagatesby the 1-st order dynamic algorithm, this coefficient takes the value:

$$k_{D,Sapp} = \frac{\sigma_{Sapp,out}}{\sigma_{Sapp}} = \frac{14 \cdot 10^{-3}}{8.2 \cdot 10^{-3}} = 1.71 \tag{5.52}$$

obtained on the basis of histograms presented in Fig. 5.8.

Experiment 5.3. This experiment aims to show properties of the error caused by neural approximation of the static inverse characteristic if this error propagates throughout the dynamic algorithm. The way of carrying out the experiment is the same as described in Example 5.2. The parameters of the exemplary neural network as in Fig. 3.25 used for the static reconstruction are taken from Fig. 3.24.

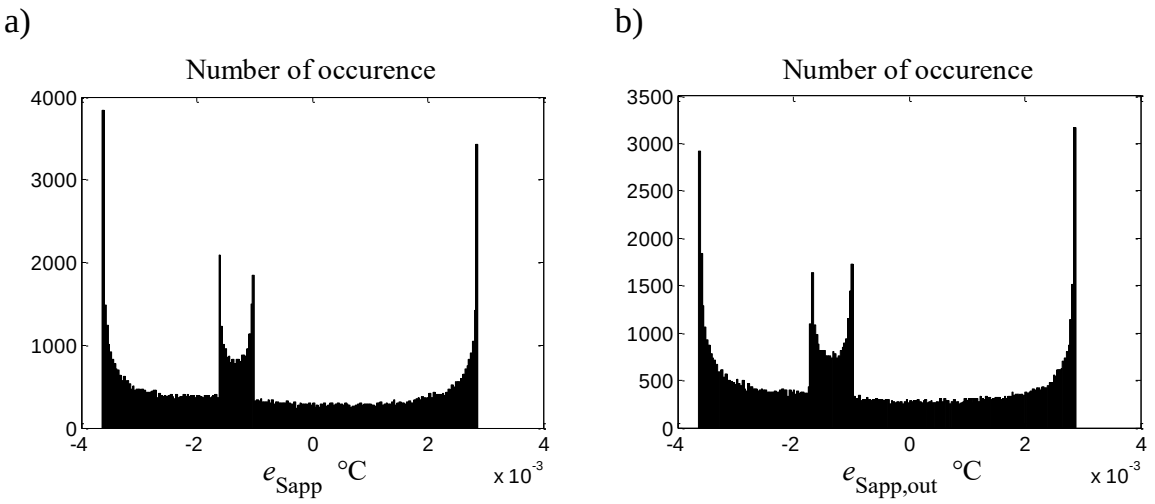

Fig. 5.9. Histograms of the neural approximation error e_{Sapp} obtained for the sinusoidal signal under the measurement condition described in Experiment 5.3: a) at the input of the 1-st order exemplary dynamic algorithm, $\sigma_{\text{Sapp}} = 2.01 \cdot 10^{-3}$°C, b) at the algorithm output, $\sigma_{\text{Sapp,out}} = 2.10 \cdot 10^{-3}$°C

On the basis of Fig. 5.9, the value of the coefficient (5.52) that describes propagation of the neural static approximation error by the 1-st order dynamic algorithm is:

$$k_{\text{D,Sapp}} = \frac{\sigma_{\text{Sapp,out}}}{\sigma_{\text{Sapp}}} = \frac{2.10 \cdot 10^{-3}}{2.01 \cdot 10^{-3}} = 1.04 \tag{5.53}$$

The second source error of the static algorithmis connected with inaccurate identification of the parameters of the static characteristic approximation. The histograms of the identification error at the output and at the input of the dynamic algorithm are determined using Experiments 5.4 and 5.5 for the analytical and neural realizations of the static reconstruction algorithms, respectively.

Experiment 5.4. The calculations are carried out in the same way as Experiment 5.2; however, the error is defined in this case as the difference between two errors connected with the linear approximation. The values of the error are calculated for the parameters contained in Tab. 3.4, which are determined on the basis on the known static characteristic (3.5). The second error is calculated for the identified parameters presented in Tab. 3.9. The obtained histograms are presented in Figs. 5.10a and b, respectively.

a) b)

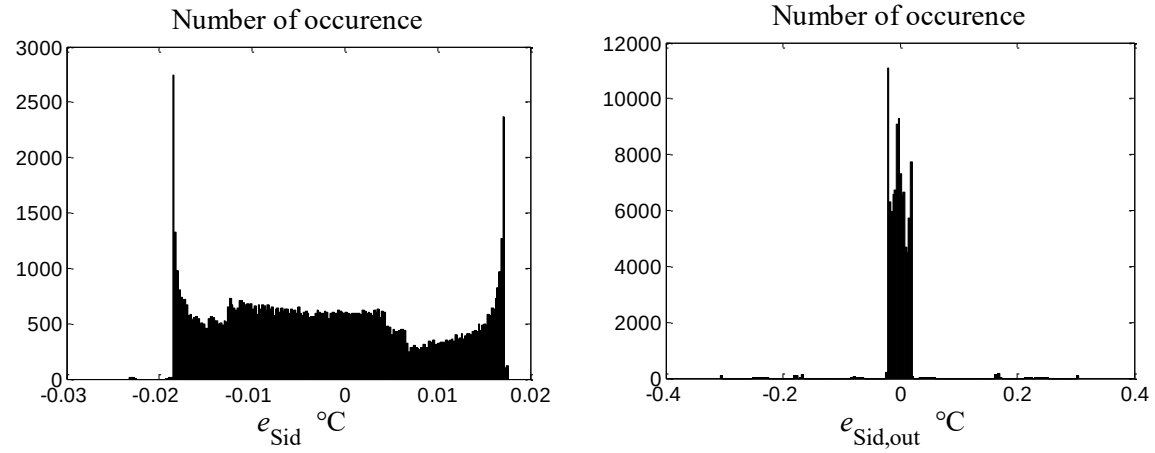

Fig. 5.10. Histograms of the static identification error e_{Sid} obtained for the sinusoidal signal if the static reconstruction is performed by the exemplary analytical algorithm: a) at the input of the 1-st order dynamic algorithm, $\sigma_{Sid} = 11.5 \cdot 10^{-3}$°C, b) at its output, $\sigma_{Sid,out} = 27 \cdot 10^{-3}$°C

The propagation coefficient (5.51) for the errors presented in Fig. 5.10 takes the value:

$$k_{D,id} = \frac{\sigma_{Sid,out}}{\sigma_{Sid}} = \frac{27}{11.5} = 2.35 \tag{5.54}$$

Experiment 5.5. It is aimed at obtaining the histograms of the errors that are connected with identification of the exemplary neural network at the input and the output of the dynamic algorithm. The parameters of the network are presented in Fig. 3.29. This experiment is carried out in the same way as the Experiment 5.4, and the obtained histograms are presented in Fig. 5.11.

a) b)

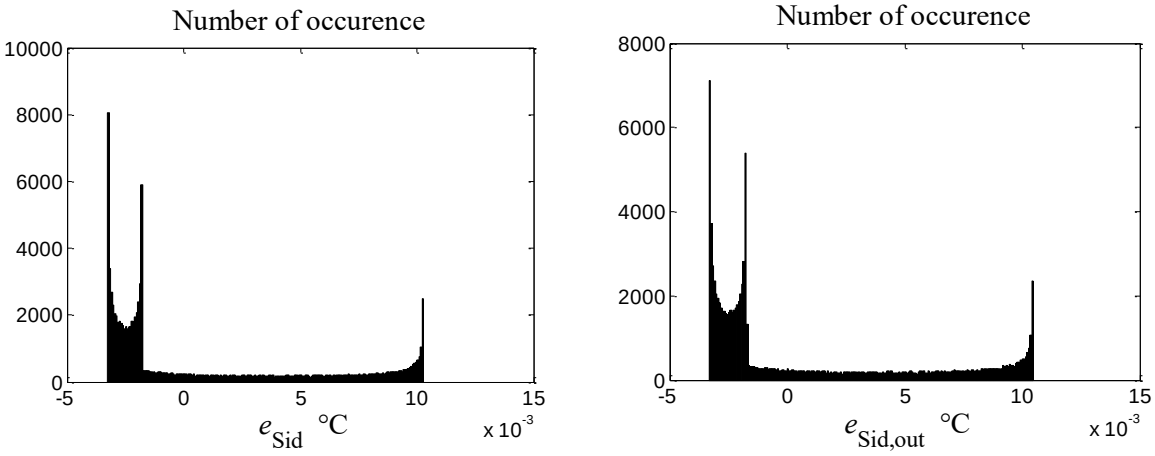

Fig. 5.11. Histograms of the static identification error e_{Sid} obtained for the sinusoidal signal if the static reconstruction is performed by the exemplary neural network, a) at the input of the exemplary 1-st order dynamic algorithm, $\sigma_{Sid} = 4.64 \cdot 10^{-3}$°C, b) at its output, $\sigma_{Sid,out} = 4.71 \cdot 10^{-3}$°C

The propagation coefficient calculated for the error characterized by Fig. 5.11 takes the value:

$$k_{\mathrm{D,Sid}} = \frac{\sigma_{\mathrm{Sid,out}}}{\sigma_{\mathrm{Sid}}} = \frac{4.71 \cdot 10^{-3}}{4.64 \cdot 10^{-3}} = 1.02 \tag{5.55}$$

As it results from Eqs. (4.52), (4.53), (4,54) and (4.55), the values of the propagation coefficient (5.51) are greater for the linear approximation error than for the neural approximation error. Moreover, the values of these errors are substantially greater for the linear approximation than for the neural one. To evaluate these differences in the output of the 1-st order exemplary dynamic algorithm, the following experiment is carried out.

Experiment 5.6. This experiment is aimed at obtaining histograms of the static reconstruction error after its propagation by the exemplary 1-st order dynamic reconstruction algorithm. The analytical static reconstruction is performed using the approximation parameters of Tab. 3.4, while the neural reconstruction on the basis of parameters from Fig. 3.29. This experiment is carried out in the same way as Experiments 5.2, and the obtained histograms are presented in Fig. 5.12.

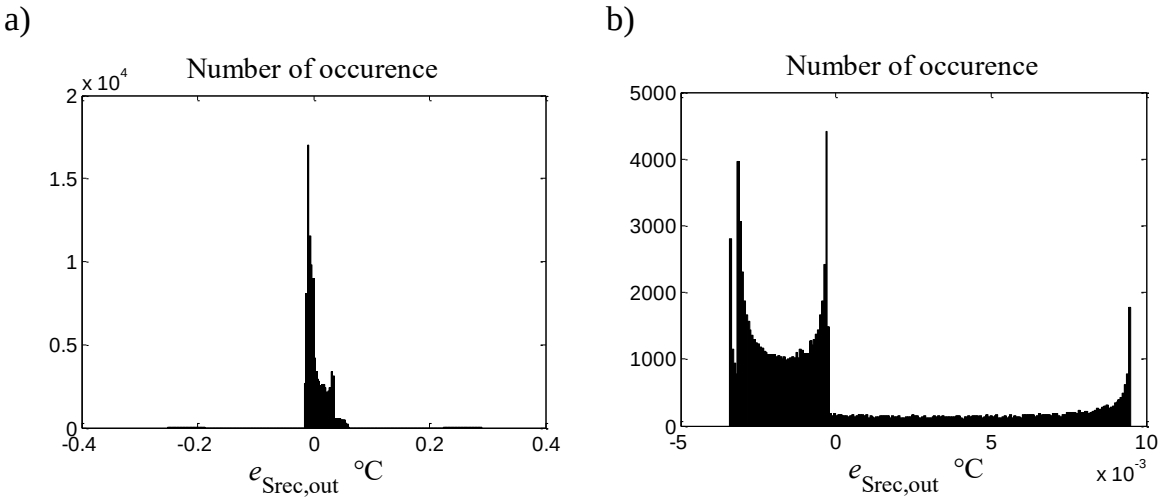

Fig. 5.12. Histograms of the output static reconstruction error $e_{\mathrm{Srec,out}}$ that is composed of the approximation and the identification errors after propagation by the exemplary 1-st order dynamic algorithm obtained for: a) the exemplary analytical static reconstruction, $\sigma_{\mathrm{Srec,out}} = 30.7 \cdot 10^{-3}$°C, b) the exemplary neural reconstruction, $\sigma_{\mathrm{Srec,out}} = 3.84 \cdot 10^{-3}$°C

The standard deviations calculated for the errors from Figs. 5.9, 5.10, 511, 5.12 and 5.12 enable determination of the correlation coefficients between the approximation and identification errors. For the analytical static reconstruction, one obtains the following:

$$c_{\mathrm{cor,Srec}} = \frac{\sigma^2_{\mathrm{Srec,out}} - \sigma^2_{\mathrm{Sapp,out}} - \sigma^2_{\mathrm{Sid,out}}}{2\sigma_{\mathrm{Sapp,out}}\sigma_{\mathrm{Sid,out}}} = \frac{30.7^2 - 14.1^2 - 27^2}{2 \cdot 14.1 \cdot 29} = 0.02 \qquad (5.56)$$

and for the neural form of the static algorithm, we have:

$$c_{\mathrm{cor,Srec}} = \frac{3.81^2 - 2.1^2 - 4.71^2}{2 \cdot 2.1 \cdot 4.71} = -0.69 \qquad (5.57)$$

The calculated values of the correlation coefficient mean that the approximation and identification errors at the output of the exemplary dynamic algorithm may be correlated. This fact and the different amplification of these errors during the propagation by the dynamic algorithm (see Eqs. 5.52, 5.53, 5.54 and 5.55) cause that, in the process of composition of standard deviations at the output of the sampling instrument, the reconstruction error should be considered instead of the partial, (i.e. approximation and identification) errors.

The coefficient describing propagation of the static reconstruction error by the dynamic algorithm depends on both the signal frequency and its amplitude as well on the parameters of the static, linear and neural, approximations. For the exemplary instrument, the most essential is the dependence of this coefficient on the frequency, which is presented below in Tabs. 5.1 and 5.2.

Table 5.1

Dependence of the propagation coefficient (5.51) of the static reconstruction error on the signal frequency f for the analytical form of the static algorithm, the standard deviation of the error is $\sigma_{\mathrm{Srec}} = 12.4 \cdot 10^{-3}$°C

f Hz	0.001	0.005	0.01	0.05
$\sigma_{\mathrm{Srec,out}} \cdot 10^{-3}$°C	15.2	23.4	30.7	71.9
$k_{\mathrm{D,Srec}}$	1.23	1.89	2.48	5.80

Table 5.2

Dependence of the propagation coefficient (5.51) of the static reconstruction error on the signal frequency f for the neural form of the static algorithm, the standard deviation of the error is $\sigma_{\mathrm{Srec}} = 3.7 \cdot 10^{-3}$°C

f Hz	0.001	0.005	0.01	0.05
$\sigma_{\mathrm{Srec,out}} \cdot 10^{-3}$°C	3.72	3.73	3.84	5.83
$k_{\mathrm{D,Srec}}$	1.005	1.008	1.038	1.576

As it results from Tabs. 5.1 and 5.2, the static reconstruction error is amplified by the dynamic algorithm in dependence of the frequency of the input signal, however, the propagation coefficient takes significantly greater values for the analytical form of the static algorithm. Making the suitable experiments one can prove that

the propagation coefficient depends on the amplitude of the signal. These properties cause that the propagation of the static reconstruction error by the dynamic algorithm should be analyzed dependently on the mentioned measurement conditions and represented separately in the error model.

5.2.3. Probabilistic description of static error propagation

As it results from the presented considerations, the most effective way of the error analysis consists in comparing standard deviations as basing parameters of the error distributions, which allows identifying the dominant sources of errors. Standard deviations of partial non-correlated errors can be composed in any point of the error propagation model on the principle of summing up the variances accordingly with Eq. (1.52). To do this, it is necessary to describe the relations between the standard deviations at the output and the input of the reconstruction chain.

It results from Fig. 5.5 that every sampling instant realization of the input static errors differs from the realization of the output error by the constant coefficient k_S that describes properties of the static reconstruction algorithm. This means that the propagation of standard deviations of every static error may be described as in Fig. 5.13.

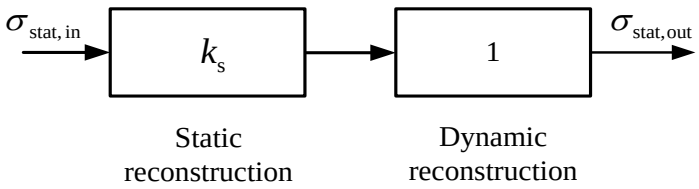

Fig. 5.13. Propagation of the standard deviation of the static error from the input to the output of the reconstruction chain

From the considerations presented in the previous chapter, it results that the static reconstruction errors propagate by the dynamic algorithm dependently on the amplitude and frequency of the input signal. This dependence is described together for the approximation and identification error by the propagation coefficient $k_{D,Srec}$, the values of which are presented in Tabs. 5.1 and 5.2. Taking this into account, the propagation of the standard deviation of the static reconstruction error to the output of the reconstruction chain may be graphically presented as shown in Fig. 5.14.

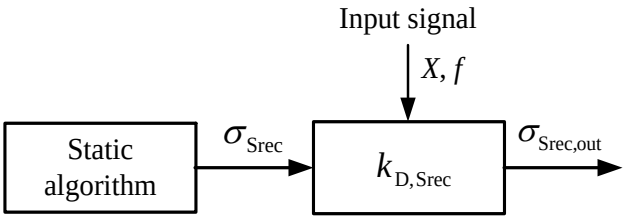

Fig. 5.14. Propagation of the standard deviation of static reconstruction error σ_{Srec} to the output of the reconstruction chain, X is the amplitude, and f the frequency of the input signal

According to Eq. (5.44), realizations of the output static errors are summing up in the output reconstruction chain, which means that we have the dependency:

$$e_{\text{stat,out}}(k) = e_{\text{sh,out}}(k) + e_{\text{inc,out}}(k) + e_{\text{Srec,out}}(k) \tag{5.58}$$

where $e_{\text{sh,out}}$ and $e_{\text{inc,out}}$ are the errors caused by the drift of the static characteristic, $e_{\text{Srec,out}}$ is the error composed of the static approximation error and the error connected with inaccurate identification of the static characteristic. All these errors are not correlated, which results from Eqs. (5.46), (5.56) and (5.57). This means that the relation between standard deviations of the errors from Eq. (5.58) may be written as:

$$\sigma_{\text{stat,out}} = \sqrt{\sigma^2_{\text{sh,out}} + \sigma^2_{\text{inc,out}} + \sigma^2_{\text{Srec,out}}} \tag{5.59}$$

Eq. (5.59) can be used for analysis of the influence of the partial errors on the standard deviation $\sigma_{\text{stat,out}}$ of the total static error. Based on values of the standard deviations given in Figs. 5.6, 5.8b and 5.12a, the value of the standard deviation of the total static error at the output of the exemplary instrument is calculated in accordance with Eq. (5.59). We have:

$$\sigma_{\text{stat,out}} = \sqrt{\left(7.3^2 + 9^2 + 33^2\right)\cdot 10^{-6}} = 35\cdot 10^{-3}\ {}^{\text{o}}\text{C} \tag{5.60}$$

As it results from Eq. (5.60), the reconstruction error dominates, which means that decreasing of this error leads to decreasing the total static error.

5.3. Propagation of dynamic errors

In the decomposed model of propagation of the errors shown in Fig. 5.4, the propagation of dynamic errors from the input to the output of the sampling instrument is described the time domain by Eq. (5.34) that may be written as:

$$e_{\text{dyn,out}}(k) = k_{\text{S}}\left[A_{k+1}e_{\text{dyn,in}}(k+1) + A_k e_{\text{dyn,in}}(k) + \ldots + A_{k-m}e_{\text{dyn,in}}(k-m)\right] + e_{\text{dyn,rec}}(k) \tag{5.61}$$

where k is the current number of the measurement window, as well as it denotes the time instant for which the specified error value is determined. The constant coefficient k_S describes the propagation of errors by the static algorithm, A_{k+1},..., A_{k-m} are coefficients of the dynamic reconstruction algorithm in the form of the sequence (4.62), $e_{dyn,in}(k+1)$,..., $e_{dyn,in}(k-m)$ are realizations of the dynamic input error in the window, $e_{dyn,rec}(k)$ is the value of the dynamic reconstruction error.

The 1-st order algorithm in the form of the sequence (4.62) consists of two terms. In this case, the expression (5.61) takes the following form:

$$e_{\mathrm{dyn,out}}(k) = k_{\mathrm{S}}\left[A_{k+1}e_{\mathrm{dyn,in}}(k+1) + A_k e_{\mathrm{dyn,in}}(k)\right] + e_{\mathrm{dyn,rec}}(k) \tag{5.62}$$

Equations (5.61) and (5.62) are mainly useful in simulative experiments, in which the arithmetical operations are performed on realizations of dynamic errors or in the error analysis that is carried out on error values changing over time.

As it is considered in Section 4.3.3, the effective error analyze for changing over time signals is performed if the input signal of the instrument is described as sinusoidal. Such an approach enables analytical description of errors in the frequency domain as spectrum forms, the effect of which is obtaining amplitudes of the analysed error that may be transformed to the probabilistic forms.

From Eq. (4.74), it results the relation between spectral forms of the errors at the input and the output of the dynamic reconstruction algorithm is to be represented by the algorithm transmittance that has the general form:

$$A(\mathrm{j}\omega) = \frac{E_{\mathrm{D,out}}(\mathrm{j}\omega)}{E_{\mathrm{D,in}}(\mathrm{j}\omega)} = A_{k+1}e^{\mathrm{j}\omega T_s} + A_k + A_{k-1}e^{-\mathrm{j}\omega T_s} + \ldots + A_{k-m}e^{-\mathrm{j}m\omega T_s} + \ldots. \tag{5.63}$$

where $E_{D,in}(j\omega)$, $E_{D,out}(j\omega)$ are the spectral forms of errors in the input and output of the algorithm, respectively, A_{k+1}, A_k, ..., A_{k-m} are constant coefficients, T_s is the sampling period. Based on this equation, the error propagation model (5.61) can be expressed in the frequency domain as:

$$E_{\mathrm{dyn,out}}(\mathrm{j}\omega) = k_{\mathrm{S}}A(\mathrm{j}\omega)E_{\mathrm{dyn,in}}(\mathrm{j}\omega) + E_{\mathrm{Drec}}(\mathrm{j}\omega) \tag{5.64}$$

where $E_{Drec}(j\omega)$ is the spectral form of the error introduced by the dynamic reconstruction algorithm. Graphical equivalent of Eq. (5.64) is shown in Fig. 5.15.

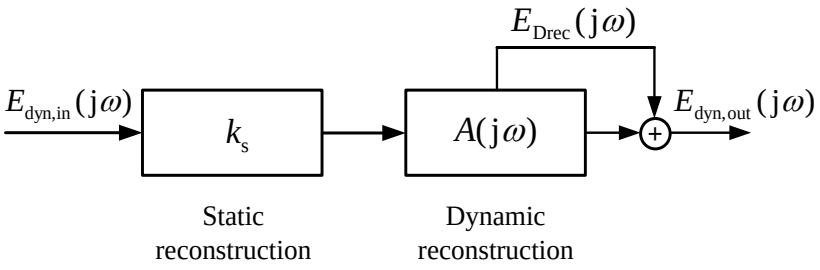

Fig. 5.15. Propagation scheme of dynamic errors

5.3.1. Propagation of input disturbances

The analysis presented in the next example is devoted to the influence of the input electromagnetic disturbance on the inaccuracy of the sampling instrument. The base of this analysis is Eq. (5.62), with the assumption that the dynamic reconstruction error E_{Drec} is omitted.

Example 5.2. The frequency of the industrial electromagnetic disturbance, generated as the voltage directly (bypassing the sensor) in the input circuit of the amplifier implemented in the exemplary instrument shown in Fig. 3.2, is $f = 50$ Hz and the amplitude of the disturbing voltage is $E_{\mathrm{dis}} = 0.1$ V. The common mode rejection ratio CMRR [J14, M2, T1] of the amplifier is equal to 100 dB, which means that this voltage amplitude in the amplifier output is equal $k_{\mathrm{A}} \cdot 0.1/10^5 = 32$ μV, where $k_{\mathrm{A}} = 32$ is the amplification coefficient. This voltage at the ADC input corresponds to about 1 (1 quantum) at its output. The sampling period is $T_{\mathrm{s}} = 0.2$ s, which means that the disturbance voltage is sampled once per 10 periods of the disturbances (for $T = 1/f = 1/50 = 20$ ms, the relative sampling frequency is $T_{\mathrm{s}}/T = 0.2/0.02 = 10$). In this case, i.e., if T_{s}/T is a positive integer, two succeeding ADC results are burdened by the error with the same value e_{dis} that changes from 0 to 1 dependently on the phase shift of the first sample in the window in relation to the disturbance signal. If the exemplary 1-st order dynamic algorithm is applied, according to Eq.(5.62), the error at the algorithm output is described as:

$$e_{\mathrm{dis,out}}(k) = k_{\mathrm{S}}\left[A_{k+1}e_{\mathrm{dis,in}}(k+1) + A_k e_{\mathrm{dis,in}}(k)\right] = k_{\mathrm{S}}\left[\frac{1}{1-\varphi}e_{\mathrm{dis}} - \frac{\varphi}{1-\varphi}e_{\mathrm{dis}}\right] = k_{\mathrm{S}}e_{\mathrm{dis}} \qquad (5.65)$$

The output error is expressed as the number of quanta. For its maximum value, this number is equal to 1; thus, it is:

$$\left|e_{\mathrm{dis,out}}\right|_{\max} = k_{\mathrm{S}}E_{\mathrm{dis}} = 6.35 \cdot 10^{-3} \cdot 1 = 6.35 \cdot 10^{-3}\ ^{\circ}\mathrm{C} \qquad (5.66)$$

where the value of the static propagation coefficient k_{S} is calculated in Example 5.1.

A more sophisticated case occurs if T_s/T is not an integer, which causes the values $e_{\mathrm{dis,in}}(k+1)$ and $e_{\mathrm{dis,in}}(k)$ of the disturbance error to be different. The worst situation is if we have: $e_{\mathrm{dis,in}}(k+1) = e_{\mathrm{dis}}$ and $e_{\mathrm{dis,in}}(k) = -e_{\mathrm{dis}}$. After introducing this values to the first expression in Eq. (5.63), we obtain the output error in the following form:

$$e_{\mathrm{dis,out}}(k) = k_{\mathrm{S}}\left[\frac{1}{1-\varphi}e_{\mathrm{dis}} - \frac{\varphi}{1-\varphi}\left(-e_{\mathrm{dis}}\right)\right] = k_{\mathrm{S}}\frac{1+\varphi}{1-\varphi}e_{\mathrm{dis}} \tag{5.67}$$

If e_{dis} takes the value equal to the error amplitude, one obtains the maximum value of the output error, which is:

$$\left|e_{\mathrm{dis,out}}\right|_{\max} = k_{\mathrm{S}}\frac{1+\varphi}{1-\varphi}E_{\mathrm{dis}} = 6.35\cdot 10^{-3}\frac{1+0.9048}{1-0.9048}\cdot 1 = 0.127\ ^{\mathrm{o}}\mathrm{C} \tag{5.68}$$

This value is relatively big, which means that it is necessary to take actions to reduce this error, for example by changing the sampling period.

5.3.2. Description of dynamic error propagation in frequency domain

The basic dynamic errors in the sampling instrument arise during analog conversion in elements described by differential equations. For sinusoidal signals, these elements are expressed in the frequency domain as transmittances, as it is shown in Fig. 5.16.

The dynamic input error occurs if the inverse dynamic model that is the basis of the dynamic reconstruction algorithm does not contain the dynamic properties of any element that is a component of the analog conversion. In such a case, the input error $E_{\mathrm{dyn,in}}(\mathrm{j}\omega)$ should contain a description of all dynamic errors that arise during the analog conversion of the instrument input signal. To obtain this description, one should use the model another than this presented in Fig. 5.15. With assumption that the static reconstruction is not taken into account, the chain of the dynamic reconstruction that contains the additive source of the dynamic input error can be described in the frequency domain as presented in Fig. 5.16.

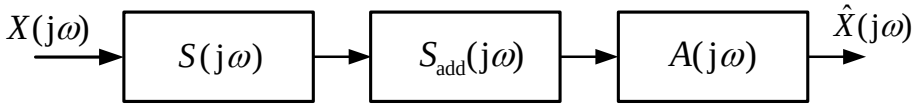

Fig. 5.16. Structure of the reconstruction chain composed of dynamic components described by transmittances: $S(\mathrm{j}\omega)$ is the transmittance of the component, the dynamic error of which is corrected by the reconstruction algorithm with the transmittance $A(\mathrm{j}\omega)$, $S_{\mathrm{add}}(\mathrm{j}\omega)$ is the transmittance of the component not contained by the reconstruction algorithm

The spectral transform of the output signal $\hat{X}(j\omega)$ of the chain from Fig. 5.16 is described as:

$$\hat{X}(j\omega) = X(j\omega)S(j\omega)S_{add}(j\omega)A(j\omega) \tag{5.69}$$

where $X(j\omega)$ is the transform of the input signal. Accordingly with the definition (4.85), the dynamic error in the output of the chain from Fig. 5.16 takes the form:

$$E_{dyn,out}(j\omega) = X(j\omega) - \hat{X}(j\omega) = X(j\omega)[1 - S(j\omega)S_{add}(j\omega)A(j\omega)] \tag{5.70}$$

With the assumption that only the dynamic error of the component $S(j\omega)$ is corrected by the reconstruction algorithm with transmittance $A(j\omega)$, Eq. (5.70) may be transformed in the following way:

$$\begin{aligned} E_{dyn,out}(j\omega) &= X(j\omega)[1 - S(j\omega)S_{add}(j\omega)A(j\omega) + S_{add}(j\omega) - S_{add}(j\omega)] = \\ &= X(j\omega)[1 - S_{add}(j\omega) + S_{add}(j\omega)(1 - S(j\omega)A(j\omega))] = \\ &= X(j\omega)[e_{add}(j\omega) + S_{add}(j\omega)(1 - S(j\omega)A(j\omega))] \end{aligned} \tag{5.71}$$

As it results from this expression, the additional element $S_{ad}(j\omega)$ introduces the error that is described as:

$$E_{add}(j\omega) = X(j\omega)[1 - S_{add}(j\omega)] \tag{5.72}$$

Based on the same definition (4.85) as used in Eq. (5.66), the dynamic reconstruction error is expressed as:

$$E_{Drec}(j\omega) = X(j\omega)[1 - S(j\omega)A(j\omega)] \tag{5.73}$$

Introducing this expression into Eq. (5.71),we have:

$$E_{dyn,out}(j\omega) = E_{add}(j\omega) + S_{add}(j\omega)E_{Drec}(j\omega) \tag{5.74}$$

which means that the output dynamic error is the sum of the additional dynamic error E_{add} and the dynamic reconstruction error after its propagation by the additional component S_{add}. If the additional component does not introduce the dynamic error, its transmittance is equal to 1. In this case, accordingly with Eq. (5.74), the output dynamic error reduces to the dynamic reconstruction error E_{Drec}.

Eq. (5.74) enables determination of the dynamic output error in the analytical spectral form, and, using the inverse Fourier transform, as the suitable time waveform.

To simplify further considerations, we define the transmittance of the source of the dynamic error $E_{dyn}(j\omega)$ as:

$$ES_{dyn}(j\omega) = \frac{E_{dyn}(j\omega)}{X(j\omega)} \tag{5.75}$$

where $X(\mathrm{j}\omega)$ is the spectral transform of the input signal. Introducing Eq. (5.74) to (5.75), we have:

$$ES_{\mathrm{dyn,out}} = \frac{E_{\mathrm{dyn,out}}(\mathrm{j}\omega)}{X(\mathrm{j}\omega)} = \frac{E_{\mathrm{add}}(\mathrm{j}\omega) + S_{\mathrm{add}}(\mathrm{j}\omega)E_{\mathrm{Drec}}(\mathrm{j}\omega)}{X(\mathrm{j}\omega)} = \\ = ES_{\mathrm{add}}(\mathrm{j}\omega) + S_{\mathrm{add}}(\mathrm{j}\omega)ES_{\mathrm{Drec}}(\mathrm{j}\omega) \tag{5.76}$$

The transmittance of the output error source can be expressed using the transmittances of the elements of the reconstruction chain. Based on Eqs. (5.72) and (5.73), Eq. (5.76) may be written as:

$$ES_{\mathrm{dyn,out}} = \frac{X(\mathrm{j}\omega)[1 - S_{\mathrm{add}}(\mathrm{j}\omega)] + S_{\mathrm{add}}(\mathrm{j}\omega)[1 - S(\mathrm{j}\omega)A(\mathrm{j}\omega)]}{X(\mathrm{j}\omega)} = 1 - S_{\mathrm{add}}(\mathrm{j}\omega)S(\mathrm{j}\omega)A(\mathrm{j}\omega) \tag{5.77}$$

To obtain the transmittance of the output error source according to Eq. (5.76), it is necessary to determine the transmittance of the reconstruction chain from Fig. 5.22. This transmittance is the product of three transmittances, which is expressed as follows:

$$S_{\mathrm{rec}} = S_{\mathrm{add}}(\mathrm{j}\omega)S(\mathrm{j}\omega)A(\mathrm{j}\omega) \tag{5.78}$$

The module of the source transmittance is described as the following product of the modules :

$$|S_{\mathrm{rec}}| = |S_{\mathrm{add}}(\mathrm{j}\omega)||S(\mathrm{j}\omega)||A(\mathrm{j}\omega)| \tag{5.79}$$

and its phase is the sum:

$$\varphi_{\mathrm{rec}} = \varphi_{\mathrm{add}} + \varphi_S + \varphi_A \tag{5.80}$$

The transmittance (5.78) can be written as:

$$S_{\mathrm{rec}}(\mathrm{j}\omega) = |S_{\mathrm{rec}}(\mathrm{j}\omega)|e^{\mathrm{j}\varphi_{\mathrm{rec}}} \tag{5.81}$$

where the module of it is described by Eq. (5.79) and the phase by Eq. (5.80). Taking these expressions into account, the transmittance of the output error source (5.77) takes the form:

$$ES_{\mathrm{dyn,out}} == 1 - |S_{\mathrm{rec}}(\mathrm{j}\omega)|e^{\mathrm{j}\varphi_{\mathrm{rec}}} = 1 - |S_{\mathrm{rec}}(\mathrm{j}\omega)|\cos\varphi_{\mathrm{rec}} - \mathrm{j}|S_{\mathrm{rec}}(\mathrm{j}\omega)|\sin\varphi_{\mathrm{rec}} \tag{5.82}$$

The module of the transmittance (5.82) is expressed as:

$$|ES_{\mathrm{dyn,out}}| = \sqrt{\mathrm{Re}\{ES_{\mathrm{dyn,out}}(\mathrm{j}\omega)\}^2 + \mathrm{Im}\{ES_{\mathrm{dyn,out}}(\mathrm{j}\omega)\}^2} = \\ = \sqrt{\{1 - |S_{\mathrm{rec}}(\mathrm{j}\omega)|\cos\varphi_{\mathrm{rec}}\}^2 + \{|S_{\mathrm{rec}}(\mathrm{j}\omega)|\sin\varphi_{\mathrm{rec}}\}^2} \tag{5.83}$$

and its phase as:

$$\varphi_{\text{rec}} = \arctan \frac{\text{Im}\{ES_{\text{dyn,out}}(\text{j}\omega)\}}{\text{Re}\{ES_{\text{dyn,out}}(\text{j}\omega)\}} = -\arctan \frac{|S_{\text{rec}}(\text{j}\omega)| \sin \varphi_{\text{rec}}}{1 - |S_{\text{rec}}(\text{j}\omega)| \cos \varphi_{\text{rec}}} \tag{5.84}$$

As it results from Eqs. (5.62) and (5.63), the transmittance of the 1-st order reconstruction algorithm is described as the sequence reduced to two terms; thus, we have in this case:

$$A(\text{j}\omega) = A_{k+1} e^{\text{j}\omega T_{\text{s}}} + A_k \tag{5.85}$$

The coefficients of this equationare calculated according to Eq. (4.72) as:

$$A_{k+1} = \frac{1}{1-\varphi}, \quad A_k = \frac{-\varphi}{1-\varphi} \tag{5.86}$$

where the value of φ is determined on the basis of parameters of the analog converter and the reconstructed signal, as it shown in example 5.3.

Introducing expressions (5.86) into Eq. (5.85), we obtain the following expression:

$$A(\text{j}\omega) = \frac{1}{1-\varphi} e^{\text{j}\omega T_{\text{s}}} - \frac{\varphi}{1-\varphi} = \frac{1}{1-\varphi}(\cos \omega T_{\text{s}} + \text{j} \sin \omega T_{\text{s}}) - \frac{\varphi}{1-\varphi} = \frac{\cos \omega T_{\text{s}} - \varphi}{1-\varphi} + \text{j} \frac{\sin \omega T}{1-\varphi} \tag{5.87}$$

from which we have that the real part of the transmittance is:

$$\text{Re}\{A(\text{j}\omega)\} = \frac{\cos \omega T_{\text{s}} - \varphi}{1-\varphi} \tag{5.88}$$

and its imaginary part:

$$\text{Im}\{A(\text{j}\omega)\} = \frac{\sin \omega T_{\text{s}}}{1-\varphi} \tag{5.89}$$

The module of the algorithm transmittance is expressed as:

$$\begin{aligned} |A(\text{j}\omega)| &= \sqrt{\text{Re}^2\{A(\text{j}\omega)\} + \text{Im}^2\{A(\text{j}\omega)\}} = \sqrt{\frac{(\cos \omega T_{\text{s}} - \varphi)^2}{(1-\varphi)^2} + \frac{\sin^2 \omega T_{\text{s}}}{(1-\varphi)^2}} = \\ &= \sqrt{\frac{\cos^2 \omega T_{\text{s}} - 2\varphi \cos \omega T_{\text{s}} + \varphi^2 + \sin^2 \omega T_{\text{s}}}{(1-\varphi)^2}} = \frac{\sqrt{1 - 2\varphi \cos \omega T_{\text{s}} + \varphi^2}}{1-\varphi} \end{aligned} \tag{5.90}$$

while its phase as:

$$\varphi_{\text{A}} = \arctan \frac{\text{Im}\{A(\text{j}\omega)\}}{\text{Re}\{A(\text{j}\omega)\}} = \arctan \frac{\dfrac{\sin \omega T_{\text{s}}}{1-\varphi}}{\dfrac{\cos \omega T_{\text{s}} - \varphi}{1-\varphi}} = \arctan \frac{\sin \omega T_{\text{s}}}{\cos \omega T_{\text{s}} - \varphi} \tag{5.91}$$

Example 5.3. The dynamic properties of the Pt100 sensor placed in a jacked are described by the series connection of two 1-st order converters with the time constant $\tau_1 = 20$ s of the first converter and $\tau_2 = 2$ s of the second. The dynamic error of the first converter dominates; therefore, it has to be corrected using the dynamic reconstruction algorithm, while the correction of the error introduced by the second converter is not necessary if this error is negligible. To resolve this issue, the transmittance of the reconstruction error source should be determined.

Let us take the reconstructed temperature signal to change sinusoidal in the input range of 0 to 100°C, which means that it is described as: $x(t) = 50\sin\omega t + 50$°C, $\omega = 2\cdot\pi\cdot f$, f is the frequency and $f = 0.002$ Hz. The signal is sampled with the period $T_s = 2$ s. For these parameters, the coefficient φ in the expressions (5.82) takes the value (see Example 4.4):

$$\varphi = e^{-\frac{T_s}{\tau_1}} = e^{-\frac{2}{20}} = 0.9048$$

Moreover, it is:

$$\omega T_s = 2\pi f T_s = 2\pi \cdot 0.002 \cdot 2 = 0.02513,\ \sin \omega T_s = 0.02513,\ \cos \omega T_s = 0.99968,$$
$$\omega \tau_1 = 2\pi f \tau_1 = 2\pi \cdot 0.002 \cdot 20 = 0.2513,\ \omega \tau_2 = 2\pi f \tau_2 = 2\pi \cdot 0.002 \cdot 2 = 0.02513$$

On the basis of these values, one can calculate the transmittances of the reconstruction chain. The module of the transmittance of the reconstruction algorithm has the following value:

$$\left|A(\mathrm{j}\omega)\right| = \frac{\sqrt{1 - 2\varphi\cos\omega T_s + \varphi^2}}{1-\varphi} = \frac{\sqrt{1 - 2\cdot 0.9048 \cdot 0.99968 + 0.9048^2}}{1 - 0.9048} = 1.0315 \quad (5.92)$$

and the phase is:

$$\varphi_A = \arctan\frac{\sin\omega T_s}{\cos\omega T_s - \varphi} = \arctan\frac{0.02513}{0.99968 - 0.9048} = \arctan 0.26486 = 0.2589 \quad (5.93)$$

The module of the transmittance of the 1-st order converter is described by Eq. (4.21). According to this equation, the module of the first dynamic converter, contained by the reconstruction algorithm, is:

$$\left|S(\mathrm{j}\omega)\right| = \frac{1}{\sqrt{1 + (\omega\tau_1)^2}} = \frac{1}{\sqrt{1 + 0.2513^2}} = 0.96985 \quad (5.94)$$

and its phase:

$$\varphi_S = -\arctan\omega\tau_1 = -\arctan 0.2513 = -0.2462 \quad (5.95)$$

The module of the second additive converter takes the value:

$$\left|S_{\text{add}}(\text{j}\omega)\right| = \frac{1}{\sqrt{1+(\omega\tau_2)^2}} = \frac{1}{\sqrt{1+0.02513^2}} = 0.99968 \tag{5.96}$$

and its phase is:

$$\varphi_{\text{add}} = -\arctan\omega\tau_2 = -\arctan 0.02513 = -0.02513 \tag{5.97}$$

According to the values obtained using Eqs. (5.92), (5.94) and (5.96), the product (5.78) of the considered modules has the value:

$$\left|S_{\text{rec}}(\text{j}\omega)\right| = \left|A(\text{j}\omega)\right|\left|S(\text{j}\omega)\right|\left|S_{\text{add}}(\text{j}\omega)\right| = 1.0315\cdot 0.96985\cdot 0.99968 = 0.99966 \tag{5.98}$$

The phase shift obtained as the sum of values calculated using expressions (5.93), (5.95) and (5.97) is:

$$\varphi_{\text{rec}} = \varphi_{\text{A}} + \varphi_{\text{S}} + \varphi_{\text{add}} = 0.2589 - 0.2462 - 0.02513 = -0.01243 \tag{5.99}$$

For the calculated values of module (5.98) and the phase (5.99), the module of the output error source (5.82) takes the value:

$$\begin{aligned}\left|ES_{\text{dyn,out}}\right| &= \sqrt{\left\{1-\left|S_{\text{rec}}(\text{j}\omega)\right|\cos\varphi_{\text{rec}}\right\}^2 + \left\{\left|S_{\text{rec}}(\text{j}\omega)\right|\sin\varphi_{\text{rec}}\right\}^2} = \\ &= \sqrt{\left[(1-0.99966\cdot\cos(-0.01243)\right]^2 + \left[0.99966\cdot\sin(-0.01243)\right]^2} = 0.0124\end{aligned} \tag{5.100}$$

Based on Eq. (5.74), one can describe the dynamic error connected to the output error source as:

$$E_{\text{dyn,out}}(\text{j}\omega) = X(\text{j}\omega)ES_{\text{dyn}}(\text{j}\omega) \tag{5.101}$$

The amplitude of this error is equal to its module that, according to Eq. (5.101), is expressed as:

$$\left|E_{\text{dyn,out}}(\text{j}\omega)\right| = \left|X(\text{j}\omega)\right|\left|ES_{\text{dyn}}(\text{j}\omega)\right| \tag{5.102}$$

The amplitude of the input signal is: $\left|X(\text{j}\omega)\right| = 50\ ^{\circ}\text{C}$; therefore, the amplitude (5.102) of the output dynamic error takes the following value:

$$E_{\text{dyn,out}} = \left|E_{\text{dyn,out}}(\text{j}\omega)\right| = \left|X(\text{j}\omega)\right|\left|ES_{\text{dyn}}(\text{j}\omega)\right| = 50\cdot 0.0124 = 0.620^{\circ}\text{C} \tag{5.103}$$

The assumption that the additive converter S_{add} does not exist in the analog conversion chain is equivalent to the description of its properties as ideal, which means that its transmittance $S_{\text{add}}(\text{j}\omega) = 1$ and the phase $\varphi_{\text{add}} = 0$. For these values, the module (5.98) is:

$$\left|S_{\text{rec}}(\text{j}\omega)\right| = \left|A(\text{j}\omega)\right|\left|S(\text{j}\omega)\right|\left|S_{\text{add}}(\text{j}\omega)\right| = 1.0315\cdot 0.96985\cdot 1 = 1.0001 \tag{5.104}$$

and the phase:

$$\varphi_{\text{rec}} = \varphi_{\text{A}} + \varphi_{\text{S}} + \varphi_{\text{add}} = 0.2589 - 0.2462 + 0 = 0.0127 \tag{5.105}$$

In this case, the amplitude (5.100) of the dynamic output error is of the following value:

$$\begin{aligned} \left|ES_{\text{dyn,out}}\right| &= \sqrt{\left\{1 - \left|S_{\text{rec}}(\text{j}\omega)\right| \cos\varphi_{\text{rec}}\right\}^2 + \left\{\left|S_{\text{rec}}(\text{j}\omega)\right| \sin\varphi_{\text{rec}}\right\}^2} = \\ &= \sqrt{\left(1 - 1.0001 \cdot \cos 0.0127\right)^2 + \left(1.0001 \cdot \sin 0.0127\right)^2} = 0.0127 \end{aligned} \tag{5.106}$$

This means that the amplitude of the error $E_{\text{dyn,out}} = 50 \cdot 0.0127 = 0.635^{\text{o}}\text{C}$ is comparable to the value (5.103) that is calculated for the case if all dynamic elements are taken into account in the signal reconstruction.

5.3.3. Analytical and probabilistic description of dynamic reconstruction error

The dynamic reconstruction error is described analytically in the same way as presented in the previous chapter, i.e., with using the transmittance of error source. The starting point of determination of this transmittance is the description of the reconstruction chain in the frequency domain presented graphically in Fig. 5.17.

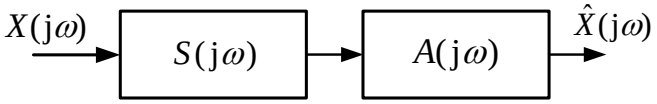

Fig. 5.17. Structure of the reconstruction chain made up of the transmittance $S(\text{j}\omega)$ of the converter, the dynamic error of which is corrected by the reconstruction algorithm with the transmittance $A(\text{j}\omega)$

According to Fig. 5.17, the transform of the output signal is as follows:

$$\hat{X}(\text{j}\omega) = X(\text{j}\omega)S(\text{j}\omega)A(\text{j}\omega) \tag{5.107}$$

where $X(\text{j}\omega)$ is the transform of the input signal. Based on the definition (4.85), the error in the output of the chain, that is, the dynamic reconstruction error in this case takes the form:

$$E_{\text{Drec}}(\text{j}\omega) = X(\text{j}\omega) - \hat{X}(\text{j}\omega) = X(\text{j}\omega)\left[1 - S(\text{j}\omega)A(\text{j}\omega)\right] \tag{5.108}$$

From Eqs. (5.75) and (5.108), we find that the source of the dynamic reconstruction error is described as:

$$ES_{\text{Drec}}(\text{j}\omega) = \frac{E_{\text{Drec}}(\text{j}\omega)}{X(\text{j}\omega)} = 1 - S(\text{j}\omega)A(\text{j}\omega) = 1 - S_{\text{rec}}(\text{j}\omega) \tag{5.109}$$

According to this equation, the amplitude of the dynamic reconstruction error is of the form:

$$E_{\text{dyn,rec}} = \left|E_{\text{dyn,rec}}(\text{j}\omega)\right| = \left|X(\text{j}\omega)\right|\left|ES_{\text{dyn,rec}}(\text{j}\omega)\right| \tag{5.110}$$

where:

$$\left|ES_{\text{Drec}}\right| = \sqrt{\left\{1-\left|S_{\text{rec}}(\text{j}\omega)\right|\cos\varphi_{\text{rec}}\right\}^2 + \left\{\left|S_{\text{rec}}(\text{j}\omega)\right|\sin\varphi_{\text{rec}}\right\}^2} \tag{5.111}$$

and it is:

$$\left|S_{\text{rec}}\right| = \left|S(\text{j}\omega)\right|\left|A(\text{j}\omega)\right|, \qquad \varphi_{\text{rec}} = \varphi_{\text{S}} + \varphi_{\text{A}} \tag{5.112}$$

Example 5.4. The dynamic properties of the sensor are described by the 1-st order converter with the time constant τ = 2 s. The reconstructed temperature signal change sinusoidal in the input range from 0 to 100°C, which means that it is described as: $x(t) = 50\sin\omega t + 50$°C, $\omega = 2\cdot\pi\cdot f$, f is the frequency and $f = 0.01$ Hz. The signal is sampled with the period $T_{\text{s}} = 0.2$ s.

For these parameters, the coefficient φ of the exemplary algorithm of 1-st order has the value (see Example 4.4): $\varphi = 0.9048$. Furthermore, we have: $\omega\tau = 2\pi f\tau = 2\pi\cdot 0.01\cdot 2 = 0.1257$, $\omega T_{\text{s}} = 2\cdot\pi f\cdot T_{\text{s}} = 2\cdot\pi\cdot 0.01\cdot 0.2 = 0.01257$.

According to the taken assumptions and Eq. (5.19), the module of the transmittance of the reconstruction algorithm has the value:

$$\left|A(\text{j}\omega)\right| = \frac{\sqrt{1-2\varphi\cos\omega T_{\text{s}}+\varphi^2}}{1-\varphi} = \frac{\sqrt{1-2\cdot 0.9048\cdot 0.99992+0.9048^2}}{1-0.9048} = 1.008 \tag{5.113}$$

and its phase is:

$$\varphi_{\text{A}} = \arctan\frac{\sin\omega T_{\text{s}}}{\cos\omega T_{\text{s}}-\varphi} = \arctan\frac{0.01257}{0.99992-0.9048} = \arctan 0.1321 = 0.1314 \tag{5.114}$$

Based on Eq. (4.21), we have the following value of the transmittance module of the 1-st order converter:

$$\left|S(\text{j}\omega)\right| = \frac{1}{\sqrt{1+(\omega\tau)^2}} = \frac{1}{\sqrt{1+0.1257^2}} = 0.9922 \tag{5.115}$$

and the phase of the transmittance is:

$$\varphi_{\text{S}} = -\arctan\omega\tau = -\arctan 0.1257 = -.0.1250 \tag{5.116}$$

Using results (5.113) and (5.115), we obtain the following value of the product of the transmittance module from Eq. (112):

$$\left|S_{\text{rec}}(\text{j}\omega)\right| = \left|A(\text{j}\omega)\right|\left|S(\text{j}\omega)\right| = 1.008\cdot 0.9922 = 1.00014 \tag{5.117}$$

The transmittance phase calculated as the sum of values (5.114) and (5.116)is:

$$\varphi_{\text{rec}} = \varphi_{\text{A}} + \varphi_{\text{S}} = 0.1314 - 0.1250 = 0.0064 \tag{5.118}$$

According to these values, the transmittance module of the error source (5.111) takes the following value:

$$\begin{aligned} |ES_{\text{Drec}}| &= \sqrt{\left\{1 - |S_{\text{rec}}(\text{j}\omega)|\cos\varphi_{\text{rec}}\right\}^2 + \left\{|S_{\text{rec}}(\text{j}\omega)|\sin\varphi_{\text{rec}}\right\}^2} = \\ &= \sqrt{\left[(1 - 1.00014\cdot\cos(0.0064)\right]^2 + \left[1.00014\cdot\sin(0.0064)\right]^2} = 0.0064 \end{aligned} \tag{5.119}$$

Thus, the amplitude of reconstruction dynamic error calculated for the amplitude of the input signal $|X(\text{j}\omega)| = 50\,^{\circ}\text{C}$ on the basis of Eq. (5.110) is as follows:

$$E_{\text{Drec}} = |E_{\text{Drec}}(\text{j}\omega)| = |X(\text{j}\omega)||ES_{\text{Drec}}(\text{j}\omega)| = 50\cdot 0.0064 = 0.32^{\circ}\text{C} \tag{5.120}$$

The analytical description of dynamic errors as transmittances enables detailed analysis of the error sources and determining relations between them, but combining of the dynamic errors with other errors needs consistent description of all errors in the probabilistic categories. Complete information about the distribution of the dynamic error is given by its histogram that is determined using Monte Carlo method as shown in the Experiment 5.7. However, the standard deviation σ_{dyn} of the sinusoidal error may be calculated on the basis of its amplitude E_{dyn} [J15, M2] as:

$$\sigma_{\text{dyn}} = \frac{E_{\text{dyn}}}{\sqrt{2}} \tag{5.121}$$

According to this expression and Eq. (5.110), the standard deviation of the dynamic output error may be determined as:

$$\sigma_{\text{dyn,out}} = \frac{E_{\text{Drec}}}{\sqrt{2}} = \frac{X|ES_{\text{Drec}}(\text{j}\omega)|}{\sqrt{2}} \tag{5.122}$$

where X denotes the amplitude of the input signal. Based on this equation, we can present the dynamic reconstruction algorithm as the source of the random error shown in Fig. 5.18a, the standard deviation of which is described by Eq. (5.122).

The amplitude of the reconstruction dynamic error calculated in Example 5.4 is: $E_{\text{Drec}} = 0.32^{\text{o}}\text{C}$. Thus, the standard deviation of this error takes the value:

$$\sigma_{\text{Drec}} = \frac{E_{\text{Drec}}}{\sqrt{2}} = \frac{0.32}{\sqrt{2}} = 0.226\,^{\circ}\text{C} \tag{5.123}$$

The same value we obtain performing Experiment 5.7.

Experiment 5.7. This experiment aims to determine of the histogram of the dynamic error in output of the exemplary algorithm (5.85) used to correct the dynamic error of the 1-st order converter with time constant $\tau = 2$ s. The input signal of the instrument changes sinusoidal in the input range of 0 to 100°C, i.e., it is described as: $x(t) = 50\sin\omega t + 50$°C, $\omega = 2 \cdot \pi \cdot f$, the frequency is $f = 0.01$ Hz. At every step of the experiment, the input signal is sampled, first at the random instant t_k located in the signal period T and, next, in the instant $t_k + T_s$, where the sampling period $T_s = 0.2$ s. At the same instants the output signal of the analog converter is sampled, too, and the obtained samples are processed by the reconstruction algorithm. The reconstruction result is subtracted from the input signal at the instant t_k to obtain the reconstruction error, the value of which is located in the set of error values. After 100 000 steps, the standard deviation of the error is calculated and the error distribution is determined in the form of the histogram presented in Fig. 5.18b.

a) b)

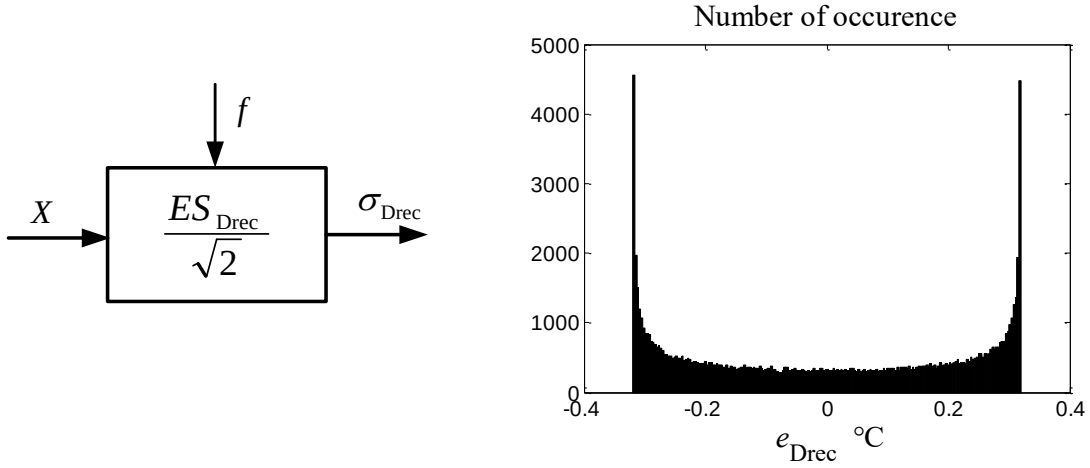

Fig. 5.18. a) Scheme of the dynamic reconstruction error as the source of the random error, b) histogram of the dynamic reconstruction error determined in Experiment 5.7, $\sigma_{\text{Drec}} = 0.226$°C

5.4. Propagation of random errors

There are two main kinds of random errors in the sampling instruments. The errors of the first kind are connected with random disturbances introduced to the input of the instrument and the noises generated in its analog and analog-to-digital converters. These errors may be modelled together as an additive noise at the input of the AD converter [M2]. The second kind of random error is connected with digitalization of the analog signal performed by sample-and-hold circuits and AD converters [J5, J14].

Both these kinds of errors are modelled at the output of the AD converter, which causes that values of them are expressed as numbers at the input of the chain of the reconstruction algorithms.

The input random error $e_{\text{ran,in}}$ is composition of the partial errors that are characterized above. The propagation of this error is described in the general model by Eq. (5.30) that may be presented in the form of the linear combination of realizations of the input error and constant coefficients A_{k+1}, A_k ... A_{k-m} of the dynamic reconstruction algorithm. Thus, we have the following:

$$e_{\text{ran,out}}(k) = k_{\text{S}}\left[A_{k+1}e_{\text{ran,in}}(k+1) + A_k e_{\text{ran,in}}(k) + \ldots + A_{k-m}e_{\text{ran,in}}(k-m)\right] \quad (5.124)$$

where k_{S} is the propagation coefficient of the static algorithm, k is the number of the current measurement window. Denoting the random error at the input of the dynamic algorithm at every sampling instant as:

$$e_{\text{Dran,in}} = k_{\text{S}}e_{\text{ran,in}} \quad (5.125)$$

and introducing this expression to Eq. (5.124), one obtains a description of the propagation of the random error by the dynamic algorithm in the form of the following equation:

$$e_{\text{ran,out}}(k) = A_{k+1}e_{\text{Dran,in}}(k+1) + A_k e_{\text{Dran,in}}(k) + \ldots + A_{k-m}e_{\text{Dran,in}}(k-m) \quad (5.126)$$

For the 1-st order algorithm, Eq. (5.126) takes the form:

$$e_{\text{ran,out}}(k) = A_{k+1}e_{\text{Dran,in}}(k+1) + A_k e_{\text{Dran,in}}(k) \quad (5.127)$$

Taking into account that realizations $e_{\text{Dran,in}}(k+1)$, $e_{\text{Dran,in}}(k)$,..., $e_{\text{Dran,in}}(k-m)$ of the error at the algorithm input are taken from the same population with the standard deviation $\sigma_{\text{Dran,in}}$, their linear combination (5.126) fulfils requirements of the Central Limit Theorem. This means that the propagation of the random error may be described as the following relation between variances of the input and output errors:

$$\sigma^2_{\text{ran,out}}(k) = \left[A_{k+1}\sigma_{\text{Dran,in}}\right]^2 + \left[A_k\sigma_{\text{Dran,in}}\right]^2 + \ldots + \left[A_{k-m}\sigma_{\text{Dran,in}}\right]^2 \quad (5.128)$$

Based on this equation, we can obtain a description of the standard deviation of the output error as the expression:

$$\sigma_{\text{ran,out}}(k) = \sigma_{\text{Dran,in}}\sqrt{A^2_{k+1} + A^2_k + \ldots A^2_{k-m}} \quad (5.129)$$

For the 1-st order reconstruction algorithm, this expression takes the form:

$$\sigma_{\text{ran,out}}(k) = \sigma_{\text{Dran,in}}\sqrt{A^2_{k+1} + A^2_k} \quad (5.130)$$

Generally, the propagation of different kinds of error by the dynamic algorithm is described by the propagation coefficient defined as expression (5.51) that is the ratio of standard deviations of the error considered at the output and input of this algorithm. According to Eq. (5.129), the propagation coefficient of the random error is described as:

$$k_{\mathrm{Dran}} = \frac{\sigma_{\mathrm{ran,out}}}{\sigma_{\mathrm{Dran,in}}} = \sqrt{A_{k+1}^2 + A_k^2 + \ldots A_{k-m}^2} \tag{5.131}$$

The coefficients of the dynamic reconstruction algorithm are constant if the sampling instrument works under stable measurement conditions. This means that, in such conditions, the random propagation coefficient has a constant value the same for every kind of random error, although it depends on the form of the reconstruction algorithm.

Example 5.5. The values of the coefficients of the exemplary algorithm of the 1-st order, calculated in Example 4.13, are: $A_{k+1} = 10.5$ and $A_k = -9.5$. For these values, the coefficient (5.114) has the following value:

$$k_{\mathrm{Dran}} = \sqrt{A_{k+1}^2 + A_k^2} = \sqrt{10.5^2 + (-9.5)^2} = 14.2 \tag{5.132}$$

As it is calculated in Example 4.11, to represent the exemplary 2-nd order algorithm accurately enough, it is necessary to take 45 initial terms of the algorithm in the form of the series. For the purpose of calculating the random propagation coefficient, it is enough to take 10 values presented in Tab. 4.4. According to Eq. (5.114), we have:

$$k_{\mathrm{Dran}} = \sqrt{10.2^2 + (-21.5)^2 + 22^2 + (-17.4)^2 + 13.8^2 + (-10.9)^2 + \ldots} = 42.8 \tag{5.133}$$

From the values calculated using the equations (5.132) and (5.133), it results that the dynamic reconstruction algorithm significantly amplifies the random errors. The coefficient k_{Dran} that quantitatively describes this amplification has the constant value, which means that influence of stable random error sources on inaccuracy of the sampling instrument does not change in time.

According to Eq. (5.35), the input random errors are multiplied by constant coefficient k_{S} during their propagation by the static algorithm. This means that this coefficient can be used to describe the relationship between the standard deviations of the random errors at the output and the input of the static algorithm. If one takes into account that the propagation of the standard deviation by the dynamic algorithm is described by the coefficient k_{Dran}, propagation of random errors by the reconstruction chain of the sampling instrument can be presented as in Fig. 5.19.

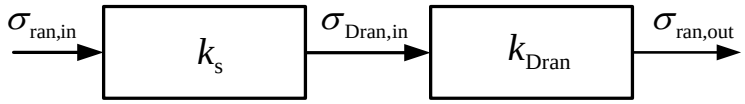

Fig. 5.19. Propagation of the standard deviation of the input random error by the chain of reconstruction algorithms, k_S is the static propagation coefficient, k_{Dran} the dynamic propagation coefficient

The scheme from Fig. 5.19 is enough to compare standard deviations of the errors in the output of the chain of algorithms. But, if we want to know how the distributions of the random errors change during their propagation, there is necessary to use probabilistic experiments. To carry out them, the random errors must be defined in the input of the reconstruction chain. The determination of error values needs knowledge about the true value of the input quantity. In the case if the reconstruction chain is considered, it is necessary to know the number representing the exact quantization result. Accordingly to Eq. (5.45), this result is obtained for the exemplary sampling instrument if we take the quantum value $q \to 0$. For this assumption we obtain the expression:

$$\dot{n}_{\mathrm{q}}(t_k) = 409.176R(t_k) \tag{5.134}$$

where $R(t_k)$ is the resistance value of the sensor at the nominal sampling instant t_k, k is the number of the current measurement window.

In the further considerations, three random input errors are taken into account: the noise error, the quantization error and the error caused by the jitter [Z1]. For these errors, the analytical description of the quantization result takes the form:

$$\tilde{n}_{\mathrm{q}}(t_k) = \mathrm{ent}\left[409.176R(\tilde{t}_k) + e_{\mathrm{noi}}(t_k) + 0.5\right] \tag{5.135}$$

where $e_{noi}(t_k)$ is the normal noise, which models composition of all noises generated in the analog and analog-to-digital parts of the instrument, $R(\tilde{t}_k)$ is the sensor resistance at the instant:

$$\tilde{t}_k = t_k + \Delta_{\mathrm{jit}}(t_k) \tag{5.136}$$

that is disturbed by the jitter $\Delta_{\mathrm{jit}}(t_k)$.

Based on the error definition (1.24) and the equations (5.134) and (5.135), the total error composed of the considered errors is expressed as:

$$e_{\mathrm{ran,in}}(t_k) = \dot{n}_{\mathrm{q}}(t_k) - \tilde{n}_{\mathrm{q}}(t_k) = 409.176R(t_k) - \mathrm{ent}\left[409.176R(\tilde{t}_k) + e_{\mathrm{noi}}(\tilde{t}_k) + 0.5\right] \tag{5.137}$$

Eq. (5.137) describes the total random error at the input of the chain of the algorithms. During propagation of this error by the static algorithm, every realization of the error is multiplied by the constant coefficient k_S. This means that

the total random error at the input of the dynamic algorithm is described by the following equation:

$$e_{\mathrm{Dran,in}}(t_k) = k_{\mathrm{S}} e_{\mathrm{ran,in}}(t_k) = k_{\mathrm{S}} \left\{409.176R(t_k) - \mathrm{ent}\left[409.176R(\tilde{t}_k) + e_{\mathrm{noi.in}}(t_k) + 0.5\right]\right\} \quad (5.138)$$

The experiments presented below are aimed at determination of histograms for the considered partial errors which propagate by the 1-st order exemplary dynamic algorithm.

Experiment 5.8. The first experiment deals with calculations of the jitter error that, accordingly with Eq. (5.138), is defined by the expression:

$$e_{\mathrm{Djit,in}}(t_k) = k_{\mathrm{S}}\left[409.176R(t_k) - 409.176R(\tilde{t}_k)\right] \quad (5.139)$$

The input temperature signal: $\vartheta(t) = 50\sin\omega t + 50^{\circ}\mathrm{C}$, $\omega = 2\cdot\pi\cdot f$, $f = 0.01$ Hz is converted at the sampling instants to the sensor resistance R accordingly with the equation (3.5). At every step of the experiment, two nominal sampling instants t_k and t_{k+1} are determined as random with the rectangular distribution in the signal period $T = 1/f$. Next, two instants disturbed by the jitter are determined on the basis of Eq. (5.136) as:

$$\tilde{t}_k = t_k + \Delta_{\mathrm{jit}}(t_k) \quad \text{and} \quad \tilde{t}_{k+1} = t_{k+1} + \Delta_{\mathrm{jit}}(t_{k+1})$$

with the assumption that the jitter takes values accordingly with the rectangular distribution in the range from Δ_{jmin} to Δ_{jmax} and $|\Delta_{\mathrm{jmin}}| = |\Delta_{\mathrm{jmax}}| = 1\cdot 10^{-6}$ s. The input error (5.139) is processed by the exemplary 1-st order dynamic algorithm using the equation:

$$e_{\mathrm{jit,out}} = A_{k+1} e_{\mathrm{Djit,in}}(t_{\mathrm{k+1}}) + A_k\, e_{\mathrm{Djit,in}}(t_{\mathrm{k}}) \quad (5.140)$$

where $A_{k+1} = 10.5$ and $A_k = -9.5$. The histograms contained 100,000 values of the output and input error are presented in Figs. 5.20a and 5.20b, respectively.

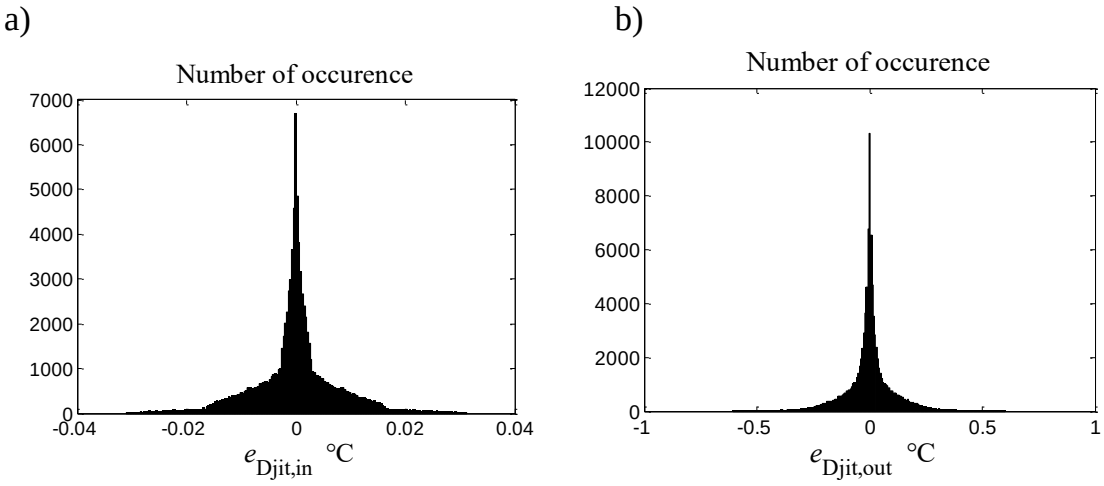

Fig. 5.20. Histograms of the jitter error: a) at the input of the exemplary dynamic algorithm of the 1-st order, $\sigma_{\mathrm{Djit,in}} = 7.6\cdot 10^{-3o}$C, b) at the algorithm output, $\sigma_{\mathrm{jit,out}} = 108\cdot 10^{-3o}$C

Experiment 5.9. Histograms of the noise error at the input and output of the dynamic algorithm, presented in Fig. 5.21, are determined in the same way as described in Experiment 5.8, but with this difference that only noise error is taken into account. According to Eq. (5.138), the noise input error is described as:

$$e_{\mathrm{Dnoi,in}}(t_k) = k_{\mathrm{S}} e_{\mathrm{noi,in}}(t_k) \tag{5.141}$$

where $e_{\mathrm{noi,in}}(t_k)$ is a realization of the normal error $N(0, 1)$, which burdens the number that is the result of the quantization of the sample at instant t_k. The realization of the noise output error is calculated by multiplying the dynamic algorithm coefficients by realizations of the input error as is performed for the jitter error.

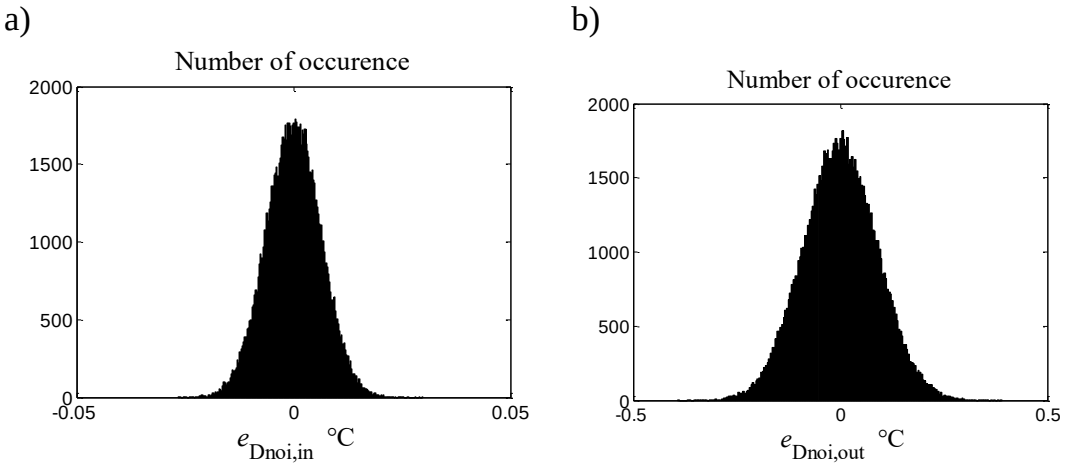

Fig. 5.21. Histograms of the noise error: a) at the input of the exemplary1-st order dynamic algorithm, $\sigma_{\mathrm{Dnoi,in}} = 6.3 \cdot 10^{-30}$C, b) at the algorithm output, $\sigma_{\mathrm{noi,out}} = 89.4 \cdot 10^{-30}$C

Experiment 5.10. This experiment aims to obtain histograms of the errors caused by the quantization for the sinusoidal signal in the same way as in Experiment 5.9. The quantization error in the input of the dynamic algorithm is described by the expression:

$$e_{\mathrm{Din,q}}(t_k) = k_{\mathrm{S}} \{409.176R(t_k) - \mathrm{ent}[409.176R(t_k) + 0.5]\} \tag{5.142}$$

obtained on the basis of Eq. (5.138). The error at the output of the exemplary dynamic algorithm is calculated in the same way as in previous experiments. The distributions of these errors in the form of histograms are shown in Fig. 5.22.

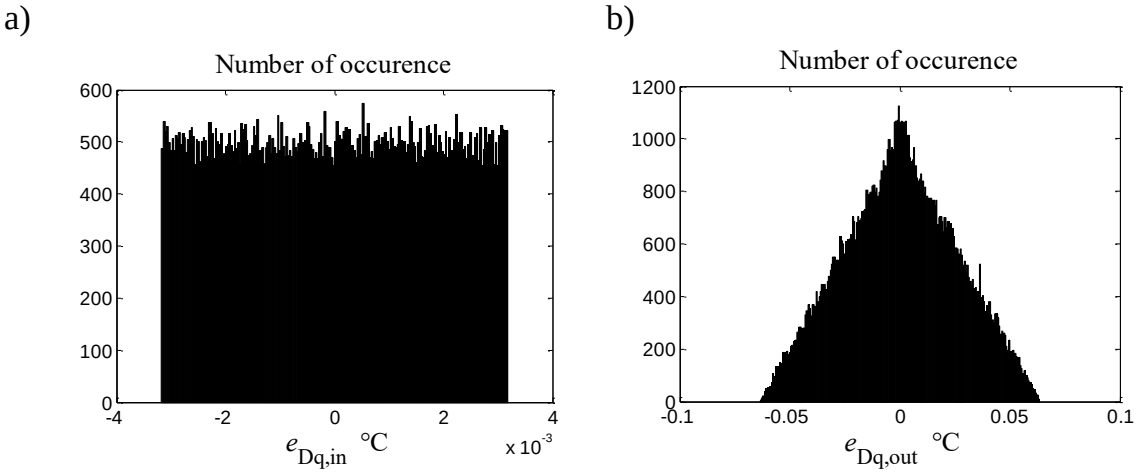

Fig. 5.22. Histograms of the quantization error for the sinusoidal input signal: a) at the input of the dynamic algorithm, $\sigma_{\mathrm{Dq,in}} = 1.8 \cdot 10^{-3}$°C, b) at the algorithm output, $\sigma_{\mathrm{Dq,out}} = 25.6 \cdot 10^{-3}$°C

Composition of standard deviation is possible if the partial errors are not correlated. The jitter error is not correlated with the other random errors because the phenomena responsible for their arising are quite different. However, it can be assumed that the noise error and the quantization error are correlated because the noise disturbs the quantized voltage. To check this, the correlation coefficient between them is calculated in the way presented in Experiment 5.6. To perform these calculations, it is necessary to determine the standard deviation of the total error using the following experiment.

Experiment 5.11. The total error that is composed of the noise error and the quantization error is described in the input of the dynamic algorithm by the expression:

$$e_{\mathrm{Dran,in}}(t_k) = k_{\mathrm{S}}\left\{409.176R(t_k) - \mathrm{ent}\left[409.176R(t_k) + e_{\mathrm{noi,in}}(t_k) + 0.5\right]\right\} \qquad (5.143)$$

obtained from Eq. (5.121). The histogram of this error determined as described in Experiment 5.8 is shown in Fig. 5.23.

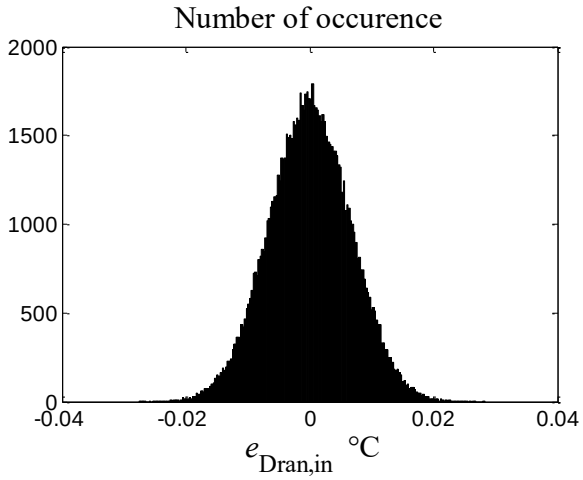

Fig. 5.23. Histogram of the error composed of noise and quantization errors at the input of the 1-st order dynamic algorithm, $\sigma_{\mathrm{Dran,in}} = 6.6 \cdot 10^{-3}$°C

The estimate of the standard deviation of the error from Fig. 5.23 is $\sigma_{\mathrm{Dran,in}} = 6.6 \cdot 10^{-3}$°C. The estimates of the standard deviations of the noise error from Fig. 5.21a is $\sigma_{\mathrm{Dnoi,in}} = 6.3 \cdot 10^{-3}$°C and of the quantization error from Fig. 5.22a is $\sigma_{\mathrm{Dq,in}} = 1.8 \cdot 10^{-3}$°C. The correlation coefficient calculated for these values is as follows:

$$c_{\mathrm{cor}} = \frac{\sigma^2_{\mathrm{Dran,in}} - \sigma^2_{\mathrm{Dnoi,in}} - \sigma^2_{\mathrm{Dq,in}}}{2\sigma_{\mathrm{Dnoi,in}}\sigma_{\mathrm{Dq,in}}} = \frac{\left(6.6^2 - 6.3^2 - 1.8^2\right)\cdot 10^{-6}}{2 \cdot 6.3 \cdot 0.1.8 \cdot 10^{-6}} = 0.028 \cong 0 \quad (5.144)$$

which means that the partial errors are not correlated.

The total random input error of the static algorithm is composed of three partial errors, realizations of which at instant t_k create the sum:

$$e_{\mathrm{ran,in}}(t_k) = e_{\mathrm{jit,in}}(t_k) + e_{\mathrm{noi,in}}(t_k) + e_{\mathrm{q,in}}(t_k) \quad (5.145)$$

where $e_{\mathrm{jit,in}}$ is the error caused by the jitter, $e_{\mathrm{noi,in}}$ – caused by the noise and $e_{\mathrm{q,in}}$ that is connected with the quantization. Based on the fact that partial random errors are not correlated, propagation of the standard deviation of the total random error by the chain of the reconstruction algorithm may by calculated using the scheme from Fig. 5.18.

According to Eq. (5.128), the standard deviation of the total random error at the input of the static algorithm can be calculated using the equation:

$$\sigma_{\mathrm{ran,in}} = \sqrt{\sigma^2_{\mathrm{jit,in}} + \sigma^2_{\mathrm{noi,in}} + \sigma^2_{\mathrm{q,in}}} \quad (5.146)$$

At the input of the dynamic algorithm, it is:

$$\sigma_{\mathrm{Dran,in}} = k_{\mathrm{S}}\sigma_{\mathrm{ran,in}} \quad (5.147)$$

where k_{S} is the propagation coefficient of the static algorithm the same for all kinds of errors. The standard deviation of the random error propagate by the dynamic algorithm with the coefficient k_{Dran}, so we have:

$$\sigma_{\mathrm{ran,out}} = k_{\mathrm{Dran}}\sigma_{\mathrm{Dran,in}} \quad (5.148)$$

Example 5.6. The standard deviation of the quantization error with the rectangular distribution in the range of -0.5 to 0.5 takes the value [J14, M2]:

$$\sigma_{\mathrm{q,in}} = \frac{0.5}{\sqrt{3}} = 0.289 \quad (5.149)$$

According to the value of the static coefficient k_S that is calculated in Example 5.1, propagation of this error by the static algorithm causes its standard deviation in the input of the dynamic algorithm input to be:

$$\sigma_{Dq,in} = k_S \sigma_{q,in} = 6.35 \cdot 10^{-3} \cdot 0.289 = 1.8 \cdot 10^{-3}\ ^{o}C \tag{5.150}$$

Comparing this calculated analytically value with the standard deviation value from Fig. 5.22a that is determined in the probabilistic experiment, one conclude that the quantization error does not depend on the input sinusoidal signal.

The standard deviation of the noise error is taken as $\sigma_{noi,in} = 1$, which means that at the input of the dynamic algorithm it takes the value:

$$\sigma_{Dnoi,in} = k_S \sigma_{noi,in} = 6.35 \cdot 10^{-3} \cdot 1 = 6.35 \cdot 10^{-3}\ ^{o}C \tag{5.151}$$

The jitter error in the input of the dynamic algorithm presented in Fig. 5.20a is of the standard deviation equal to $\sigma_{Djit,in} = 7.6 \cdot 10^{-3}$°C. Taking this value and the values calculated in Eqs.(5.150) and (5.151) into account, one obtains the standard deviation of the total random error in the input of the dynamic algorithm as:

$$\sigma_{Dran,in} = \sqrt{\sigma_{Djit,in}^2 + \sigma_{Dnoi,in}^2 + \sigma_{Dq,in}^2} = 10^{-3}\sqrt{7.6^2 + 6.35^2 + 1.8^2} = 10 \cdot 10^{-3}\ ^{o}C \tag{5.152}$$

The value of the propagation coefficient k_{Dran} of the exemplary 1-st order dynamic algorithm is calculated in Example 5.5. Multiplying this value by the standard deviation (5.152) at the input of the algorithm gives the standard deviation of total random error at the algorithm output:

$$\sigma_{ran,out} = k_{Dran} \sigma_{Dran,in} = 14.2 \cdot 10 \cdot 10^{-3} = 0.14 \cdot 10^{-3}\ ^{o}C \tag{5.153}$$

Complete knowledge of the distribution of the output random error may be obtained on the basis of the set of error values that is determined using the probabilistic experiment described in the following.

Experiment 5.12. Two random nominal instants and two instants burdened by jitter are determined according to the measurement conditions described in Experiment 5.8. For these instants, two realizations of the input error are determined on the basis of Eq. (5.121), and then, they are processed by the exemplary 1st order algorithm. The obtained values of the input and the output errors are located in the suitable sets of error values and after ending the experiment presented in Fig. 5.24.

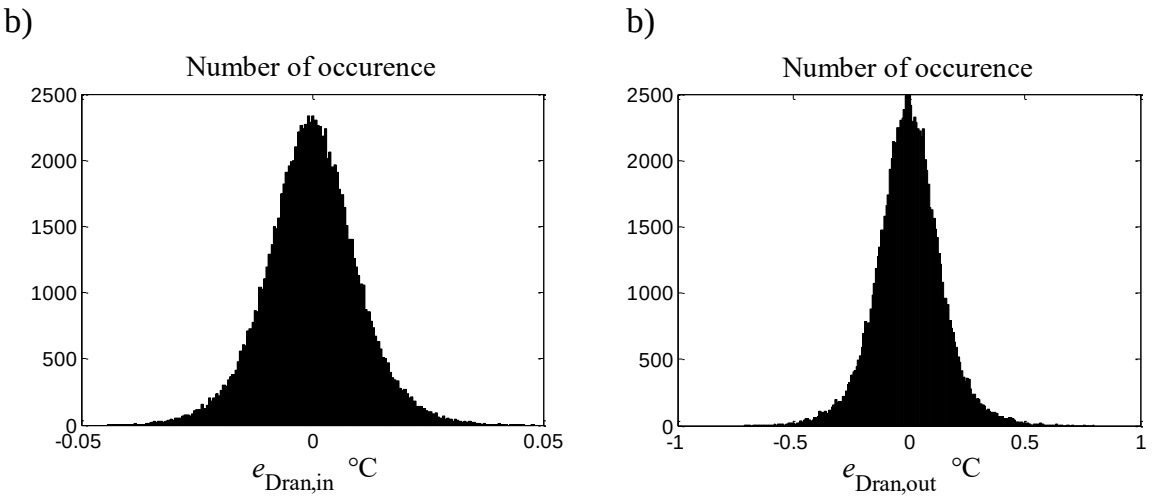

Fig. 5.24. Histograms of the total random error composed of the jitter error, noise error and quantization error, a) at the input of the exemplary 1-st order dynamic algorithm, $\sigma_{Dran,in} = 10.1 \cdot 10^{-3o}$C, b) at the algorithm output, $\sigma_{ran,out} = 142 \cdot 10^{-3o}$C

The dynamic reconstruction algorithm that is performed by the neural network has the same form of linear equations as the analytical algorithm. The only difference is related to obtaining values of the algorithm coefficients, which, for the neutral network, are obtained in the learning process, while, for the analytical form, they are determined using calculations. This means that all considerations presented in this chapter deals with both the analytical and the neural dynamic reconstruction.

5.5. Propagation model of standard deviations of sampling instrument

The considerations presented in Sections 5.2, 5.3 and 5.4 make it possible creation of the general propagation model of the standard deviations that describe the errors typical for the sampling instrument. This instrument measures, on the principle of the reconstruction, samples of the input signal that, for the purposes of the error analysis, is considered as sinusoidal. The model, presented in the graphical form in Fig. 5.25, is created for the exemplary instrument, but the structure of the model is of universal character for the analog converter described by the Wiener model. For stable measurement conditions, the parameters of the model are constant.

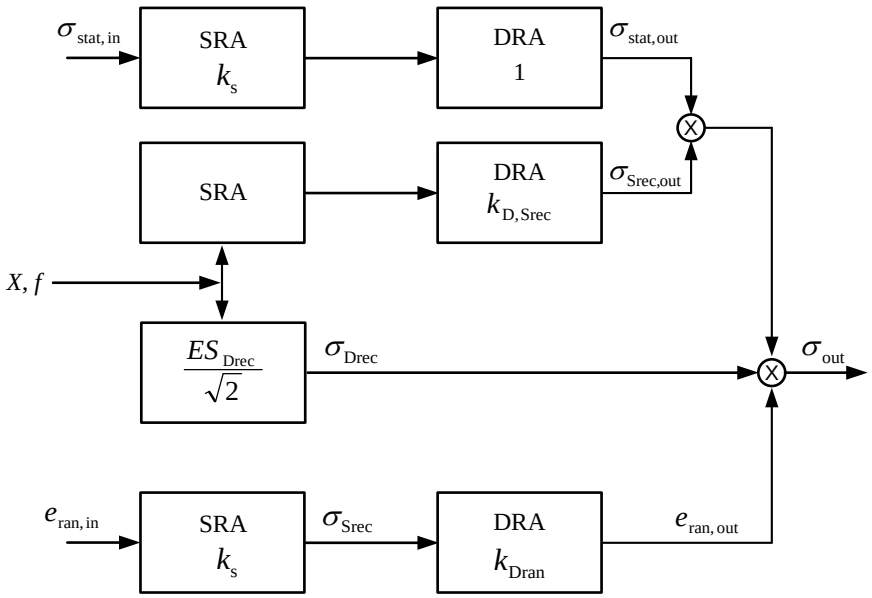

Fig. 5.25. The structure of general propagation model of standard deviations in the exemplary instrument for sinusoidal input signal, SRA – static reconstruction algorithm, DRA – dynamic reconstruction algorithm, X, f – the amplitude and frequency of the signal

The errors modelled in the input of the chain of the reconstruction algorithms arise during the analog and analog-to-digital conversions, and they are expressed as numbers burdening the number of quanta obtained in the output of the AD converter. The input errors are divided into two groups: the static errors and the random errors because of their specificity of the propagation. The third group of errors depend on the amplitude X and the frequency f of the input signal. This group includes the dynamic reconstruction error and the static reconstruction error processed by the dynamic algorithm. All these errors are represented in Fig. 5.25 by their standard deviations. The standard deviation of the total output error is calculated as the geometrical sum of standard deviations of the suitable partial errors, i.e., as the square root of the sum of squares. The considered partial errors are not correlated as is proved in Sections 5.2, 5.3 and 5.4, in which detailed analysis of the propagation of these errors is carried out.

The basic application of the model from Fig. 5.25 is used in the analysis of participations of the errors in the total output error. Knowledge about these participations enables selection of dominating errors and takes measures to reduce their values, which leads to increased accuracy of the output results. This kind the model is illustrated by the following examples. The table containing the standard deviations of the partial output errors is called the error budget. The complete description of every error should include, except for the standard deviation, its type of distribution, although in the case of the exemplary instrument it may be impossible

because many of the partial errors are characterized by non-standard distributions. If the knowledge about the concrete error distribution is needed, one can find this information in the chapter, in which this error is considered.

Example 5.7. Let us take that the amplitude of the input signal of the exemplary instrument is $X = 50^{o}$C and its frequency $f = 0.01$ Hz. The time constant of the sensor is $\tau = 2$ s and the sampling period is equal to $T_s = 0.2$ s. The standard deviations of the output errors presented in the Tab. 5.4 are taken for the analytical reconstruction from Figs. 5.6a, 5.6b, 5.12a, 5.18b, 5.20b, 5.21b and 5.22b. The table 5.3 contains the appropriate standard deviations determined for the neural reconstruction, which differ from the values contained in Tab. 5.4 in one position, i.e.in the value from Fig. 12b, that describes the static reconstruction error after its propagation by the dynamic algorithm.

Table 5.3

Budget of errors, represented by their standard deviations, of the exemplary instrument with analytical reconstruction for sinusoidal input signal changing in the range from 0 to 100^{o}C with the frequency $f = 0.01$ Hz and the amplitude $X = 50^{o}$C

Standard deviation	$\sigma_{sh,out}$	$\sigma_{inc,out}$	$\sigma_{Srec,out}$	σ_{Drec}	$\sigma_{jit,out}$	$\sigma_{q,out}$	$\sigma_{noi,,out}$
Value·10^{-3o}C	7.3	9	30.7	226	108	25.6	89.4

Table 5.4

Budget of errors, represented by their standard deviations, of the exemplary instrument with neural reconstruction for sinusoidal input signal changing in the range from 0 to 100^{o}C with the frequency $f = 0.01$ Hz and the amplitude $X = 50^{o}$C

Standard deviation	$\sigma_{sh,out}$	$\sigma_{inc,out}$	$\sigma_{Srec,out}$	σ_{Drec}	$\sigma_{jit,out}$	$\sigma_{q,out}$	$\sigma_{noi,,out}$
Value·10^{-3o}C	7.3	9	3.84	226	108	25,6	89.4

The standard deviation of the total error in the output of the exemplary instruments for the considered partial errors is calculated using the expression:

$$\sigma_{out} = \sqrt{\sigma_{sh,out}^2 + \sigma_{inc,out}^2 + \sigma_{Srec,out}^2 + \sigma_{dyn,rec}^2 + \sigma_{jit,out}^2 + \sigma_{noi,out}^2 + \sigma_{q,out}^2} \qquad (5.154)$$

Introducing the values from Tab. 5.3 into Eq. (5.154) gives:

$$\sigma_{out} = 10^{-3}\sqrt{7.3^2 + 9^2 + 30.7^2 + 226^2 + 108^2 + 25.6^2 + 89.4^2} = 0.269\ ^{o}\text{C} \qquad (5.155)$$

while, for the values from Tab. 5.4, we have:

$$\sigma_{out} = 10^{-3}\sqrt{7.3^2 + 9^2 + 3.84^2 + 226^2 + 108^2 + 25.6^2 + 89.4^2} = 0.267\ ^{o}\text{C} \qquad (5.156)$$

Comparison of the values (5.155) and (5.156) comes to the conclusion that different kinds of the static reconstruction have the minor meaning in the budget of the output errors in the considered measurement conditions. Analysis of the values presented in Tabs. 5.3 and 5.4 shows that there is no single dominant error, which means that reducing the value of any error does not significantly reduce the total error. The opposite kind of situation is considered in the next example.

Example 5.8. Let us take that the input signal frequency is $f = 0.05$ Hz, while the others parameters of the signal reconstruction are the same as described in Example 5.7. The standard deviations of the partial error in the output of the exemplary instrument working under these conditions are presented in Tab. 5.5. In this table, two standard deviations differ from these in Tab. 5.3 because the suitable errors depend on the signal frequency that is 5 times greater than in Example 5.7. The dependencies of the standard deviations $\sigma_{\text{Srec,out}}$ and σ_{Drec} of these errors on the signal frequency are described in Sections 5.2.3 and 5.3, respectively.

Table 5.5

Error budget of the exemplary instrument for the frequency $f = 0.05$ of the sinusoidal input signal with amplitude $X = 50^{o}$C

Standard deviation	$\sigma_{\text{sh,out}}$	$\sigma_{\text{inc,out}}$	$\sigma_{\text{Srec,out}}$	σ_{Drec}	$\sigma_{\text{jit,out}}$	$\sigma_{\text{q,out}}$	$\sigma_{\text{noi, ,out}}$
Value·10^{-3}°C	7.3	9	71.9	1129	108	25,6	89.4

In this case, the dynamic reconstruction error e_{Drec} dominates. The analysis of the impact of this error on inaccuracy of the instrument may be performed analytically by comparison of standard deviations of the total error under different measurement conditions. Introducing the values from Tab. 5.5 in Eq. (5.154), we have:

$$\sigma_{\text{out}} = 10^{-3}\sqrt{7.3^2 + 9^2 + 71.9^2 + 1129^2 + 108^2 + 25.6^2 + 89.4^2} = 1140 \cdot 10^{-3}\ ^{o}\text{C} = 1.14\ ^{o}\text{C} \tag{5.157}$$

The standard deviation determined by Eq. (5.157) is substantially greater than calculated in Eq. (5.155), which is caused by the dominance of the dynamic reconstruction error. Such a situation inspires seeking some means to decrease this error if the values of the total error is greater than the allowable one.

5.6. Reduction of total error

The total error is a composition of several partial errors. As in the results from Fig. 5.25, some of the errors do not depend on the reconstructed signal, but the others

are dependent on the signal parameters that influence properties of the dynamic algorithm. This causes the problem of reduction of the total error by the actions that lead to decreasing values of the partial errors to be complex.

As a rule, the error, the values of which are the most significant in the error budget, are connected with the frequency of the reconstructed signal. In this chapter, two ways to decrease such a kind of errors are considered.

In the case if the error caused by the dynamic reconstruction dominates, one can reduce it by decreasing the sampling period (see Section 5.3). However, this way is connected with increasing the output random error, because the dynamic coefficient k_{Dran} increases with grow of the sampling period. Dependencies of these errors from the sampling period for the exemplary instrument working with the signal frequency f = 0.05 Hz are presented in Fig. 5.26.

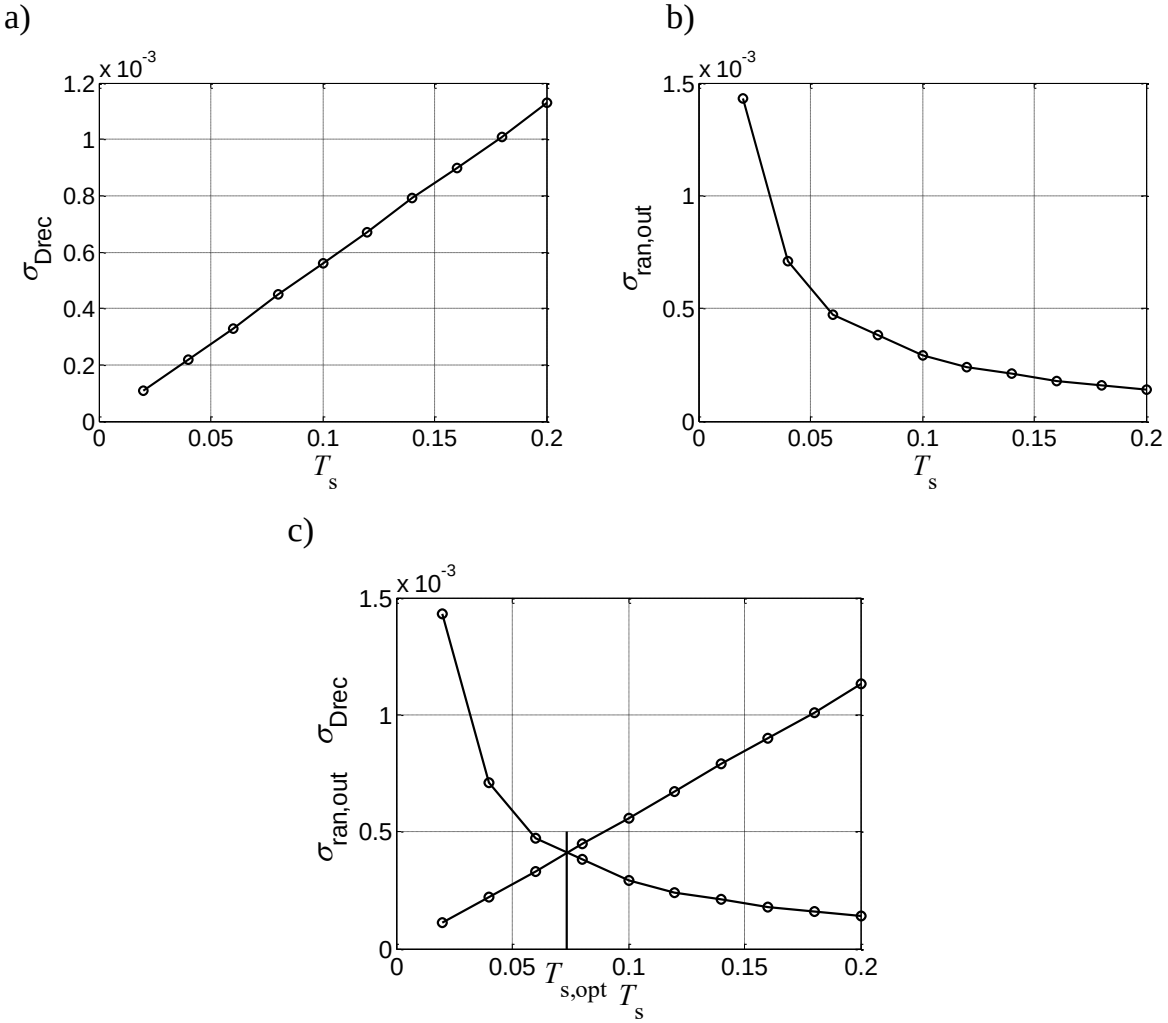

Fig. 5.26. Dependencies of standard deviations of the selected errors on the sampling period in the output of the exemplary instrument with the 1-st order dynamic reconstruction for the input signal frequency f = 0.05 Hz: a) the dynamic reconstruction error, b) the random error, c) the error composed of these errors

As in Fig. 5.26, the standard deviation of the error composed of the discussed two partial errors reaches a minimum if the partial standard deviations have the same values. This minimum is obtained for the optimal sampling period $T_{s,opt}$ that is about 0.07 s. The values of the standard deviations read from this figure is about 0.4°C, but they also can be determined analytically in the way presented below.

For the optimal sampling period $T_{s,opt} = 0.07$ s, the parameter φ of the discrete dynamic model takes the value:

$$\varphi = e^{-\frac{T_{s,opt}}{\tau}} = e^{-\frac{0.07}{2}} = 0.9656 \tag{5.158}$$

for which the coefficients of the dynamic reconstruction algorithm are:

$$A_{k+1} = \frac{1}{1-\varphi} = \frac{1}{1-0.9656} = 29,\ A_k = -\frac{\varphi}{1-\varphi} = -\frac{0.9656}{1-0.9656} = -28 \tag{5.159}$$

On the basis of these values, one obtains that the dynamic coefficient describing amplification of random error by the 1-st order dynamic algorithm is:

$$k_{Dran} = \sqrt{A_{k+1}^2 + A_k^2} = \sqrt{29^2 + (-28)^2} = 40.4 \tag{5.160}$$

The standard deviation of the total input random errors is calculated in Eq. (5.152) as $\sigma_{ran,in} = 10 \cdot 10^{-3}$°C. Taking into account this value and the result of Eq. (5.160), we obtain the standard deviation of the output error that is determined according to Eq. (5.48) as:

$$\sigma_{ran,out} = k_{Dran}\sigma_{ran,in} = 40.3 \cdot 10 \cdot 10^{-3} = 404 \cdot 10^{-3}\ ^\circ\text{C} \cong 0.4\ ^\circ\text{C} \tag{5.161}$$

From Fig. 5.26c, it results the standard deviation of the dynamic reconstruction error to be of the same value as the value of the standard deviation calculated above; thus, it is:

$$\sigma_{Drec} = \sigma_{ran,out} \cong 0.4\ ^\circ\text{C} \tag{5.162}$$

The values of standard deviations of the partial errors at the output of the exemplary instrument working with the optimum sampling period are presented in Tab. 5.6. One should notice that the value of the standard deviation of the static reconstruction error differs of the value from Tab. 5.5. These differences are connected with changes of coefficients of the dynamic algorithm, which depend on the sampling period, and this in turn causes that the dynamic algorithm processed the error of the static reconstruction differently.

Table 5.6

Error budget of the exemplary instrument for sinusoidal input signal with the frequency f = 0.05 Hz and the amplitude X = 50°C determined for the optimal sampling period $T_{s,opt}$ = 0.07 s

Standard deviation	$\sigma_{sh,out}$	$\sigma_{inc,out}$	$\sigma_{Srec,out}$	σ_{Drec}	$\sigma_{ran,out}$
Value·10^{-3}°C	7.3	9	109	400	400

For the values from Tab. 5.6, the standard deviation of the total output error takes the value:

$$\sigma_{out} = 10^{-3}\sqrt{7.3^2 + 9^2 + 109^2 + 400^2 + 400^2} = 0.576\ ^{\circ}\mathrm{C} \tag{5.163}$$

This value is significantly less than the value calculated in Eq. (5.157), but, in some applications of the sampling instrument, it may be too big. In such cases, the other method of reducing the dynamic reconstruction error, even more effective than the described above, may be used. This method consists in changing the point in the measurement window to which the output result is assigned.

Suppose that the output result is not assigned to the first sampling point in the window but to the point shifted by half the sampling period $h = T_s/2$. This causes that all terms of the transmittance (4.75) of the dynamic algorithm are multiplied by $-\mathrm{j}\omega h$ [L1], so we have:

$$A_{sh}(\mathrm{j}\omega) = A(\mathrm{j}\omega)e^{-\mathrm{j}\omega\frac{T_s}{2}} = A_{k+1}e^{0.5\mathrm{j}\omega T_s} + A_k e^{-0.5\,\mathrm{j}\omega T_s} + A_{k-1}e^{-1.5\mathrm{j}\omega T_s} + \ldots + A_{k-m}e^{-(m-0.5)\mathrm{j}\omega T_s} + \ldots \tag{5.164}$$

For the 1-st order algorithm, this expression takes the form:

$$A_{sh}(\mathrm{j}\omega) = A_{k+1}e^{0.5\mathrm{j}\omega T_s} + A_k e^{-0.5\,\mathrm{j}\omega T_s} \tag{5.165}$$

The transmittance of the 1-st order dynamic converter is described by Eq. (4.3). Based on these equations, the transmittance (5.109) of the reconstruction error source for the algorithm transmittance (5.148) is expressed as:

$$ES_{Drec,sh}(\mathrm{j}\omega) = 1 - A_{sh}(\mathrm{j}\omega)S_1(\mathrm{j}\omega) = 1 - \frac{A_{k+1}e^{0.5\mathrm{j}\omega T_s} + A_k e^{-0.5\mathrm{j}\omega T_s}}{1 + \mathrm{j}\omega\tau} \tag{5.166}$$

After transformation of this equation, we obtain the following expression:

$$ES_{Drec,sh}(\mathrm{j}\omega) = \frac{1 + (\omega\tau)^2 - A_{k+1}e^{0.5\mathrm{j}\omega T_s} - A_k e^{-0.5\mathrm{j}\omega T_s} + \left(A_{k+1}e^{0.5\mathrm{j}\omega T_s} + A_k e^{-0.5\mathrm{j}\omega T_s}\right)\mathrm{j}\omega\tau}{1 + (\omega\tau)^2} \tag{5.167}$$

The real part of the transmittance (5.167) is:

$$\mathrm{Re}\{ES_{Drec,sh}\} = \frac{1 + (\omega\tau)^2 + \omega\tau\left[(A_k - A_{k+1})\sin 0.5\omega T_s\right] - (A_k + A_{k+1})\cos 0.5\omega T_s}{1 + (\omega\tau)^2} \tag{5.168}$$

and the imaginary part:

$$\mathrm{Im}\left\{ES_{\mathrm{Drec,sh}}\right\}=\frac{\omega\tau\left(A_k+A_{k+1}\right)\cos 0.5\omega T_{\mathrm{s}}+\left(A_k-A_{k+1}\right)\sin 0.5\omega T_{\mathrm{s}}}{1+\left(\omega\tau\right)^2} \tag{5.169}$$

Example 5.9. The measurement conditions are the same as in Example 5.7 with this difference that the input signal frequency is f = 0.05 Hz. According to Eqs. (5.168) and (5.169), the real part of the transmittance of the dynamic error source has the value:

$$\mathrm{Re}\left\{ES_{\mathrm{Drec,sh}}\right\}=1.64\cdot 10^{-4} \tag{5.170}$$

and the imaginary part is:

$$\mathrm{Im}\left\{ES_{\mathrm{Drec,sh}}\right\}=-5.23\cdot 10^{-4} \tag{5.171}$$

Based on these values, we obtain the module of the error source transmittance as:

$$\left|ES_{\mathrm{Drec,sh}}(\mathrm{j}\omega)\right|=\sqrt{\mathrm{Re}^2\left\{ES_{\mathrm{Drec,sh}}\right\}+\mathrm{Im}^2\left\{ES_{\mathrm{Drec,sh}}\right\}}=10^{-4}\sqrt{1.64^2+\left(-5.23\right)^2}=5.49\cdot 10^{-4} \tag{5.172}$$

Having given this transmittance, one can calculate the amplitude of the output dynamic error accordingly with Eq. (5.105). For the amplitude X of the input signal equal to 50°C, the standard deviation of the error takes the value:

$$\sigma_{\mathrm{Drec,sh}}=\left|ES_{\mathrm{Drec,sh}}(\mathrm{j}\omega)\right|\frac{X}{\sqrt{2}}=\frac{5.49\cdot 10^{-4}\cdot 50}{\sqrt{2}}=19.4\cdot 10^{-3}\ ^{\mathrm{o}}\mathrm{C} \tag{5.173}$$

The error budget for the shifted reconstruction instant is presented in Tab. 5.7.

Table 5.7

Error budget of the exemplary instrument for sinusoidal input signal with f = 0.05 Hz and amplitude X = 50°C if the reconstruction instant is shifted by $T_{\mathrm{s}}/2$, T_{s} is the sampling period

Standard deviation	$\sigma_{\mathrm{sh,out}}$	$\sigma_{\mathrm{inc,out}}$	$\sigma_{\mathrm{Srec,out}}$	$\sigma_{\mathrm{Drec,sh}}$	$\sigma_{\mathrm{jit,out}}$	$\sigma_{\mathrm{q,out}}$	$\sigma_{\mathrm{noi,out}}$
Value·10^{-3}°C	7.3	9	73.6	19.4	105	25	87.6

Introducing values from Tab. 5.7 into expression (5.154), one obtains the following standard deviation:

$$\sigma_{\mathrm{tot,out}}=10^{-3}\sqrt{\left(7.3^2+9^2+73.6^2+27^2+105^2+25^2+87.6^2\right)}=160\cdot 10^{-3}\ ^{\mathrm{o}}\mathrm{C}=0.16\ ^{\mathrm{o}}\mathrm{C} \tag{5.174}$$

that is substantially less than the standard deviations of the other discussed total errors. This means that this method is effective in decreasing the total reconstruction error.

5.7. Uncertainty evaluation of reconstruction results

As discussed in Chapter 1, the inaccuracy of every measurement instrument must be described quantitatively, which enables comparison of basic metrological properties of the same kind of instruments. The most commonly used measure of the inaccuracy is the uncertainty [B1, B2, G1, J1, J2, K3, M6, S2] treated in this book as the parameter of the uncertainty interval that is calculated on the basis of distribution of total error burdening the estimate of reconstructed sample. If the measurement conditions, in which the instrument works, are stable, the uncertainty is the same for all estimates, which means that the inaccuracy of instrument may be described by one number. In this case, every reconstructed sample can be written in the interval form (1.45):

$$\vec{x}(k) = \left[\hat{x}(k) - u_{\text{out}},\ \hat{x}(k) + u_{\text{out}}\right] = \hat{x}(k) \pm u_{\text{out}} \tag{5.175}$$

where $\hat{x}(k)$ is the estimate of the input sample $x(k)$, k is the instant, for which the estimate is determined, u_{out} is the uncertainty, the value of which is the same for every sample.

If the measurement conditions change, uncertainties of individual samples depends on time variations of the parameters that describes these conditions. This means that every change of the measurement conditions should result in determination of the suitable value of the uncertainty. In this case, the reconstructed sample is described as:

$$\vec{x}(k) = \left[\hat{x}(k) - u_{\text{out}}(k),\ \hat{x}(k) + u_{\text{out}}(k)\right] = \hat{x}(k) \pm u_{\text{out}}(k) \tag{5.176}$$

Determination of the current uncertainty $u_{\text{out}}(k)$, requires keeping track of changes of the measurement conditions and the knowledge about relations between quantities that describe these conditions is necessary.

Calculation of the uncertainty is the simplest if partial output errors take comparable values. In this case, the Central Limit Theorem may be used [P1,Y1], accordingly with which the distribution of the sum of random uncorrelated errors tends to the normal distribution if no one error dominates. Having given standard deviations of the partial errors, one can calculate in this case the standard deviation σ_{out} of the total output error accordingly with Eq. (1.52). Denoting the expanded uncertainty for the confidence level $p = 0.95$ as U, we have [K3, Y1]:

$$U = 2\sigma_{\text{out}} \tag{5.177}$$

One should notice that qualification of the total error distribution as normal do not have to be carried out statistically strictly because the inaccuracy of uncertainty itself

equal to about 10% can be treated as good enough for industrial conditions. If there is any doubt about normality of the error distribution, one may carry out the simulative probabilistic experiment [M6] assuming the suitable measurement conditions in the way described below.

The reconstruction chain in the exemplary sampling instrument consists of the static and the dynamic algorithms. The coefficients of static algorithm in the analytical form are presented in Tab. 3.9, while of the neural form in Fig. 3.29. These coefficients are calculated as the effect of the identification, which means that the algorithms introduce both the approximation and the identification errors. The exemplary dynamic algorithm is of 1-st order; thus, it is composed of two terms the values of which are determined with assumption that the time constant τ of the sensor is known, and $\tau = 2$ s. In this case, the measurement window contains two quantization results, which are described as:

$$\tilde{n}_q(t_k) = \mathrm{ent}\left[409.176R(\tilde{t}_k) + e_{\mathrm{sh}}(t_k) + e_{\mathrm{inc}}(t_k) + e_{\mathrm{noi.in}}(t_k) + 0.5\right] \qquad (5.178)$$

and

$$\tilde{n}_q(t_{k+1}) = \mathrm{ent}\left[409.176R(\tilde{t}_{k+1}) + e_{\mathrm{sh}}(t_k) + e_{\mathrm{inc}}(t_k) + e_{\mathrm{noi.in}}(t_{k+1}) + 0.5\right] \qquad (5.179)$$

where t_k and t_{k+1} are the nominal sampling instants distant in time by the sampling period T_s.

The quantization results are burdened by the errors connected with: jitter, drift of the shift and of inclination of the static characteristic, noise, and caused by the quantization. The standard deviations of these errors are contained by the error budget presented in Tabs. 5.4 and 5.5. One should notice that the shift error e_{sh} and the inclination error e_{inc} are static in the window, which means that they have the same values in these two sampling instants. It is assumed that the value of the drift error is taken, for every window, from the population described as random in the range from -2 to 2 with the rectangular distribution. The inclination error is expressed as: $e_{\mathrm{inc}} = n_q \cdot \varepsilon_{\mathrm{inc}}$, wherein n_q is the quantization result, and the inclination coefficient $\varepsilon_{\mathrm{inc}}$ changes accordingly with the rectangular distribution in the range from $-5 \cdot 10^{-5}$ to $5 \cdot 10^{-5}$.

The sampling instant is burdened by the jitter, which means that they are determined as:

$$\tilde{t}_k = t_k + \Delta_{\mathrm{jit}}(t_k) \quad \text{and} \quad \tilde{t}_{k+1} = t_{k+1} + \Delta_{\mathrm{jit}}(t_{k+1}) \qquad (5.180)$$

where the jitter takes values $\Delta_{\mathrm{jit}}(t_k)$ and $\Delta_{\mathrm{jit}}(t_{k+1})$ accordingly with the rectangular distribution in the range from Δ_{jmin} to Δ_{jmax} and $|\Delta_{\mathrm{jmin}}| = |\Delta_{\mathrm{jmax}}| = 1 \cdot 10^{-6}$ s. Except of the jitter error, the quantization result is burdened by the normal noise error $N(0, 1)$ and by the quantization error that is presented in Fig. 5.22a.

The experiments described below are performed for the temperature sinusoidal signal $\vartheta(t) = 50\sin\omega t$°C, wherein $\omega = 2\pi f$, f is the frequency. For every measurement window, the input signal is sampled two times in the signal period $T = 1/f$: first, at the instant t_k that is determined randomly accordingly with the rectangular distribution, next, at the instant $t_{k+1} = t_k + T_s$, T_s is the sampling period. The number of measurement windows used in the experiment presented below is $K = 100{,}000$.

Experiment 5.13. This experiment is aimed at obtaining two histograms of the total error in the output of the exemplary sampling instrument for the signal frequency $f = 0.01$ Hz, which is sampled with the period $T_s = 0.2$ s. The first histogram is determined for the analytical static reconstruction, and presented in Fig. 5.27a. The second, shown in Fig. 5.27b, is obtained with assumption that the neural static reconstruction is performed.

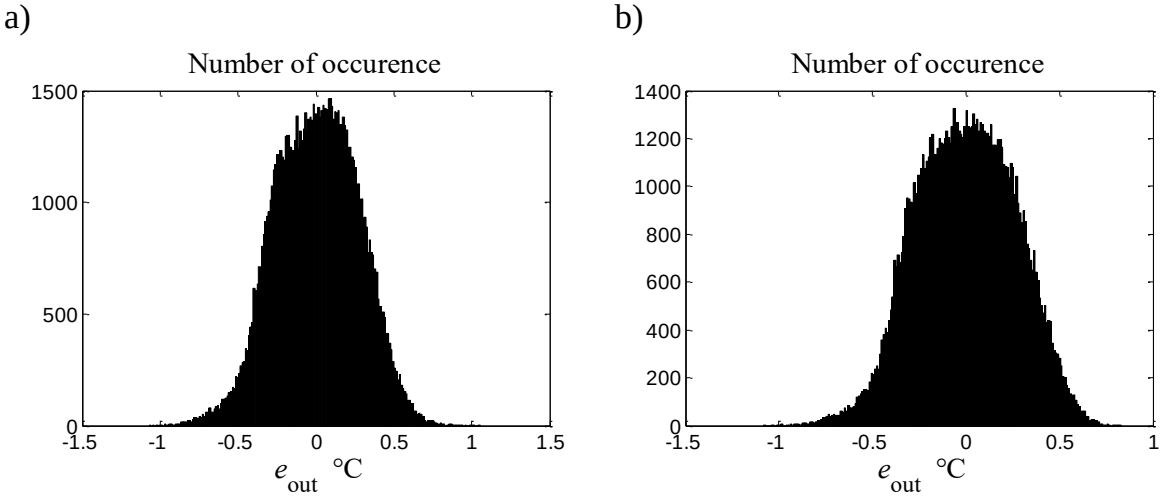

Fig. 5.27. Histograms of the total error of the samples reconstructed using the exemplary instrument for the input signal frequency $f = 0.01$ Hz: a) if the analytical static reconstruction is performed, $\sigma_{out} = 0.268$°C, the uncertainty obtained from definition (1.49) is $U = 0.56$°C, b) for the neural static reconstruction, $\sigma_{out} = 0.266$°C, $U = 0.55$°C

Based on the standard deviation from Fig. 5.27a, the expanded uncertaintythat is calculated using Eq. (5.177) with assumption that the error distribution is normal has the value:

$$U = 2\sigma_{out} = 2 \cdot 0.268 = 0.54\ ^{o}\text{C} \tag{5.181}$$

If we calculate the uncertainty on the basis of the set of error values presented as the histogram in Fig. 5.27a, the obtained value is $U = 0.56$°C. Both values differ insignificantly from accuracy requirement point of view, which means that the distribution of the total error presented in Fig. 5.27a may be treated as close enough to the normal in the considered measurement conditions.

Experiment 5.14. This experiment is aimed at obtaining two histograms of the total error at the output of the exemplary sampling instrument for the signal frequency $f_1 = 0.05$ Hz, which is sampled with the period $T_s = 0.2$ s. The first histogram is determined for the analytical static reconstruction, and presented in Fig. 5.28a. The second, shown in Fig. 5.28b, is obtained if the neural static reconstruction is performed by the sampling instrument.

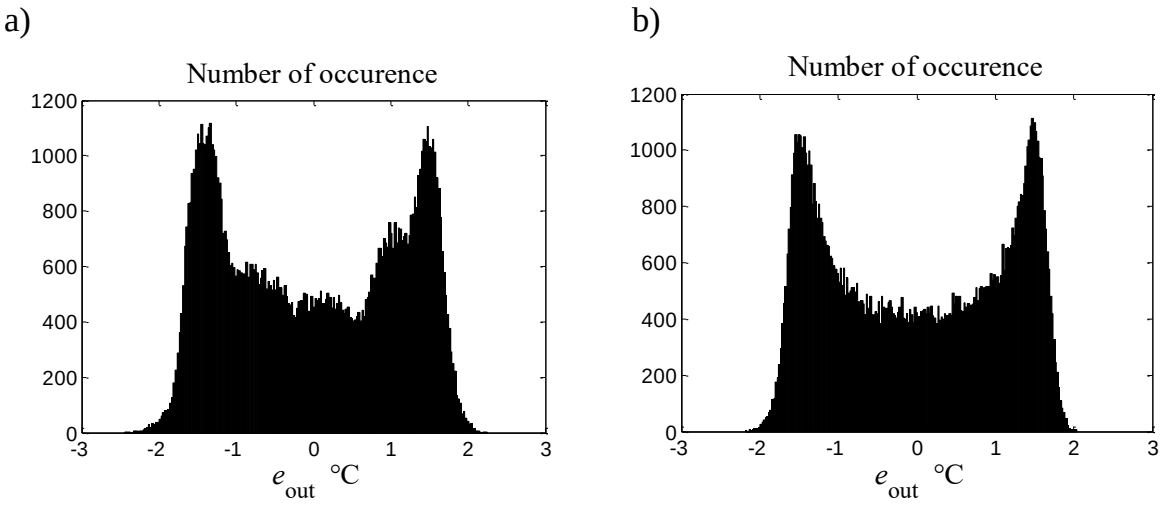

Fig. 5.28. Histograms of the total error of the samples reconstructed using the exemplary instrument for the input signal frequency $f = 0.05$ Hz: a) the analytical static reconstruction is performed, $\sigma_{out} = 1.12^{o}$C, b) the neural static reconstruction is performed, $\sigma_{out} = 1.14^{o}$C

The distributions of the errors shown in Fig. 5.28 are significantly different from the normal distribution, which means that the uncertainties of these errors must be calculated from the definition on the basis of the histograms. Accordingly with Eqs. (1.30) and (1.31), we may determine the lower bound of the uncertainty interval as:

$$\int_{-\infty}^{\underline{u}} \hat{g}(e_{out})\mathrm{d}e_{out} = \frac{1-p}{2} \tag{5.182}$$

and the upper bound as:

$$\int_{\bar{u}}^{\infty} \hat{g}(e_{out})\mathrm{d}e_{out} = \frac{1-p}{2} \tag{5.183}$$

where the confidence level $p = 0.95$ and $\hat{g}(e_{out})$ is the probability density function of the error e_{out}, which is obtained by the normalization of its histogram in this way that every value of the histogram bar is divided by the number of occurrence equal to 10^5. For the histogram from Fig. 5.28a, we obtain that:

$$\underline{u} = -1.7\ ^{o}\mathrm{C} \qquad \text{and} \qquad \bar{u} = 1.7\ ^{o}\mathrm{C} \tag{5.184}$$

which means that, according to Eq. (1.50), the uncertainty takes the value:

$$U = \frac{\overline{u} - \underline{u}}{2} = \frac{1.7 - (-1.7)}{2} = 1.7\ ^{\circ}\mathrm{C} \tag{5.185}$$

Based on this uncertainty, one can describe the value of every reconstructed sample in the interval form (1.34) as:

$$\vec{\vartheta}(k) = \left[\hat{\vartheta}(k) - 1.7,\ \ \hat{\vartheta}(k) + 1.7\right]\ ^{\circ}\mathrm{C} = \hat{\vartheta}(k) \pm 1.7\ ^{\circ}\mathrm{C} \tag{5.186}$$

The same values as (5.184) can be obtained on the basis of the histogram from Fig. 5.28b. It means that the output values of the sampling instrument using the exemplary neural static reconstruction are described by the same interval (5.186) as determined for the exemplary analytical algorithm.

One can point one more analytical method of calculation of the uncertainty. It consists in application of the reductive interval arithmetic [J13, J15] to determinate the uncertainty of the total error on the basis of uncertainties of the partial errors. However, this method, as well as the other methods considered here, are numerically sophisticated and they can be used only for stable measurement conditions, in which all partial errors does not change their parameters. In such conditions, the uncertainty can be calculated one times before the sampling instrument is used and next every sample is characterized by the same uncertainty. In this the case, the time necessary to calculate the uncertainty is not important. But the calculation time is critical for the sampling instrument working in real-time if the parameters of the input signals, i.e., its amplitude and frequency, change significantly in time. In this situation, the uncertainty may have different values for successive samples, which causes that all calculations connected with the uncertainty determination must be performed between the sampling instants. In practice, the only way possible to obtain the current uncertainty consists in using a look-up table to store selected values of the uncertainty as a function of the measurement conditions. Calculation of the intermediate values is performed using the linear approximation as it is illustrated by the next example.

Example 5.10. Let us take that the frequency of the input signal of the exemplary sampling instrument varies from $f_{\min} = 10^{-3}$ Hz to $f_{\max} = 0.1$ Hz, which means that the signal period T changes from 10 s to 1000 s. The others quantities, which influence the measurement conditions, are stable. In Tab. 5.8, there are presented values of the uncertainty determined in the way described above for the selected values of the signal period.

Table 5.8

Uncertainties of the reconstructed samples in relation to the signal period T calculated for the exemplary sampling instrument

T s	10	20	50	100	500	1000
Uncertainty ^{o}C	3.3	1.7	0.81	0.54	0.43	0.39

Let us take that the measured value of the period is $T = 72$ s. Using the linear approximation of values lying between these contained in Tab. 5.8, we obtain the uncertainty value as:

$$\hat{U}(72) = U(50) + \frac{U(100) - U(50)}{100 - 50}(72 - 50) = 0.81 + \frac{0.54 - 0.81}{50}22 = 0.69\ ^{\circ}\mathrm{C} \qquad (5.187)$$

The value of the uncertainty determined for this period in the same way as described in Experiment 5.13 is $U = 0.67^{o}$C, which means that estimated value (5.187) is close enough to this one obtained experimentally. The time necessary to calculate the uncertainty accordingly with Eq. (5.187) is the same as for performing the static reconstruction using the linear approximation.

5.8. Final remarks

As it results from Example 5.10, the method of the uncertainty determination based on the look-up table needs only few arithmetical operations and may be performed in real-time by a microcontroller. One should notice that these operations may be reduced to seeking the suitable value of the uncertainty in the memory if the data stored in the look-up table are so close that this value is read as the closest to this one that corresponds to the measured value of signal period. In this case, other calculation are not needed. Capacities of EEPROM memories in modern microcontrollers are so big that there is no problem with storing many values of uncertainties in them [Y6].

If the total uncertainty is dependent both on the period of signal and its amplitude, one may use the two-dimensional linearization method described in Chapter 3. Much more complicated problem occurs if the signal is poliharmonic because, in this case, the total uncertainty depends both on the amplitudes of harmonics and their beginning phases; and, what is more, these dependencies are non-linear. This problem of evaluation of the uncertainty can be solved by using the reductive interval arithmetic [J15], although the calculations are numerically complex, which means that this

method can’t be used in the real-time. However, one may use in this case the same means as described above to make the calculations quickly enough.

The decomposed general model of error propagation presented in Fig. 5.4 can be extended to include other errors than those described in this chapter. For example, when a sampling instrument is used in a measurement system, additional errors may occur due to delays in data transmission [J11]. The probabilistic description of these errors allows them to be included in the output of the model in Fig. 5.4 and included in the error budget of the sampling device.

6. REAL-TIME EXECUTION OF RECONSTRUCTION BY MICROCONTROLLERS

The presented analytical forms of the reconstruction algorithms characterize very small number of arithmetical operations, which means that they may be performed efficiently by microcontrollers. This property also applies to neural reconstruction if one takes into account that the transfer functions of the neurons may be approximated by linear segments, which enables rapid realization of these functions with the acceptable inaccuracy. Short execution times of the presented algorithms cause that they may be performed in the real-time mode, that is, all arithmetic operations connected with the signal reconstruction are executed between the succeeding sampling instants. The basic question is how often the input signal may be sampled if microcontrollers are applied to the signal reconstruction in this mode.

To evaluate the reconstruction execution time, it is useful to define a unit arithmetic operation as the number of instructions necessary to perform one operation by a microprocessor. This definition requires some assumptions. At first, it is assumed that 16-bit microcontrollers are used and all operations are performed using the fixed--point arithmetic. This kind of arithmetic is computationally effective, and moreover, it is possible to use it because the coefficients of the algorithm may be stored in look-up tables in such a form that enables obtaining accurate enough results expressed in units of the sampled quantity. In second, results of the A/D conversion are positive integer numbers in the binary code and arithmetic operations are performed in this code. It enables one to evaluate the execution time of the arithmetic instructions as approximately equal to the time of moving data. Based on these assumptions, it is defined a unit of arithmetic operation as the sequence of three processor instructions: move + operation + move, for which one takes that two transfers of data are needed per one arithmetic operations. To simplify the considerations, one assumes that all instructions are executed in the same time that is equal to one cycle of the microcontroller.

6.1. Execution time of static reconstruction

6.1.1. Execution time of analytical static reconstruction

Accordingly with Eq. (3.13), three arithmetical operations are necessary to obtain the result of the analytical static reconstruction: one to determine the distance of the working point from the node, one to multiply the distance by the inclination and one to add the obtained result to the shift coefficient. These operations must be preceded by two activities. The first one concerns obtaining a measurement result from the AD converter. Taking into account that the AD converter handling can be carried out by using an interrupt, one can evaluate it execution time as approximately equal to one unit. The second activity consists in the determination of the node number, and it is performed by comparing the AD indication with the nodal values, which causes the number of comparisons to depend on the total number of nodes. One can point the more efficient method of determination of the node number than described. It requires a different look-up table structure than this one used in this work, namely the even distribution of nodes along the axis of indications is necessary. In this case, the AD converter result may be split into two parts: higher, which is used to determine addresses of three nodal values and lower, which represents the distance from the node. Such a splitting can be carried out by using two logical operations, so it needs about two units. The addresses are determined in about three units.

Taking the presented analysis into account, on can set together all units necessary to obtain one estimate of the input sample that reconstructed by using the static algorithm. One obtains the following list:

- measurement of a value of the input signal sample by using AD converter – 1 unit,
- splitting the ADC result into the bits that represent the node number and the distance from the node – 2 units,
- the determination of addresses of 3 node values – 3 units,
- calculation of the estimate of the reconstructed sample by using the static algorithm according to Eq. (3.13) – 3 units.

Summing up the values of units, one obtains 9 units. Adding 1 unit to perform other operations, we find that the number of unit necessary to reconstruct one sample using the static algorithm is about 10. Taking into account that one unit consists of 3 instructions, and with assumption that the execution time of each instruction is 1 μs, one obtains that the static reconstruction is performed in $3 \cdot 10 \cdot 1\ \mu s = 30\ \mu s$, which means that the maximum sampling frequency for the exemplary sampling instrument performing in the real-time only the static reconstruction is about $1/30 \cdot 10^{-6} = 33$ kHz.

If the two-dimensional static reconstruction is applied, the influence quantity have to be measured. In the exemplary sampling instrument, this quantity is measured by the second AD converter of the microcontroller, which means that measurements of both the input and the influence quantities are performed in parallel at the same time. In this case, the static reconstruction requires 3 units more than the one-dimensional reconstruction: one for determining the address of the coefficient, one for calculating the correction and one for correcting the AD indication. Therefore, if the two--dimensional reconstructionis performed accordingly with the algorithm described in Section 3.3.2, it requires 13 calculation units, which means that its execution time is $3 \cdot 13 \cdot 1\ \mu s = 39\ \mu s$, i.e., the maximum sampling frequency is about 25 kHz.

6.1.2. Execution time of neural static reconstruction

Neurons in layers of artificial neural networks perform operations in parallel. It means that to obtain a minimum execution time of the static reconstruction, we must use as many microcontrollers as the number of neurons is applied in the hidden layer. For the exemplary network of Fig. 3.18, 3 microcontrollers should be used. They execute the same kinds of operation except the last that consists in addition of the output data of the neurons. This operation is carried out by the microcontroller selected as the main on the basis of the partial results obtained from the remaining microcontrollers.

The main problem that must be solved if microcontrollers are used to perform operations suitable for a neuron is caused by non-linearity of the transfer function. The most time-efficient solution consists in using the linear approximation of the transfer function, which requires the same calculation units as the one-dimensional static reconstruction. As it results from considerations presented in Section 3.2.5, this approximation requires many nodes if the nonlinearity is strong, but the number of arithmetical operations do not depend on the number of nodes.

Based on Fig. 3.18 and taking the above into account, one may state that the operations that perform the exemplary static reconstruction in parallel are:

- measurement of a value of the input signal sample by using ADC converter – 1 unit,
- multiplication of the indication by the suitable coefficient and addition of the result to the bias – 2 units,
- processing this result by the transfer function using the linear approximation – 9 units,

- multiplication of transfer function output result by the coefficient suitable for the neuron – 1 unit,
- summing up output results of 3 neurons by the main microcontroller and connected with addition of the bias – 4 units.

Summing up the presented above numbers of units, one obtains 15 units, which means that the parallel execution of the one-dimensional reconstruction algorithm using the neural network is about 50 % longer than of the analytical algorithm.

As it results from Fig. 3.38, each neuron in the hidden layer of the network that performs two-dimensional neural reconstruction processes two measurement results. If as many microcontrollers as the neurons are used, 2 more arithmetical units are necessary to multiply the indication obtained for the influence quantity by the suitable coefficient and to add the result the second input value. This means that the total number of units is equal to 17, 4 units more than for the two-dimensional analytical reconstruction.

6.2. Execution time of signal reconstruction

The signal reconstruction based on the Wiener model is performed in series: the static reconstruction algorithm is executed as first, and next, the dynamic algorithm is performed on the basis of the estimates obtained from the static reconstruction. Thus, the execution time of the signal reconstruction is the sum of the times at which the static and dynamic algorithms are executed.

Accordingly with Eq. (4.51), the first-order dynamic reconstruction requires 3 units: 2 for making the multiplications plus 1 for the addition. If the reconstruction is realized accordingly with the second-order dynamic algorithm described by Eqs. (4.52) and (4.53) – 6 operations of addition and 4 of multiplication are required, which gives 10 arithmetic units.

Summing up the presented considerations, we obtain that the different combinations of the exemplary signal reconstruction algorithms require the following number of units:

- the analytical one-dimensional static algorithm + 1-st order dynamic algorithm – 9 + 3 = 12 units,
- the analytical two-dimensional static algorithm + 1-st order dynamic algorithm – 12 + 3 = 15 units,

- the analytical one-dimensional static algorithm + 2-nd order dynamic algorithm – 9 + 10 = 19 units,
- the analytical two-dimensional static algorithm + 2-nd order dynamic algorithm – 12 + 10 = 22 units,
- the neural one-dimensional static algorithm + 1-st order dynamic algorithm – 15 + 3 = 18 units,
- the neural two-dimensional static algorithm + 1-st order dynamic algorithm – 17 + 3 = 20 units,
- the neural one-dimensional static algorithm + 2-nd order dynamic algorithm – 15 + 10 = 25 units,
- the neural two-dimensional static algorithm + 2-nd order dynamic algorithm – 17 + 10 = 27 units.

As it results from the presented list, the number of the units required to perform the signal reconstruction in the conditions considered in this book does not exceed 27. Taking into account that the execution time of the unit takes 3 instructions, this number of units needs $27 \cdot 3 \cdot 1$ μs = 81 μs. Taking other operations needed into account, one can evaluate the execution time as about 100 μs. This means that the maximum sampling frequency of the instrument working in real-time mode o is about $1/(100 \cdot 10^{-6})$ = 10 kHz. This frequency is limited exclusively by the execution time of mathematical operations necessary to obtain the estimate of the input sample for the execution time of one instruction by the exemplary microcontroller. However, if we take into account that the instrument processes varying over time signals, the suitable number of samples per one period must be performed to obtain the required uncertainty of the estimate, which is connected with property of the discretization error. As resulted from the considerations presented in Chapter 4, for the first order dynamic converter, about 100 samples per the period is needed to obtain about 1 % uncertainty related to the measurement range. In this case, the maximum frequency of the sinusoidal signal is about $10 \cdot 10^3/100$ = 100 Hz. This frequency is limited exclusively by properties of the mathematical tools used to perform the reconstruction in the considered conditions.

6.3. Real-time calculation of uncertainty

A single sample of the instrument input signal is treated as the measurand, which means that the result of the reconstruction is expressed in the form of the interval,

which is presented in Chapter 1. The radius of this interval is described by the defined uncertainty. If the sampling instrument works in stable measurement conditions, the uncertainty is the same for each sample, thus, the uncertainty can determined only once as the result of the error analysis. However, for changing conditions, the uncertainty must be calculated dependently of the their actual state. Quantities that substantially affect measurement results are contained in the measurement model as influence quantities. Embracing these quantities by the model means that the suitable errors that burden the results are eliminated from them as an effect of the reconstruction. However, there are parameters of the measurement conditions which do not affect measurement results, but they influence on the instrument inaccuracy. In this situation, the uncertainties of the reconstructed samples should be calculated based on values of these parameters.

It results from considerations presented in Chapter 5 that two parameters of the reconstructed signal mainly influence the uncertainty of the estimates obtained: the frequency and the amplitude of the signal. Both parameters can be calculated based on the samples reconstructed for at least one signal period. These calculations are performed with assumption that these parameters change in time relatively slowly, therefore, a value of the parameter determined for the current period may be used in the next. Taking this into account, one can state that the calculations of these parameters may be performed in background of the reconstruction execution. The signal period may be determined by countering the samples, while the amplitude as the maximum value of them in the period, which means that these calculations do not consume essential part of the microcontroller time.

The basic way of the sampling instrument adjustment to the signal amplitude variations consists in suitable changes of the amplification coefficient of the amplifier working in the analog part of this instrument. It causes the parameters of the linear approximation of the static characteristic to be changed dependently on the coefficient value. The fastest way of obtaining the suitable parameters is to store them in a look-up table for every values of the amplification coefficient and use the actual parameters to perform the reconstruction.

Variations of the signal frequency are important from properties of the dynamic algorithm point of view because, for the constant sampling frequency, the number of samples in the signal period changes. This causes in turn the discretization error to change, which may influence significantly the uncertainty of the reconstructed samples. We have two ways to proceed in this situation. The first consists in using a look-up table to store the selected values of uncertainty dependently on

the frequency values to use them as in Example 5.7 to calculate the current value of the uncertainty. The essence of the second way is to change the sampling frequency so that the uncertainty is constant. This way needs suitable changes of parameters of the dynamic algorithm, the current values of which may be determined with using look-up tables. Such a working mode of the sampling instrument can be considered as adaptive [G2].

BIBLIOGRAPHY

A1. Andria G.T.: Approximation of continuous functions by polynomials with integral coefficients. Journal of Approximation Theory, Vol. 4 (4), 1971, pp. 357–362.

A2. Ablameyko S., Goras L., Goris M., Piuri V.: Neural Networks for Instrumentation, Measurement and Related Industrial Applications. IOS Press, 2003.

A3. Armato A., Fanucci L., Scilingo E. P., De Rossi D.: Low-error digital hardware implementation of artificial neuron activation functions and their derivative. Microprocessors and Microsystems, Vol. 35, Issue 6, August 2011, pp. 557–567.

A4. Arpaia P., Daponte P., Grimaldi D., Michaeli L.: Systematic error correction for experimentally modeled sensors by using ANNs. Instrumentation and Measurement Technology Conference, 1999.IMTC/99. Proceedings of the 16th IEEE, Vol. 3, 1999, pp. 1635–1640.

B1. Betta G., Lignori C., Pietrosanto A.: A Structural Approach to Estimate the Measurement Uncertainty in Digital Signal Elaboration Algorithms. IEE Proc. Part A, Sci. Measur. Technol. 146 (1), 1999, pp. 21–26.

B2. Betta G., Lignori C., Pietrosanto A.: Propagation of Uncertainty in a Discrete Fourier Transform Algorithm. Measurement, 27 (4), 2000, pp. 231–239.

B3. Battiti R.: First and second order methods for learning: Between steepest descent and Newton's method. Neural Computation, Vol. 4, No. 2, 1992, pp. 141–166, 1992.

B4. Bicle L.W., Dove R.C.: Numerical Correction of Transient Measurements. Adv. Instrum., Vol. 27, Part 2, Pittsburgh 1972.

C1. Chudzik S., Grys S, Minkina W. The application of the artificial neural network and hot probe method in thermal parameters determination of heat insulation materials. Part: 1-thermal model consideration. 2009 IEEE International Conference on Industrial Technology, 2009, pp. 1–6.

C2. Cichy A., Roj J.: Applications of artificial neural networks in quasi-balanced measuring circuits. Diagnostic of electrical machines and materials: DESAM 2014. 3rd International conference, Papradno, Slovak Republic, 19-20.06.2014. Proceedings, 2014, EDIS − Zilina University Publisher, pp. 7–11.

D1. Daponte P., Grimaldi D.: Artificial neural networks in measurements. Measurement, Vol. 23, Issue 2, March 1998, pp. 93–115.

G1. Godec Z.: Standard Uncertainty in Each Measurement Result Explicit or Implicit. Measurement 20 (2), 1997, pp. 97–101.

G2. Gröchenig K.: A discrete theory of irregular sampling. Elsevier Inc., 1993.

G3. Guo F.: A new identification method for Wiener and Hammerstein systems. Forschungszentrum Karlsruhe, 2004.

H1. Hornik K.: Approximation capabilities of multilayer feedforward networks. Neural Networks, Vol. 4, Issue 2, Elsevier 1991, pp. 251–257.

H2. Hsu Y.-L., Wang J.-S.: A Wiener-type recurrent neural network and its control strategy for nonlinear dynamic applications. Journal of Process Control, Vol. 19, Issue 6, June 2009, pp. 942–953.

H3. Hagel R., Zakrzewski J.: Miernictwo dynamiczne. WNT, Warszawa 1984.

J1. Jakubiec J., Topór-Kamiński T.: Uncertainty Modelling Method of Data Series Processing Algorithms. IMEKO TC-4 Symposium on Development in Digital Measuring Instrumentation and 3rd Workshop on ADC Modelling and Testing, Sep. 17-18, 1998, Naples, Italy, pp. 631–636.

J2. Jakubiec J., Konopka K.: Uncertainty Propagation Model of A/D Measuring Chain. IMEKO TC-4 Symposium on Development in Digital Measuring Instrumentation and 3rd Workshop on ADC Modelling and Testing, Sep. 17–18, 1998, Naples, pp. 831–836.

J3. Jakubiec J., Konopka K.: Reductive Interval Arithmetic in Dynamic Error Evaluation. Proc. XVI IMEKO World Con., Sept. 25–28, 2000. Vienna, Austria. Vol. X, pp. 195–200.

J4. Jakubiec J., Konopka K.: Coherence Coefficient as Uncertainty Parameter of Error Value Set. Proc. of the IMEKO-TC7 Symposium „Measurement Science of the Information Era", Cracow, Poland, June 25-27 2002, pp. 76–81.

J5. Jakubiec J., Konopka K.: A Method of Error Source Identification of A/D Measuring Chain. Proc. 20th IEEE Instrumentation and Measurement Technology Conference IMTC/03, Vail, CO, USA, 20-22 May 2003, pp. 1659–1664.

J6. Jakubiec J.: Reductive Interval Arithmetic Application to Uncertainty Calculation of Measurement Result Burdened Correlated Errors. Metrology and Measurement Systems. Vol. X, No. 2 (2003), pp. 137–156.

J7. Jakubiec J.: System Oriented Mathematical Model of Single Measurement Result. Metrology and Measurement Systems. Vol. XIII, No. 4 (2006), pp. 405–419.

J8. Jakubiec J., Makowski P., Roj J.: Error Model Application in Neural Reconstruction of Nonlinear Sensor Input Signal. IEEE Transactions on Instrumentation and Measurement, Vol. 58, No. 3, March 2009, pp. 649–656.

J9. Jakubiec J.: Błędy i niepewności w systemie pomiarowo-sterującym. Wydawnictwo Politechniki Śląskiej, Gliwice 2010.

J10. Jakubiec J.: A New Conception of Measurement Uncertainty Calculation. Acta Physica Polonica A. Vol. 124 (2013), No. 3, pp. 436–444.

J11. Jakubiec J., Wymysło M.: Errors caused by delays in measuring and control systems. Proceedings of Metrology Commission of Katowice Branch of Polish Academy of Sciences, Conferences Nr 20.PPM'15, Kościelisko, 07–10 June 2015, pp. 49–52.

J12. Jakubiec J.: A Complex Method of Systematic Error Correction in AD Measuring Chain. Proc. IMEKO TC-4 Int. Work. on ADC Modelling, Smolenice, May 7–9, 1996, pp.13–18.

J13. Jakubiec J., Konopka K.: Reductive Interval Arithmetic in Dynamic Error Evaluation. Proc. XVI IMEKO World Congr., Sept. 25–28, 2000. Vienna, Austria. Vol. X, pp. 195–200.

J14. Jakubiec J., Roj J.: Pomiarowe przetwarzanie próbkujące. Wydawnictwo Politechniki Śląskiej, Gliwice 2000.

J15. Jakubiec J.: Application of reductive interval arithmetic to uncertainty evaluation of measurement data processing algorithms. Wyddawnictwo Politechniki Śląskiej, Gliwice 2002.

J16. Jackowska-Strumiłło L.: Analytical and neural correctors of temperature sensors dynamic errors. Automatyka, tom 14, zeszyt 3/2 (2010), s. 773–783.

J17. Jackowska-Strumiłło L. et al.: Modelling and MBS experimentation for temperature sensors. Measurement. Vol. 20, Issue 1, Jan. 1997, pp. 49–60.

K1. Kluk P., Morawski R.Z.: Static Calibration of Transducers Using Parametrization and Neural-Network based Approximation. Proc. IEEE Transactions on Instrumentation and Measurement, 1995, pp. 49–53.

K2. Konopka K., Topór-Kamiński T.: Identification of Measurement Data Processing Algorithm Coefficients Presented on Selected Form of FFT Algorithm. XIX IMEKO World Congress, Lizbona, Portugalia, 6–11.09.2009, pp. 2400–2404.

K3. Korczyński J.: Calculation of Expanded Uncertainty. Proc. Joint IMEKO TC-1 & XXXIV Conference 2002, Wrocław, 8–12 Sept. 2002, Vol. I, pp. 107–114.

K4. Kroese D.P., Taimre T., Botev Z.I.: Handbook of Monte Carlo Methods. Wiley Series in Probability and Statistics, John Wiley & Sons, New York 2011.

L1. Layer E., Tomczyk K.: Measurement Modelling and Simulation of Dynamic Systems. Springer, 2010.

L2. Layer E., Tomczyk K.: Signal Transforms in Dynamic Measurements. Studies in Systems, Decision and Control, Vol. 16, Springer 2015.

L3. Luque J., Escudero I., Pérez F.: Analytic Model of the Measurement Errors Caused by Communications Delay, IEEE Transactions on Power Delivery, Vol. 17, No. 2, 2002, pp. 334–337.

L4. Leondes C.T.: Algorithms and Architectures. Neural Network Systems Techniques and Applications. Vol. 1, Academic Press, 1998.

M1. McGhee J., Kulesza W., Henderson I.A., Korczyński M.J.: Measurement Data Handling. Theoretical Technique. Vol. 1. The Technical University of Lodz, Łódź 2001.

M2. McGhee J., Kulesza W., Henderson I. A., Korczyński M. J.: Measurement Data Handling. Hardware Technique. Vol. 2. The Technical University of Lodz, Łódź 2001.

M3. Morawski R.Z.: Basic Problems of Measurement Signal Reconstruction. Advances in Science and Technology and Engineering of Instrumenation, 1989, pp. 80–84.

M4. Morawski R.Z.: Unified Approach to Measurement Signal Reconstruction. Measurement 9 (3), 1991, pp. 140–144.

M5. Morawski R.Z.: Unified Approach to Measurand Reconstruction. IEEE Transactions on Instrumentation and Measurement, Vol. 43, No. 2, 1994, pp. 226–231.

M6. Morawski R.Z., Miękina A.: Monte-Carlo Evaluation of Measurement Uncertainty using a New Generator of Pseudorandom Numbers. Measurement Automation Monitoring, Vol. 59, No. 5, 2013, pp. 390–393.

M7. Minkina W., Gryś S.: Application of adaptive signal processing in error compensation of transient temperature measurements. Metrology and Measurement Systems 9 (2), 125–139, pp. 2002.

M8. Minkina W.: Theoretical and experimental identification of the temperature sensor unit step response non-linearity during air temperature measurement. Sensors and Actuators A: Physical 78 (2–3), 1999, pp. 81–87.

M9. Minkina W., Chudzik S.: Determination of Thermal Parameters of Heat--Insulating Materials Using Artificial Neural Networks. Metrol. and Measur. Sys. Vol. 10, No. 1, 2003, pp. 33–49.

M10. Minkina W., Gryś S.: Correction of dynamic characteristics of thermometric sensors – methods, systems, algorithms. Publishing House of Czestochowa University of Technology, 2023.

M11. Mirri D., Luculano G., Filicori F., Pasini G., Vannini G., Pellegrini G.P.: A modified Volterra series approach for nonlinear dynamic systems modeling. IEEE Transactions on Circuits and Systems,Vol. 49, Issue 8, 2002, pp. 118–1128.

M12. Meditch J.S.: Stochastic optimal linear estimation and control. McGraw Hill, New York 1969.

N1. Neumaier A.: Interval Methods for System of Equations. Cambridge Univer. Press, 1990.

O1. Orfanidis S.J.: Optimum Signal Processing. Sec. Ed., Macmillan Publ. Company, New York 1988.

O2. Olyaee S., Hamedi S.: Neural network approximation of nonlinearity in laser nanometrology system based on TLMI. 3rd International Photonics &OptoElectronics Meetings (POEM 2010), Journal of Physics: Conference Series 276, 2011, pp. 1–8.

P1. Papoulis A.: Probability, Random Variables, and Stochastic Processes. McGraw-Hill, Inc., New York 1965.

P2. Patra J.C., Chakraborty G., Meher P.K.: Neural-Network-Based Robust Linearization and Compensation Technique for Sensors Under Nonlinear Environmental Influences. Circuits and Systems I: Regular Papers, IEEE Transactions on Instr., Vol. 55, Issue 5, 2008, pp. 1316–1327.

R1. Roj J.: Correction of dynamic errors of a gas sensor based on a parametric method and a neural network technique. Sensors, Multidisciplinary Digital Publishing Institute, Vol. 16, No. 8, 2016, art. No. 1267.

R2. Roj J., Urzędniczok H.: Correction of gas sensor dynamic errors by means of neural networks. Measurement Automation Monitoring, Wyd. PAK, Vol. 61, No. 12, 2015, pp. 538–541.

R3. Roj J., Cichy A.: Method of measurement of capacitance and dielectric loss factor using artificial neural networks. Measurement Science Review, De Gruyter Open, Vol. 15, No. 3, 2015, pp. 127–131.

R4. Roj J.: Estimation of the artificial neural network uncertainty used for measurand reconstruction in a sampling transducer. IET Science Measurement & Technology, Institute of Electrical and Electronics Engineers, Vol. 8, No. 1, 2014, pp. 23–29.

R5. Roj J.: Neuronowe odtwarzanie sygnałów pomiarowych. Wydawnictwo Politechniki Śląskiej, Gliwice 2013.

R6. Roj J.: Neural approximation of empirical functions. Acta Physica Polonica A, Polish Academy of Sciences Institute of Physics, Vol. 124, No. 3, 2013, pp. 554–557.

R7. Roj J.: Neural network based real-time correction of transducer dynamic errors. Measurement Science Review, De Gruyter Open, Vol. 13, No. 6, 2013, pp. 286–291.

R8. Roj J.: Właściwości metrologiczne radialnych i sigmoidalnych sieci neuronowych zastosowanych do korekcji błędów statycznych w przetworniku próbkującym. Przegląd Elektrotechniczny, Sigma NOT, Vol. R. 89, nr 1a, 2013, s. 84–87.

R9 Roj J.: Neuronowa korekcja błędów dynamicznych przetwornika II-go rzędu. Measurement Automation Monitoring, Wydawnictwo PAK, Vol. 56, nr 11, 2010, s. 1315–1317.

R10. Roj J.: Modele odcinkowo-liniowe w zastosowaniu do budowy szybkich algorytmów korekcji błędów systematycznych złożonych nieliniowych przetworników pomiarowych. PAK, nr 11, Warszawa 1999, s. 2–5.

S1. Szczeciński L., Barwicz A.: Quickly Converging Iterative Algorithms for Measurand Reconstruction. Measurement 20 (3), 1997, pp. 211–217.

S2. Szafrański T., Morawski R.Z.: Efficient Estimation of Uncertainty in Weakly Non-linear Algorithms for Measurand Reconstruction. Measurement 29, 2001, pp. 77–85.

S3. Szczeciński L., Morawski R.Z., Barwicz A.: Numerical Correction of Spectrometric Data Using a Bilinear Operator of Measurand Reconstruction. Instrumentation Science & Technology, Vol. 25, No. 3, 1997, pp. 197–205.

S4. Stone H.: Approximation of curves by linear segments. Math. Comp. 15, 1961, pp. 40–47.

S5. Smith B.A., McClendon R.W., Hoogenboom G.: Improving air temperature prediction with artificial neural networks. International Journal of Computational Intelligence, 3(3), 2006, pp. 179–186.

S6. Sabatier P.C.: Inverse problems – An Introduction. Inverse problems, Vol. 1, No. 1, Feb. 1985.

S7. Sasai T. Nakamura M., Yamazaki E., Matsushita A., Okamoto S., Horikoshi K., Kisaka Y.: Wiener-Hammerstein model and its learning for nonlinear digital pre-distortion of optical transmitters. Optics Express**,** Vol. 28, Issue 21, 2020, pp. 30952–30963.

T1. Terrell D.L.: Op Amps, Design, Application, and Troubleshooting. Second Edition. Elsevier Inc., 1996.

V1. Vopalensky M., Platil A.: Temperature Drift of Offset and Sensitivity in Full--Bridge Magnetoresistive Sensors. EEE Transactions on Magnetics, Vol. 49, Issue 1, 2012.

W1. Wiliams C.M.: An efficient algorithm for the piecewise linear approximation of planar curves. Comp. Graphics Image Processing, 8, 1978, pp. 286–293.

W2. Wu D., Huang S., Zhao W., Xin J.: Infrared thermometer sensor dynamic error compensation using Hammerstein neural network. Sensors and Actuators A, Physical, Vol. 149, Issue 1, 15 January 2009, pp. 152–158.

W3. Wiliamowski B., Yu H.: Improved Computation for Levenberg–Marquardt Training. IEEE Transactions on Neural Networks and Learning Systems, 21 (6), 2010, pp. 930–937.

Z1. Zieliński M., Kowalski M., Frankowski R., Chaberski D., Grzelak S., Wydźgowski L.: Accumulated Jitter Measurement of Standard Clock Oscillators. Metrology and Measurement Systems. Vol. XVI (2009), No. 2, pp. 259–266.

Z2. Żuchowski A.: Technika pomiarów dynamicznych. Wyd. Pol. Szczecińskiej, Szczecin 1974.

Y1. Guide to the Expression of Uncertainty in Measurement. ISO, 1992, 1995.

Y2. International vocabulary of metrology – Basic and general concepts and associated terms. JCGM 200:2012\.

Y3. Guide to Expression of Uncertainty in Measurement. Supplement 1. Numerical Methods for the Propagation of Distributions. BIPM 2004.

Y4. EN IEC 60751:2022. “Industrial platinum resistance thermometers and platinum temperature sensors”. https://standards.iteh.ai/catalog/standards/clc/61d80f27-74a7-4165-97ad-67edd99b8f7d/en-iec-60751-2022

Y5. ASTM E1137/E1137M-08(2020). “Standard Specification for Industrial Platinum Resistance Thermometers”. https://webstore.ansi.org/standards/astm/astme1137e1137m082020j

Y6. ADuC 386. https://www.analog.com/media/en/technical-documentation/data-sheets/ADUC836.pdf

ERROR ANALYSIS OF ANALYTICAL AND NEURAL REAL-TIME RECONSTRUCTION OF ANALOG SIGNALS

Summary

This monography is devoted to signal reconstruction by a sampling instrument, which can operate autonomously or be an element of a measurement and control system. The reconstruction consists in calculation of the input signal sample values based on quantized signal samples at the output of the analog part of the device, assuming that this signal is burdened by dynamic errors and errors caused by the nonlinearity of analog processing. The book considers the reconstruction algorithms that can be implemented in real time by microcontrollers, which means that all calculations are performed in the period between successive sampling instants. Two types of the algorithms are analyzed: analytical, whose parameters are specyfied as programming constants, and neural, implemented using artificial neural networks and learned during the identification of analog processing parameters. The reconstructed samples must have the required accuracy, which in the book is expressed quantitatively by the uncertainty interval of the sample estimate of the input signal. The main goal of the book is to analyze errors in the reconstruction process, on the basis of which a model of error propagation in the sampling instrument is created. The uncertainty interval is determined based on the distribution of the instrument output error using the proposed mathematical apparatus adapted to the algorithmic processing of measurement data.

ANALIZA BŁĘDÓW ANALITYCZNEGO I NEURONOWEGO ODTWARZANIA SYGNAŁÓW ANALOGOWYCH W CZASIE RZECZYWISTYM

Streszczenie

Monografia ta poświęcona jest odtwarzaniu sygnału przez przyrząd próbkujący, który może działać autonomicznie lub być elementem systemu pomiarowo-sterującego. Odtwarzanie to polega na obliczaniu wartości próbek sygnału wejściowego na podstawie skwantowanych próbek sygnału na wyjściu części analogowej przyrządu, przy założeniu że sygnał ten obarczony jest błędami dynamicznymi i błędami powodowanymi nieliniowością przetwarzania analogowego. W monografii rozpatrywane są takiego rodzaju algorytmy, które mogą być realizowane w czasie rzeczywistym przez mikrokontrolery, co oznacza, że wszystkie obliczenia wykonywane są w okresie między kolejnymi chwilami próbkowania. Analizowane są właściwości dwojakiego rodzaju algorytmów: analitycznych, których parametry określane są jako stałe programistyczne, oraz neuronowych, realizowanych przy użyciu sztucznych sieci neuronowych i uczonych w trakcie identyfikacji parametrów przetwarzania analogowego. Odtwarzane próbki muszą cechować się wymaganą dokładnością, która w monografii wyrażana jest ilościowo za pomocą przedziału niepewności estymaty próbki sygnału wejściowego. Głównym celem pracy jest analiza błędów procesu odtwarzania, na podstawie której tworzony jest model propagacji błędu w przyrządzie próbkującym. Wyznaczanie przedziału niepewności realizowane jest na podstawie rozkładu błędu wyjściowego przyrządu przy użyciu zaproponowanego aparatu matematycznego dostosowanego do algorytmicznego przetwarzania danych pomiarowych.

WYDAWNICTWO POLITECHNIKI ŚLĄSKIEJ
ul. Akademicka 5, 44-100 Gliwice
tel. (32) 237-13-81
wydawnictwo@polsl.pl
www.wydawnictwopolitechniki.pl

UIW 48600

Sprzedaż i Marketing
tel. (32) 237-18-48
wydawnictwo_mark@polsl.pl

Nakł. 100 + 44	Ark. wyd. 19	Ark. druk. 15	Papier 80 g

Zam. 37/24
Monografia 1030

ISBN 978-83-7880-959-3

Wydawnictwo Politechniki Śląskiej
44-100 Gliwice, ul. Akademicka 5
tel. (32) 237-13-81
www.wydawnictwopolitechniki.pl
Dział Sprzedaży i Reklamy
tel.(32) 237-18-48
e-mail: wydawnictwo_mark@polsl.pl
http://www.polsl.pl/rjo2-wps